# 1

# Evolution of DC Drives

Direct current (dc) motors have been used in variable-speed drives for a long time. The versatile control characteristics of dc motors[1-3] have contributed to their extensive use in industry. Dc motors can provide high starting torques, which are required for traction drives. Control over a large speed range both below and above the rated speed can be easily achieved. The methods of control are simpler and less expensive than those of alternating current (ac) motors. Although commutators prohibit their use in certain applications, such as high-speed drives and operation in hazardous atmospheres, dc motors play a significant role in many industrial drives.

The technology of speed control of dc drives has evolved considerably. The present state of the art of dc motor drives is far advanced compared to what it was just a quarter century ago. A brief history of the evolution of the dc drives is presented in the following section.

## 1.1 HISTORY OF DC DRIVES

During the last century the available power supply was constant-voltage direct current, and the use of electric power to any significant extent was confined to larger cities. In industrial plants, located in urban areas, dc motors were used to drive machinery. The dc motors were operated from a constant-voltage bus. Variable-speed drives were made possible only by the adjustment of motor field flux. This in turn produced such severe problems as commutator sparking and the consequent limitation on the life of brushes and commutators. In fact, the phenomenon of commutation was not well understood at that time. As a result, most drives were constant-speed drives. Any variable-speed drives, achieved by changing field flux, as shown in Fig. 1.1, used rugged durable motors that generally had poor mechanical and electrical time constants.

But the demand for wider ranges of speed control rapidly increased. The commutation phenomenon became better understood. Interpole and pole-face

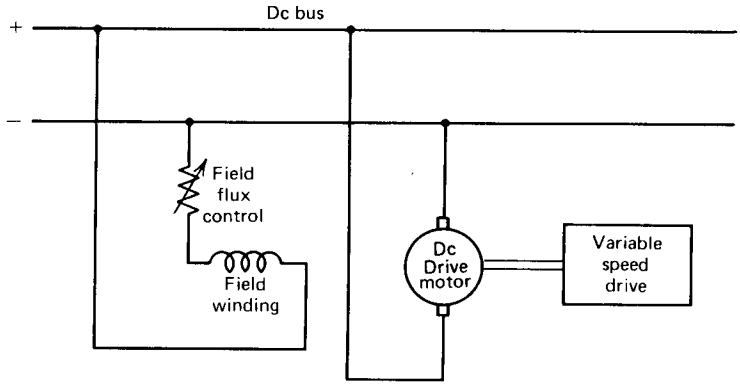


*Fig. 1.1* Basic schematic diagram of the classical variable-speed dc drive.

windings were developed to improve commutation and were put to use with fair success.

### 1.1.1 Ward-Leonard System

The development of the Ward-Leonard system,[1,2] which was introduced in the 1890s, was a significant step in the evolution of dc drives. The system uses a motor-generator (M-G) set to power the dc drive motor. The motor of the M-G set runs at constant speed. By varying the generator field excitation, the generator voltage is changed, which, in turn, can provide continuous control of speed of the drive motor over a wide range. In this method of speed control by armature voltage control, the field flux of the drive motor is kept constant, thereby avoiding the attendant problem of poor motor commutation. Figure 1.2 shows the basic schematic diagram of the Ward-Leonard speed control system. The Ward-Leonard system provided a constant torque as well as constant horsepower drive as shown in Fig. 1.3. In the constant torque mode, the field flux of the drive motor is kept constant and the armature voltage is controlled. In the constant horsepower mode, the armature voltage is held constant at the rated value and the field current is controlled. This system was the first to provide successfully better performance in terms of increased speed range, improved commutation, and precise speed control.

Meanwhile, development of ac systems for generation, transmission, and distribution continued. Ac motors were developed and became attractive because of their simplicity and ruggedness. In expanding plants, ac distribution systems were installed as plants ran out of dc capacity, and ac motors were used for constant-speed drive systems. In new plants only ac distribution systems were installed. Even in old plants, dc distribution was eventually replaced by the ac system. Machines requiring variable-speed drives used

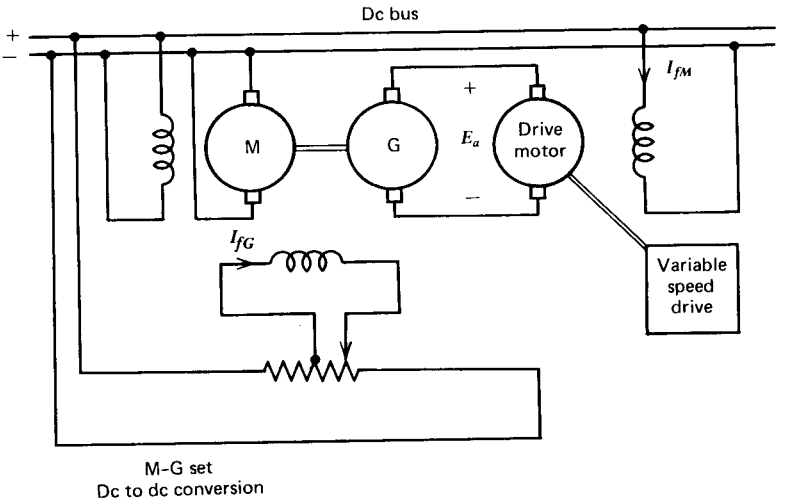


*Fig. 1.2* Basic schematic diagram of the Ward-Leonard system.

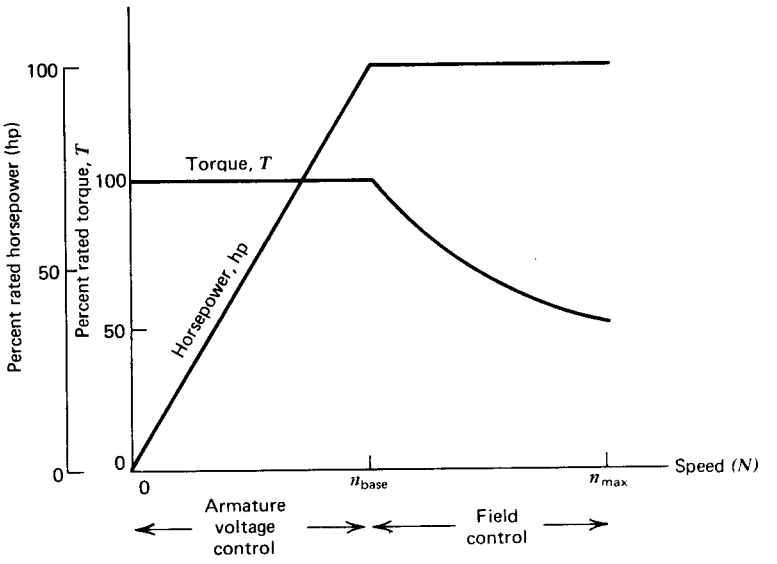


*Fig. 1.3* Constant torque and constant horsepower operation of the Ward-Leonard system.

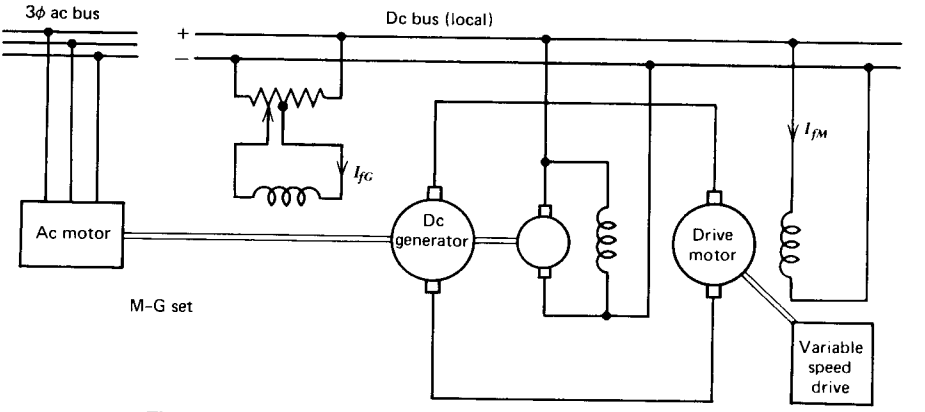


*Fig. 1.4* Ward-Leonard system with ac motor and dc generator.

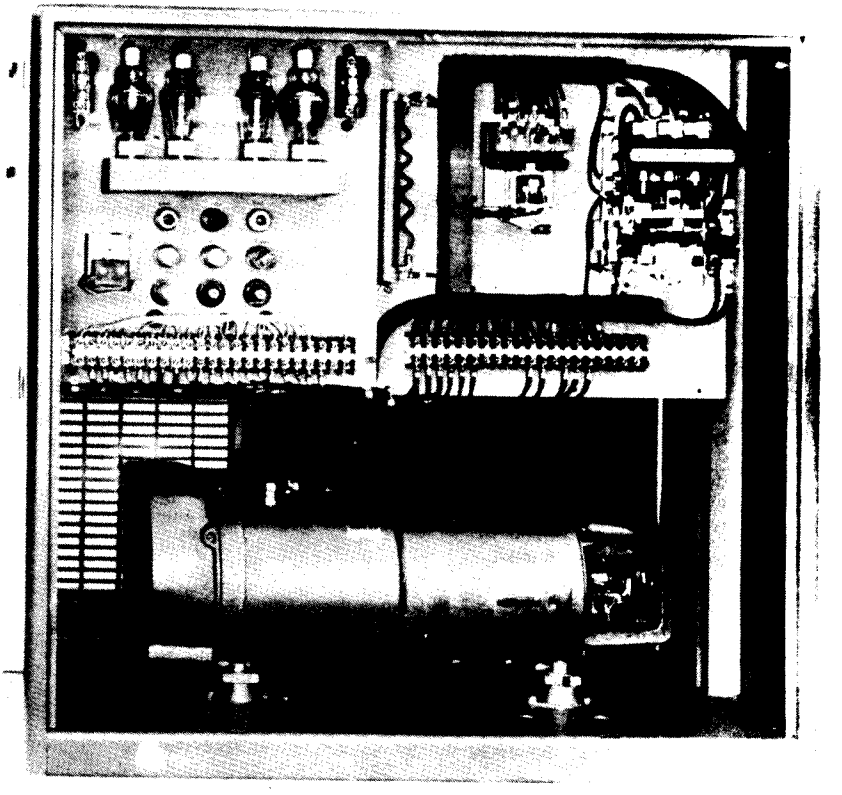

*Fig. 1.5* Packaged Ward-Leonard M-G set using tube-type regulator. (Courtesy of Reliance Electric Co.)

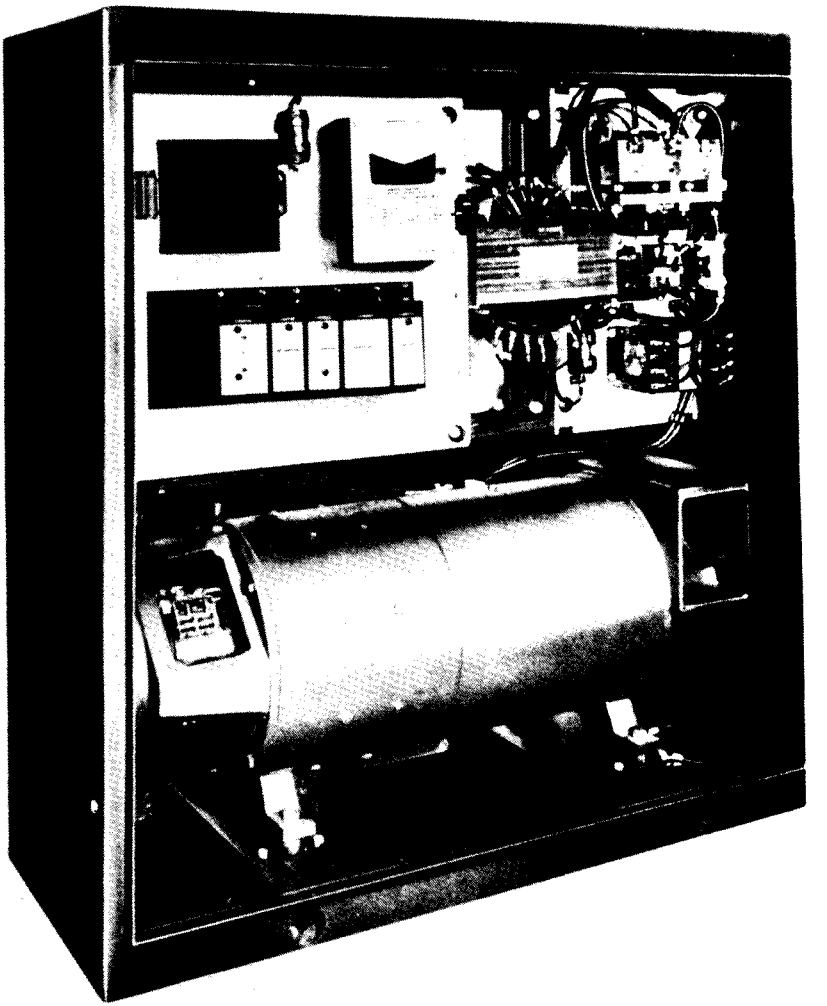

*Fig. 1.6* Packaged Ward-Leonard system using solid-state regulator. (Courtesy of Reliance Electric Co.)

Ward-Leonard M-G sets comprising an ac motor and a dc generator as shown in Fig. 1.4.

Initially the Ward-Leonard system was available in discrete components that were mounted and interconnected at the plant site. In the early 1940s the packaged Ward-Leonard system was introduced. The M-G set, regulators, and controls were mounted and wired in a common enclosure to provide a preassembled drive system. Figures 1.5 and 1.6 show the packaged M-G set system.

The Ward-Leonard system has the following advantages:

1 Full forward and reverse speed can be achieved.
2 Power is automatically regenerated to the ac line through the M-G set when speed is reduced.
3 Short-time overload capability is large.
4 The armature current of the motor is smooth.

However, it has the following disadvantages:

1 The capital cost is high.
2 The overall efficiency is low, less than 80%.
3 A large amount of space is required.
4 Periodic inspection and lubrication are necessary.

### 1.1.2 Electronic Control

In the late 1940s and early 1950s electronic control brought about a significant improvement in dc drive systems. In the initial phase, industrial-type gas-filled rectifier and controlled rectifier (thyratron) tubes were used in exciters and regulators for the M-G set as shown in Fig. 1.5. This system provided improved response and better accuracy and allowed automatic closed-loop control to be used in place of earlier manual or electromechanical control methods. Later on, these tubes became available in high current capacity and were used in rectifier circuits to convert ac to dc for speed control of the dc drive motor. Single-phase rectifier circuits using tube-type rectifiers were used in low horsepower drives. In ratings above 10 hp, tube-type rectifier systems were not found reliable.

### 1.1.3 Solid-State Control

In the late 1950s solid-state devices, silicon diodes, and silicon-controlled rectifiers (SCRs)[4,5] became available in the market at economic prices. These devices were first available in low power ratings and therefore were used in generator field regulators as a replacement for tube-type regulators. Solid-state regulators offered long life, high reliability, a smaller package, and significant improvement in performance. Figure 1.6 shows a picture of such a packaged M-G set system using a solid-state regulator.

Later on high-power versions of silicon diodes and SCRs (also called *thyristors*) became available. These solid-state devices were used to convert ac power to dc power for direct control of the drive motor. At first, silicon diodes of high-power rating were developed and were used with saturable reactors in variable-speed dc drives, as shown in Fig. 1.7. Compared to M-G

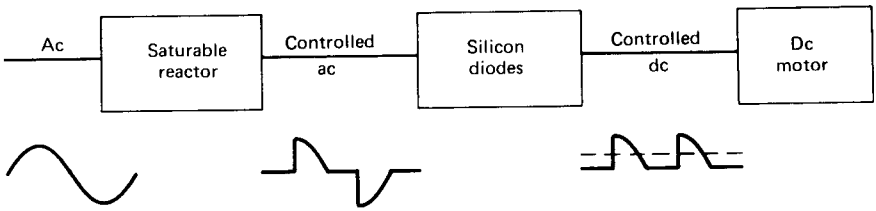


(*a*)

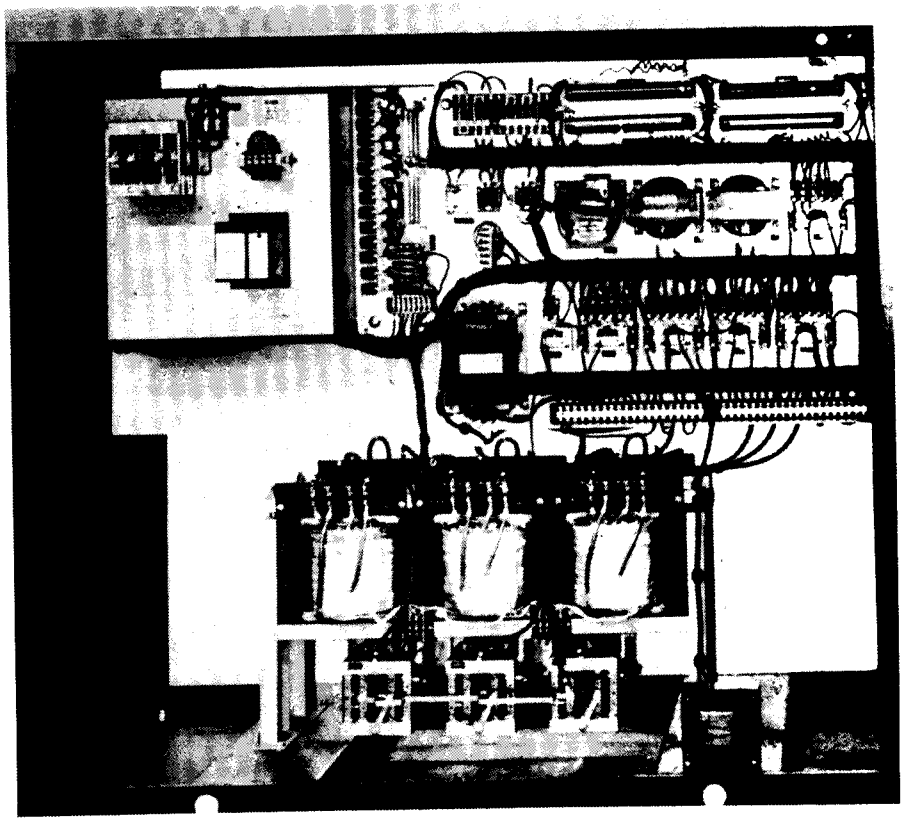

(*b*)

***Fig. 1.7*** Saturable reactor, adjustable speed, dc drive system. (*a*) Block diagram and waveform. (*b*) Photograph of the system. (Courtesy of Reliance Electric Co.)

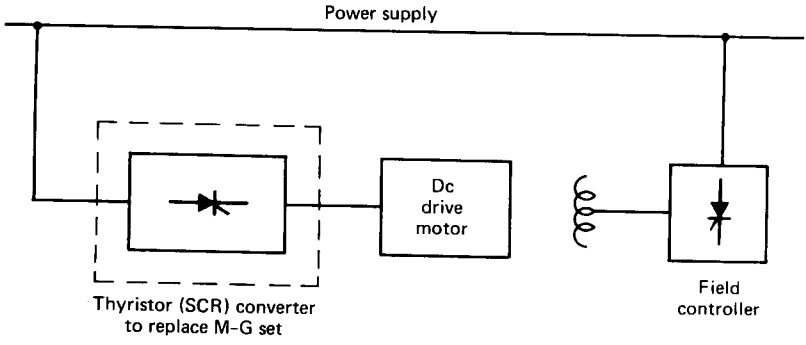


(*a*)

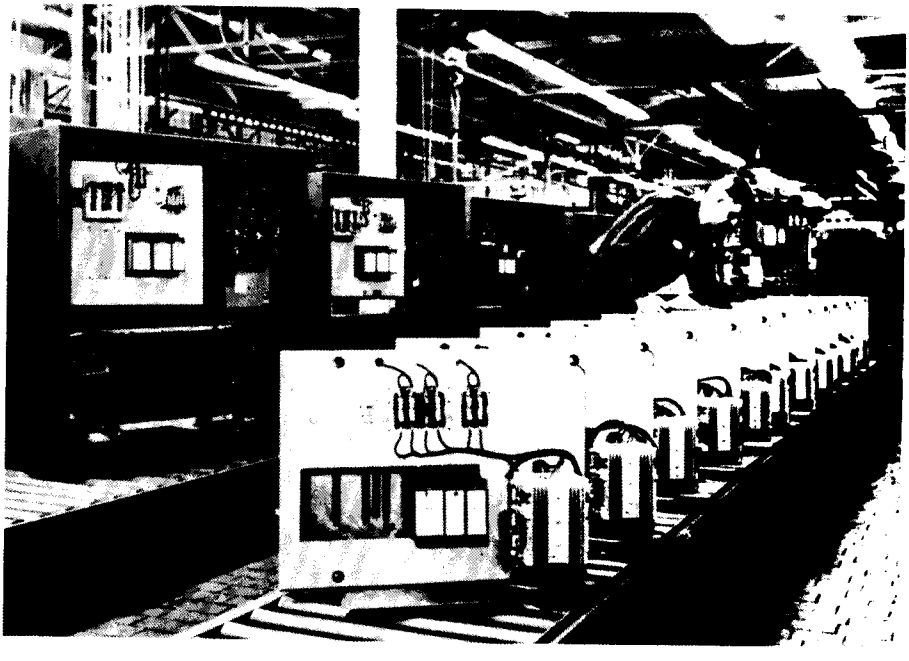

(*b*)

***Fig. 1.8*** Thyristor-controlled dc drive. (*a*) Block diagram. (*b*) First generation thyristor-controlled dc drives (foreground) and earlier M-G set drives (background). (*c*) Close-up view of a thyristor power module. [(*b*) and (*c*) Courtesy of Reliance Electric Co.]

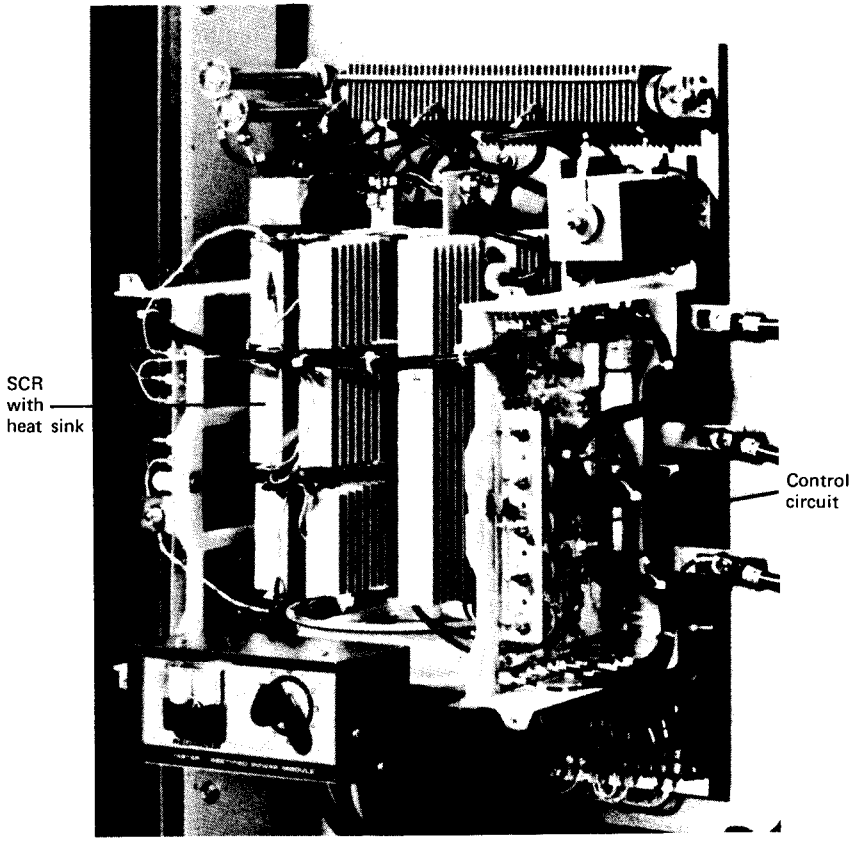


(c)

*Fig. 1.8* (*Continued*)

set systems, saturable reactor drive systems were rugged, more reliable, and provided better performance. However, they were fairly large and expensive.

Availability of high-power thyristors in the early 1960s brought about a minor revolution in industrial control equipment and drive system performance. During the decade of the 1960s, the attention of engineers designing high-capacity variable-voltage dc supply systems was diverted from generating power using an M-G set to converting power using thyristors. Figure 1.8*a* shows the block diagram of a thyristor-controlled dc drive. Virtually all new variable-speed dc drives use thyristor (SCR) converters. The M-G set that was used in variable-speed dc drives for over 50 years has been largely replaced by thyristor converters. Figure 1.8*b* shows a thyristor-controlled dc drive and its M-G set predecessor. A close-up view of a thyristor power module is shown in Fig. 1.8*c*. The thyristor drive has the following advantages:[6]

1 The thyristor-power module eliminates the electrical time lag of the generator field and armature. Time response is therefore faster, limited only by dc motor commutating ability and the inertia of the drive.
2 Basic operation is simple and reliable.
3 Minimal maintenance is required.
4 Operating efficiency is high, above 95%.
5 Small size, less weight, and packaging flexibility result in reduced space requirements, lower initial cost, and lower installation and operating costs.

The thyristor drive has the following disadvantages:[6–8]

1 The higher ripple content of the converter output adds to motor heating and commutation problems. The addition of a reactor in the armature circuit may be required to smooth out the ripple current.
2 Under certain operating conditions, the power factor in the ac supply is low. In the M-G set system, if a synchronous motor is used, the supply power factor can be kept high by adjusting the field excitation of the synchronous motor.
3 The overload capability is lower than that of a comparable M-G set.
4 Distortion of the ac supply voltage and telephone interference may be produced due to the switching action of SCRs.
5 An M-G set can regenerate automatically. In the thyristor converter, complex control circuitry is required to achieve regeneration. Either a dual converter (two bridges back-to-back) or a single converter together with a reversing switch of some kind is required to achieve regeneration. Both methods are complex and expensive.

## 1.2 STATE OF THE ART

At present separately excited dc motors controlled by thyristor converters are the most widely used motor drive systems in industry. These systems provide speed control over a wide range. The speed adjustment from base speed downward is obtained by armature voltage control. Speed control above base speed is obtained by field weakening. Horsepower and speed limitations are determined by the dc motors, not by the semiconductor devices. Thyristors (SCRs) can be connected in series and parallel for higher voltages and current ratings. The armature current and torque are limited by the motor temperature rise.

The thyristor converter shown in the block diagram of Fig. 1.8*a* provides variable armature voltage for the drive motor. The three basic methods—phase control, integral cycle control, and chopper control—for obtaining a variable dc output voltage from a fixed supply voltage (ac or dc) are

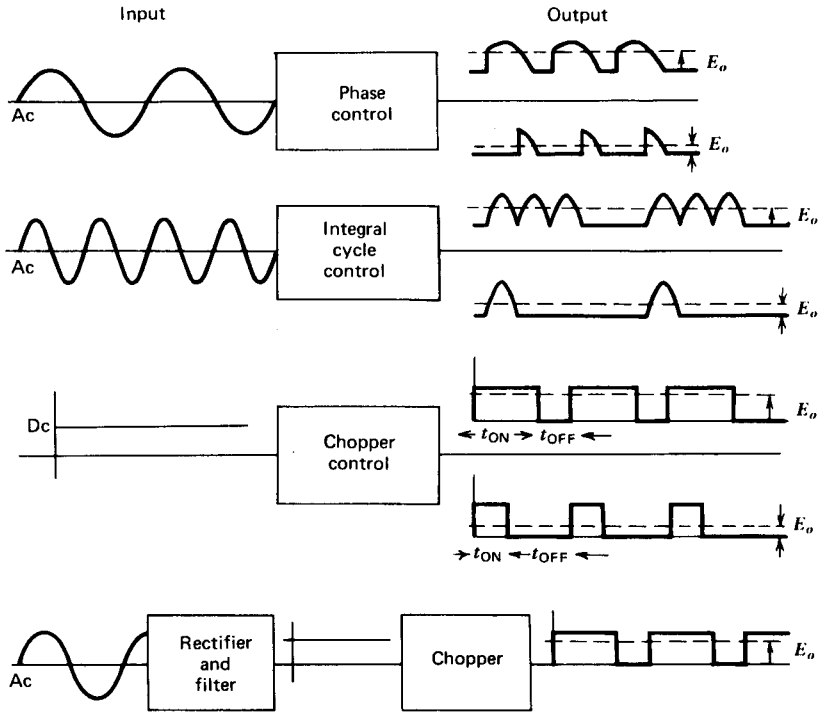


*Fig. 1.9* Control techniques for obtaining variable-voltage dc output from a fixed-voltage input supply.

illustrated in Fig. 1.9. In all these methods thyristors connect the supply to and disconnect it from the motor terminals. The frequency of switching is rapid. Therefore the motor responds to the average output voltage level and not to the individual voltage pulses.

In both phase control and integral cycle control schemes, the conversion from ac to dc is achieved by rectification. In phase control, the thyristor connects the supply to the motor during certain periods in each half-cycle and disconnects the motor from the supply for the remainder of each half-cycle. In the integral cycle control scheme, the thyristor connects the supply to the motor for a few half-cycles and disconnects the motor from the supply for several half-cycles. In the chopper control scheme, the thyristor switches on and off rapidly and provides a chopped voltage for the drive motor. The average value of the chopped voltage can be controlled by the ratio of the conducting time ($t_{ON}$) to the blocking time ($t_{OFF}$) of the thyristor. A combination of rectifier and chopper is also used if the supply is ac.

In phase control and integral cycle control, the supply ac voltage turns off the thyristor and no commutation circuit is necessary. These schemes are therefore simple and inexpensive. Phase control is widely used. It can control

the output voltage smoothly over a wide range. However, the power factor at the input ac supply decreases at lower output voltages. Integral cycle control is satisfactory if the supply frequency is high; otherwise the motor will oscillate about its mean speed. This system has not been found satisfactory for speed control of motors. If the supply is dc, chopper circuits are used. Auxiliary circuits are required to turn off the thyristors. Choppers are operated at a higher switching frequency to reduce ripple in the motor current. High-speed switching requires special thyristors. Therefore, chopper control is relatively complex, but nevertheless it is widely used. The combination of rectifier and chopper is costly but has the advantage of high supply power factor due to the input diode bridge.

Braking in a speed drive system is important in most applications. Friction brakes usually have been used to stop dc motors. If braking is required often, the frequent maintenance and ultimate replacement of the brake shoes make friction brakes uneconomic and undesirable. In order to exploit the full potential of thyristor control, electrical braking, both dynamic and regenerative, is widely used at present in most thyristor-controlled dc drives. In electrical braking the kinetic energy of the drive system is converted to electrical energy. In dynamic braking the electrical energy is dissipated in a stack of braking resistors, whereas in regenerative braking the electrical energy is returned to the supply, thereby making the drive system more efficient. In most transit vehicles or battery-operated electric cars propulsion power is provided by a thyristor converter and regenerative braking is used.

Thyristor dc drives frequently require sophisticated control systems. Both analog and digital feedback controls are used. Phase-locked loop control techniques are employed in some dc drives to provide precise speed control and essentially zero speed regulation. Microcomputer control of complex drive systems can provide great operating flexibility when required.

The techniques of thyristor control of dc drives have developed rapidly in recent years. The technology is now highly advanced.[4-19]

## REFERENCES

1 G. R. Slemon, *Magnetoelectric Devices*, John Wiley & Sons, New York, 1966.

2 A. E. Fitzgerald, C. Kingsley, Jr., and A. Kusko, *Electric Machinery*, McGraw-Hill Book Company, New York, 1971.

3 S. A. Nasar and L. E. Unnewehr, *Electromechanics and Electric Machines*, John Wiley & Sons, New York, 1979.

4 General Electric Co., *General Electric SCR Manual*, Fifth Edition, Electronics Park, Syracuse, NY, 1977.

5 Westinghouse Electric Corp., *Westinghouse SCR Designers Handbook*, Second Edition, Youngwood, PA, 1970.

6 P. C. Sen and S. Mukhopadhyay, "On Solid State DC Motor Control," *IEEE Conference Record*, IGA-71, New York, 1971.

7 C. A. Schwartz, "Trends in Variable Speed in DC Drive Equipment," Reliance Electric Company, Paper D-7092, Cleveland, OH.

8 C. E. Robinson, "Redesign of DC Motors for Applications with Thyristor Power Supplies," *IEEE Transactions on Industry and General Applications*, Vol. IGA-4, No. 5, September 1968.

9 A. Kusko, *Solid State DC Motor Drives*, MIT Press, Cambridge, MA, 1969.

10 S. B. Dewan and A. Straughen, *Power Semiconductor Circuits*, Wiley-Interscience, New York, 1975.

11 B. R. Pelly, *Thyristor Phase-Controlled Converters and Cycloconverters*, Wiely-Interscience, New York, 1971.

12 R. S. Ramshaw, *Power Electronics*, Chapman and Hall, London, 1973.

13 M. Ramamoorty, *Thyristors and Their Applications*, East-West Press Pvt. Ltd., New Delhi, 1977.

14 F. F. Mazda, *Thyristor Control*, John Wiley & Sons, New York, 1973.

15 B. D. Bedford and R. G. Hoft, *Principles of Inverter Circuits*, John Wiley & Sons, New York, 1964.

16 B. Berman, "Battery Powered Regenerative SCR Drive," *IEEE Transactions on Industry Applications*, Vol. IA-8, No. 2, March 1972.

17 P. C. Sen and M. L. MacDonald, "Thyristorized DC Drives with Regenerative Braking and Speed Reversal," *IEEE Transactions on Industrial Electronics and Control Instrumentation*, Vol. IECI-25, No. 4, November 1978.

18 R. H. Osman and R. Krukowski, "A High Performance Tow Tank Drive Using Phase Locked Loop Techniques," *IEEE Conference Record*, ISPCC-77, New York, March 1977.

19 T. Izumi, M. Yamazoe, and T. Nakano, "A Microprocessor-Based Control System of Thyristor Converter Fed DC Motor Drives," *IEEE Conference Record*, IECI-79, New York, March 1979.

# 2

# Single-Phase Drives

In phase-controlled dc drives an ac to dc phase-controlled converter is used to control the dc drive motor. The converter changes the ac input voltage to a controllable dc output voltage. In such converters thyristor commutation (i.e., transfer of current from one thyristor to the next) is easily achieved by a process referred to as *natural* or *line* commutation. When an incoming thyristor is turned on, it immediately reverse-biases the outgoing thyristor and turns it off. No additional circuitry is required for the commutation process. Phase-controlled converters are therefore simple and less expensive and are extensively used in industries. Power conversion efficiency in these converters is generally high, above 95%, because of relatively low losses in thyristors. Phase-controlled dc drives are used in many applications. In small sizes they are used as speed controllers for fractional-horsepower dc motors. In large sizes they are used as replacements for rotating Ward-Leonard systems—in applications such as variable-speed reversing drives for rolling mills, the ratings may be as high as several megawatts.

Phase-controlled converters are broadly classified as single-phase converters and three-phase converters. Some single-phase converters are shown in Table 2.1, and some three-phase converters are shown in Table 3.1 (Chapter 3). The converter used for a particular application depends on such factors as supply available ($1\phi$ or $3\phi$), rating of the drive, amount of voltage ripple to be tolerated, reversible or nonreversible drive, need for regeneration, etc.

Semi-converters are one-quadrant converters, that is, they have one polarity of voltage and current at the dc terminals. Full-converters are two-quadrant converters in which voltage polarity can reverse, but current remains unidirectional because of the unidirectional thyristors. Dual-converters can operate in all four quadrants. When a reversing switch is used at the dc terminals, semi-converters can be operated in two quadrants and full-converters in four quadrants. The use of a reversing switch is satisfactory if the time delay associated with the mechanical changeover of the reversing switch is satisfactory. The dual-converter provides virtually instantaneous reversals of current at the dc terminals.

*Table 2.1* **Single-Phase Thyristor Phase-Controlled Converter Circuits**

| Circuit | Type | Typical hp | Ripple frequency | Quadrant operation |
|---|---|---|---|---|
| 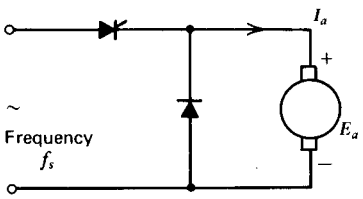 | Half-wave | Below $\frac{1}{2}$ hp | $f_s$ | 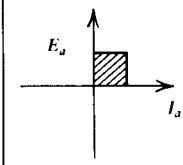 |
| 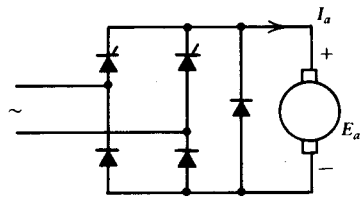 | Semi-converter | Up to 20 hp (100 hp in traction systems) | $2f_s$ | 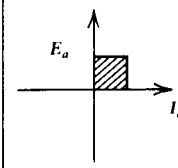 |
| 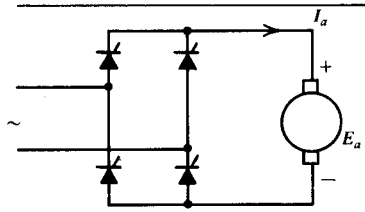 | Full-converter | Up to 20 hp (100 hp in traction systems) | $2f_s$ | 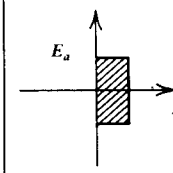 |
| 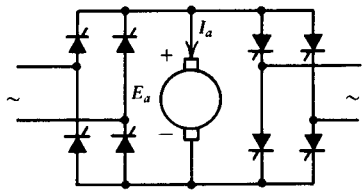 | Dual-converter | Up to 20 hp | $2f_s$ | 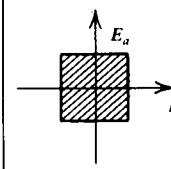 |

Regeneration of power, that is, power flow from the dc motor to the ac supply, is possible with full-converters. Where regeneration is not required, semi-converters are used for the sake of economy.

A diode is sometimes used across the motor terminals. This diode is referred to as a *free-wheeling diode*. It dissipates the stored energy in the motor inductance when the thyristor blocks. It may also provide protection against transients.

In the single-phase half-wave circuit, the motor current is always discontinuous. This causes the performance of the drive to deteriorate. In other single-phase converters, the motor current may or may not be discontinuous. It depends on the operating conditions. In three-phase converters, the motor current is mostly continuous.

In this chapter, the performance characteristics of single-phase drives using separately excited dc motors and series dc motors are studied. Three-phase drives are dealt with in Chapter 3.

## 2.1 PERFORMANCE PARAMETERS

In phase-controlled dc drives the motor current is not constant, nor is the supply current sinusoidal. The nature of these currents depends on the types of converters and motors used and significantly influences the performance of the drive. In order to evaluate the overall performance of a converter-motor combination, certain performance parameters for the dc motor and the input supply have to be considered. Some important ones are defined in the following section.

### 2.1.1 Motor Performance Parameters

The performance of the motor can be assessed in terms of the following parameters.

1 **Torque-Speed Characteristic** This characteristic will show the variation of motor speed with torque and thus will indicate the speed regulations of the drive.

2 **Nature of the Motor Current** The motor current can be continuous or discontinuous. This will influence the speed regulation and dynamic response of the drive.

3 **Average Motor Armature Current $I_a$** This current is defined as follows:

$$I_a = \frac{1}{T}\int_{t_1}^{t_1+T} i_a\,dt \tag{2.1}$$

where $i_a$ = instantaneous motor armature current
$T$ = time period for one cycle of variation of $i_a$.

In a separately excited dc machine, the developed torque is proportional to the average armature current. This current $I_a$ is known as the *torque-producing component* of the motor current.

4 **Rms (Root Mean Square) Motor Armature Current $I_{ar}$** This is defined as follows:

$$I_{ar} = \left(\frac{1}{T}\int_{t_1}^{t_1+T} i_a^2\,dt\right)^{1/2} \tag{2.2}$$

The heat produced in the armature of the motor is proportional to the square of this current. This current $I_{ar}$ is known as the *heat-producing component* of the motor current.

5 **Peak Motor Armature Current $i_{ap}$** The commutating capability of the dc motor depends on the peak value of the armature current. This current $i_{ap}$ is known as the *commutation component* of the motor current.

### 2.1.2 Input Supply Performance Parameters

The ac supply current in a phase-controlled drive is nonsinusoidal. This will affect the performance of the drive as far as supply is concerned. The performance can be assessed in terms of the following parameters:

1 **Input Power Factor *PF***

$$PF = \frac{\text{mean input power}}{\text{rms input volt-amperes}}$$

If the supply voltage is an undistorted sinusoid, only the fundamental component of the input current will contribute to the mean input power. Therefore,

$$PF = \frac{VI_1 \cos\phi_1}{VI} \tag{2.3}$$

where $V$ = rms supply phase voltage
$I$ = rms supply phase current
$I_1$ = rms fundamental component of the supply current
$\phi_1$ = angle between supply voltage and fundamental component of supply current

Input power factor is an important parameter because it decides the volt-ampere requirement of the drive system. For the same power demand, if the power factor is poor more volt-amperes (and hence more current) are drawn from the supply.

2 **Input Displacement Factor *DF*** This may also be called *fundamental power factor* and is defined as

$$DF = \cos\phi_1 \tag{2.4}$$

where $\phi_1$ is known as the *input displacement angle*. For the same power demand, if the displacement factor is low, more fundamental current is drawn from the supply.

3 **Harmonic Factor *HF*** The input current, being nonsinusoidal, contains currents of harmonic frequencies. The harmonic factor is defined as

$$HF = \frac{(I^2 - I_1^2)^{1/2}}{I_1} \tag{2.5}$$

$$= \frac{\left(\sum_{n=2}^{\infty} I_n^2\right)^{1/2}}{I_1} \tag{2.5a}$$

$$= \frac{I_h}{I_1} \tag{2.5b}$$

where $I_n$ = rms value of the $n$th harmonic current
$I_h$ = rms value of the net harmonic current.

The harmonic factor indicates the harmonic content in the input supply current and thus measures the distortion of the input current.

The input supply current $i$ can be expressed in terms of Fourier series as follows:

$$i = I_0 + \sum_{n=1}^{\infty} (a_n \cos n\omega t + b_n \sin n\omega t) \tag{2.6}$$

$$= I_0 + \sum_{n=1}^{\infty} \sqrt{2}\, I_n \sin(n\omega t + \phi_n) \tag{2.6a}$$

The dc component $I_0$ and the Fourier coefficients $a_n, b_n$ are obtained as follows:

$$I_0 = \frac{1}{T}\int_0^T i\, dt \tag{2.7}$$

$$a_n = \frac{2}{T}\int_0^T i \cos n\omega t\, dt \tag{2.8}$$

$$b_n = \frac{2}{T}\int_0^T i \sin n\omega t\, dt \tag{2.9}$$

$$I_n = \left(\frac{a_n^2 + b_n^2}{2}\right)^{1/2} \tag{2.10}$$

$$\phi_n = \tan^{-1}\left(\frac{a_n}{b_n}\right) \tag{2.11}$$

Phase-controlled dc drives are discussed in the following sections in terms of the above performance parameters. Single-phase half-wave converters are used only in fractional horsepower applications, and the effect of such drives on the supply is insignificant. Single-phase full-wave drives are used in low- and medium-horsepower applications and are discussed in detail. The analytical techniques can be easily applied to three-phase drives if desired. Three-phase drives provide better performance because armature current is mostly continuous.

## 2.2 SINGLE-PHASE SEPARATELY EXCITED DC MOTOR DRIVES

The basic circuit for a single-phase separately excited dc motor drive is shown in Fig. 2.1. The armature voltage is controlled by a semi-converter or full-converter and the field circuit is fed from the ac supply through a diode bridge. The motor current cannot reverse due to the thyristors in the converters. If semi-converters are used, the average dc output voltage ($E_a$) is always positive. Therefore power flow ($E_a I_a$) is always positive, that is, from the ac supply to the dc load. In drive systems using semi-converters, regeneration or reverse power flow from motor to ac supply is not possible. In semi-converters free-wheeling action (i.e., dissipation of armature inductance energy through the free-wheeling path) takes place when the thyristor blocks.

Single-phase full-wave drives are used for low- and medium-horsepower applications as indicated in Table 2.1. Such drives have poor speed regulation on open-loop firing angle control. However, with armature voltage or tachometer feedback, good regulation can be achieved.

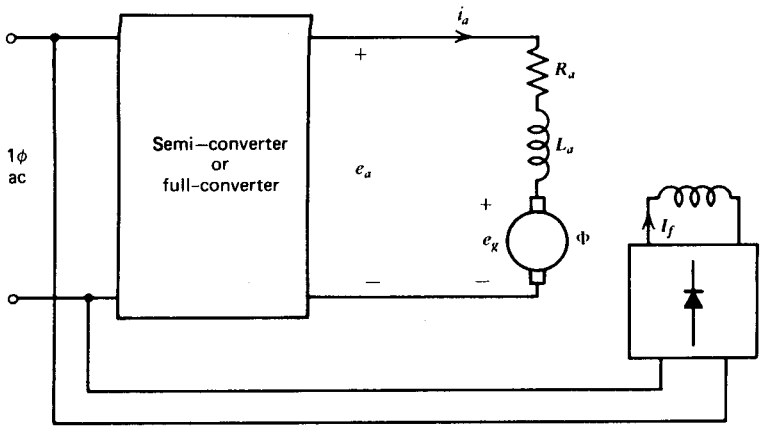


*Fig. 2.1* Basic single-phase circuit for the speed control of a separately excited dc motor.

***Basic Equations***[1]

The armature circuit of the dc motor is represented by its back voltage $e_g$, armature resistance $R_a$, and armature inductance $L_a$ as shown in Fig. 2.1.

Back voltage:

$$e_g = K_a \Phi n \tag{2.12}$$

Average back voltage:

$$E_g = K_a \Phi N \tag{2.13}$$

Developed torque:

$$t = K_a \Phi i_a \tag{2.14}$$

Average developed torque:

$$T = K_a \Phi I_a \tag{2.15}$$

The armature circuit voltage equation is

$$e_a = R_a i_a + L_a \frac{di_a}{dt} + e_g \tag{2.16}$$

In terms of average values,

$$E_a = R_a I_a + E_g \tag{2.17}$$

Note that the inductance $L_a$ does not absorb any average voltage.

From equations 2.13 and 2.17, the average speed is

$$N = \frac{E_a - R_a I_a}{K_a \Phi} \tag{2.18}$$

Although the time variation of voltages, currents, torque, and speed can take various forms, the basic dc motor equations (2.13, 2.15, 2.17, and 2.18) still hold good for the phase-controlled drive in terms of average quantities.

In single-phase converters, the armature voltage $e_a$ and current $i_a$ change with time. This is unlike the M-G set drive in which both $e_a$ and $i_a$ are essentially constant. In phase-controlled converters, the armature current $i_a$ may not even be continuous. In fact, for most operating conditions, $i_a$ is discontinuous. This makes prediction of performance difficult. Analysis is simplified if continuity of armature current can be assumed. Analysis for both continuous and discontinuous current is presented in the following sections.

### 2.2.1 Continuous Armature Current

Let us assume that the armature current is continuous over the whole range of operation. Typical voltage and current waveforms are shown in Figs. 2.2 and 2.3 for semi-converter and full-converter systems, respectively. The thyristors are symmetrically triggered. In the semi-converter system shown in Fig. 2.2, thyristor $S_1$ is triggered at an angle $\alpha$ and $S_2$ at an angle $\alpha + \pi$ with respect to the supply voltage $v$. In the full-converter system shown in Fig. 2.3, thyristors $S_1$ and $S_3$ are simultaneously triggered at $\alpha$, and thyristors $S_2$ and $S_4$ are triggered at $\pi + \alpha$.

In Fig. 2.2, the motor is connected to the input supply for the period $\alpha < \omega t < \pi$ through $S_1$ and $D_2$, and the motor terminal voltage $e_a$ is the same as the supply input voltage $v$. Beyond $\pi$, $e_a$ tends to reverse as the input voltage changes polarity. This will forward-bias the free-wheeling diode and $D_{FW}$ will start conducting. The motor current $i_a$, which was flowing from the supply through $S_1$, is transferred to $D_{FW}$ (i.e., $S_1$ commutates). The motor terminals are shorted through the free-wheeling diode during $\pi < \omega t < (\pi + \alpha)$, making $e_a$ zero. Energy from the supply is therefore delivered to the armature circuit when the thyristor conducts ($\alpha$ to $\pi$). This energy is partially stored in the inductance, partially stored in the kinetic energy (K.E.) of the moving system, and partially used to supply the mechanical load. During the free-wheeling period, $\pi$ to $\pi + \alpha$, energy is recovered from the inductance and is converted to mechanical form to supplement the K.E. in supplying the mechanical load. The free-wheeling armature current continues to produce electromagnetic torque in the motor. No energy is fed back to the supply during this period.

In Fig. 2.3, the motor is always connected to the input supply through the thyristors. Thyristors $S_1$ and $S_3$ conduct during the interval $\alpha < \omega t < (\pi + \alpha)$ and connect the motor to the supply. At $\pi + \alpha$, thyristors $S_2$ and $S_4$ are triggered. Immediately the supply voltage appears across the thyristors $S_1$ and $S_3$ as a reverse-bias voltage and turns them off. This is called *natural* or *line* commutation. The motor current $i_a$, which was flowing from the supply through $S_1$ and $S_3$, is transferred to $S_2$ and $S_4$. During $\alpha$ to $\pi$, energy flows from the input supply to the motor (both $v$ and $i$ are positive, and $e_a$ and $i_a$ are positive, signifying positive power flow). However, during $\pi$ to $\pi + \alpha$, some of the motor system energy is fed back to the input supply ($v$ and $i$ have opposite polarities and likewise $e_a$ and $i_a$, signifying reverse power flow).

In Fig. 2.3*c* voltage and current waveforms are shown for a firing angle greater than 90°. The average motor terminal voltage $E_a$ is negative. If the motor back emf $E_g$ is reversed, it will behave as a dc generator and will feed power back to the ac supply. This is known as the *inversion operation* of the converter, and this mode of operation is used in the regenerative braking of the motor.

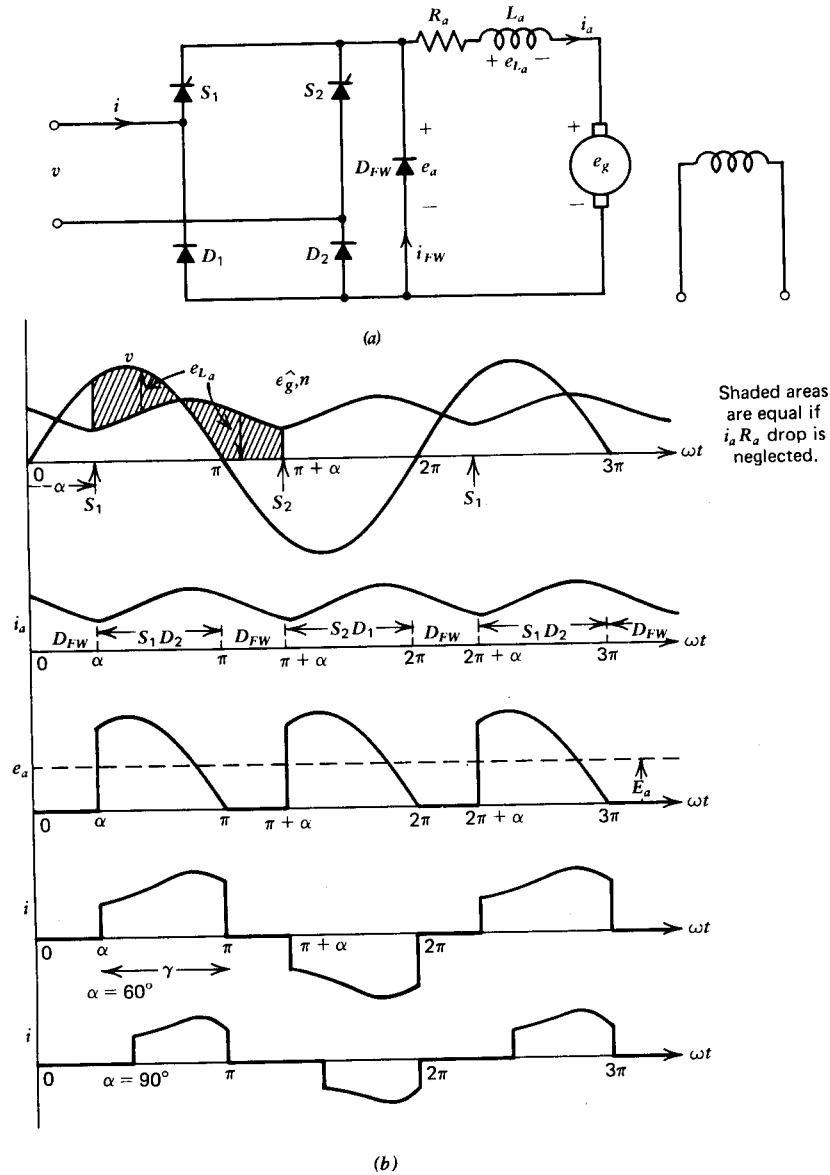


*Fig.* 2.2 Speed control of a separately excited dc motor by a single-phase semi-converter. (*a*) Power circuit. (*b*) Voltage and current waveforms for continuous motor current.

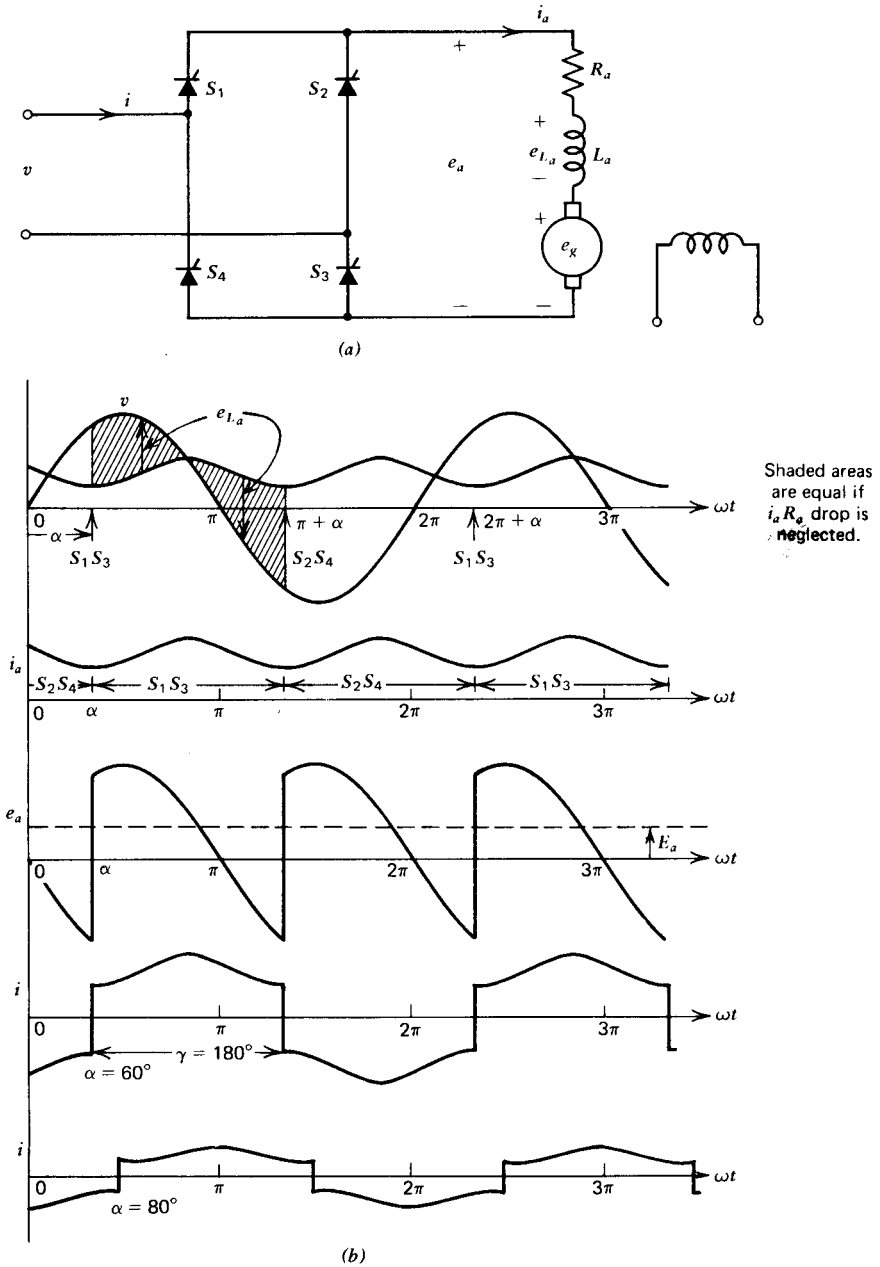


*Fig. 2.3* Speed control of a separately excited dc motor by a single-phase full-converter. (*a*) Power circuit. (*b*) Voltage and current waveforms for continuous motor current (motor operation). (*c*) Waveforms for inversion operation.

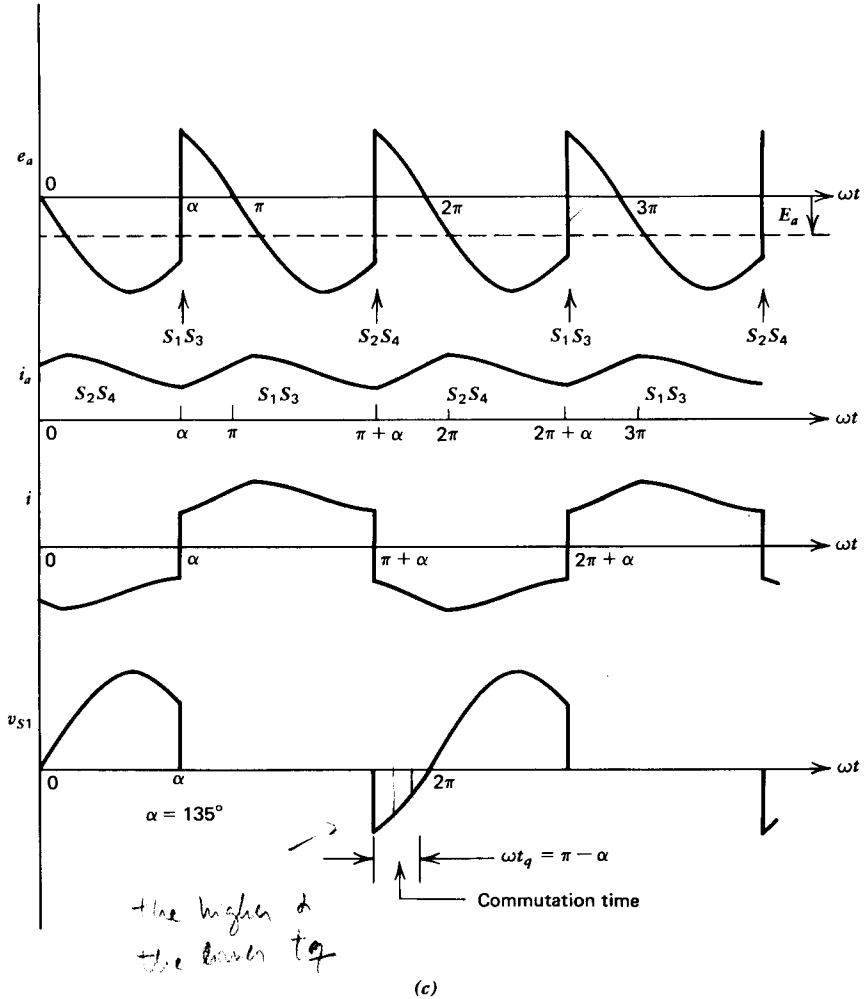


(c)

*Fig. 2.3 (Continued)*

### *Torque Speed Characteristics*

For a semi-converter with free-wheeling action the armature circuit equations are:

$$e_a = v = R_a i_a + L_a \frac{di_a}{dt} + e_g \qquad \alpha < \omega t < \pi \tag{2.19}$$

$$e_a = 0 = R_a i_a + L_a \frac{di_a}{dt} + e_g \qquad \pi < \omega t < \pi + \alpha \tag{2.20}$$

The armature circuit equation for a full-converter is:

$$e_a = v = R_a i_a + L_a \frac{di_a}{dt} + e_g \qquad \alpha < \omega t < \pi + \alpha \tag{2.21}$$

Let $v = \sqrt{2}\, V \sin\theta$. The average motor terminal voltages are:

With a semi-converter:

$$E_a = \frac{1}{\pi}\int_{\alpha}^{\pi} \sqrt{2}\, V \sin\theta\, d\theta = \frac{\sqrt{2}\, V}{\pi}(1 + \cos\alpha) \tag{2.22}$$

With a full-converter:

$$E_a = \frac{1}{\pi}\int_{\alpha}^{\pi+\alpha} \sqrt{2}\, V \sin\theta\, d\theta = \frac{2\sqrt{2}\, V}{\pi}\cos\alpha \tag{2.23}$$

The variation of motor terminal voltage $E_a$ as a function of the firing angle $\alpha$ is shown in Fig. 2.4*a* for both semi-converter and full-converter systems. The inverter operation of the full-converter occurs in the range $90° < \alpha < 180°$ for continuous motor armature current.

From equations 2.15, 2.18, 2.22, and 2.23, the average speed is given as follows:

With a semi-converter:

$$N = \frac{(\sqrt{2}\, V/\pi)(1 + \cos\alpha)}{K_a \Phi} - \frac{R_a}{(K_a \Phi)^2} T \tag{2.24}$$

With a full-converter:

$$N = \frac{2\sqrt{2}\, V \cos\alpha}{\pi K_a \Phi} - \frac{R_a}{(K_a \Phi)^2} T \tag{2.25}$$

The first term in equations 2.24 and 2.25 represents the theoretical no-load speed. The second term represents the speed drop produced by armature current $I_a$ and hence torque $T$. The theoretical no-load speed is varied by the firing angle $\alpha$. The torque-speed characteristics based on equations 2.24 and 2.25 are shown in Fig. 2.4*b*. These characteristics show that good speed regulation is obtained with continuous armature current.

**Example 2.1**

The speed of a 10 hp, 230 V, 1200 rpm separately excited dc motor is controlled by a single-phase full-converter as shown in Fig. 2.3*a*. The rated motor armature current is 38 A, and the armature resistance is $R_a = 0.3\ \Omega$.

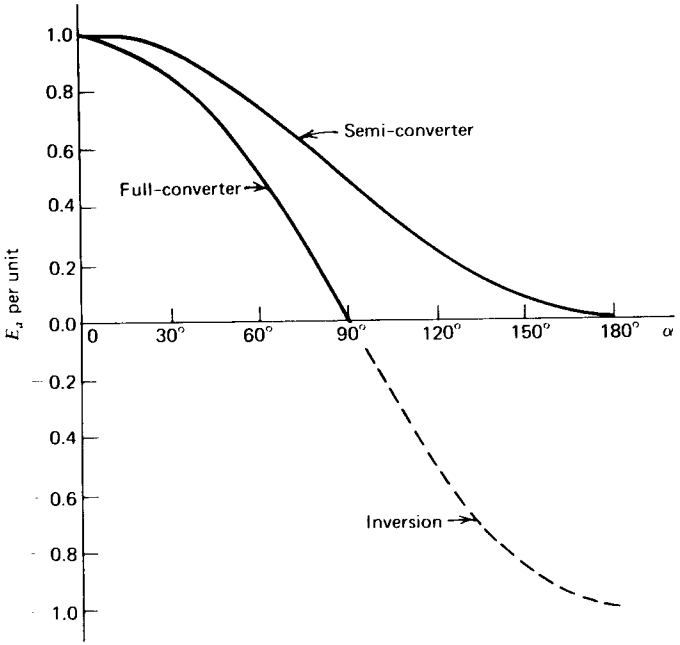


(a)

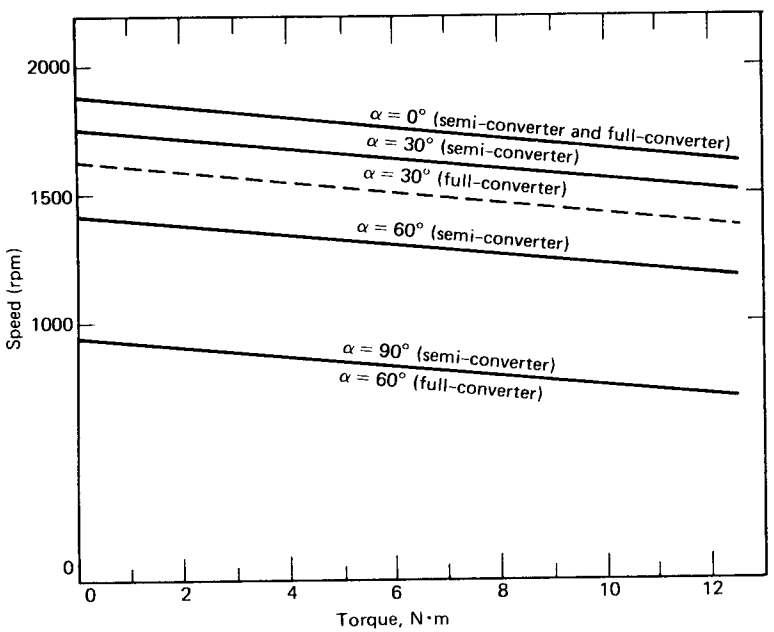


(b)

***Fig. 2.4*** Converter and motor characteristics for continuous motor current. (*a*) Converter output voltage as a function of firing angle. (*b*) Torque speed relation at different firing angles from equations 2.24 and 2.25. $R_a = 0.6\Omega$, $K_a\Phi = 0.55$ N·m/A, and V = 120 V.

The ac supply voltage is 260 V. The motor voltage constant is $K_a\Phi = 0.182$ V/rpm. Assume that sufficient inductance is present in the armature circuit to make the motor current continuous and ripple-free.

1 **Rectifier Operation (Motoring Action)** For a firing angle $\alpha = 30°$ and rated motor current, calculate:
   - **a** The motor torque.
   - **b** The speed of the motor.
   - **c** The supply power factor.

2 **Inverter Operation (Regenerating Action)** The polarity of the motor back emf $E_g$ is reversed, say by reversing the field excitation. Calculate:
   - **a** The firing angle to keep the motor current at its rated value.
   - **b** The power fed back to the supply.

*Solution*

1 **a** $K_a\Phi = 0.182$ V/rpm

$$= \frac{0.182 \times 60}{2\pi} \text{ V}\cdot\text{sec/rad}$$

$$= 1.74 \text{ V}\cdot\text{sec/rad}$$

From equation 2.15:

$$T = 1.74 \times 38$$

$$= 66.12 \text{ N}\cdot\text{m}$$

**b** From equation 2.23:

$$E_a = \frac{2\sqrt{2} \times 260}{\pi} \cos\alpha$$

$$= 234.2 \cos\alpha$$

$$= 234.2 \cos 30°$$

$$= 202.82 \text{ V}$$

From equation 2.17:

$$E_g = 202.82 - (38 \times 0.3)$$

$$= 191.42 \text{ V}$$

From equation 2.13:

$$N = \frac{191.42}{0.182}$$

$$= 1051.8 \text{ rpm}$$

or, from equation 2.25:

$$N = \frac{2\sqrt{2} \times 260 \cos 30°}{\pi \times 1.74} - \frac{0.3}{1.74^2} \times 66.12$$

$$= 116.56 - 6.55 \text{ rad/sec}$$

$$= 110.01 \text{ rad/sec}$$

$$= \frac{110.01}{2\pi} \times 60 \text{ rpm}$$

$$= 1051 \text{ rpm}$$

c If the motor current is constant and ripple-free, the supply current is a square wave (Fig. 2.3) of amplitude 38 A. The rms supply current is:

$$I = 38 \text{ A}$$

Supply volt-ampere is

$$U = VI$$

$$= 260 \times 38$$

$$= 9880 \text{ VA}$$

If losses in the converter are neglected the power from the supply is

$$P_s = E_a I_a$$

$$= 202.82 \times 38$$

$$= 7707.2 \text{ W}$$

Therefore, the supply power factor is

$$PF = \frac{P_s}{U}$$

$$= \frac{7707.2}{9880}$$

$$= 0.78$$

**2 a** At the time of polarity reversal, the back emf is:

$$E_g = 191.42 \text{ V}$$

From equation 2.17:

$$E_a = E_g + I_a R_a$$

$$= -191.42 + (38 \times 0.3)$$

$$= -180.02 \text{ V}$$

Now, $E_a' = \dfrac{2\sqrt{2} \times 260}{\pi} \cos\alpha = -180.02$

or $\alpha = 140.2°$

**b** Power from the dc machine is

$$P_g = 191.42 \times 38 = 7273.96 \text{ W}$$

Power lost to the armature resistance is

$$P_R = 38^2 \times 0.3 = 433.2 \text{ W}$$

Power fed back to the ac supply is

$$P_s = 7273.96 - 433.2 = 6840.76 \text{ W}$$

or $$P_s = E_a I_a = 180.02 \times 38 = 6840.76 \text{ W}$$

Note that if there is no mechanical input to the dc machine, its speed (as well as back emf) will decrease as it feeds power back to the ac supply because kinetic energy is converted to electrical energy. If armature current is to be maintained constant at its rated value during deceleration, the firing angle has to be adjusted continuously. This adjustment can be made with a closed-loop current feedback control system (discussed in Chapter 6).

### 2.2.2. Discontinuous Armature Current

The torque-speed characteristics shown in Fig. 2.4*b* are drawn on the crude assumption that the armature current is continuous over the whole range of operation. It is very doubtful that the armature current will be continuous at high values of the firing angle $\alpha$, high speed, and low values of torque. In fact, armature current is discontinuous for these operating conditions. If the armature current is discontinuous, the no-load speeds will be higher than those shown in Fig. 2.4*b*, and the speed regulation will be significantly poor in the region of discontinuous armature current. The motor performance

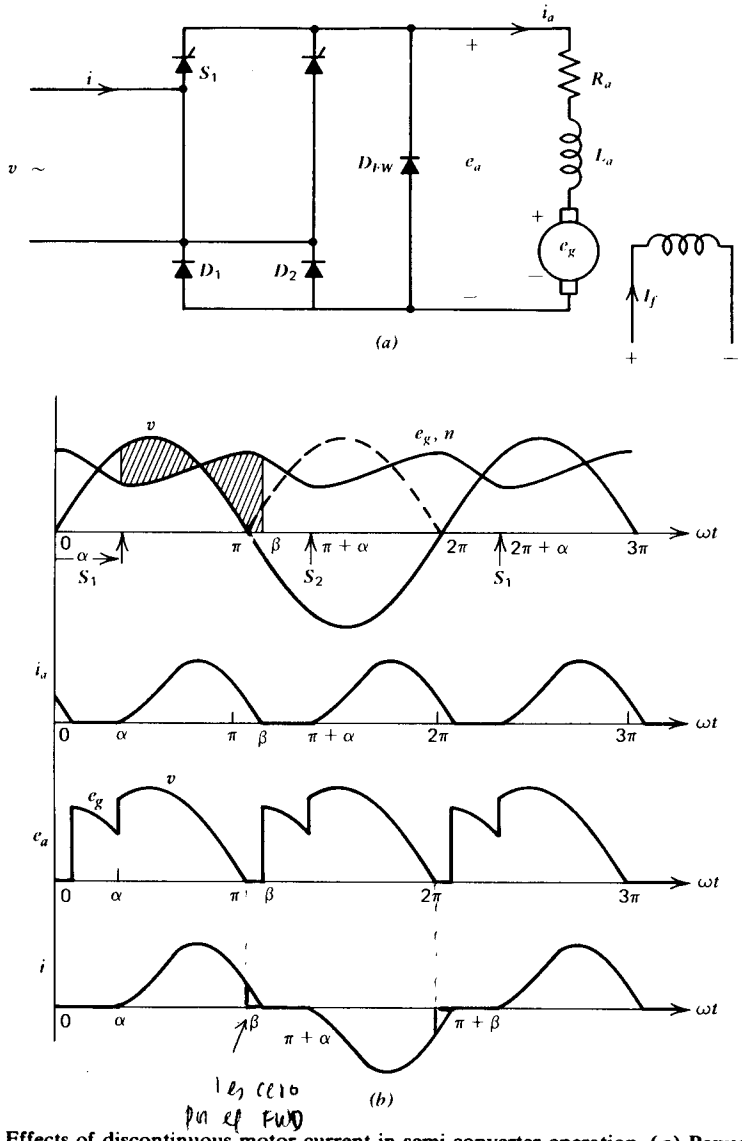


*Fig. 2.5* Effects of discontinuous motor current in semi-converter operation. (*a*) Power circuit. (*b*) Voltage and current waveforms.

deteriorates if the armature current is discontinuous. The ratio of peak to average and rms to average armature current increases. In addition, the dynamic response becomes slow.[2] It is therefore desirable to operate the dc motor in the continuous armature current mode. This is promoted by having free-wheeling action and using an external armature circuit choke to increase the time constant of the armature circuit.

The waveforms with semi-converter and full-converter with discontinuous armature current are shown in Fig. 2.5 and Fig. 2.6, respectively.

In Fig. 2.5, the motor is connected to the input supply for the period $\alpha < \omega t < \pi$ through $S_1$ and $D_2$. Beyond $\pi$, the motor terminal is shorted through the free-wheeling diode $D_{FW}$. The armature current decays to zero at $\beta$ before the thyristor $S_2$ is triggered at $\pi + \alpha$, thereby making the armature current discontinuous. During $\alpha$ to $\pi$ (i.e., the conduction period of the thyristor $S_1$), motor terminal voltage $e_a$ is the same as the supply voltage $v$. However, during $\pi$ to $\beta$, the motor current free-wheels through $D_{FW}$ and so $e_a$ is zero. In the interval $\beta < \omega t < \pi + \alpha$, the motor coasts and the motor terminal voltage $e_a$ is the same as the back voltage $e_g$.

In Fig. 2.6, the motor is connected to the supply during $\alpha < \omega t < \beta$ and it coasts during $\beta < \omega t < \pi + \alpha$. As long as the motor is connected to the supply, its terminal voltage is the same as the input supply voltage.

If the armature current can be assumed to be continuous, the torque-speed characteristics can be calculated merely from average values of the motor terminal voltage and current. In the discontinuous current mode, these calculations are cumbersome. The difficulty arises in the calculation of the average motor terminal voltage $E_a$, because $\beta$ (called the *extinction angle*, the instant at which the thyristor or motor current becomes zero) depends on the average speed $N$, average armature current $I_a$, and the firing angle $\alpha$. A general approach, valid for both continuous and discontinuous armature current, is therefore necessary.

### 2.2.3 General Analysis

There are three possible modes of operation: Thyristors conduct, free-wheeling action takes place through the free-wheeling diode, and motor coasts. The governing equations for the different modes of operation are as follows:

***Mode 1*** Thyristors conduct and motor is connected to the supply.

The duration of this mode of operation is as follows: With semi-converter $\alpha < \omega t < \pi$ ($\alpha < \omega t < \beta$ if $\beta < \pi$). With full-converter $\alpha < \omega t < \beta$. The voltage equation is

$$e_a = \sqrt{2}\,V \sin \omega t = L_a \frac{di_a}{dt} + R_a i_a + K_a \Phi n \tag{2.26}$$

The electrodynamic equation is

$$t = K_a \Phi i_a = J \frac{dn}{dt} + Bn + T_L \tag{2.27}$$

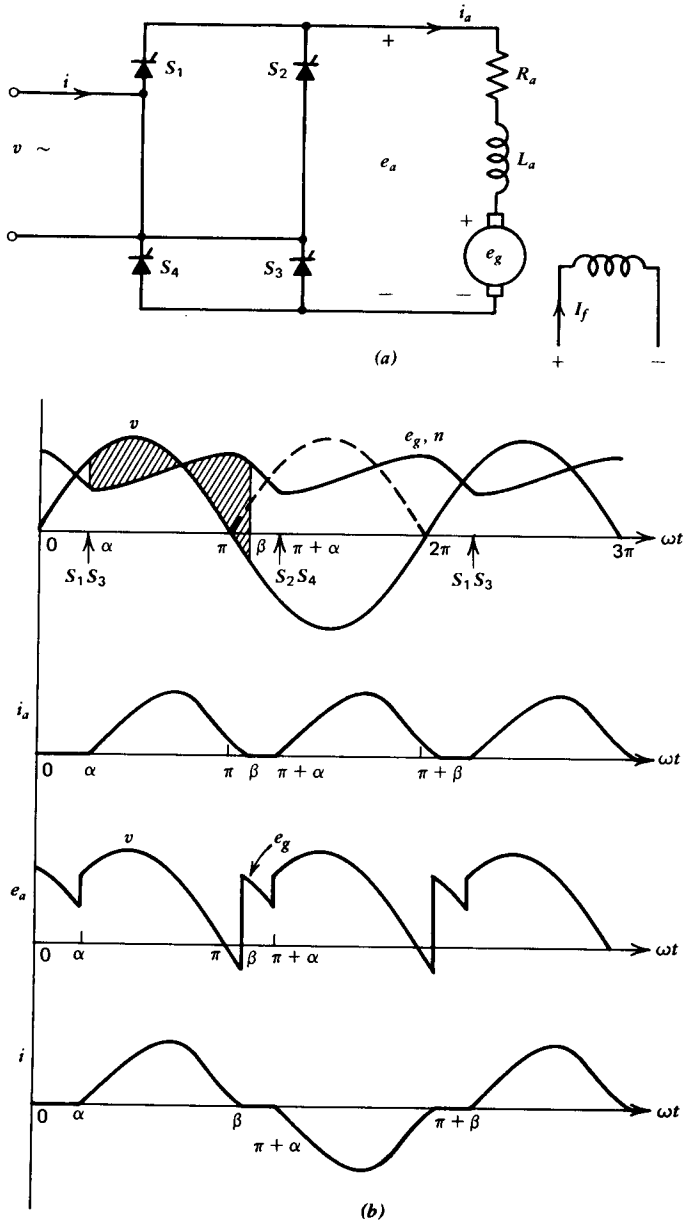


*Fig.* 2.6 Effects of discontinuous motor current in full-converter operation. (*a*) Power circuit. (*b*) Voltage and current waveforms.

***Mode 2*** Free-wheeling action is present only with the semi-converter, during the interval $\pi < \omega t < \beta$.

$$0 = R_a i_a + L_a \frac{di_a}{dt} + K_a \Phi n \tag{2.28}$$

$$K_a \Phi i_a = J \frac{dn}{dt} + Bn + T_L \tag{2.29}$$

If $\beta < \pi$, mode 2 will be absent.

***Mode 3*** Motor coasts during the interval $\beta < \omega t < \pi + \alpha$.

$$i_a = 0 \tag{2.30}$$

$$0 = J \frac{dn}{dt} + Bn + T_L \tag{2.31}$$

Two methods, numerical and analytical, can be used to solve these equations in order to determine the preformance of the phase-controlled dc drives.

***Numerical Method***

In the numerical method, the motor is considered to be at rest initially. Speed and current are then computed during each cycle until a steady state is reached by solving the appropriate equations digitally using the Runge-Kutta fourth-order approximation method.[3] The equations to be solved in different modes of operation are as follows:

***Mode 1*** From equations 2.26 and 2.27:

$$\frac{di_a}{dt} = \frac{\sqrt{2} V \sin \omega t}{L_a} - \frac{R_a}{L_a} i_a - \frac{K_a \Phi}{L_a} n = \psi(i_a, n) \tag{2.32}$$

$$\frac{dn}{dt} = \frac{K_a \Phi}{J} i_a - \frac{B}{J} n - \frac{T_L}{J} = \psi_2(i_a, n) \tag{2.33}$$

***Mode 2*** From equations 2.28 and 2.29:

$$\frac{di_a}{dt} = -\frac{R_a}{L_a} i_a - \frac{K_a \Phi}{L_a} n \tag{2.34}$$

$$\frac{dn}{dt} = \frac{K_a \Phi}{J} i_a - \frac{B}{J} n - \frac{T_L}{J} \tag{2.35}$$

*Mode 3*

$$i_a = 0 \tag{2.36}$$

$$\frac{dn}{dt} = -\frac{B}{J}n - \frac{T_L}{J} \tag{2.37}$$

Both steady-state and dynamic performance can be studied by this method. For dynamic response, this is essential. For steady-state characteristics, since the computation is to be carried from standstill to steady-state speed, this method requires computation over many cycles before the steady-state condition is reached. This method is thus costly in terms of computer time. This is discussed further in Chapter 6 where dynamic response is studied.

### *Analytical Method*

In the analytical method, a steady-state speed is assumed, and therefore only the electrical equations 2.26, 2.28, and 2.30 have to be considered. This makes it possible to obtain analytical expressions for the motor current, such as equations 2.40, 2.43, and 2.44. These equations are used to compute the motor current, and the steady-state condition is noted by observing the variation of the motor current at a particular instant (or the motor average current over a cycle) over successive cycles. By this method, the steady state is reached after only a few cycles of computation. The performance parameters are determined after the steady state is reached.

If the current is discontinuous and if at the instant of firing the thyristor the supply voltage is less than the motor back emf (i.e., $v(\alpha) < e_g$), then the thyristor will not turn on at $\alpha$. It will start conducting when the input voltage $v$ equals back voltage $e_g$. For the sake of generality, let $\theta_s$ be the angle at which a thyristor turns on.

***Mode 1*** Thyristor conducts,

$\theta_s < \omega t < \beta$ with full-converter

$\theta_s < \omega t < \pi$ with semi-converter

$(\theta_s < \omega t < \beta$ if $\beta < \pi)$.

The voltage equation is

$$\sqrt{2}\,V \sin \omega t = L_a \frac{di_a}{dt} + R_a i_a + E_g \tag{2.38}$$

The solution for $i_a$ is

$$i_a = \frac{\sqrt{2}\,V}{Z}\sin(\omega t - \theta_z) - \frac{E_g}{R_a} + A_1 \varepsilon^{-(R_a/L_a)t} \tag{2.39}$$

where $A_1$ is a constant, and

$$Z = [R_a^2 + (\omega L_a)^2]^{1/2}$$
$$\theta_z = \tan^{-1}\frac{\omega L_a}{R_a}$$

The first term is the component of armature current due to the input supply voltage. The second term is due to the back voltage, which tends to send a current opposite to the assigned direction of $i_a$. The third term is the transient component of current.

Let the current $i_a$ at $\omega t = \theta_s$ be $I_{as}$. From equation 2.39,

$$I_{as} = \frac{\sqrt{2}\,V}{Z}\sin(\theta_s - \theta_z) - \frac{E_g}{R_a} + A_1 \varepsilon^{-(R_a/\omega L_a)\theta_s} \tag{2.39a}$$

Then,

$$A_1 = \left[ I_{as} - \frac{\sqrt{2}\,V}{Z}\sin(\theta_s - \theta_z) + \frac{E_g}{R_a} \right] \varepsilon^{(R_a/\omega L_a)\theta_s} \tag{2.39b}$$

From equations 2.39 and 2.39b,

$$i_a = \frac{\sqrt{2}\,V}{Z}\left[\sin(\omega t - \theta_z) - \sin(\theta_s - \theta_z)\varepsilon^{(R_a/\omega L_a)(\theta_s - \omega t)}\right]$$
$$+ \frac{E_g}{R_a}(\varepsilon^{(R_a/\omega L_a)(\theta_s - \omega t)} - 1) + I_{as}\,\varepsilon^{(R_a/\omega L_a)(\theta_s - \omega t)} \tag{2.40}$$

***Mode 2*** Free-wheeling action present with a semi-converter, during the interval $\pi < \omega t < \beta$.

The voltage equation is

$$0 = L_a \frac{di_a}{dt} + R_a i_a + E_g \tag{2.41}$$

The solution for $i_a$ is

$$i_a = A_2 \varepsilon^{-(R_a/\omega L_a)\omega t} - \frac{E_g}{R_a} \tag{2.42}$$

where $A_2$ is a constant. The value of $i_a$ at $\omega t = \pi$ can be computed from equation 2.40.

Let $i_a(\pi) = I_{a\pi}$. Therefore, from equation 2.42,

$$I_{a\pi} = A_2\, \varepsilon^{-(R_a/\omega L_a)\pi} - \frac{E_g}{R_a} \tag{2.42a}$$

or

$$A_2 = \left( I_{a\pi} + \frac{E_g}{R_a} \right) \varepsilon^{(R_a/\omega L_a)\pi} \tag{2.42b}$$

From equations 2.42 and 2.42b,

$$i_a = I_{a\pi}\, \varepsilon^{(R_a/\omega L_a)(\pi - \omega t)} + \frac{E_g}{R_a} \left( \varepsilon^{(R_a/\omega L_a)(\pi - \omega t)} - 1 \right) \tag{2.43}$$

Mode 2 will be absent if $\beta < \pi$. Mode 2 is absent with a full-converter.

***Mode 3*** Motor coasts during the interval $\beta < \omega t < \pi + \alpha$ .

$$i_a = 0 \tag{2.44}$$

***Supply Current***

***Mode 1***

$$i = i_a \qquad \theta_s < \omega t < \pi \text{ with semi-converter}$$
$$\theta_s < \omega t < \beta \text{ with full-converter} \tag{2.45}$$

$$i = -i_a \qquad \pi + \theta_s < \omega t < 2\pi \text{ with semi-converter}$$
$$\pi + \theta_s < \omega t < \pi + \beta \text{ with full-converter} \tag{2.46}$$

***Modes 2 and 3***

$$i = 0 \tag{2.47}$$

### 2.2.4 Performance Evaluation

The quality of a particular phase-controlled drive is assessed in terms of the performance parameters defined in Section 2.1. These performance parameters can be obtained by either a numerical method or an analytical method. Computation over a large number of cycles is required in the numerical method before the steady state is reached. In most motors, the mechanical time constant is large, and the time variation of speed in the steady state is insignificant. This justifies the assumption of a constant steady-state speed in the analytical method. The back voltage $E_g$ of the motor is constant if the

speed is assumed constant. With an assumed steady-state speed, armature current reaches the steady-state value within a few cycles. If the current is discontinuous, the steady state is reached in one-half cycle. If the current is continuous, computation over a few cycles may be necessary before the steady state is reached. This is illustrated in the following discussion.

**$0 < \alpha < \pi/2$**

The theoretical maximum value of $E_g$ is $\sqrt{2}\,V$. The assumed speed can be such that $E_g > \sqrt{2}\,V \sin\alpha$ or $E_g < \sqrt{2}\,V \sin\alpha$, where $\alpha$ is the triggering angle.

1 If $E_g > \sqrt{2}\,V \sin\alpha$ as shown in Fig. 2.7*a*, the thyristor will not turn on at $\alpha$. It will turn on at $\theta_s$ where

$$\theta_s = \sin^{-1}\frac{E_g}{\sqrt{2}\,V} \tag{2.48}$$

Using this value of $\theta_s$, the computation is performed and if $i_a(\pi + \alpha) \leqslant 0$, the current is discontinuous and further computation is not necessary, because the next half-cycle will start with the same initial conditions when the next thyristor is triggered at $\pi + \alpha$. The steady state is therefore reached in half a cycle.

If $i_a(\pi + \alpha) > 0$ as shown in Fig. 2.7*b*, then the next thyristor will turn on when it is triggered at $\pi + \alpha$, although at this instant the back voltage $E_g$ is higher than the supply voltage. Note that since the outgoing thyristor was conducting at this instant, the incoming thyristor is forward-biased at $\pi + \alpha$ and so it turns on when a triggering pulse is applied. The current $i_a(\pi + \alpha)$ computed from the previous half-cycle becomes the initial current for the second half-cycle. If $i_a(\pi + \theta_s) \leqslant 0$ [which may happen because the supply voltage $v$ is less than the back voltage $E_g$ during the period $(\pi + \alpha) < \omega t < (\pi + \theta_s)$], initial conditions at $\theta_s$ and $\pi + \theta_s$ are identical and the armature current during the second and following half-cycles will be the same. That is, the steady state is reached and the armature current is discontinuous as shown in Fig. 2.7*b*.

If, however, $i_a(\pi + \theta_s) > 0$ as shown in Fig. 2.7*c*, the armature current is likely to be continuous during the subsequent half-cycles. The steady-state condition will be reached after a few half-cycles.

2 If $E_g < \sqrt{2}\,\sin\alpha$, as shown in Fig. 2.7*d*, the thyristor will turn on at $\alpha$ and therefore $\alpha = \theta_s$. Computation for such firing angles and speed will be less complicated.

**$\pi/2 < \alpha < \pi$**

The theoretical maximum value of $E_g$ will be

$$E_{g_{max}} = \sqrt{2}\,V \sin\alpha \tag{2.49}$$

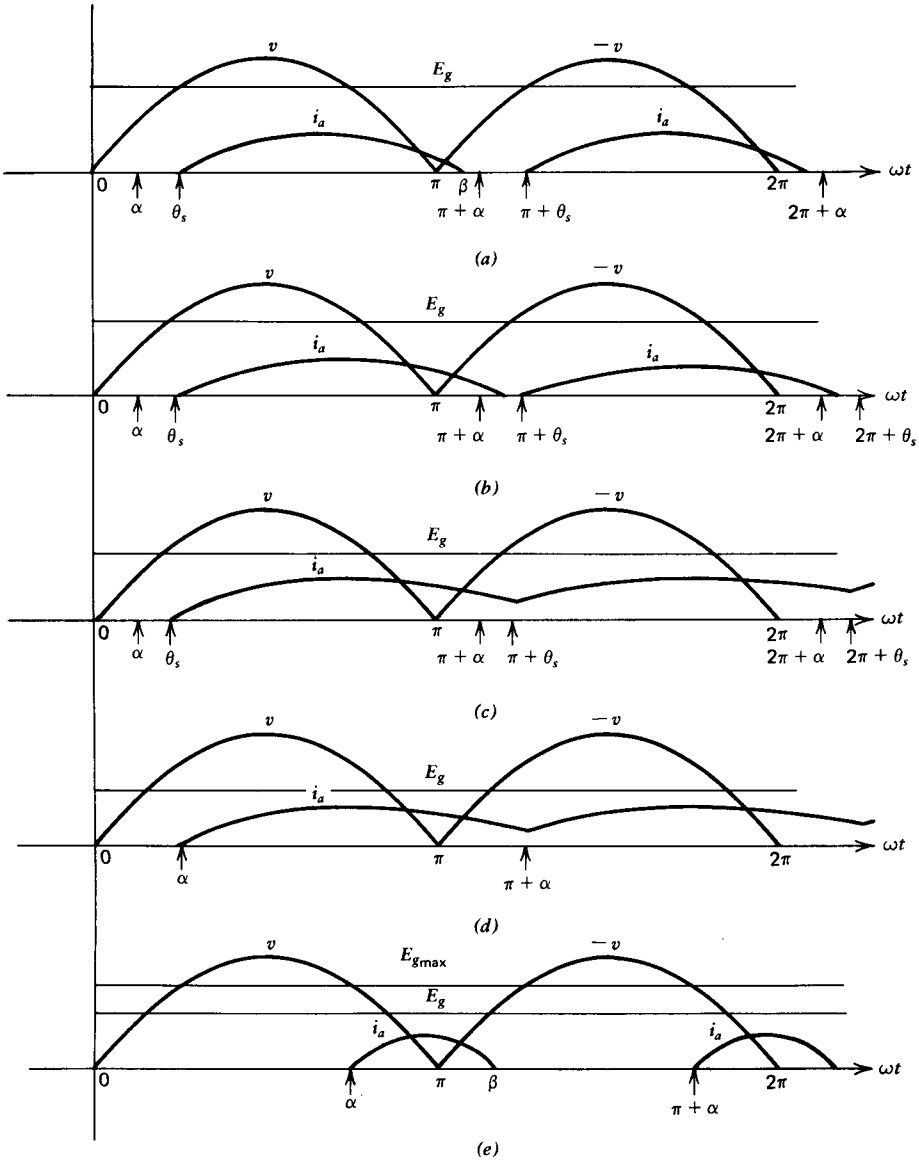


***Fig. 2.7*** **Motor current waveforms for various triggering angles and motor back voltages.**

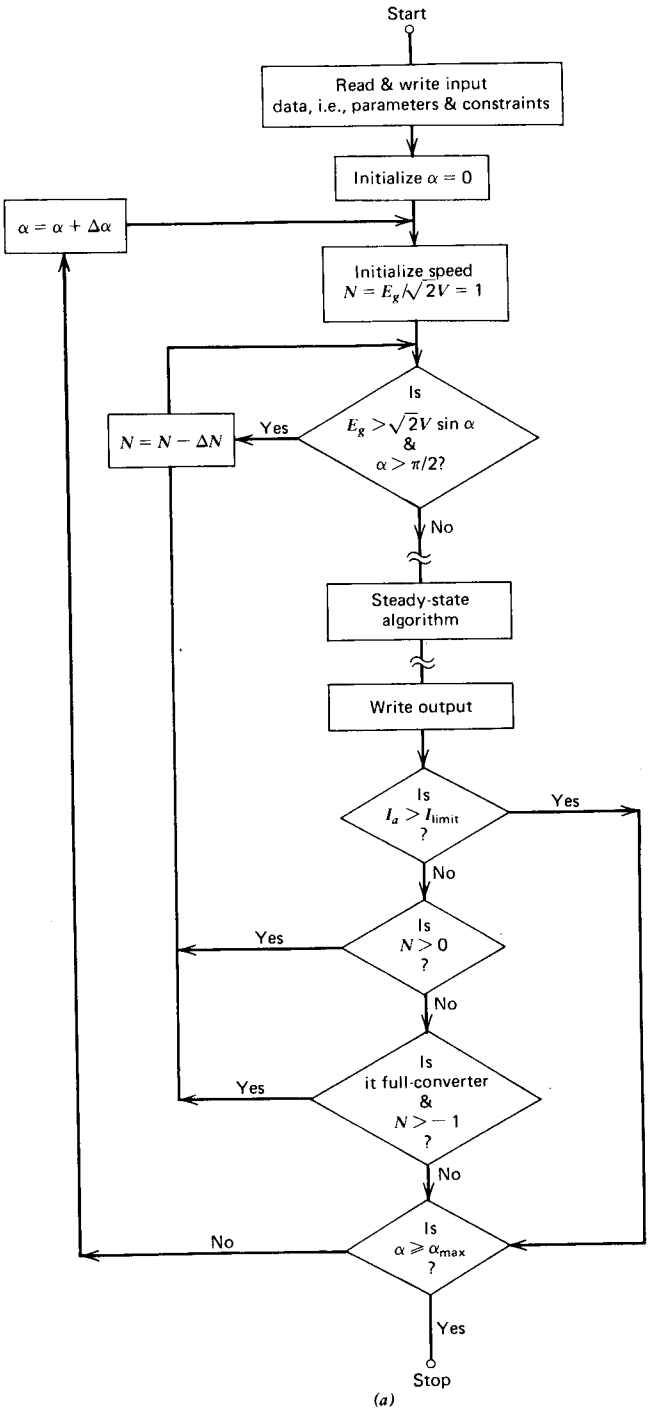


*Fig. 2.8* Flowchart for computer analysis of converter-motor system. (*a*) Steady-state operation of separately excited dc motor. (*b*) Steady-state algorithm—applicable in (*a*) and (*c*). (*c*) Constant torque operation.

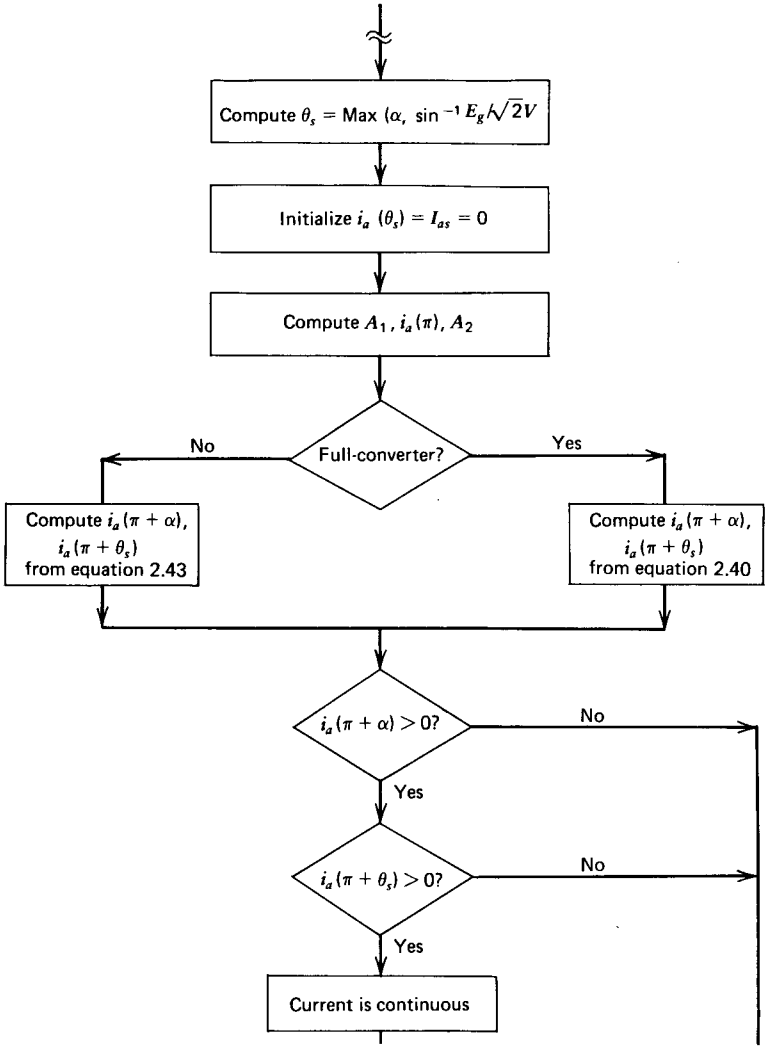
Compute $\theta_s$ = Max ($\alpha$, $\sin^{-1} E_g/\sqrt{2}V$
Initialize $i_a$ ($\theta_s$) = $I_{as}$ = 0
Compute $A_1$, $i_a(\pi)$, $A_2$
Full-converter?
No
Yes
Compute $i_a(\pi + \alpha)$, $i_a(\pi + \theta_s)$ from equation 2.43
Compute $i_a(\pi + \alpha)$, $i_a(\pi + \theta_s)$ from equation 2.40
$i_a(\pi + \alpha) > 0$?
No
Yes
$i_a(\pi + \theta_s) > 0$?
No
Yes
Current is continuous

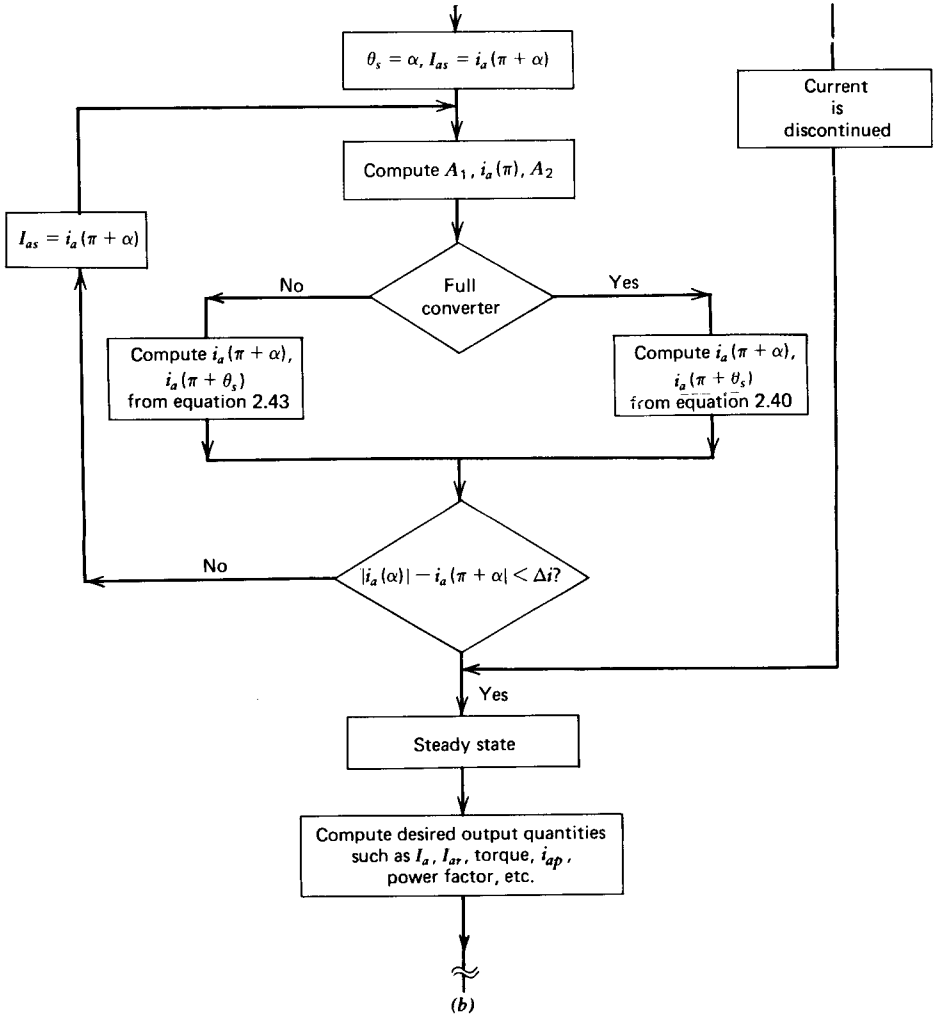


*Fig. 2.8* (*Continued*)

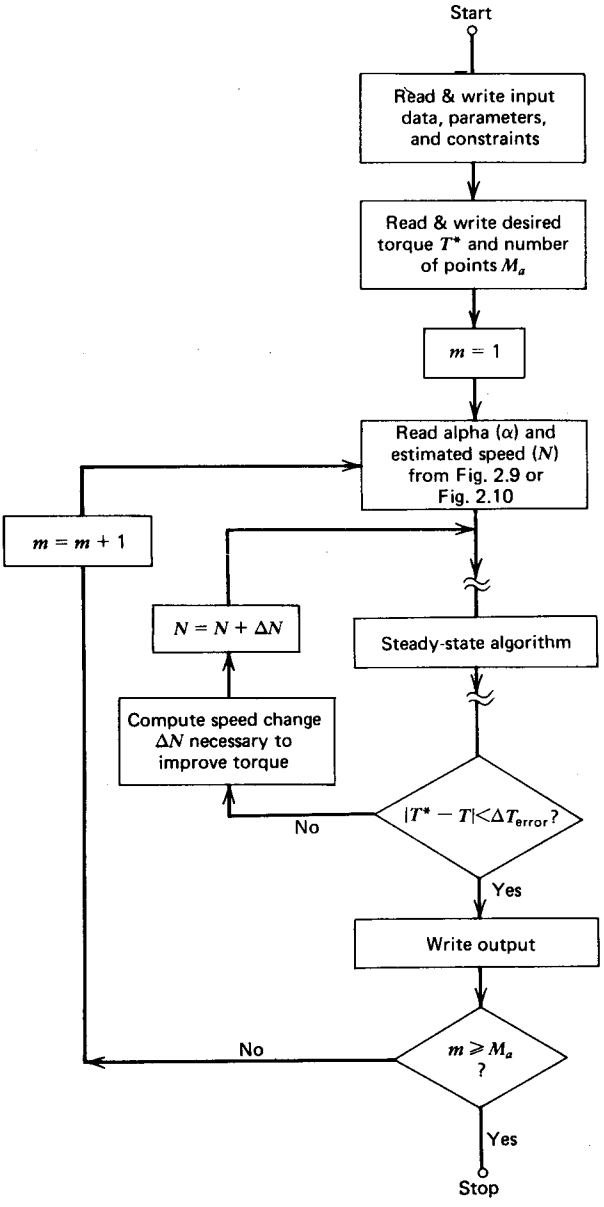


(c)

*Fig. 2.8 (Continued)*

and for any speed less than that corresponding to $E_{g_{max}}$, the thyristor turns on as soon as it is triggered (i.e., $\theta_s = \alpha$) as shown in Fig. 2.7*e*.

After the steady state is reached for a particular triggering angle and speed, the information obtained during the last cycle can be processed to determine the performance parameters of the drive. The average developed torque can be obtained from the average armature current. In the full-converter, the instantaneous value of the supply current is the same as the motor current. In the semi-converter, the instantaneous supply current is the same as the motor current when the thyristor conducts, and it is zero when the motor current flows through the free-wheeling diode. This is evident from Figs. 2.2, 2.3, 2.5, and 2.6. From a Fourier analysis of the supply current, we can evaluate input power factor, displacement factor (fundamental power factor), and harmonic factor.

### 2.2.5 Computer Study

If the parameters, constants, and constraints of the motor, converter, and supply are known, the performance characteristics of any phase-controlled dc drive can be obtained by using a digital computer. The flowcharts shown in Fig. 2.8 illustrate the computer simulation and are self-explanatory. In the following sections, studies on a phase-controlled drive using a laboratory-size separately excited dc motor (110 V, 1800 rpm, 2.5 hp) are presented.

#### *Torque-Speed Characteristics*

The torque-speed characteristics at different firing angles are shown in Figs. 2.9 and 2.10 for semi-converter and full-converter, respectively. In both cases the large drop in speed at low torque region is due to discontinuous motor current. With a full-converter the motor current is discontinuous over almost the entire range of operation. The negative speed in Fig. 2.10 implies inverter operation of the full-converter. The average output voltage of the full-converter can reverse. If the dc machine terminal voltage is reversed due to reversal of speed or field by some means, the machine will act as a generator and invert power to the ac supply.

#### *Effect of Armature Circuit Inductance: $L_a$*

Addition of inductance in the motor armature circuit has significant effects on the performance of the converter motor system. Figures 2.11 and 2.12 indicate that it reduces the region of discontinuous motor current. If a large inductor is used, the motor will operate essentially at constant speed for a particular firing angle over a wide range of torque. This significantly improves the speed regulation of the drive.

Armature circuit inductance also affects other motor and supply performance parameters, as shown in Figs. 2.13, 2.14, 2.15, and 2.16 for the semi-converter system. These results are shown for operation of the motor at

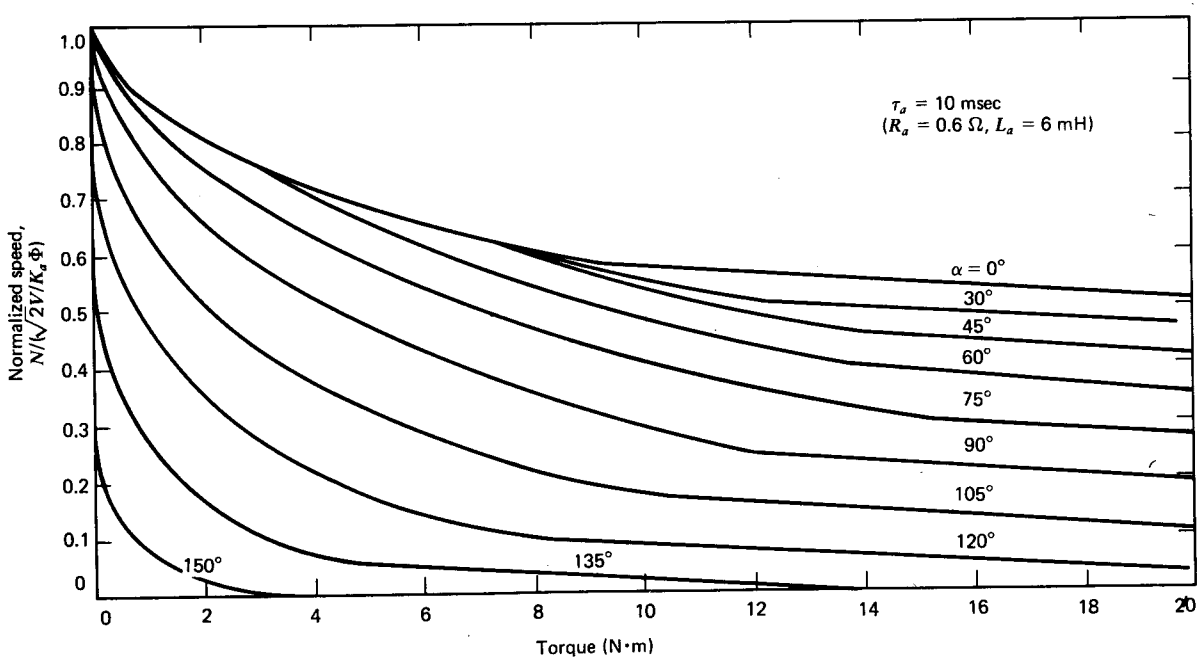


*Fig. 2.9* Torque-speed characteristics of a separately excited dc motor (2.5 hp, 110 V, 1800 rpm) controlled by a single-phase semi-converter.

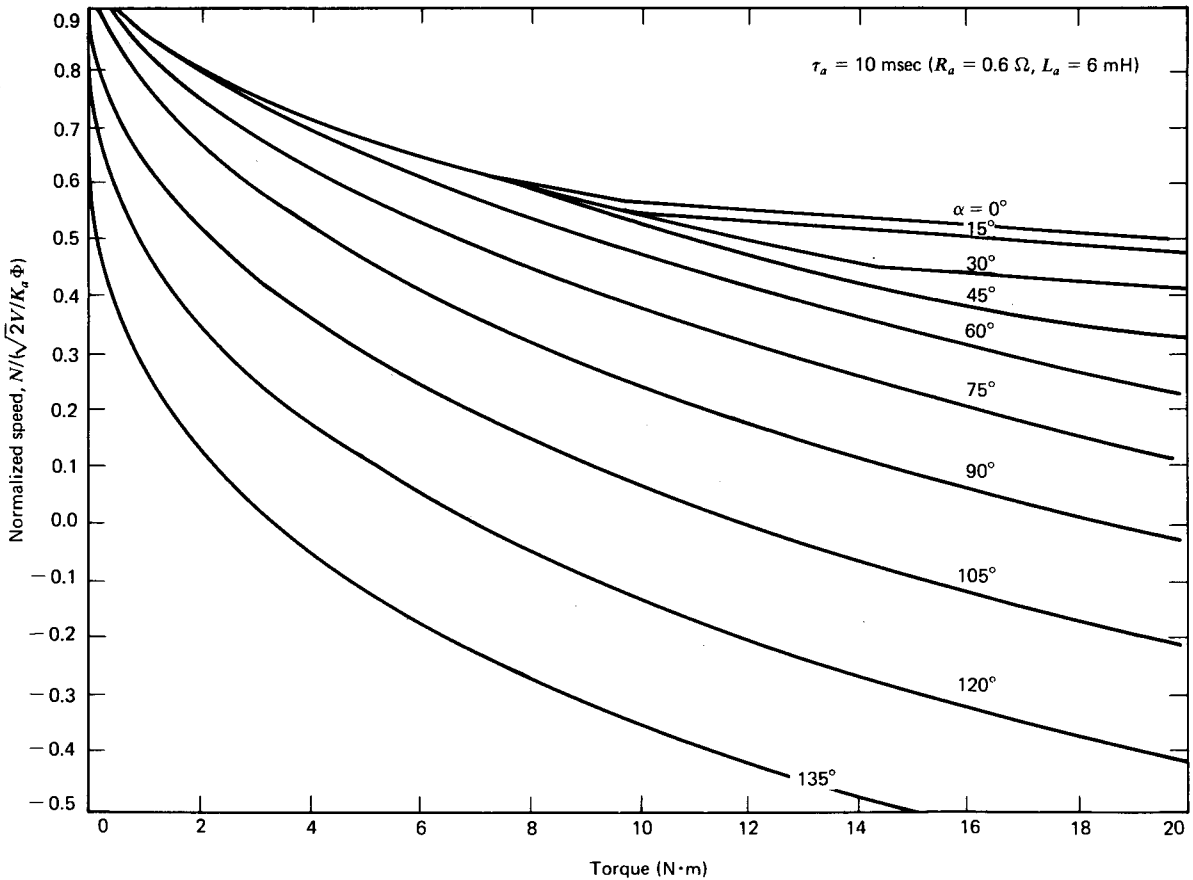


*Fig. 2.10* Torque-speed characteristics of a separately excited dc motor (2.5 hp, 110 V, 1800 rpm) controlled by a single-phase full-converter.

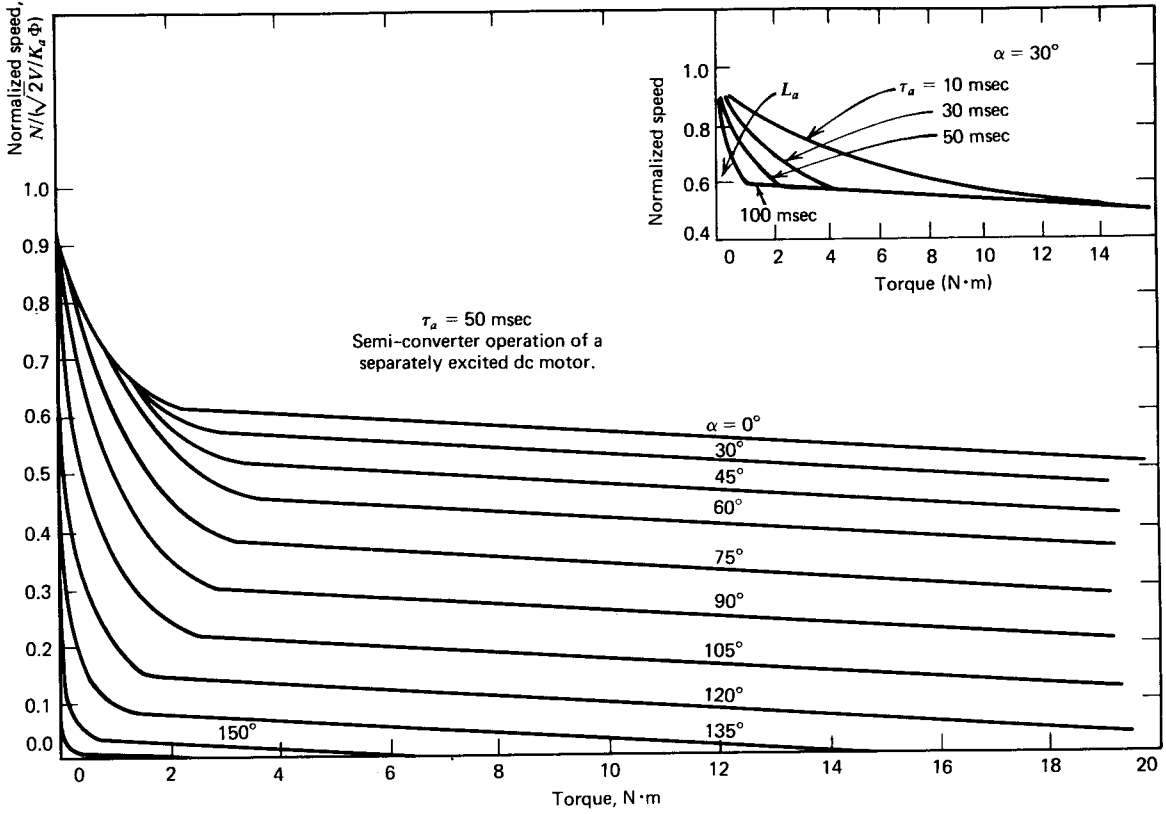


*Fig. 2.11* Torque-speed characteristics with added inductance in motor armature circuit. Inset shows the effects of changing $L_a$ at a particular firing angle (semi-converter operation).

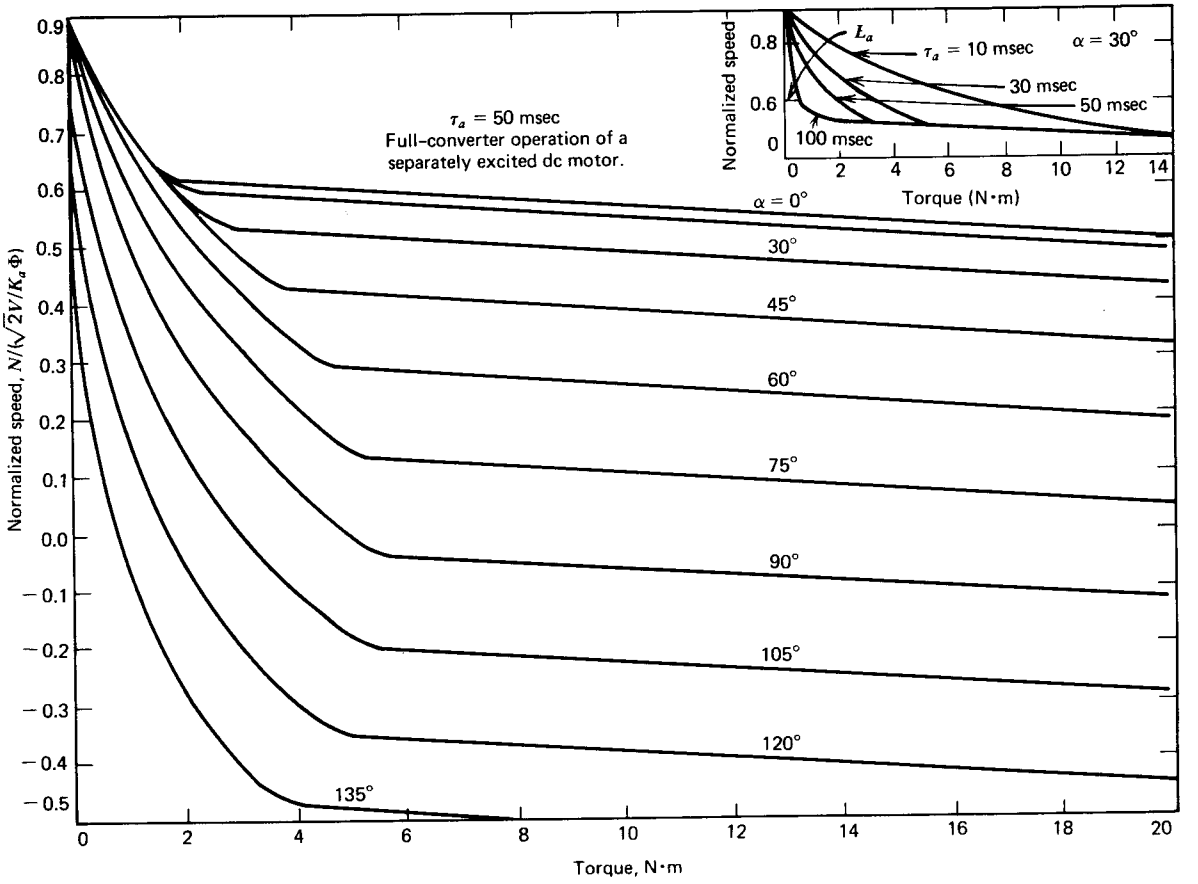


*Fig. 2.12* Torque-speed characteristics with added inductance in the motor armature circuit. Inset shows the effects of changing $L_a$ at a particular firing angle. (Full-converter operation.)

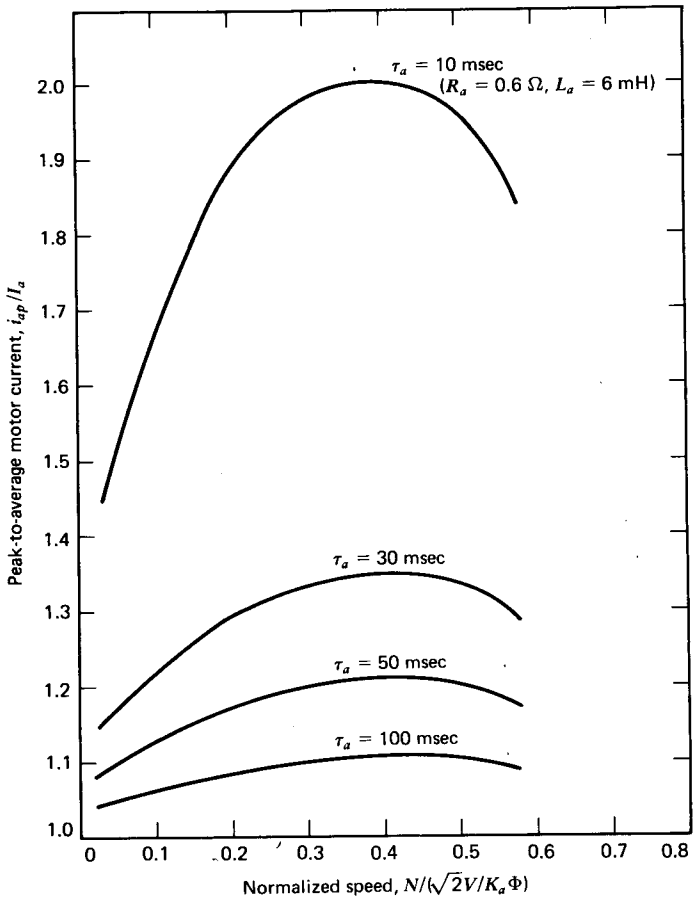


*Fig. 2.13* Constant-torque operation of a separately excited dc motor controlled by a semi-converter. Torque = 10 N·m. Peak-to-average motor current versus motor speed for various values of motor armature circuit time constant $\tau_a$.

rated torque condition (10 N·m for the motor considered). The flowchart for obtaining the performance parameters at a desired torque value is shown in Fig. 2.8*c*. The study indicated that additional armature circuit inductance improves the motor as well as the supply performance. For the full-converter system similar improvements occur with the addition of inductance, except for the harmonic content.

Figure 2.17 shows the effects of armature circuit inductance on the harmonic content in a full-converter system. The harmonic factor first decreases as the inductance is decreased, but increases again as the inductance is further decreased. At some value of $L_a$ the motor ripple current makes the supply current essentially sinusoidal. The ripple current is undesirable for the

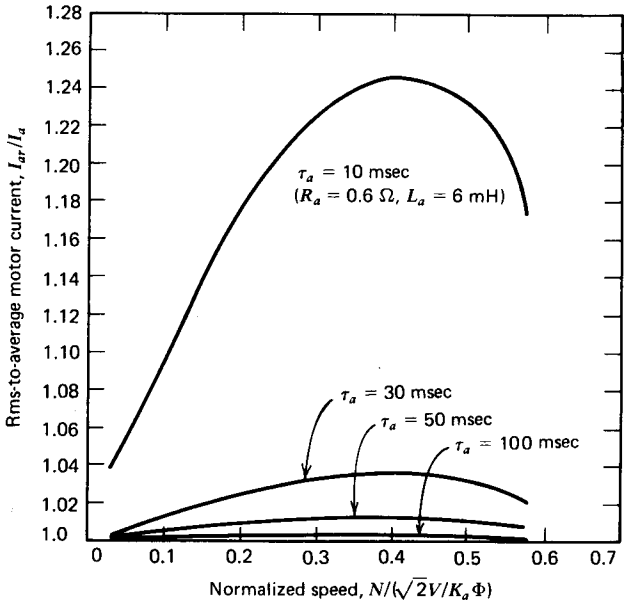


*Fig. 2.14* Constant-torque operation of a separately excited dc motor controlled by a semiconverter. Torque = 10 N·m. Rms-to-average motor current versus motor speed for various $\tau_a$.

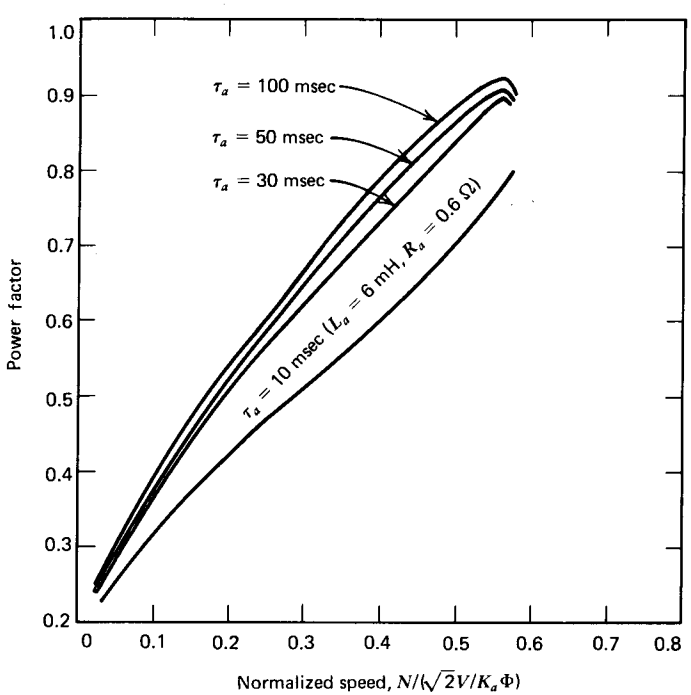


*Fig. 2.15* Constant-torque operation of a separately excited dc motor controlled by a semiconverter. Torque = 10 N·m. Supply power factor versus motor speed for various $\tau_a$.

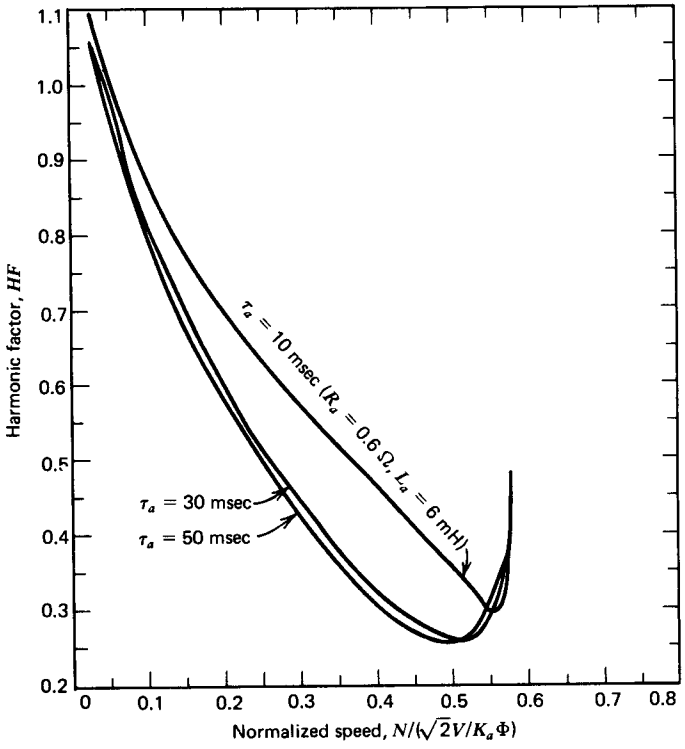


***Fig. 2.16*** Constant-torque operation of a separately excited dc motor controlled by a semi-converter. Torque = 10 N·m. Supply harmonic factor versus motor speed for various $\tau_a$.

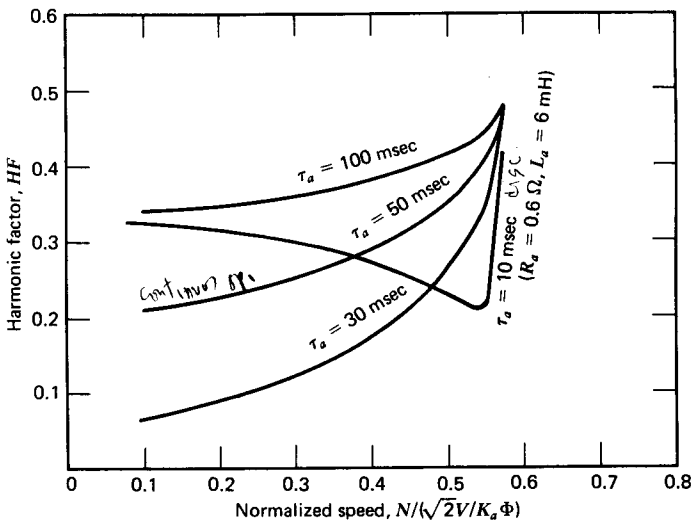


***Fig. 2.17*** Constant-torque operation of a separately excited dc motor controlled by a full-converter. Torque = 10 N·m. Supply harmonic factor versus motor speed for various $\tau_a$.

motor, but it makes the supply current look more sinusoidal. A single-phase diode rectifier with resistive load produces maximum ripple current (the output is a rectified sine wave), but it makes the supply current sinusoidal. With a dc motor load, the harmonic content increases at very low values of $L_a$ (Fig. 2.17) because the motor current becomes discontinuous and the supply current is in the form of pulses (Fig. 2.6).

Figure 2.13 shows that the ratio of peak-to-average motor current becomes maximum at approximately 0.4 normalized speed, which is about 63% rated speed. If no additional inductance is added to the armature circuit (i.e., $\tau_a = 10$ msec), the peak current is double the average current at this speed. The commutating capability is seriously affected. The peak current decreases as additional inductances are added to the armature circuit.

Figure 2.14 shows that with no additional armature circuit inductance, the rms motor current can become almost 1.25 times the average current. This will produce $(1.25)^2 = 1.56$ times the rated armature heating. This may require special design[4] of motors to be used in phase-controlled drives. Addition of inductances in the armature circuit reduces the rms-to-average current ratio and therefore decreases armature heating.

Figure 2.15 shows that power factor becomes poorer as the speed decreases. This is a serious disadvantage of a phase-controlled drive. Addition of inductance in the armature circuit does not significantly improve the power factor.

### *Comparison: Semi-Converter versus Full-Converter*

The type of converter, semi-converter, or full-converter affects the performance of the separately excited dc motor speed control system, as is shown in Figs. 2.18 to 2.22.

Supply power factor and displacement factor deteriorate with a decrease in speed in both semi-converter and full-converter. Semi-converter systems have an edge over full-converter systems and are preferred where inverter operation for regenerative braking is not required.

Figure 2.20 shows that, in the lower speed range, harmonic content in the input supply current is substantially higher in a semi-converter system. In the lower speed range, as the speed decreases, harmonic content increases in the semi-converter system while it remains essentially the same in the full-converter system. This is due to the fact that the supply current waveform remains essentially the same in a full-converter (Fig. 2.3, $\gamma = 180°$), whereas it changes in a semi-converter (Fig. 2.2, $\gamma = \pi - \alpha$) as the firing angle is changed.

Figure 2.21 shows that peak motor current is less in the semi-converter system. This is due to the smoothing action of the free-wheeling diode in semi-converters. The commutating capability of semi-converters is therefore higher, and this effect is significantly pronounced in the low-speed and low-torque region. Semi-converter systems also produce less rms current (Fig.

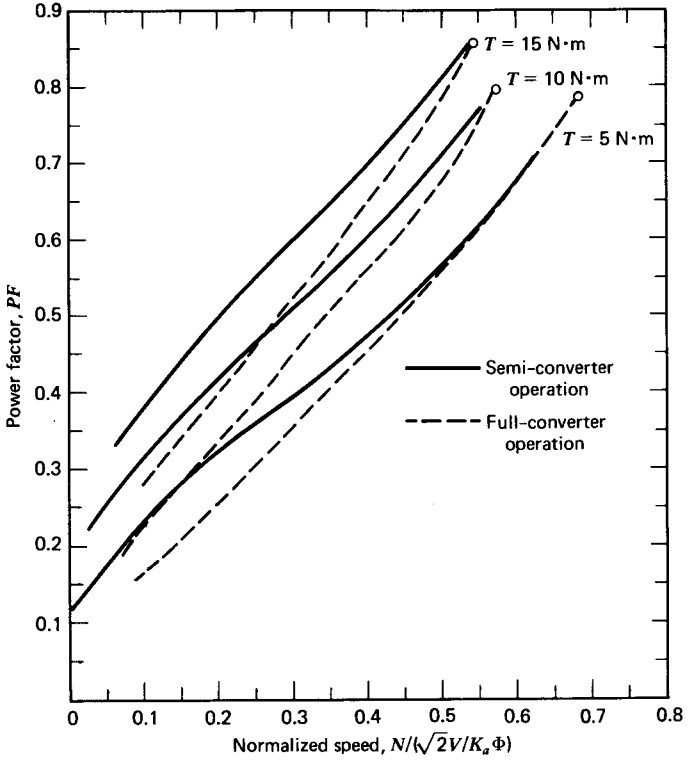


*Fig. 2.18* Supply power factor versus motor speed. Comparison for semi-converter and full-converter operation. Separately excited dc motor, $R_a = 0.6\ \Omega$, $L_a = 6$ mH, and $\tau_a = 10$ msec.

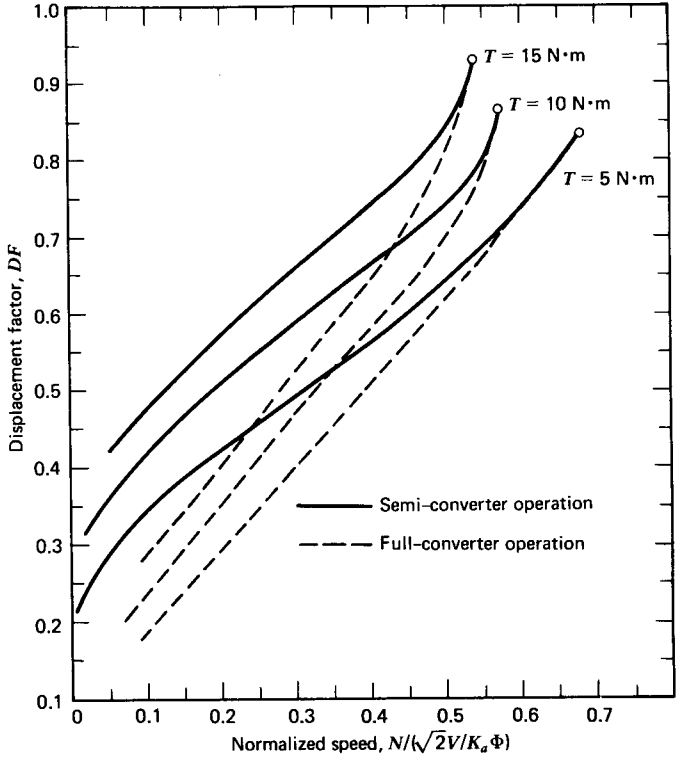


*Fig. 2.19* Supply displacement factor versus motor speed. Comparison for semi-converter and full-converter operation. Separately excited dc motor, $\tau_a = 10$ msec.

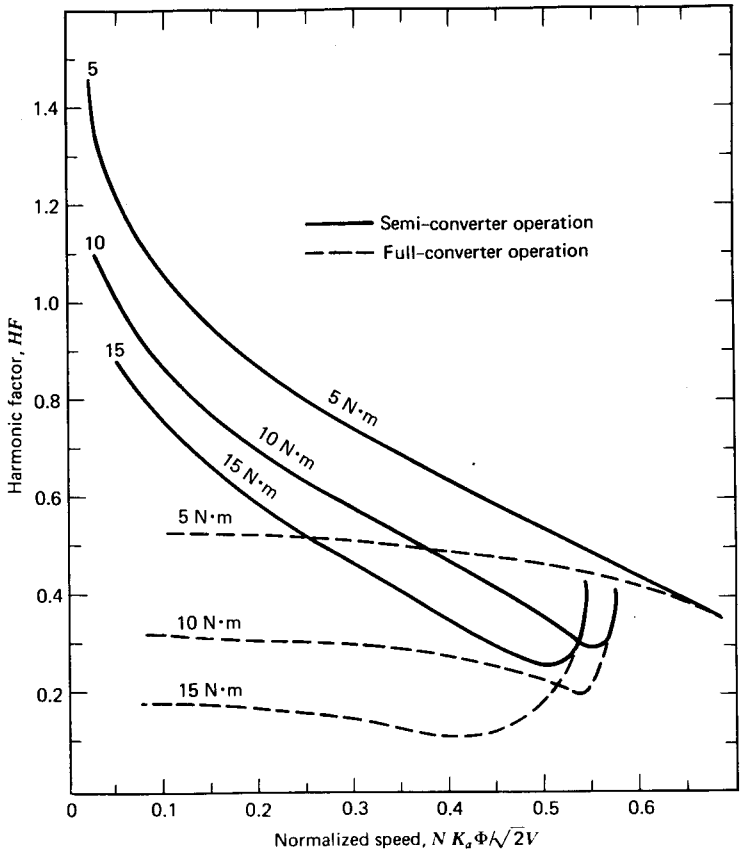


*Fig. 2.20* Supply harmonic factor versus motor speed. Comparison for semi-converter and full-converter operation. Separately excited dc motor, $\tau_a = 10$ msec.

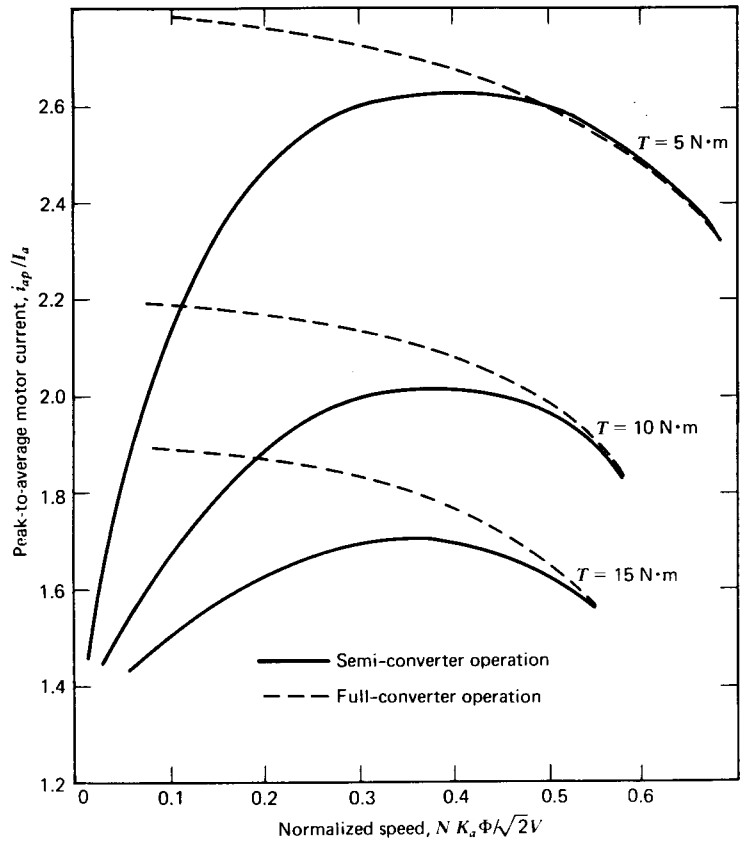


*Fig. 2.21* Peak-to-average motor current ratio versus motor speed. Comparison for semi-converter and full-converter operation. Separately excited dc motor, $\tau_a = 10$ msec.

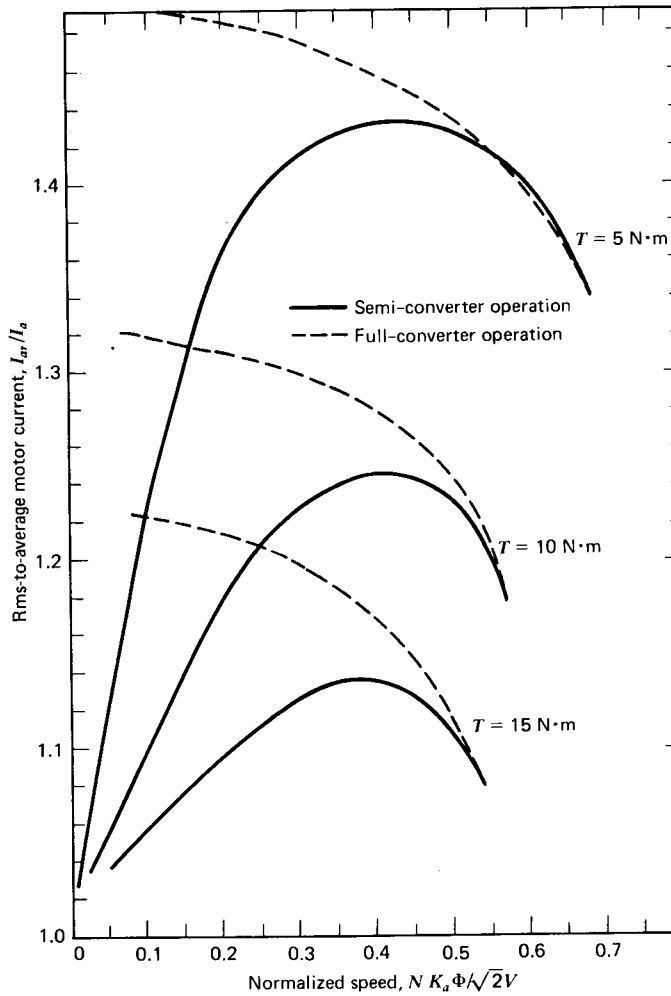


*Fig. 2.22* Rms-to-average motor current versus motor speed. Comparison for semi-converter and full-converter operation. Dc motor: separately excited, $\tau_a$ = 10 msec.

2.22), and hence there is less heating of the motor. At rated torque (10 N·m for the motor considered) and 0.1 normalized speed (approximately 15% rated speed), full-converter operation produces $(1.32/1.1)^2 = 1.44$ times (i.e., 44% extra) the heating produced by semi-converter operation.

Although a typical laboratory-size dc motor (2.5 hp) is considered in this study, the results represent the general behavior of dc drives controlled by thyristor converters. The various performance characteristics obtained here should provide the reader with an appreciation of the first-order effects expected of phase control in dc drives.

## 2.3 SINGLE-PHASE SERIES DC MOTOR DRIVES

In a series motor, the field circuit is connected in series with the armature, and the motor terminal voltage is controlled by a semi-converter or full-converter as shown in Fig. 2.23. Series motors are extensively used in many applications. They are particularly suited for applications that require high starting torque, such as cranes, hoists, elevators, vehicles, etc. Inherently, series motors can provide essentially constant power output and are therefore particularly suitable for traction drives.

### *Basic Equations*

The armature circuit resistance $R_a$ and inductance $L_a$ include the resistance and inductance of the series field winding. Back voltage is

$$e_g = K_a \Phi n \tag{2.50}$$

The flux $\Phi$ has two components. One component, say $\Phi_a$, is produced by the armature current flowing through the series field winding. The other component, say $\Phi_{res}$, is due to the so-called residual magnetism. The latter is small and can be assumed constant.

$$\Phi = \Phi_a + \Phi_{res} \tag{2.51}$$

If magnetic linearity is assumed,

$$\Phi_a = K_f i_a \tag{2.52}$$

From equations 2.50, 2.51, and 2.52

$$\begin{aligned} e_g &= K_a(K_f i_a + \Phi_{res})n \\ &= K_a K_f i_a n + K_a \Phi_{res} n \\ &= K_{af} i_a n + K_{res} n \end{aligned} \tag{2.53}$$

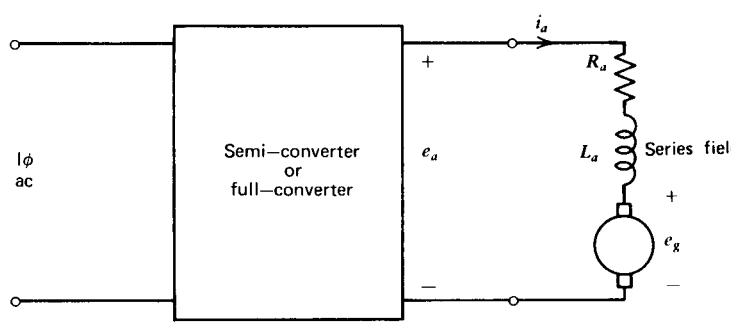


*Fig. 2.23* Basic single-phase (1ϕ) circuit for series motor speed control.

The back voltage due to residual magnetism is very small and is proportional to speed. The back voltage due to the flux produced by the armature current is the major voltage, and it is present when both $i_a$ and $n$ are present. Average back voltage is

$$E_g = K_{af} N I_a + K_{res} N \tag{2.54}$$

Developed torque is

$$t = K_a \Phi i_a \tag{2.55}$$

If the flux $\Phi_{res}$ is neglected, then from equations 2.51, 2.52, and 2.55

$$t \simeq K_{af} i_a^2 \tag{2.56}$$

Therefore, for either direction of current, torque is developed in the same direction. Hence in the series motor, speed reversal can be achieved by reversing either the field winding or the armature terminals, but not both.

Average torque is

$$T = K_{af} i_a^2 |_{\text{average}}$$

$$= K_{af} I_{ar}^2 \tag{2.57}$$

The armature circuit voltage equation is

$$e_a = R_a i_a + L_a \frac{di_a}{dt} + e_g \tag{2.58}$$

In terms of average quantities:

$$E_a = R_a I_a + E_g \tag{2.59}$$

Thus, although the time variations of voltages, currents, torque, and speed can assume various forms, the basic dc motor equations (2.54, 2.57, and 2.59) hold good for the phase-controlled series dc motor drives in terms of average quantities.

### 2.3.1 Waveforms

Current and voltage waveforms for semi-converter and full-converter series motor drives are shown in Figs. 2.24 and 2.25, respectively. The waveforms are drawn for both discontinuous and continuous motor armature current. In separately excited motors a large back voltage $E_g$ is always present, even when the motor armature current is absent. The back voltage $E_g$ tends to

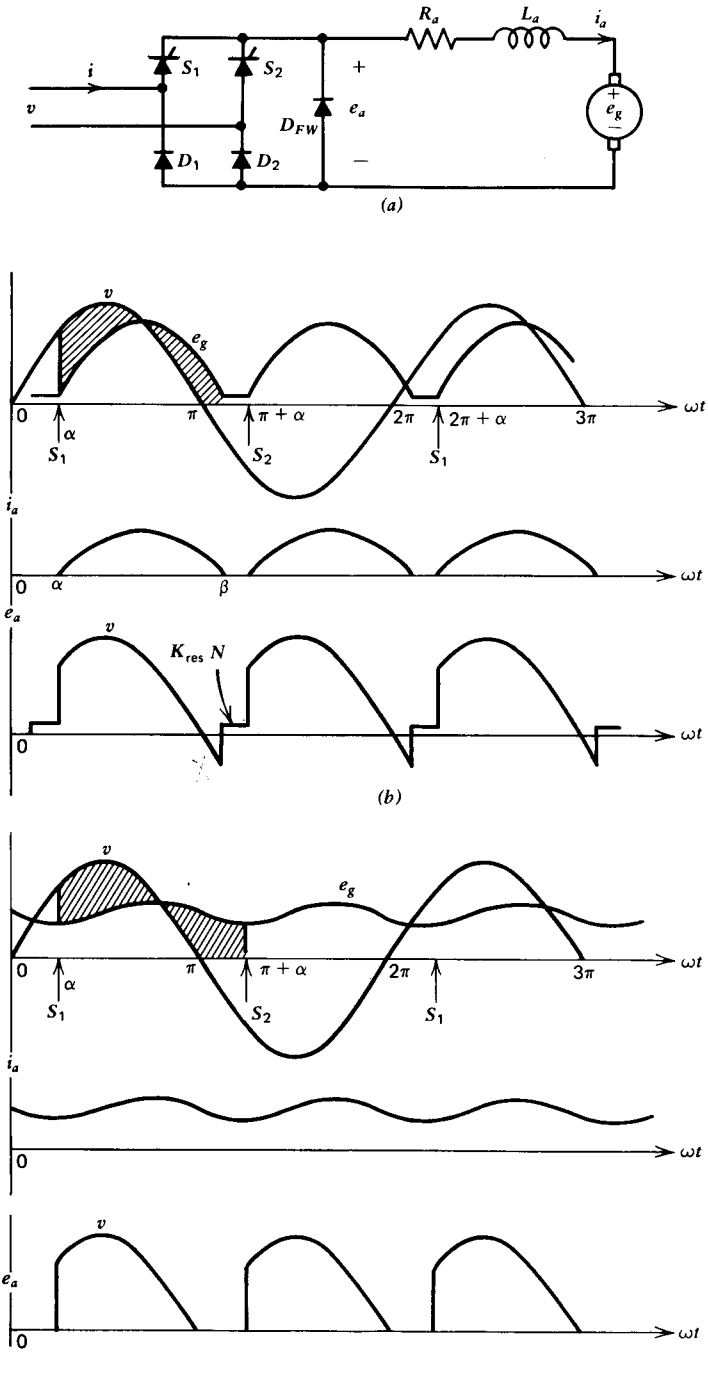


*Fig. 2.24* Speed control of a dc series motor by a single-phase semi-converter. (*a*) Power circuit. (*b*) Waveforms for discontinuous motor current. (*c*) Waveforms for continuous motor current.

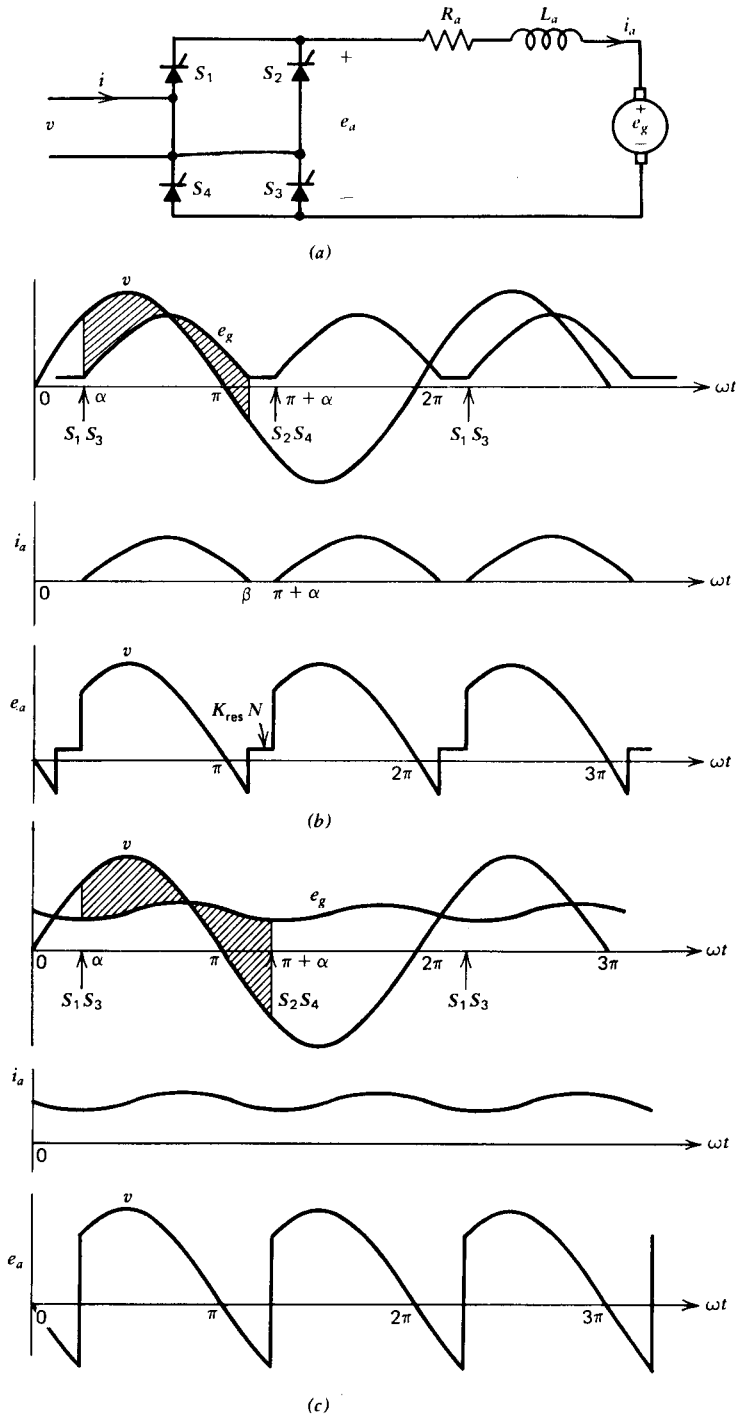


***Fig. 2.25*** Speed control of a dc series motor by a single-phase full-converter. (*a*) Power circuit. (*b*) Waveforms for discontinuous motor current. (*c*) Waveforms for continuous motor current.

oppose the motor current and so the motor current decays rapidly. This leads to discontinuous motor current over a wide range of operation. In series motors, the back voltage is proportional to the motor current (speed is assumed constant and back voltage due to residual magnetism is very small and neglected). Therefore, the back voltage decreases (unlike the separately excited motor where $E_g$ stays constant and accelerates the decay of $i_a$) as the motor current decreases and so the motor current tends to be continuous. In fact, motor current is continuous over a wide range of operation in dc series motor drives. Only at high speed and low current is the motor current likely to become discontinuous. In the discontinuous current mode, the motor terminal voltage $e_a$ is the same as the back voltage due to residual magnetism, which is very small.

### 2.3.2 Defining Equations

The system can operate in three modes. The governing equations for these modes are as follows:

***Mode 1*** Thyristor conducts during the interval:

$\alpha < \omega t < \pi$ with semi-converter and

$\alpha < \omega t < \beta$ with full-converter

The voltage equation is

$$e_a = \sqrt{2}\, V \sin \omega t = R_a i_a + L_a \frac{di_a}{dt} + K_{af} i_a n + K_{res} n \tag{2.60}$$

The electrodynamic equation is

$$t = K_{af} i_a^2 = J \frac{dn}{dt} + Bn + T_L \tag{2.61}$$

***Mode 2*** Free-wheeling action in semi-converter systems during the interval:

$\pi < \omega t < \beta$ for discontinuous current and

$\pi < \omega t < (\pi + \alpha)$ for continuous current

Free-wheeling action will be absent if $\beta < \pi$:

$$e_a = 0 = R_a i_a + L_a \frac{di_a}{dt} + K_{af} i_a n + K_{res} n \tag{2.62}$$

$$t = K_{af} i_a^2 = J \frac{dn}{dt} + Bn + T_L \tag{2.63}$$

***Mode 3*** Motor coasts during the interval:

$$\beta < \omega t < (\pi + \alpha)$$

$$i_a = 0 \tag{2.64}$$

$$t = 0 = J\frac{dn}{dt} + Bn + T_L \tag{2.65}$$

In terms of average values,

$$E_a = R_a I_a + K_{af} I_a N + K_{res} N \tag{2.66}$$

$$T = K_{af} I_{ar}^2 = BN + T_L \tag{2.67}$$

***Continuous Motor Current***

In phase-controlled series motor drives, the motor current is mostly continuous. An explanation was given earlier in Section 2.3.1. For a continuous motor current, well-defined expressions for the motor terminal voltage can be obtained, and these are given by equations 2.22 and 2.23. Therefore, in terms of average voltages, the voltage equations are as follows.

For semi-converter systems,

$$E_a = \frac{\sqrt{2}\,V}{\pi}(1 + \cos\alpha) = R_a I_a + K_{af} I_a N + K_{res} N \tag{2.68}$$

For full-converter systems,

$$E_a = \frac{2\sqrt{2}\,V}{\pi}\cos\alpha = R_a I_a + K_{af} I_a N + K_{res} N \tag{2.69}$$

Hence the average speed is

$$N = \frac{(\sqrt{2}\,V/\pi)(1 + \cos\alpha) - R_a I_a}{K_{af} I_a + K_{res}} \tag{2.70}$$

for the semi-converter system and

$$N = \frac{(2\sqrt{2}\,V/\pi)\cos\alpha - R_a I_a}{K_{af} I_a + K_{res}} \tag{2.71}$$

for the full-converter system.

These expressions relate average speed to average motor current. However, we are more interested in the torque-speed characteristics of the drive.

In series motors, the torque developed is proportional to the square of the motor rms current (equation 2.57). The relationship between the average and rms motor currents is not straightforward, and therefore an explicit expression relating torque and speed cannot be easily obtained.

However, if the ripple in the motor current can be neglected, then $I_a \simeq I_{ar}$. This will provide a well-defined expression relating speed and torque.

$$T = K_{af} I_{ar}^2$$

$$\simeq K_{af} I_a^2 \tag{2.72}$$

If the values of $I_a$ obtained from equations 2.68 and 2.69 are substituted in equation 2.72,

$$T \simeq K_{af} \left[ \frac{(\sqrt{2}\, V/\pi)(1 + \cos\alpha) - K_{res} N}{R_a + K_{af} N} \right]^2 \tag{2.73}$$

for the semi-converter system and

$$T \simeq K_{af} \left[ \frac{(2\sqrt{2}\, V/\pi) \cos\alpha - K_{res} N}{R_a + K_{af} N} \right]^2 \tag{2.74}$$

for the full-converter system.

The torque-speed characteristics under the assumption of continuous and ripple-free motor current can be obtained from equations 2.73 and 2.74 for different values of the firing angle $\alpha$. These characteristics are shown in Fig. 2.26.

**Example 2.2**

The speed of a 20 hp, 230 V, 900 rpm series motor is controlled by a single-phase semi-converter. The combined field and armature circuit resistance is 0.15 Ω. Motor constants are $K_{af} = 0.03$ N·m/A$^2$ and $K_{res} = 0.075$ V·sec/rad. Supply voltage is 260 V. Assuming continuous and ripple-free motor current, calculate the following for a firing angle $\alpha = 30°$ and speed $N = 900$ rpm:

1 Motor torque, motor current, and supply power factor.
2 Calculate these values if the converter is a full-converter.

*Solution*

1 $N = 900 \text{ rpm} = \dfrac{900}{60} \times 2\pi = 94.2 \text{ rad/sec.}$

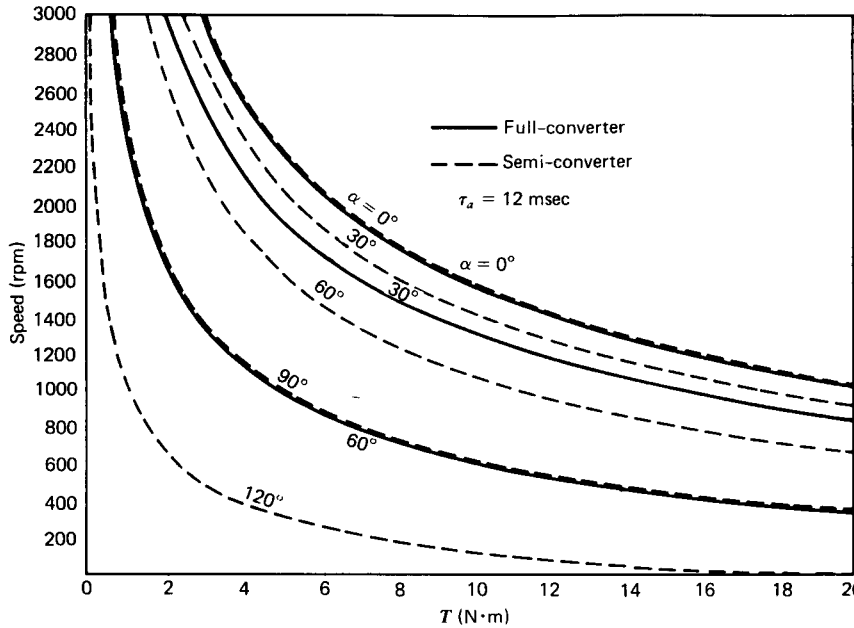


*Fig. 2.26* Torque-speed characteristics of a dc series motor (110 V, 2 hp, 1800 rmp) that is controlled by a single-phase converter. Ripple-free armature current assumed.

From equation 2.73

$$T = 0.03\left[\frac{(\sqrt{2} \times 260/\pi)(1 + \cos 30°) - (0.075 \times 94.2)}{0.15 + (0.03 \times 94.2)}\right]^2$$

$$= 0.03\left[\frac{218.48 - 7.07}{2.98}\right]^2$$

$$= 150.99 \text{ N}\cdot\text{m}$$

From equation 2.72

$$I_a = \left(\frac{150.99}{0.03}\right)^{1/2}$$

$$= 70.94 \text{ A}$$

From equation 2.68, motor terminal voltage is

$$E_a = \frac{\sqrt{2} \times 260}{\pi}(1 + \cos 30°)$$

$$= 218.48 \text{ V}$$

If losses in the converter are neglected, input power is

$$P_s = E_a I_a = 218.48 \times 70.94$$

$$= 15499 \text{ W}$$

Input volt-ampere is

$$U = 260 \times 70.94 \times \left(\frac{5}{6}\right)^{1/2} = 16837.4 \text{ VA}$$

Supply power factor is

$$PF = \frac{15499}{16837.4} = 0.92$$

**2** Full-converter. From equation 2.74

$$T = 0.03\left[\frac{(2\sqrt{2} \times 260/\pi)\cos 30° - 7.07}{2.98}\right]^2$$

$$= 0.03\left(\frac{202.79 - 7.07}{2.98}\right)^2$$

$$= 129.41 \text{ N}\cdot\text{m}$$

From equation 2.72

$$I_a = \left(\frac{129.41}{0.03}\right)^{1/2} = 65.68 \text{ A}$$

From equation 2.69

$$E_a = \frac{2\sqrt{2} \times 260}{\pi} \cos 30° = 202.79 \text{ V}$$

Now,

$$P_s = 202.79 \times 65.68 = 13318.8 \text{ W}$$

$$U = 260 \times 65.68 = 17076.8 \text{ VA}$$

$$PF = \frac{13318.8}{17076.8} = 0.78$$

Note that for the same firing angle, the power factor is better in the semi-converter system.

### *Rippled or Discontinuous Motor Current*

If ripple cannot be neglected and/or motor current is discontinuous, either the numerical method or the analytical method has to be used (as in the case of a separately excited motor drive) to obtain the torque-speed and other performance characteristics. These methods will now be discussed.

### *Numerical Method*

The motor is considered at standstill to start with. Torque, speed, and current are then computed during each cycle until steady state is reached by solving equations 2.60 to 2.65 digitally using the Runge-Kutta fourth-order approximation method.[3] This method requires computation over many cycles before the steady-state condition is reached and is therefore costly in terms of computer time.

### *Analytical Method*

In the analytical method, a steady-state speed is assumed, and therefore only equations 2.60, 2.62, and 2.64 have to be considered. From these equations it is possible to obtain analytical expressions for the armature current, such as equations 2.78, 2.83, and 2.84. These equations are used to compute the motor current during each cycle for a particular triggering angle until steady-state condition in the armature current is reached.

If the motor current is absent at the instant the thyristor is triggered, the back voltage at that instant is the small voltage due to residual magnetism. Therefore the thyristor turns on at the instant it is triggered because supply voltage is higher than the residual magnetism voltage, unless $\alpha$ is so low that $v(\alpha) < K_{res}N$. Recall that in a separately excited motor, if current is absent at the instant the thyristor is triggered, the back voltage $E_g$ is normally large and if $v(\alpha) < E_g$, the thyristor will not turn on at $\alpha$.

***Mode 1*** Thyristor conducts during the interval:

$\alpha < \omega t < \pi$ with semi-converter and

$\alpha < \omega t < \beta$ with full-converter

From equation 2.60,

$$\sqrt{2}\,V \sin \omega t = (R_a + K_{af}N)i_a + L_a\frac{di_a}{dt} + K_{res}N$$

$$= R_1 i_a + L_a\frac{di_a}{dt} + K_{res}N \tag{2.75}$$

where $R_1 = R_a + K_{af}N$.

The solution for $i_a$ is

$$i_a = \frac{\sqrt{2}\,V}{\left[R_1^2 + (\omega L_a)^2\right]^{1/2}} \sin(\omega t - \theta_z) - \frac{K_{res}N}{R_1} + A_1\,\varepsilon^{-(R_1/\omega L_a)\omega t} \tag{2.76}$$

where $A_1$ = a constant
$\theta_z = \tan^{-1}(\omega L_a / R_1)$.

Let $i_a(\alpha) = I_\alpha$ and $[R_1^2 + (\omega L_a)^2]^{1/2} = Z_1$. Then from equation 2.76

$$I_\alpha = \frac{\sqrt{2}\,V}{Z_1} \sin(\alpha - \theta_z) - \frac{K_{res}N}{R_1} + A_1\,\varepsilon^{-(R_1/\omega L_a)\alpha}$$

Therefore the constant $A_1$ is

$$A_1 = \left[ I_\alpha + \frac{K_{res}N}{R_1} - \frac{\sqrt{2}\,V}{Z_1} \sin(\alpha - \theta_z) \right] \varepsilon^{(R_1/\omega L_a)\alpha} \tag{2.77}$$

From equations 2.76 and 2.77,

$$i_a = \frac{\sqrt{2}\,V}{Z_1}\left[\sin(\omega t - \theta_z) - \sin(\alpha - \theta_z)\,\varepsilon^{(R_1/\omega L_a)(\alpha - \omega t)}\right]$$

$$+ \frac{K_{res}N}{R_1}\left(\varepsilon^{(R_1/\omega L_a)(\alpha - \omega t)} - 1\right) + I_\alpha \varepsilon^{(R_1/\omega L_a)(\alpha - \omega t)} \tag{2.78}$$

Note that $I_\alpha = 0$ for the first cycle of computation.

***Mode 2*** Free-wheeling action present with a semi-converter during the interval $\pi < \omega t < (\pi + \alpha)$ if motor current is continuous, or during the interval $\pi < \omega t < \beta$ if motor current is discontinuous.

The voltage equation is

$$0 = R_1 i_a + L_a \frac{di_a}{dt} + K_{res}N \tag{2.79}$$

The solution for $i_a$ is

$$i_a = A_2 \varepsilon^{-(R_1/\omega L_a)\omega t} - \frac{K_{res}N}{R_1} \tag{2.80}$$

where $A_2$ = a constant.

The value of $i_a$ at $\omega t = \pi$ can be computed from equation 2.78.

Let $i_a(\pi) = I_{a\pi}$. Therefore, from equation 2.80

$$I_{a\pi} = A_2 \varepsilon^{-(R_1/\omega L_a)\pi} - \frac{K_{res}N}{R_1} \tag{2.81}$$

or,

$$A_2 = \left( I_{a\pi} + \frac{K_{res}N}{R_1} \right) \varepsilon^{(R_1/\omega L_a)\pi} \tag{2.82}$$

From equations 2.80 and 2.82

$$i_a = I_{a\pi} \varepsilon^{-(R_1/\omega L_a)(\omega t - \pi)} + \frac{K_{res}N}{R_1} (\varepsilon^{-(R_1/\omega L_a)(\omega t - \pi)} - 1) \tag{2.83}$$

Mode 2 is absent if $\beta < \pi$, and it is also absent in a full-converter system.

***Mode 3*** Motor coasts during the interval $\beta < \omega t < (\pi + \alpha)$:

$$i_a = 0 \tag{2.84}$$

***Supply Current***

***Mode 1***

$$i = i_a \qquad \alpha < \omega t < \pi \quad \text{with semi-converter}$$

$$\alpha < \omega t < \beta \quad \text{with full-converter} \tag{2.85}$$

$$= -i_a \qquad \pi + \alpha < \omega t < 2\pi \quad \text{with semi-converter}$$

$$\pi + \alpha < \omega t < \pi + \beta \quad \text{with full-converter} \tag{2.86}$$

***Modes 2 and 3***

$$i = 0 \tag{2.87}$$

### 2.3.3 Performance Characteristics

The performance characteristics of a series motor drive are obtained by the analytical method. In most motors the mechanical inertia is large enough to make the time variation of speed in the steady state insignificant. The assumption of constant speed in the analytical method is therefore justified.

Since speed is assumed constant, the back voltage $e_g$ is approximately proportional to motor current, provided the residual magnetism voltage is

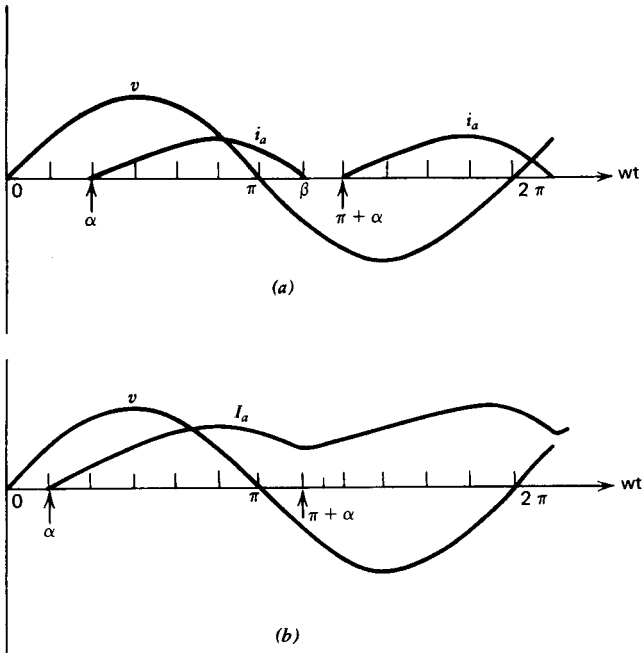


*Fig. 2.27* Series motor armature current waveform. (*a*) Discontinuous motor current. (*b*) Continuous motor current.

neglected. A thyristor turns on at the instant it is triggered because $v(\alpha) > K_{res}N$. If the current is discontinuous, as shown in Fig. 2.27*a*, steady state is reached in one half-cycle of computation because the second half-cycle will start with the same initial condition. If computation over the first half-cycle indicates that current is continuous—that is, $i_a(\pi + \alpha) > 0$ as shown in Fig. 2.27*b*—computation over a few cycles is required to reach the steady-state condition.

After the motor current reaches the steady state for a particular triggering angle and speed, the information obtained during the last cycle can be processed to determine the performance of the drive. The average developed torque can be obtained from the rms motor current. In the following sections, performance characteristics are presented for a phase-controlled drive using a laboratory-size dc series motor (110 V, 1800 rpm, 2 hp).

### *Torque-Speed Characteristics*

The torque-speed characteristics at different firing angles are shown in Figs. 2.28 and 2.29 for semi-converter and full-converter systems, respectively. Comparison of these characteristics with those for separately excited dc motors, shown in Figs. 2.9 and 2.10, reveals that the region of discontinuous motor current is reduced with the series motor. In the semi-converter system,

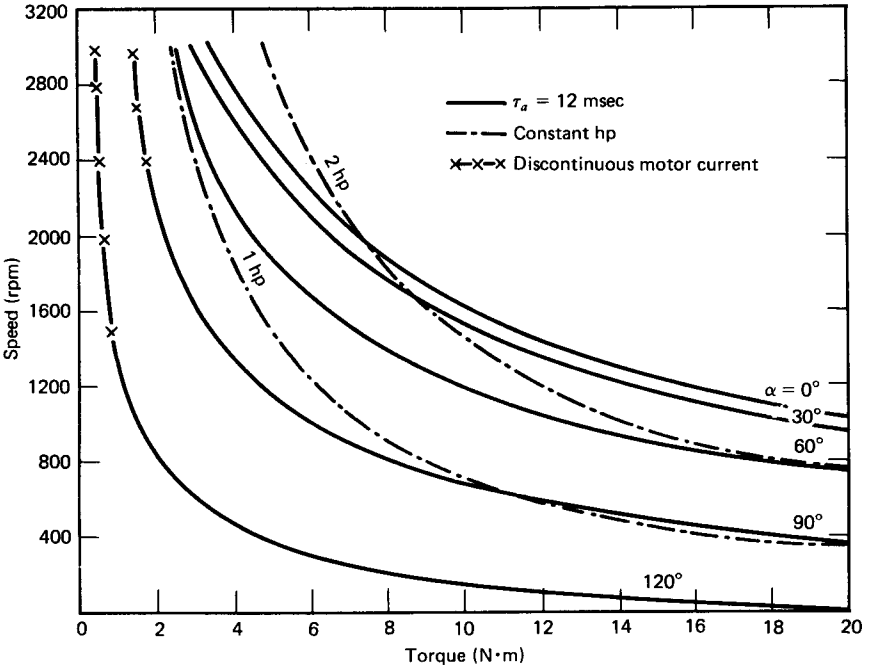


*Fig. 2.28* Torque-speed characteristics of a dc series motor (110 V, 2 hp, 1800 rpm) controlled by a single-phase semi-converter. Data obtained by the analytical method.

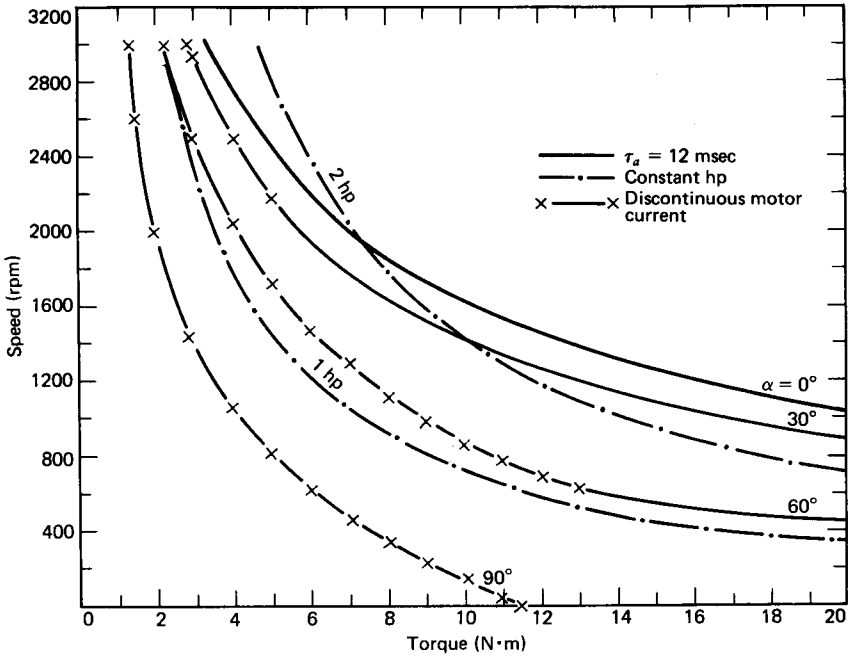


*Fig. 2.29* Torque-speed characteristics of a dc series motor (110 V, 2 hp, 1800 rpm) controlled by a single-phase full-converter. Data obtained by the analytical method.

the motor current is continuous over almost the entire operating region, except at a very low torque operation. Addition of inductance in the armature circuit can make the motor current continuous over the entire range of operation.

### *Constant-Hp Operation*

The torque-speed characteristics are drooping in nature. The drive system produces high torque at low speed and low torque at high speed, typical of a series motor. Series motors are normally used for constant-horsepower applications. However, the torque-speed ($T$-$N$) curves for a particular firing angle do not conform to constant power characteristics over the entire speed range, as can be seen from the constant-horsepower curves drawn in Figs. 2.28 and 2.29. If the motor drive system is required to operate at a constant power level over a given range of speed, the triggering angle has to be adjusted accordingly.

Some performance characteristics at two power levels are presented in Figs. 2.30 to 2.32. The semi-converter, as expected, provides better motor performance than the full-converter because the semi-converter, due to its free-wheeling action, assists in making the motor current continuous. Furthermore, the motor current tends to be smoother in a series motor, as explained earlier, than in a separately excited motor. The ratios of peak-to-average and rms-to-average motor current are smaller for series motors than for separately

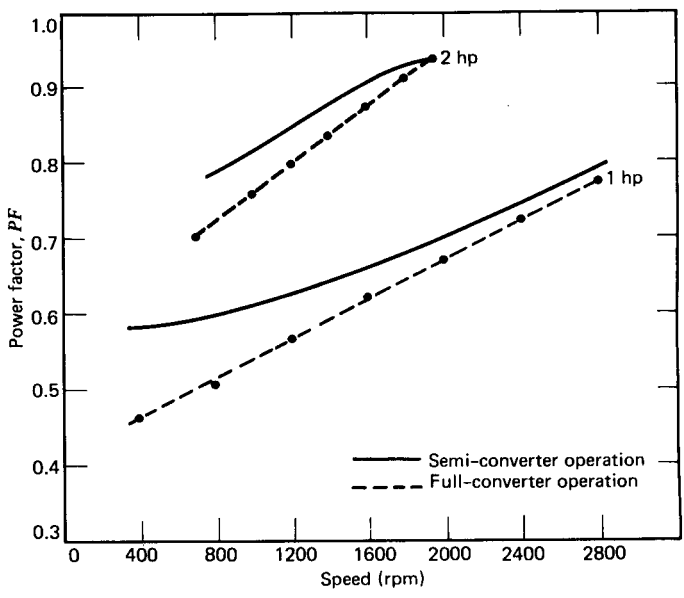


***Fig. 2.30*** Supply power factor versus motor speed. Comparison for semi-converter and full-converter operation. Dc series motor, $R_a = 1\ \Omega$, $L_a = 12$ mH, $\tau_a = 12$ msec.

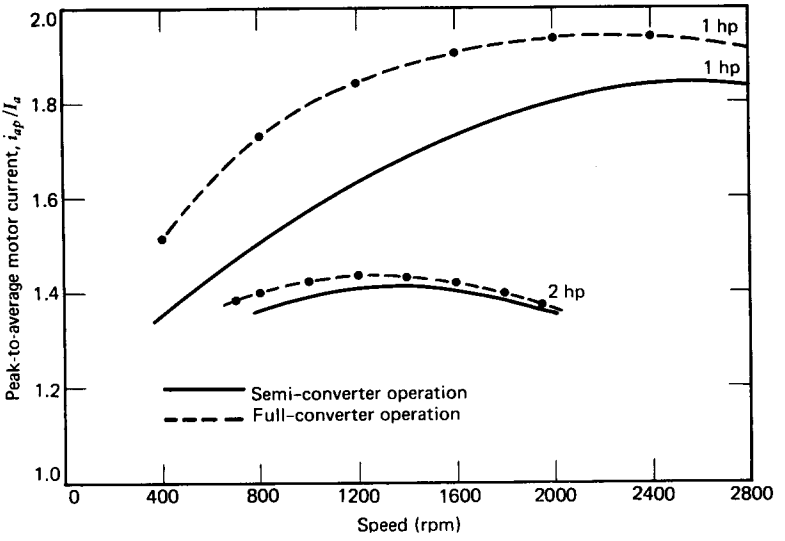


*Fig. 2.31* Motor peak-to-average current ratio versus speed. Comparison for semi-converter and full-converter operation. Dc series motor, $\tau_a = 12$ msec.

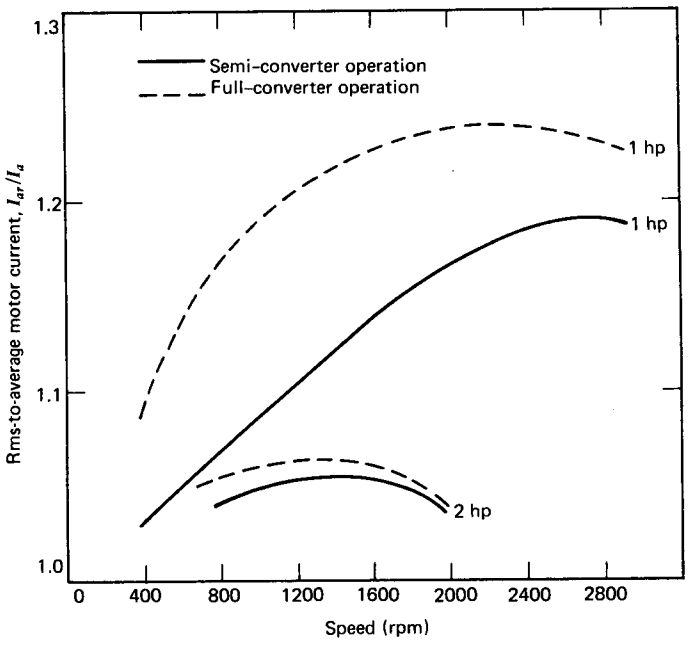


*Fig. 2.32* Motor rms-to-average current ratio versus speed. Comparison for semi-converter and full-converter operation. Dc series motor, $\tau_a = 12$ msec.

excited motors. This study shows that the series motor semi-converter combination provides superior performance.

## 2.4 POWER FACTOR IMPROVEMENT

Phase-controlled converters are widely used because these converters are simple, less expensive, reliable, and do not require any commutation circuit. However, the supply power factor in phase-controlled converters is low when the output voltage is less than the maximum, that is, when the firing angle is large. As the firing angle increases, the displacement angle between the supply voltage and current increases and the converter draws more lagging reactive power, thereby decreasing the power factor. Semi-converter systems provide better power factors than full-converter systems, although the improvement is not remarkable. This poor power factor operation is a major concern in variable-speed drives and in high-power applications. In the following sections, various techniques to improve power factor in phase-controlled converters are discussed. To facilitate analysis, it is assumed that motor current is constant (i.e., ripple-free) and the ac supply is ideal (i.e., has no supply impedance).

### 2.4.1 Phase Angle Control (PAC)

Certain performance characteristics, assuming constant motor current and ideal source, are studied first so that various techniques for improving power factor can be compared. For ripple-free motor current, the supply voltage and supply current waveforms are shown in Fig. 2.33. The magnitude of the supply current is the same as that of the motor current.

***Full-Converter***

The average output voltage is

$$E_a = \frac{1}{\pi}\int_{\alpha}^{\pi+\alpha} \sqrt{2}\, V \sin \omega t \, d(\omega t) = \frac{2\sqrt{2}\, V}{\pi} \cos \alpha \tag{2.88}$$

$$= E_{\max} \cos \alpha \tag{2.89}$$

If $E_{\max}$ is taken as base (i.e., 1 pu)

$$E_a = \cos \alpha \text{ pu} \tag{2.90}$$

The rms supply current $I$ is

$$I = I_a \tag{2.91}$$

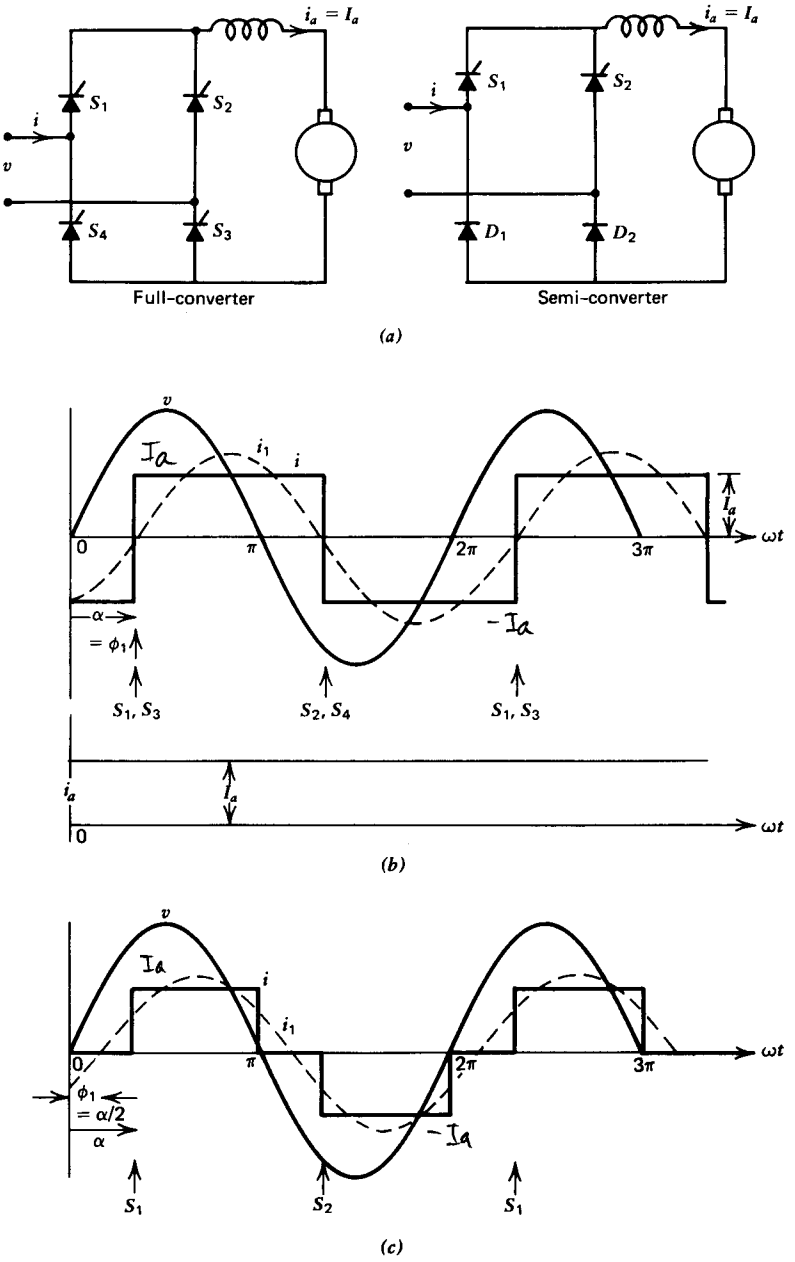


*Fig. 2.33* Phase angle control. (*a*) Full-converter and semi-converter drive circuits. (*b*) Waveforms in the full-converter circuit. (*c*) Waveforms in the semi-converter circuit.

The supply current $i$ may be represented by the Fourier series of equation 2.6.

The dc component is

$$I_0 = \frac{1}{2\pi}\int_{\alpha}^{2\pi+\alpha} i\, d(\omega t) = 0 \tag{2.92}$$

The Fourier coefficients are

$$a_n = \frac{1}{\pi}\left[\int_{\alpha}^{2\pi+\alpha} i \cos n\omega t\, d(\omega t)\right]$$

$$= \frac{1}{\pi}\left[\int_{\alpha}^{\pi+\alpha} I_a \cos n\omega t\, d(\omega t) + \int_{\pi+\alpha}^{2\pi+\alpha} -I_a \cos n\omega t\, d(\omega t)\right]$$

$$= \frac{2I_a}{n\pi}\left[\sin n(\pi+\alpha) - \sin n\alpha\right] \tag{2.93}$$

$$b_n = \frac{1}{\pi}\left[\int_{\alpha}^{2\pi+\alpha} i \sin n\omega t\, d(\omega t)\right]$$

$$= \frac{2I_a}{n\pi}\left[\cos n\alpha - \cos n(\pi+\alpha)\right] \tag{2.94}$$

From equations 2.93 and 2.94 both $a_n$ and $b_n$ are zero for even harmonics. This is also evident from the symmetry of the supply current waveform, shown in Fig. 2.33*b*. For odd harmonics

$$a_n = -\frac{4I_a}{n\pi}\sin n\alpha \tag{2.95}$$

$$b_n = \frac{4I_a}{n\pi}\cos n\alpha \tag{2.96}$$

The rms $n$th harmonic current is

$$I_n = \left(\frac{a_n^2 + b_n^2}{2}\right)^{1/2} = \frac{2\sqrt{2}\, I_a}{n\pi} \tag{2.97}$$

The displacement angle of the $n$th harmonic is

$$\phi_n = \tan^{-1}\frac{a_n}{b_n} = -n\alpha \tag{2.98}$$

The displacement angle of the fundamental current is therefore the same as the firing angle, that is, $\phi_1 = -\alpha$. The negative sign indicates that the fundamental current lags the supply voltage.

The supply power factor from equations 2.3, 2.91, 2.97, and 2.98 is

$$PF = \frac{I_1 \cos \phi_1}{I} = \frac{2\sqrt{2}}{\pi} \cos \alpha \tag{2.99}$$

The displacement factor is

$$DF = \cos \phi_1 = \cos \alpha \tag{2.100}$$

Therefore, both the power factor and displacement factor decrease as the firing angle increases.

The harmonic factor from equations 2.91 and 2.97 is

$$HF = \frac{(I^2 - I_1^2)^{1/2}}{I_1} = 0.4834 \tag{2.101}$$

***Semi-Converter***

The average output voltage is

$$E_a = \frac{1}{\pi} \int_{\alpha}^{\pi} \sqrt{2}\, V \sin \omega t \, d(\omega t) = \frac{\sqrt{2}\, V}{\pi} (1 + \cos \alpha)$$

$$= \frac{1}{2} (1 + \cos \alpha) \text{ pu} \tag{2.102}$$

Again, because of symmetry, even harmonics are absent. The Fourier coefficients and other parameters are:

$$a_n = \frac{2}{\pi} \int_{\alpha}^{\pi} I_a \cos n\omega t \, d(\omega t)$$

$$= -\frac{2I_a}{n\pi} \sin n\alpha \tag{2.103}$$

$$b_n = \frac{2}{\pi} \int_{\alpha}^{\pi} I_a \sin n\omega t \, d(\omega t)$$

$$= \frac{2I_a}{n\pi} (1 + \cos n\alpha) \tag{2.104}$$

$$I_n = \frac{2\sqrt{2}\, I_a}{n\pi} \cos \frac{n\alpha}{2} \tag{2.105}$$

$$\phi_n = -\frac{n\alpha}{2} \tag{2.106}$$

$$I = \left[ \frac{1}{\pi} \int_{\alpha}^{\pi} I_a^2 \, d(\omega t) \right]^{1/2} = I_a \left( 1 - \frac{\alpha}{\pi} \right)^{1/2} \tag{2.107}$$

$$PF = \frac{\sqrt{2}\,(1 + \cos\alpha)}{\pi \left( 1 - \frac{\alpha}{\pi} \right)^{1/2}} \tag{2.108}$$

$$DF = \cos\frac{\alpha}{2} \tag{2.109}$$

$$HF = \left[ \frac{\pi(\pi - \alpha)}{4(1 + \cos\alpha)} - 1 \right]^{1/2} \tag{2.110}$$

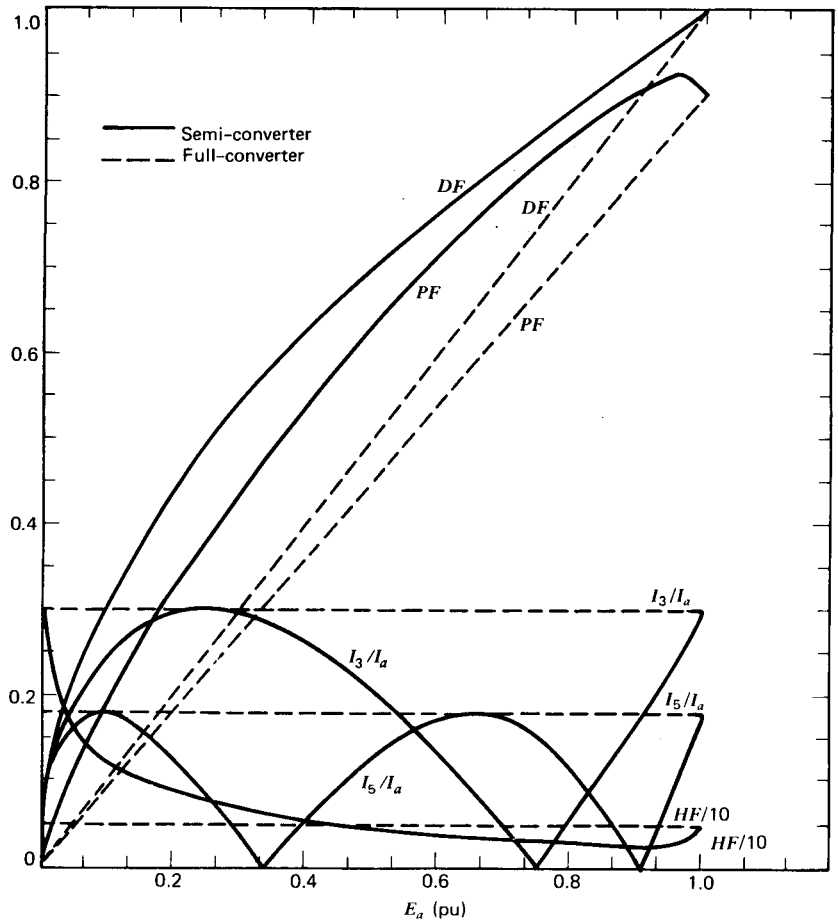


*Fig. 2.34* Performance characteristics in semi-converter and full-converter systems.

Variations of power factor, displacement factor, third and fifth harmonic currents (i.e., the two low-order harmonics), and harmonic factor as a function of the output voltage $E_a$ are shown in Fig. 2.34. The motor current $I_a$ is taken as a base (i.e., $I_a = 1$ pu). In both semi-converter and full-converter systems, power factor and displacement factor decrease as the output voltage decreases (or as firing angle increases). The semi-converter provides some improvement in power factor, displacement factor, and lower-order harmonics. Higher values of harmonic factor in the low-speed region in semi-converters are due to the presence of more higher-order harmonics, which can be filtered out easily.

### 2.4.2 Semi-Converter Operation of Full-Converters

A semi-converter is commonly used where regeneration is not required. This is because a semi-converter system is cheaper (fewer SCRs are required) and provides better performance, as can be seen from Fig. 2.34. If, however, regeneration is required, that is, feedback of dc power to the ac supply during regenerative braking of dc motors, full-converter systems are necessary. With some complexity in the control logic circuit, it is possible, however, to operate a full-converter as a semi-converter in both rectifying and inverting modes in order to exploit the better performance characteristics of semi-converters. This is illustrated in Fig. 2.35. In the rectification mode (i.e., positive output voltage, Fig. 2.35*b*), thyristors $S_3$ and $S_4$ are gated during the whole of the positive half-cycle and negative half-cycle respectively of the supply voltage. These thyristors $S_3$ and $S_4$ therefore behave as diodes during the respective half-cycles. The firing angle $\alpha$ for $S_1$ and $S_2$ is varied to change the output voltage. In the inverting mode (i.e., negative output voltage, Fig. 2.35*c*), thyristors $S_1$ and $S_2$ are gated during the whole of the negative and positive half-cycles respectively of the supply voltage so that they behave as diodes during their respective half-cycles. The firing angle for $S_3$ and $S_4$ is varied to change the output voltage.

When two SCRs of the same leg (such as $S_1$ and $S_4$ or $S_2$ and $S_3$) conduct, the motor current free-wheels through them producing zero output voltage. The nature of the motor terminal voltage $e_a$ and the supply current $i$ is the same as that in a semi-converter system. Therefore performance is improved at the cost of complexity in the control logic circuit.

Another interpretation of the foregoing control scheme is as follows: In the rectification mode, the firing of the negative group of thyristors (i.e., $S_3$ and $S_4$) is kept at zero. Therefore when the firing angle of the positive group of thyristors $S_1$ and $S_2$ is zero, the output voltage is maximum; when it is 180°, the output voltage is zero. In the inverting mode, the firing of the positive group of thyristors is kept at 180° and when the firing angle for the negative group is also 180°, the output voltage has its maximum negative value. In practice, the firing angle must be limited to less than 180° in all

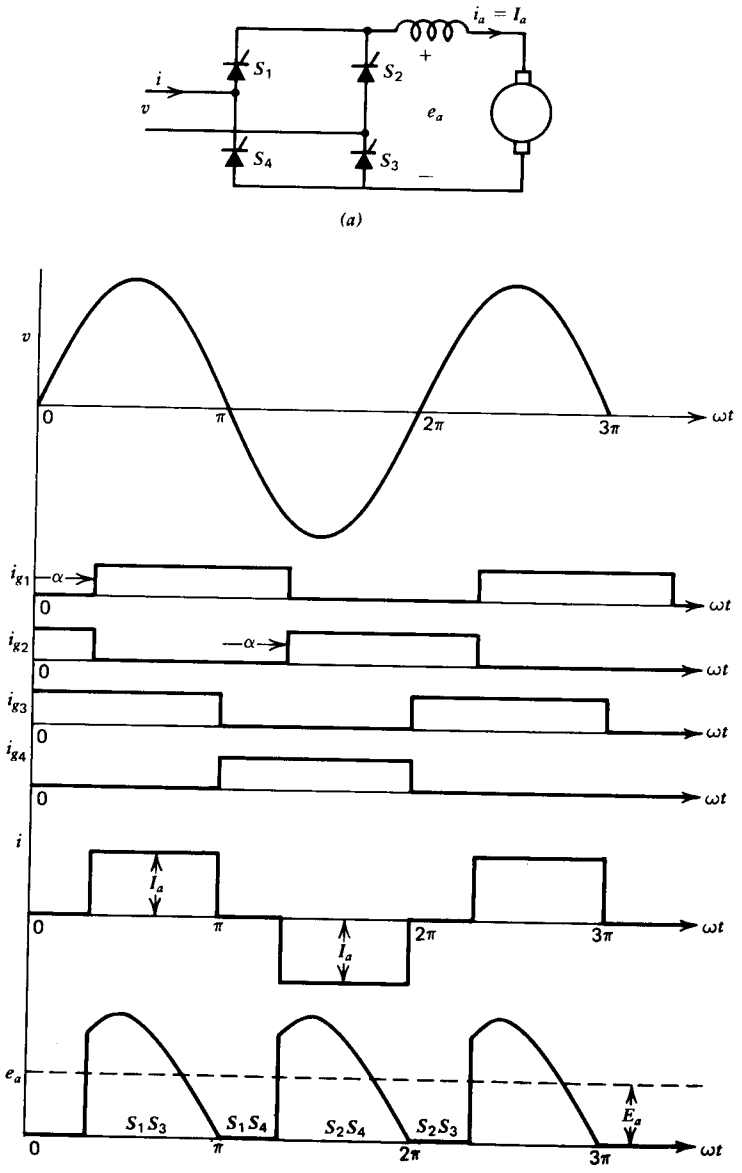


*Fig. 2.35* Semi-converter operation of a full-converter. (*a*) Full-converter drive circuit. (*b*) Waveforms for rectification. (*c*) Waveforms for inversion.

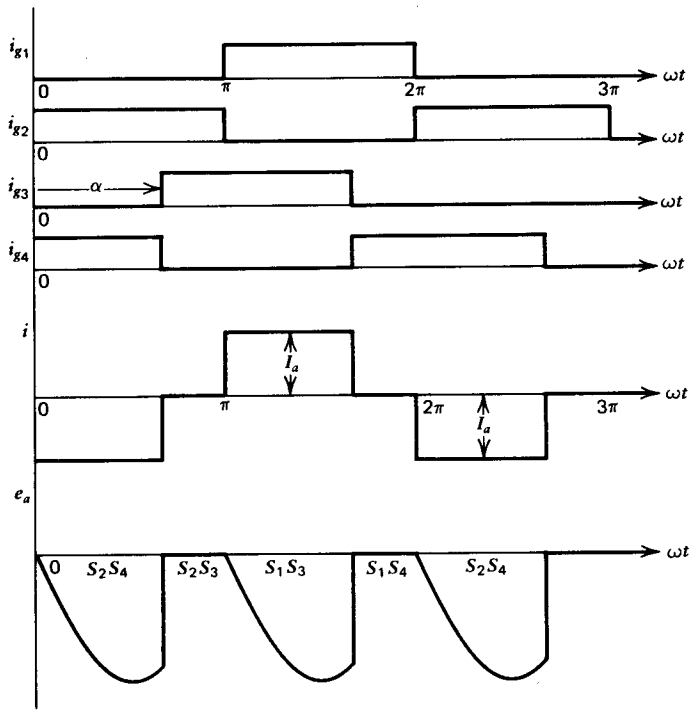


(c)

***Fig. 2.35*** *(Continued)*

cases to allow a margin for commutation (Fig. 2.3*c*). As the firing angle for $S_3$ and $S_4$ is reduced from 180°, the output voltage becomes less negative. This interpretation helps in understanding the application of this control scheme in three-phase full-converters,[5] where it is called *sequential control*. The firing angle for the positive group of thyristors is kept constant at zero and that for the negative group of thyristors is varied for the rectification mode. For the inversion mode, the firing angle for the positive group is varied, and that for the negative group is kept at 180°. This control scheme, although it improves power factor in both single-phase and three-phase converters, is not recommended for three-phase converters because of three major disadvantages:

1 Even harmonic currents are present in the supply line current.
2 Third harmonic ripple is present in the output.
3 There is a danger of commutation failure.

### 2.4.3 Asymmetrical Firing[5,6]

Further improvement in power factor can be achieved by a technique known as *asymmetrical firing*, illustrated in Fig. 2.36*c*. In this scheme thyristors are

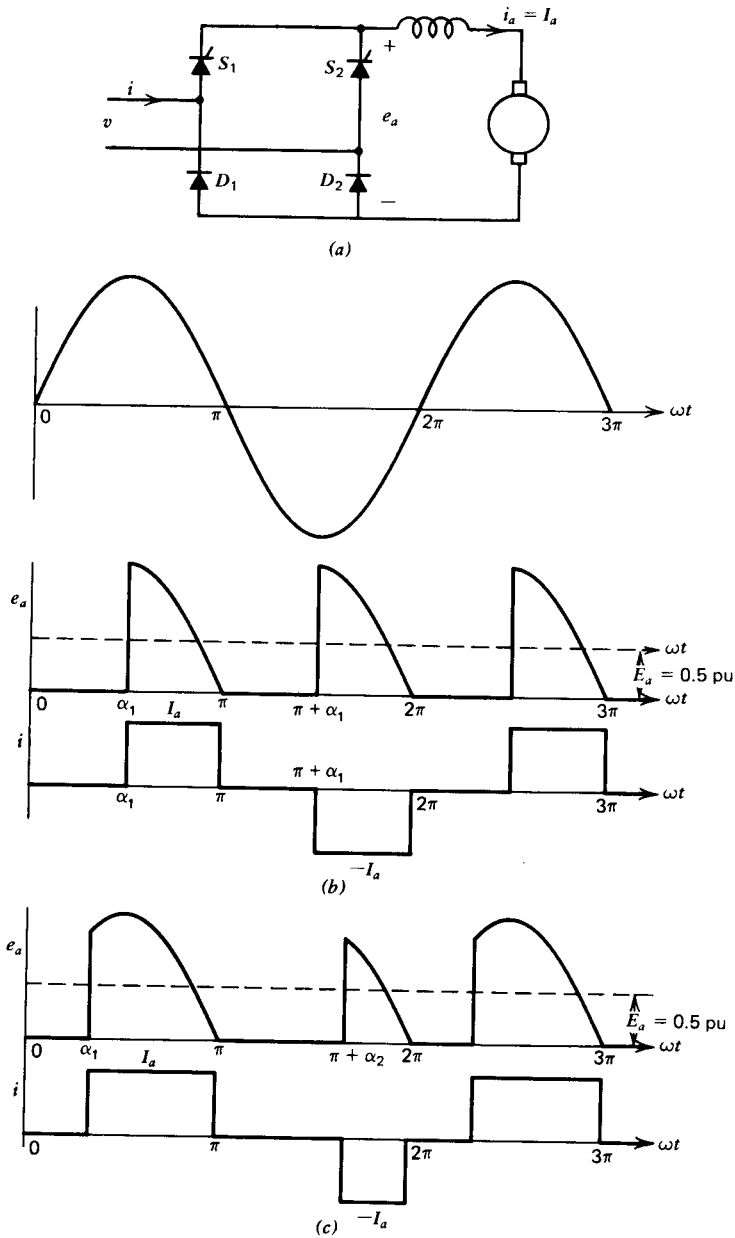


*Fig. 2.36* Symmetrical and asymmetrical triggering. (*a*) Semi-converter circuit. (*b*) Waveforms in symmetrical triggering. (*c*) Waveforms in asymmetrical triggering.

fired at different angles, whereas in the symmetrical firing scheme (Fig. 2.36*b*) both thyristors are fired at the same firing angle. For example, if 0.5 pu average output voltage is required, thyristors are fired at $\alpha = 90°$ in the symmetrical firing scheme. To obtain the same average output voltage in the asymmetrical firing scheme, if thyristor $S_1$ is fired at $\alpha_1 = 60°$, then thyristor $S_2$ is fired at $\alpha_2 = 120°$. Because one thyristor is fired at a lower value of the firing angle, the power factor is slightly improved in asymmetrical firing. However, asymmetrical firing produces several disadvantages. It generates dc and even harmonic currents in the supply line current. The dc component can, however, be avoided if the firing angles are alternated in successive cycles. If sufficient inductance is not present in the motor armature circuit, asymmetrical firing makes the motor current very peaky and discontinuous. The disadvantages outweigh the advantages of minor improvement in power factor, and therefore asymmetrical firing is only of theoretical interest.

### 2.4.4 Forced Commutation

In conventional phase-controlled converters a thyristor is commutated by the line voltage whenever the next thyristor is fired. However, if each thyristor is provided with its own commutation circuitry, it can be commutated at any desired instant. The thyristor inside the dotted square of Fig. 2.37*a* represents an SCR and its commutation circuitry. To keep the circuit simple, details of commutation circuitry, which can take various forms,[7–9] are not shown. The thyristor switch is a chopper and can be turned on and off at any desired instant.

Three control schemes[10] implementing forced commutation, which can improve the power factor and other performance characteristics, are discussed here.

#### *Extinction Angle Control (EAC)*

In the extinction angle control scheme, shown in Fig. 2.37*b*, the thyristor $S_1$ is turned on at 0° and turned off (by forced commutation) at $\beta$. The average output voltage changes as the turn-off instant $\beta$ is changed. The fundamental component $i_1$ of the supply current $i$, shown in Fig. 2.37*b*, leads the supply voltage. The displacement factor is leading, and this feature may be desirable to compensate for line voltage drop.

Expressions for various parameters can be derived as before, and only the final equations are presented here.

$$E_a = \tfrac{1}{2}(1 - \cos\beta) \text{ pu} \tag{2.111}$$

$$I = I_a\sqrt{\frac{\beta}{\pi}} \tag{2.112}$$

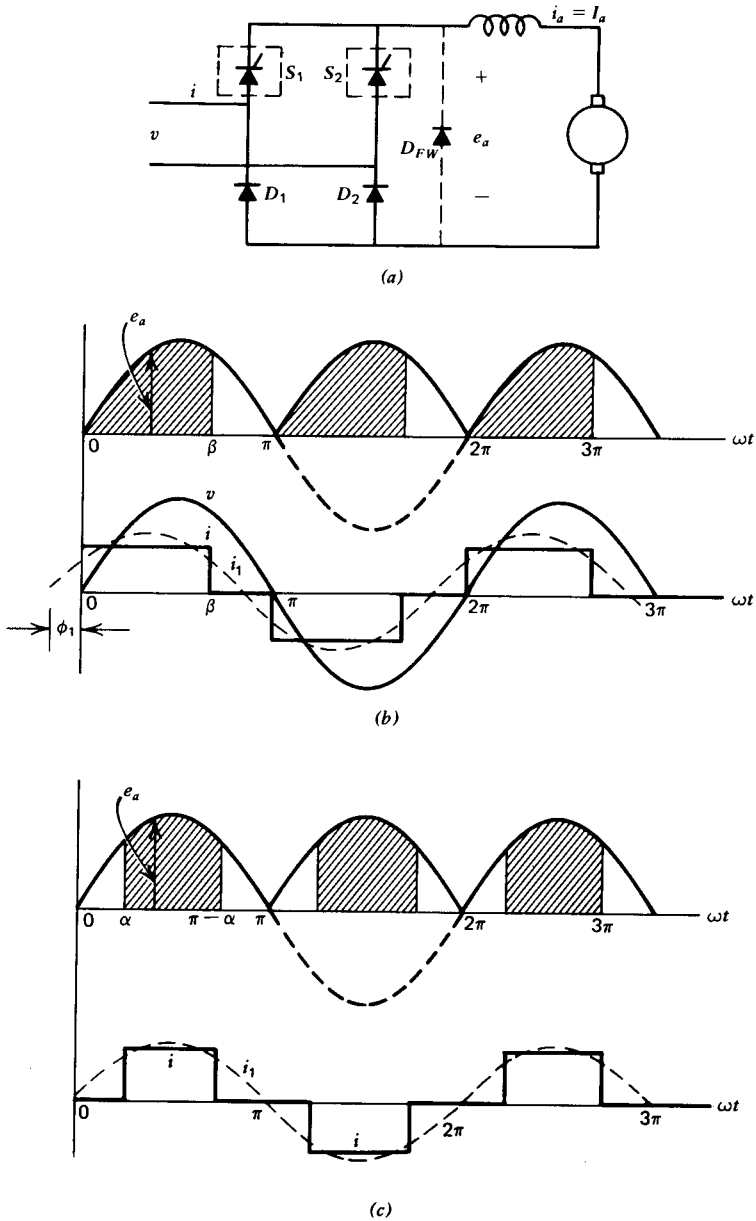


*Fig. 2.37* Forced commutation to improve power factor. (*a*) Power circuit. (*b*) Extinction angle control. (*c*) Symmetrical angle control. (*d*) Pulse-width modulation control.

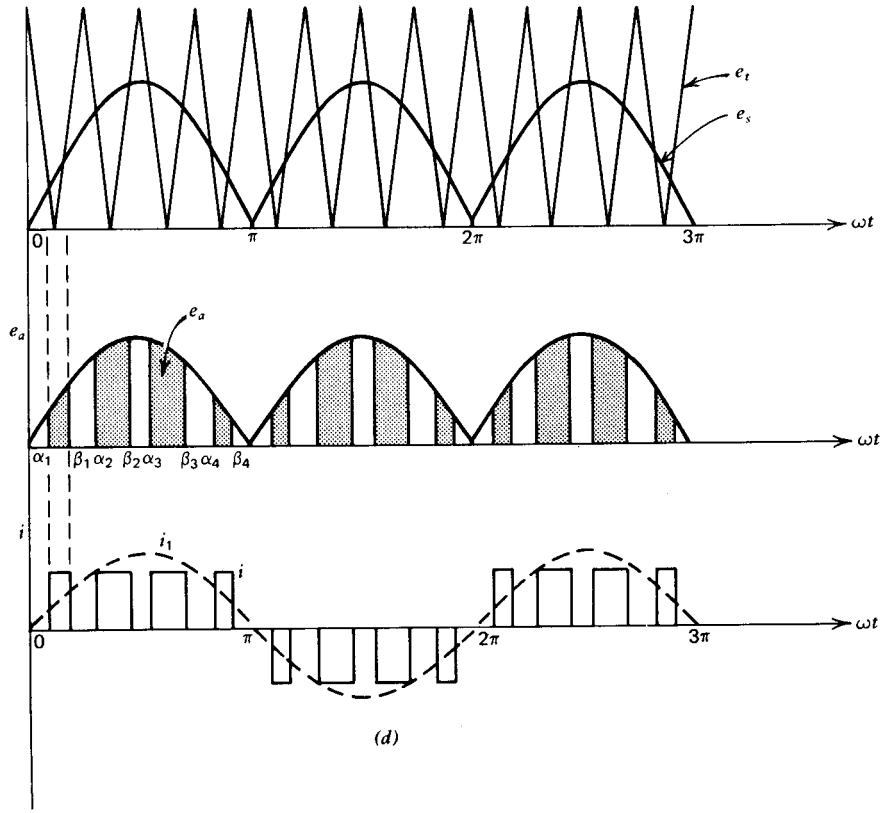


(d)

*Fig. 2.37* (*Continued*)

$$I_n = \frac{2\sqrt{2}\, I_a}{n\pi} \sin \frac{n\beta}{2} \qquad \text{where } n \text{ is odd} \tag{2.113}$$

$$\phi_n = n\left(\frac{\pi}{2} - \frac{\beta}{2}\right) \qquad \text{where } n \text{ is odd} \tag{2.114}$$

$$PF = \frac{\sqrt{2}\,(1 - \cos\beta)}{\sqrt{\pi\beta}} \tag{2.115}$$

$$DF = \sin\frac{\beta}{2}, \text{ leading} \tag{2.116}$$

$$HF = \left[\frac{\pi\beta}{4(1 - \cos\beta)} - 1\right]^{1/2} \tag{2.117}$$

In a semi-converter system performance of the converter under extinction angle control is similar to that of phase angle control, with the exception that the displacement factor is leading in extinction angle control, whereas it is lagging in phase angle control.

***Symmetrical Angle Control (SAC)***

In the symmetrical angle control scheme, shown in Fig. 2.37*c*, the thyristor $S_1$ is fired at $\alpha$ and turned off at $\pi - \alpha$. Expressions for the important parameters are as follows:

$$E_a = \cos\alpha \text{ pu} \tag{2.118}$$

$$I = I_a\left(1 - \frac{2\alpha}{\pi}\right)^{1/2} \tag{2.119}$$

$$I_n = \frac{2\sqrt{2}\, I_a}{n\pi}\cos n\alpha \qquad \text{where } n \text{ is odd} \tag{2.120}$$

$$\phi_n = 0 \tag{2.121}$$

$$PF = \frac{2\sqrt{2}\,\cos\alpha}{\pi\left(1 - \frac{2\alpha}{\pi}\right)^{1/2}} \tag{2.122}$$

$$DF = 1 \tag{2.123}$$

$$HF = \left[\frac{\pi(\pi - 2\alpha)}{8\cos^2\alpha} - 1\right]^{1/2} \tag{2.124}$$

In this scheme the supply current pulse is placed symmetrically with respect to the supply voltage peak, and therefore the fundamental current $i_1$ is in phase with the supply voltage. This makes the displacement factor unity and improves the power factor.

***Pulse-Width Modulation (PWM)***

In phase angle control, extinction angle control, and symmetrical angle control schemes, the supply current consists of one pulse per half-cycle and the lowest-order harmonic is the third. Lower-order harmonics are difficult to filter out. If the supply current has more than one pulse per half-cycle, lower-order harmonics can be eliminated and/or reduced. In the pulse-width modulation scheme, shown in Fig. 2.37*d*, a thyristor is turned on and off several times during each half-cycle. The width of the pulses is varied to change the output voltage. Lower-order harmonics can be eliminated or reduced by selecting the type of modulation for the pulse widths and the

number of pulses per half-cycle. Higher-order harmonics may increase, but these are of no concern because they can be eliminated easily by filters.

A sinusoidal pulse-width control technique is illustrated in Fig. 2.37*d*. In this method firing signals for the thyristors are obtained by comparing a triangular voltage $e_t$ with a rectified sinusoidal voltage $e_s$, which is in phase with the supply voltage $v$. The output voltage $e_a$ is varied by changing the amplitude of $e_s$ or the modulation index $m$, where $m$ is defined by

$$m = \frac{\text{amplitude of } e_s}{\text{amplitude of } e_t}$$

To obtain expressions for various performance parameters, the instants of turn-on (i.e., $\alpha$'s) and turn-off (i.e., $\beta$'s) are obtained by using Newton's method[11] to solve for the intersecting points between the signals $e_s$ and $e_t$.

Once these values (i.e., the $\alpha$'s and $\beta$'s) are obtained, expressions for the performance parameters can be obtained as follows:

$$E_a = \frac{1}{\pi}\int_0^{\pi} e_a \, d(\omega t)$$

$$= \frac{\sqrt{2}\,V}{\pi}\sum_{k=1}^{p}\int_{\alpha_k}^{\beta_k} \sin \omega t \, d(\omega t)$$

$$= \frac{1}{2}\sum_{k=1}^{p}(\cos\alpha_k - \cos\beta_k) \text{ pu} \tag{2.125}$$

where $p$ = number of pulses per half-cycle.

Because of symmetry in the current waveform $i$, even harmonics are absent and also:

$$I_0 = 0 \tag{2.126}$$

$$a_n = 0 \tag{2.127}$$

$$b_n = \frac{2}{\pi}\int_0^{\pi} i \sin n\omega t \, d(\omega t)$$

$$= \frac{2}{\pi}\sum_{k=1}^{p}\left[\cos n\alpha_k - \cos n\beta_k\right] \text{ pu} \tag{2.128}$$

$$I_n = \frac{b_n}{\sqrt{2}} \tag{2.129}$$

$$\phi_n = 0°$$

$$I = \left[ \frac{1}{\pi} \int_0^{\pi} i^2 \, d(\omega t) \right]^{1/2}$$

$$= \frac{I_a}{\sqrt{\pi}} \left[ \sum_{k=1}^{p} (\beta_k - \alpha_k) \right]^{1/2} \tag{2.130}$$

$$PF = \frac{I_1}{I} \tag{2.131}$$

$$DF = \cos \phi_1 = 1 \tag{2.132}$$

$$HF = \left[ \frac{I^2 - I_1^2}{I_1^2} \right]^{1/2} \tag{2.133}$$

In sinusoidal modulation of the PWM control scheme, the displacement angle $\phi_1$ is zero, the displacement factor is unity, and the power factor tends to remain high. The lowest-order harmonic is the fifth for four pulses per half-cycle, and the seventh for six pulses per half-cycle. Therefore, lower-order harmonics that are difficult to filter out are eliminated or reduced by selecting the number of pulses per half-cycle. Note that sinusoidal modulation is maintained as long as the modulation index $m$ is limited to less than unity.

The performance characteristics of phase angle control (PAC), extinction angle control (EAC), symmetrical angle control (SAC), and pulse-width modulation control (PWM) are compared in Figs. 2.41 to 2.44. Converters using forced commutation show definite improvement in performance.

### 2.4.5 Sequence Control of Series Converters

Converters can be connected in series to share the output voltage and can be controlled so that the supply power factor is improved. For example, consider two phase-controlled semi-converters connected in series (Fig. 2.38*a*) such that each converter can be controlled to provide 0 to 0.5 pu output voltage. Control strategy for the converters can be such that to obtain output voltage from 0 to 0.5 pu, only one converter is operated and the other one is bypassed through its free-wheeling diode. Therefore, at 0.5 pu output voltage, one converter is fully turned on (i.e., its firing angle is zero). This is equivalent to moving the characteristics of Fig. 2.34 to the left. This means that in the region of low output voltage the power factor is improved. To obtain output voltage from 0.5 to 1 pu, one converter is fully turned on (i.e., $\alpha = 0$) and the firing angle of the other converter is controlled. This control scheme is called *sequence control* of series converters. In high-voltage drives, instead of using a single converter with thyristors connected in series in the converter, two or more converters can be connected in series and sequence control of the converters can be implemented to improve supply power factor.

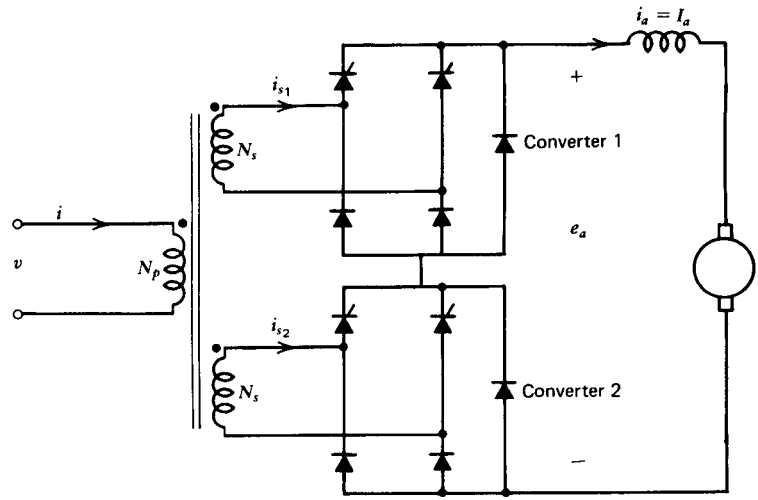


(a)

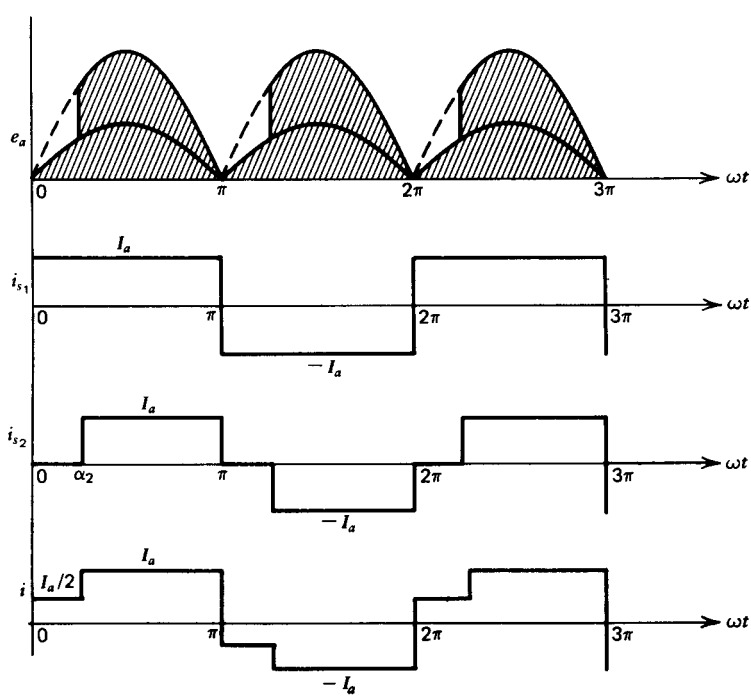


(b)

*Fig. 2.38* Sequence control of series semi-converters. $N_s/N_p = 0.5$. (*a*) Power circuit. (*b*) Waveforms for phase-angle control.

### *Phase-Controlled Semi-Converters*

Figure 2.38*a* shows the scheme for sequence control of two phase-controlled semi-converters. The converters are connected to the secondaries of a transformer. Each secondary has the same number of turns, and the turns ratio between secondary and primary is $N_s/N_p = 0.5$.

**$0 < E_a < 0.5$ pu**

The output voltage can be controlled in this range by changing the firing angle $\alpha_1$ for converter 1 and either keeping the firing angle $\alpha_2$ for converter 2 at $\pi$, or inhibiting the firing pulses for converter 2. Expressions for the various parameters are as follows.

$$\alpha_2 = \pi \qquad 0 < \alpha_1 < \pi$$

$$E_a = \tfrac{1}{4}(1 + \cos\alpha_1) \text{ pu} \tag{2.134}$$

$$I = \frac{I_a}{2}\left(1 - \frac{\alpha_1}{\pi}\right)^{1/2} \tag{2.135}$$

$$I_n = \frac{\sqrt{2}\, I_a}{n\pi} \cos n\alpha_1 \qquad n \text{ is odd} \tag{2.136}$$

$$\phi_n = -\frac{n\alpha_1}{2} \qquad n \text{ is odd} \tag{2.137}$$

$$PF = \frac{\sqrt{2}\,(1 + \cos\alpha_1)}{\pi\left(1 - \dfrac{\alpha_1}{\pi}\right)^{1/2}} \tag{2.138}$$

$$DF = \cos\frac{\alpha_1}{2} \tag{2.139}$$

$$HF = \left[\frac{\pi(\pi - \alpha_1)}{4(1 + \cos\alpha_1)} - 1\right]^{1/2} \tag{2.140}$$

**$0.5 < E_a < 1.0$ pu**

In this range of the output voltage, converter 1 is fully turned on and converter 2 is controlled; that is, $\alpha_1 = 0$ and $0 < \alpha_2 < \pi$. Figure 2.38*b* shows voltage and current waveforms for $\alpha_1 = 0$ and $\alpha_2 = 45°$.

$$E_a = \tfrac{1}{4}(3 + \cos\alpha_2) \tag{2.141}$$

$$I = I_a\left(1 - \frac{3\alpha_2}{4\pi}\right)^{1/2} \tag{2.142}$$

$$I_n = \frac{I_a}{n\pi}(5 + 3\cos n\alpha_2)^{1/2} \qquad n \text{ is odd} \tag{2.143}$$

$$\phi_n = -\tan^{-1}\frac{\sin n\alpha_2}{3 + \cos n\alpha_2} \qquad n \text{ is odd} \tag{2.144}$$

$$PF = \frac{3 + \cos\alpha_2}{\pi\left(2 - \dfrac{3\alpha_2}{2\pi}\right)^{1/2}} \tag{2.145}$$

$$DF = \frac{3 + \cos\alpha_2}{(10 + 6\cos\alpha_2)^{1/2}} \tag{2.146}$$

$$HF = \left[\frac{\pi(\pi - 3\alpha_2/4)}{5 + 3\cos\alpha_2} - 1\right]^{1/2} \tag{2.147}$$

The power factor variation with the output voltage is shown in Fig. 2.41. When compared with phase control of single converters, the improvement is significant. If more than two converters are connected in series, further improvement is possible.

***Symmetrical Angle Control***

The symmetrical angle control scheme in a single converter provides better power factor than the phase angle control scheme. In sequence control of series converters, symmetrical angle control can be implemented. Figure 2.39 shows two converters in series: one is line commutated and the other is forced commutated.

**$0 < E_a < 0.5$ pu**

To control voltage in this range the line commutated converter is bypassed through the free-wheeling diode and the forced commutated converter is controlled ($0 < \alpha_1 < 90°$).

$$E_a = \frac{\cos\alpha_1}{2} \text{ pu} \tag{2.148}$$

$$I = \frac{I_a}{2}\left(1 - \frac{2\alpha_1}{\pi}\right) \tag{2.149}$$

$$I_n = \frac{\sqrt{2}\, I_a}{n\pi}\cos n\alpha_1 \tag{2.150}$$

$$\phi_n = 0 \tag{2.151}$$

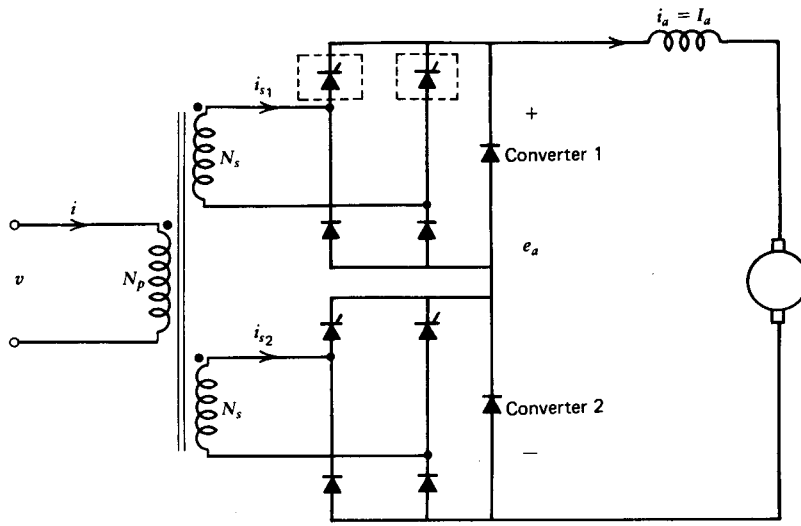


(a)

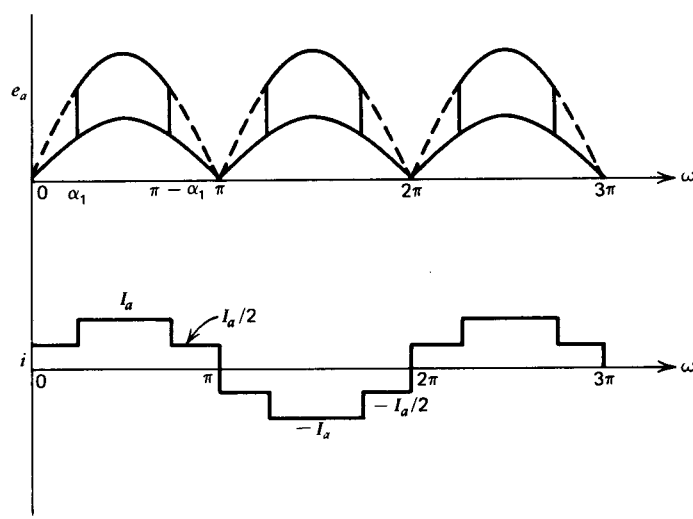


(b)

***Fig. 2.39*** Sequence control of series semi-converters. $N_s/N_p = 0.5$. (*a*) Power circuit. (*b*) Waveforms for symmetrical angle control.

$$PF = \frac{2\sqrt{2}\cos\alpha_1}{\pi\left(1 - \frac{2\alpha_1}{\pi}\right)^{1/2}} \tag{2.152}$$

$$DF = 1 \tag{2.153}$$

$$HF = \left[\frac{\pi(\pi - 2\alpha_1)}{8\cos^2\alpha_1} - 1\right]^{1/2} \tag{2.154}$$

**$0.5 < E_a < 1.0$ pu**

To control the output voltage in this range of $E_a$ the line commutated converter is fully turned on and the forced commutated converter is controlled ($0 < \alpha_1 < 90°$).

$$E_a = \tfrac{1}{2}(1 + \cos\alpha_1)\ \text{pu} \tag{2.155}$$

$$I = I_a\left(1 - \frac{3\alpha_1}{2\pi}\right)^{1/2} \tag{2.156}$$

$$I_n = \frac{\sqrt{2}\,I_a}{n\pi}(1 + \cos n\alpha_1) \tag{2.157}$$

$$\phi_n = 0 \tag{2.158}$$

$$PF = \frac{\sqrt{2}\,(1 + \cos\alpha_1)}{\pi\left(1 - \frac{3\alpha_1}{2\pi}\right)^{1/2}} \tag{2.159}$$

$$DF = 1 \tag{2.160}$$

$$HF = \left[\frac{\pi\left(\pi - \frac{3\alpha_1}{2}\right)}{2(1 + \cos\alpha_1)^2} - 1\right]^{1/2} \tag{2.161}$$

The power factor as function of the output voltage is shown in Fig. 2.41. A significant improvement in power factor is obtained in this control scheme.

***Sequence Control of Full-Converters***

Some applications require motoring as well as regenerative braking operation of the dc motors. In this case full-converters, as shown in Fig. 2.40*a*, are required. Because of the absence of the free-wheeling diodes the converters

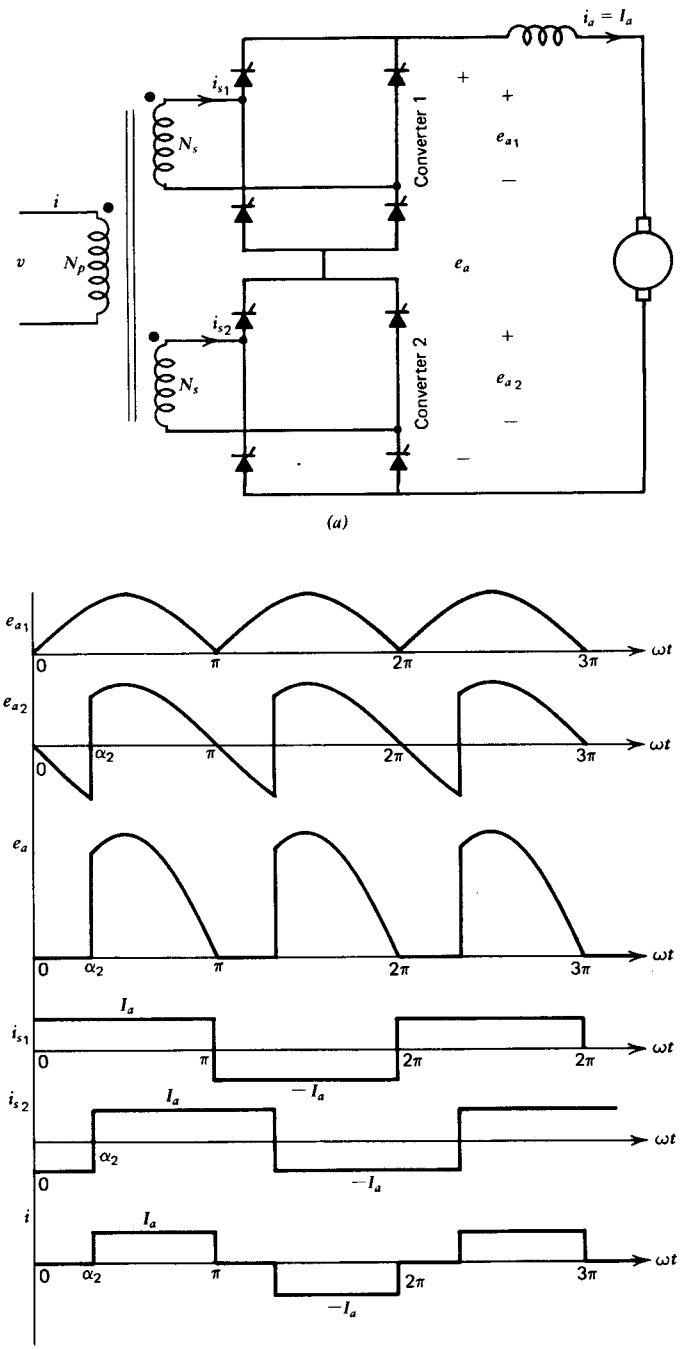


***Fig. 2.40*** Sequence control of full-converters. $N_s/N_p = 0.5$. (*a*) Power circuit. (*b*) Waveforms for rectification. (*c*) Waveforms for inversion.

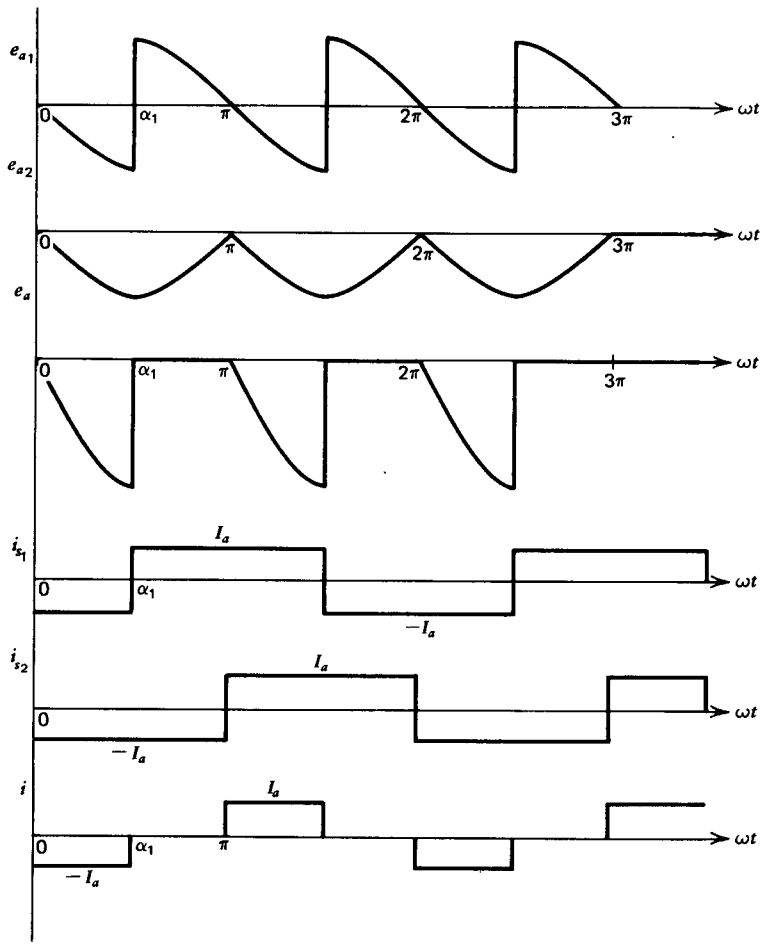


(c)

*Fig. 2.40* (*Continued*)

cannot be bypassed. Therefore both converters must stay in operation. Sequence control can be implemented by turning on one converter fully advanced (i.e., $\alpha = 0°$) or fully retarded (i.e., $\alpha = 180°$) and controlling the firing angle of the other converter.

In the rectifying (or motoring) mode of operation, the firing angle of converter 1 is kept fully advanced (i.e., $\alpha_1 = 0°$) and the firing angle of converter 2 is controlled in the range $0 < \alpha_2 < 180°$. This produces positive average output voltage. At $\alpha_2 = 0°$, both converters are fully turned on and the output voltage is maximum. At $\alpha_2 = 180°$, the output voltages of the two converters cancel each other, and thus the output voltage is zero. Voltage and current waveforms for $\alpha_1 = 0°$ and $\alpha_2 = 60°$ are shown in Fig. 2.40*b*.

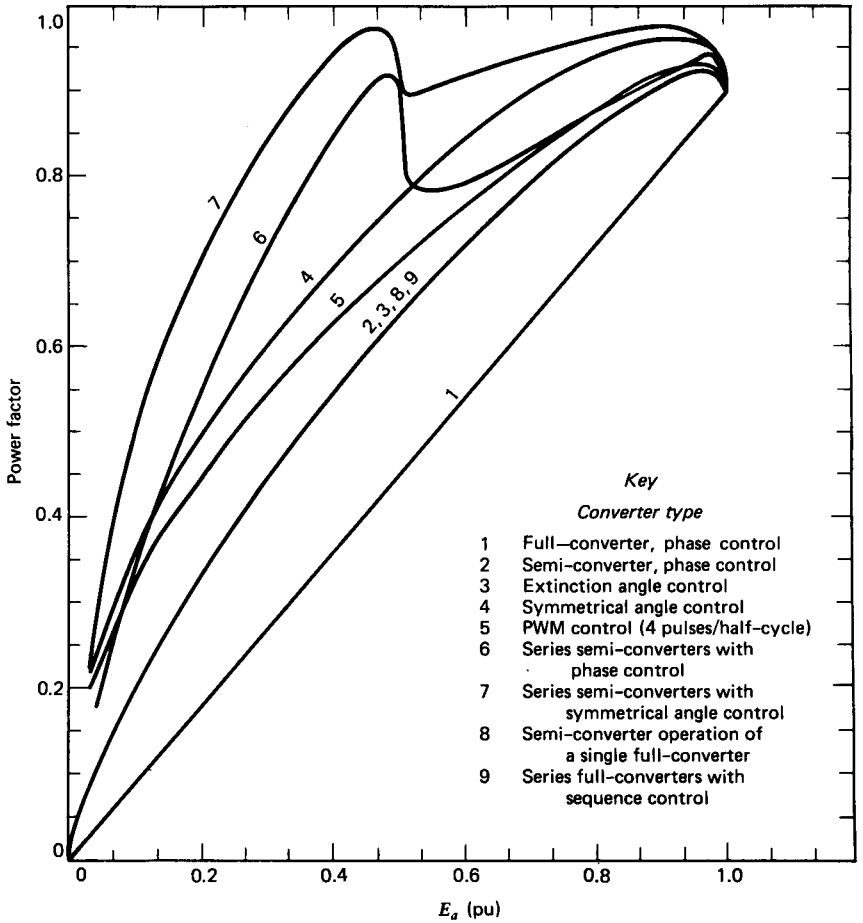


*Fig. 2.41* Supply power factor as a function of average motor voltage for various converter controls.

In the inverting (or regenerating) mode of operation, the firing angle of converter 2 may be kept fully retarded ($\alpha_2 = 180°$) while that of converter 1 is controlled in the range of $0 < \alpha_1 < 180°$. This produces negative average output voltage, as can be seen from the waveform for $e_a$ in Fig. 2.40*c*.

The waveforms of the supply current $i$ and the output voltage $e_a$ shown in Fig. 2.40 are the same as those obtained in a single phase-controlled semi-converter, and therefore the performance characteristics are similar. The sequence control of full-converters can provide the power factor of a single semi-converter. This power factor performance is better than that of a single full-converter but inferior to that of series operation of semi-converters.

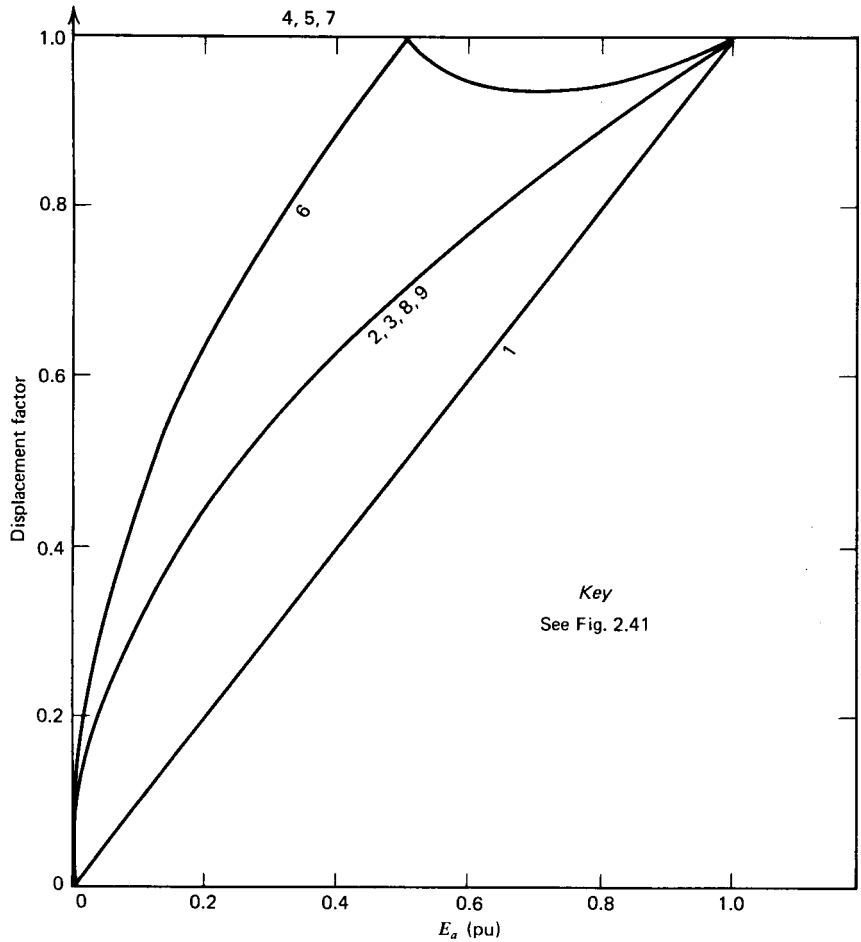


*Fig. 2.42* Supply displacement factor versus average motor voltage for various converter controls.

### 2.4.6 Comparative Evaluation of Schemes

Various techniques for improving the supply power factor of phase-controlled drives have been discussed in the preceding sections. The performance characteristics resulting from these control techniques are shown in Figs. 2.41 to 2.44 for convenience of comparison. Information about the total harmonic content (Fig. 2.43) is important only if input filters are not used. Current with high harmonic content may distort the supply voltage. In some control schemes the harmonic factor is high in the low-speed region (Fig. 2.43). This is due to high contents of higher-order harmonics, which are easily filtered out if input filters are used. The important current harmonics that the filter

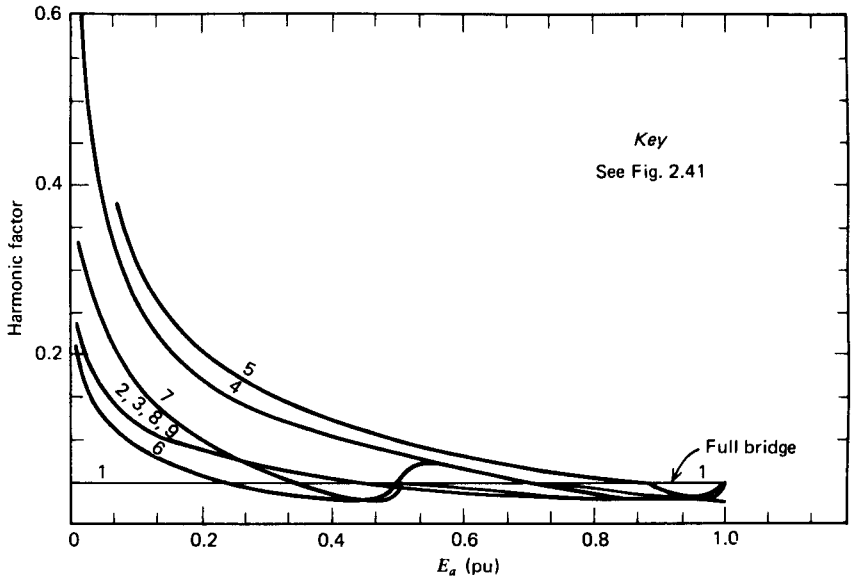


*Fig. 2.43* Harmonic factor as a function of average motor voltage for various converter controls.

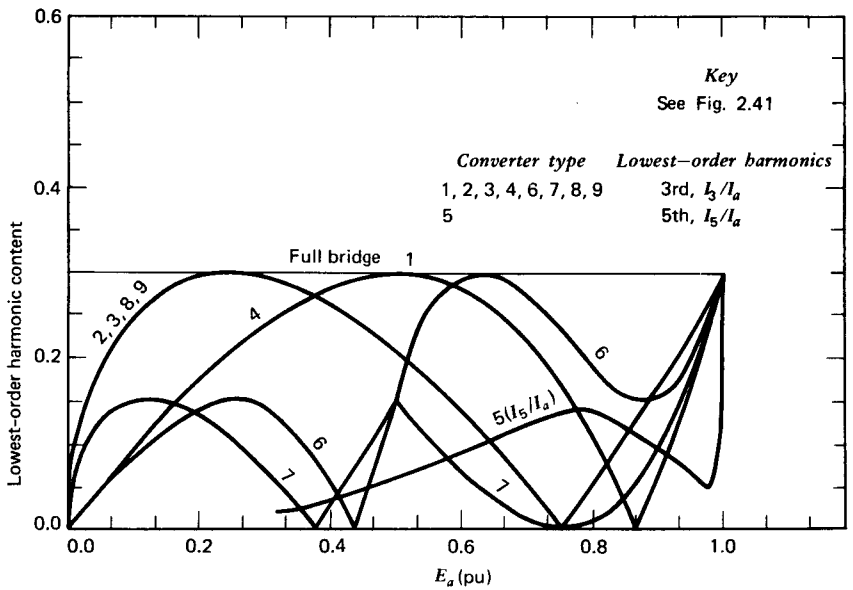


*Fig. 2.44* Lowest-order harmonic content in supply current as a function of average motor voltage for various converter controls.

designer needs to consider are those of the lowest order. In this respect, the PWM control scheme has an advantage, because by a proper choice of the number of pulses per half-cycle, the lowest-order harmonics can be eliminated. An input filter can eliminate most of the harmonic currents from the line, thereby making the line current essentially sinusoidal. A higher number of pulses per half-cycle increases the ripple frequency of the motor current. The armature circuit inductance may be sufficient to smooth out the motor current, and additional inductance may not be necessary in the armature circuit. The number of pulses per half-cycle should not be too large. If it is, the switching loss of the thyristors increases and special costly thyristors having low turn-off time are required. Six pulses per half-cycle appear to be a good choice, in which case harmonic currents below the seventh are eliminated. The PWM control scheme is receiving serious consideration in single-phase traction systems.[8, 12]

Power factor (Fig. 2.41) and displacement factor (Fig. 2.42) improve in forced commutation schemes. Extinction angle control and phase angle control schemes provide similar characteristics. However, extinction angle control makes power factor leading, which may be desirable in supply systems that feed other large inductive loads.

Sequence control of series converters improves supply power factor. Forced commutation in series connected converters can further improve power factor. This scheme has been tried in traction systems in Europe.[9] Of course, forced commutation of thyristors increases cost and complexity. However, improvement in power factor and other performance parameters may justify the added cost for a particular application.

## REFERENCES


1 G. R. Slemon, *Magnetoelectric Devices*, John Wiley & Sons, New York, 1966.

2 P. C. Sen and S. Mukhopadhyay, "On Solid State DC Motor Control," *IEEE Conference Record*, IGA-71, New York, 1971.

3 D. G. Moursund and C. S. Davis, *Elementary Theory and Application of Numerical Analysis*, McGraw-Hill Book Company, New York, 1967.

4 C. E. Robinson, "Redesign of DC Motors for Applications with Thyristor Power Supplies," *IEEE Transactions on Industry and General Applications*, Vol. IGA-4, No. 5, September 1968.

5 W. McMurray, "A Study of Asymmetrical Gating for Phase-Controlled Converters," *IEEE Transactions on Industry Applications*, Vol. IA-8, No. 3, May 1972.

6 P. Mehta and S. Mukhopadhyay, "Improvement in DC Motor Performance by Asymmetrical Triggering, Part I–One Quadrant Drive," *IEEE Conference Record*, IAS-77, New York, 1973.

7 S. R. Doradla and P. C. Sen, "Time Ratio Control (TRC) Scheme for a DC Series Motor, Part II: Commutation Circuit Analysis," *Canadian Electrical Engineering Journal*, Vol. 3, No. 2, April 1978.

8 T. Kataoka, K. Mizumachi, and S. Miyairi, "A Pulse-Width Controlled AC to DC Converter to Improve Power Factor and Waveform of AC Line Current," *IEEE Conference Record*, ISPCC-77, New York, 1977.

9 K. H. Bezold, J. Forster, and H. Zander, "Thyristor Converters for Traction DC Motor Drives," *IEEE Conference Record*, ISPCC-72, New York, 1972.

10 P. C. Sen and S. R. Doradla, "Evaluation of Control Schemes for Thyristor Controlled DC Motors," *IEEE Transactions on Industrial Electronics and Control Instrumentation*, Vol. IECI-25, No. 3, August 1978.

11 F. S. Acton, *Numerical Methods That Work*, Harper & Row, New York, 1970.

12 H. Kielgas and R. Nill, "Converter Propulsion Systems with 3-Phase Induction Motors for Electric Traction Vehicles," *IEEE Conference Record*, ISPCC-77, New York, 1977.

# 3

# Three-Phase Drives

Large-horsepower dc drives take power from three-phase sources. In such drives the drive motor is controlled by three-phase phase-controlled converters. Some of these converter circuits are shown in Table 3.1. The ripple frequency of the motor terminal voltage is higher than that of the single-phase converters. Consequently the filtering requirements for smoothing out the motor current are less. The motor current is mostly continuous, and therefore the motor performance is better compared to single-phase drives.

The three-phase half-wave converter is impractical for most purposes because the supply currents would contain dc components. Semi-converters and full-converters are most commonly used in practice. Dual-converters are used in reversible drives having power ratings as high as several megawatts.

## 3.1 SEMI-CONVERTER AND FULL-CONVERTER DRIVES

Understanding the operation of three-phase converters is not straightforward. In each cycle of the input supply, switching of the thyristors occurs several times. Each input cycle can thus be divided into several time intervals during which various pairs of devices conduct. In the following sections, the operation of three-phase converters is described with the help of waveforms during various time intervals.

### 3.1.1 Semi-Converter Operation

Figure 3.1 shows a three-phase semi-converter drive circuit and waveforms of voltages and currents. The diodes $D_1$, $D_2$, and $D_3$ conduct during the intervals $t_4$ to $t_6$, $t_6$ to $t_8$, and $t_2$ to $t_4$, respectively. If the thyristors $S_1$, $S_2$, and $S_3$ were diodes, they would conduct during the intervals $t_1$ to $t_3$, $t_3$ to $t_5$, and $t_5$ to $t_7$, respectively. Therefore the references for the triggering angles for $S_1$, $S_2$, and $S_3$ are the instants $t_1$, $t_3$, and $t_5$, respectively; that is, these are the crossing points of the phase voltages $v_A$, $v_B$, and $v_C$.

The firing instants of the thyristors are marked for the triggering angle $\alpha = 90°$. The interval at which thyristors are fired is 120°. Recall that the

***Table 3.1*** **Three-Phase Thyristor Phase-Controlled Converter Circuits**

| Circuit | Type | Typical hp | Ripple frequency | Quadrant operation |
|---|---|---|---|---|
| 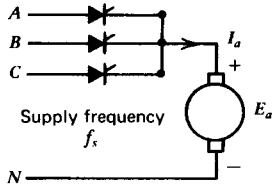 | Half-wave | 10-50 | $3f_s$ | 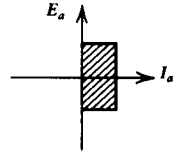 |
| 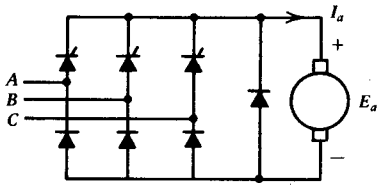 | Semi-converter | 15-150 ↑ limited for even harmonics | $3f_s$ | 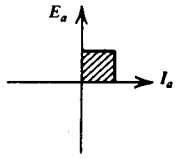 |
| 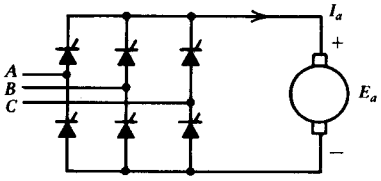 | Full-converter | 100-150 | $6f_s$ | 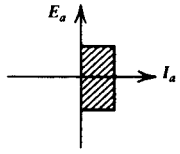 |
| 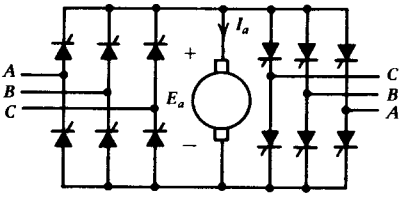 | Dual-converter | 200-2000 | $6f_s$ | 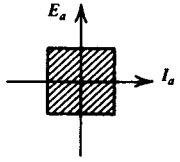 |

firing interval is 180° in single-phase converters. Thyristors are switched faster in three-phase converters, and therefore the time available for any current decay is less compared to the single-phase case. This tends to make the motor current continuous.

During the interval $(\pi/6 + \alpha) < \omega t < \omega t_4$, $S_1$ and $D_3$ conduct. Therefore motor terminal $X$ is connected to phase voltage $v_A$, and terminal $Y$ is connected to phase voltage $v_C$. Thus the motor terminal voltage during this period is $e_a = v_A - v_C = v_{AC}$. At $\omega t_4$, $e_a$ is zero, and from this time onward $e_a$ tends to be negative. The free-wheeling diode $D_{FW}$ thus becomes forward-biased at $\omega t_4$, and motor current flows through it until the next thyristor $S_2$ is turned on at $\pi/6 + \alpha + 2\pi/3$. In the absence of the free-wheeling diode, free-wheeling action would have taken place through $S_1$ and $D_1$. At large

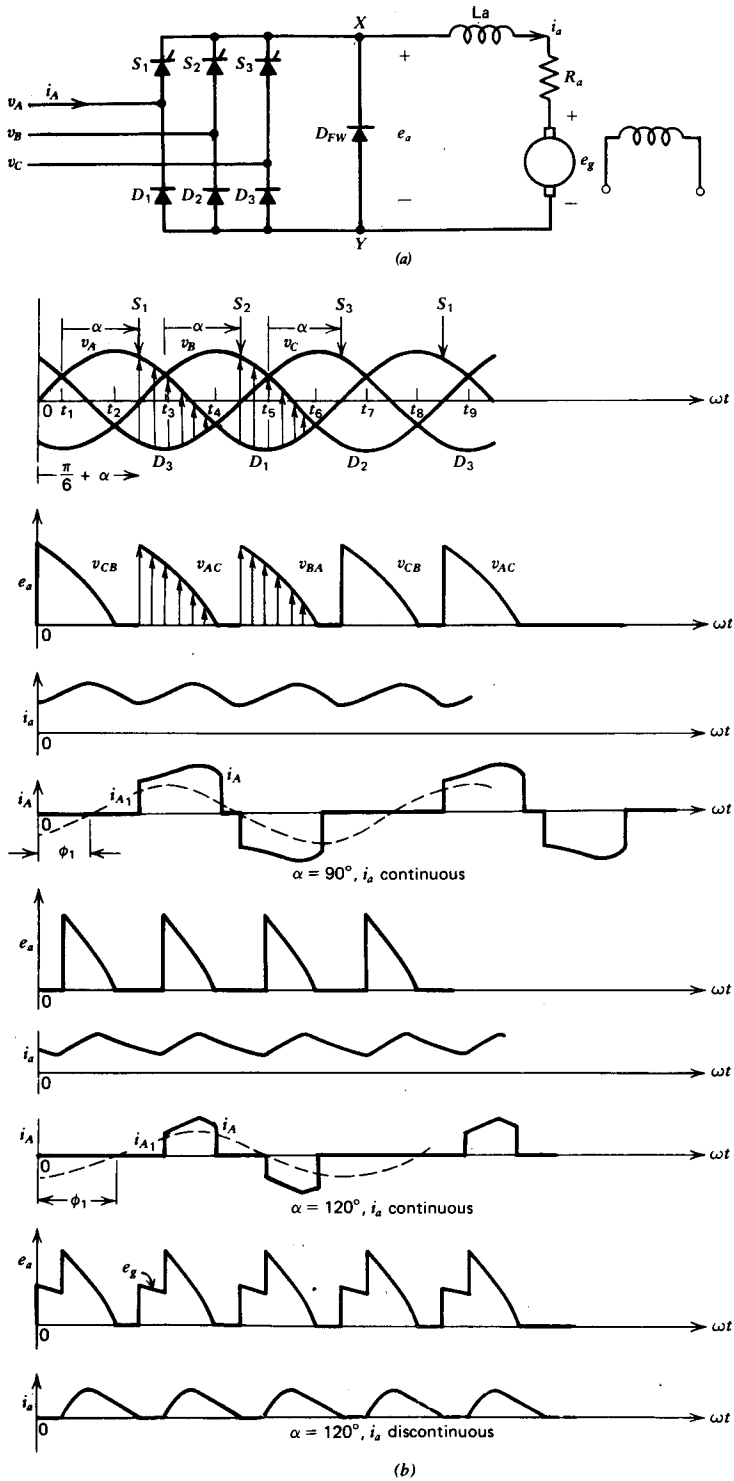


*Fig. 3.1* Three-phase semi-converter-controlled dc motor system. (*a*) Power circuit. (*b*) Waveforms for different firing angles.

firing angles the motor current can be continuous or discontinuous, depending on the current demand and speed.

If the current demand is low and the speed is not low, the motor current may be discontinuous at large firing angles. Waveforms of voltages and currents are shown in Fig. 3.1*b* at $\alpha = 120°$ for both continuous and discontinuous motor currents.

In terms of average voltages,

$$E_a(\alpha) = I_a R_a + E_g$$

$$= R_a I_a + K_a \Phi N$$

$$N = \frac{E_a(\alpha) - R_a I_a}{K_a \Phi} \tag{3.1}$$

Let the supply phase voltages be as follows.

$$v_A = \sqrt{2}\, V \sin \omega t$$

$$v_B = \sqrt{2}\, V \sin\left(\omega t - \frac{2\pi}{3}\right)$$

$$v_C = \sqrt{2}\, V \sin\left(\omega t + \frac{2\pi}{3}\right)$$

If the motor current is continuous,

$$E_a(\alpha) = \frac{3}{2\pi} \int_{\pi/6+\alpha}^{\pi/6+\alpha+2\pi/3} (v_A - v_C)\, d(\omega t)$$

$$= \frac{3\sqrt{6}\, V}{2\pi}(1 + \cos \alpha) \tag{3.2}$$

The fundamental component of the input current is shown dotted in Fig. 3.1*b*. The displacement angle $\phi_1$ increases as the firing angle increases. The input power factor will thus decrease as the firing angle increases.

### 3.1.2 Full-Converter Operation

Figure 3.2 shows a full-converter drive circuit and the voltage and current waveforms. The instants of firing the thyristors are marked for $\alpha = 60°$. The thyristors are fired at an interval of 60°, and the ripple in the motor terminal voltage is 6 pulses per cycle. Since the thyristors are triggered at a faster rate, the motor current is mostly continuous. The filtering requirement is therefore less than that in the semi-converter system.

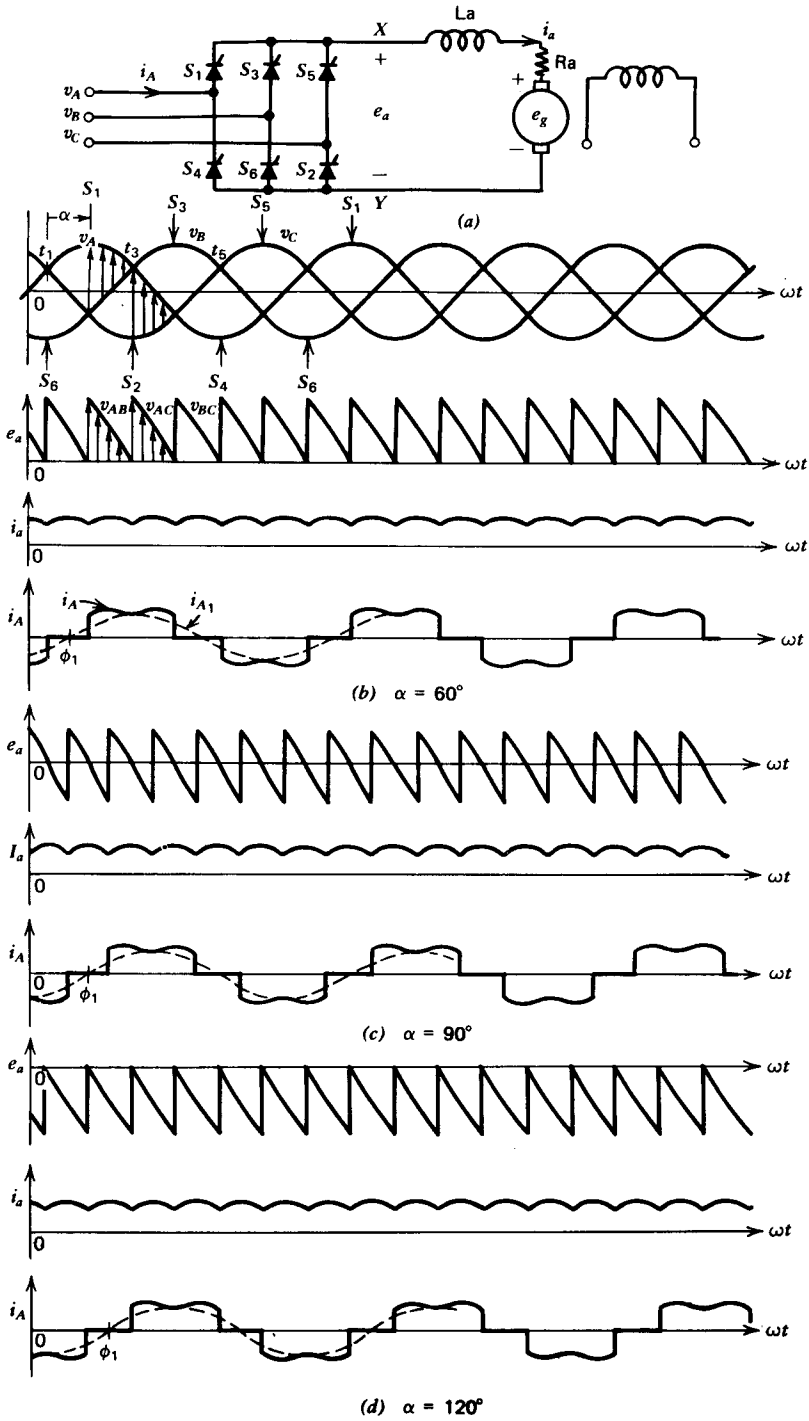


*Fig. 3.2* Three-phase full-converter drive system. (*a*) Power circuit. (*b*)–(*d*) Waveforms at different firing angles for continuous motor current.

At $\omega t = \pi/6 + \alpha$, $S_1$ turns on. Prior to this instant $S_6$ was turned on. Therefore, during the interval $(\pi/6 + \alpha) < \omega t < (\pi/6 + \alpha + \pi/3)$, thyristors $S_1$ and $S_6$ conduct, and the motor terminals are connected to phase $A$ and phase $B$, making $e_a = v_{AB}$. At $\omega t = \pi/6 + \alpha + \pi/3$, thyristor $S_2$ is fired, and immediately thyristor $S_6$ is reverse-biased and turns off (*natural* or *line* commutation). The current from $S_6$ is transferred to $S_2$, and therefore the motor terminals are connected to phase $A$ through $S_1$ and phase $C$ through $S_2$, making $e_a = v_{AC}$. This process repeats after every 60° whenever a thyristor is fired. Note that the thyristors are numbered in the sequence in which they are fired.

The motor terminal voltage can become negative, as shown in Fig. 3.2*d* for the triggering angle $\alpha = 120°$. This is the inversion mode of operation of the converter. If the motor voltage is reversed with a reversing contactor or by reversing the field current, power can be transferred from the motor to the ac supply. This is what is commonly known as *regeneration*. The motor will slow down due to power feedback, and thus the motor voltage will decrease. Therefore, as the motor slows down, the firing angle of the converter has to be adjusted to keep the current up and to regenerate power.

The average motor terminal voltage is

$$E_a(\alpha) = \frac{3}{\pi}\int_{\pi/6+\alpha}^{\pi/6+\alpha+\pi/3} (v_A - v_B)\,d(\omega t)$$

$$= \frac{3\sqrt{6}\,V}{\pi}\cos\alpha \tag{3.3}$$

The average speed is

$$N = \frac{E_a(\alpha) - R_a I_a}{K_a \Phi}$$

In a separately excited motor, $T = K_a \Phi I_a$. Therefore,

$$N = \frac{E_a(\alpha)}{K_a \Phi} - \frac{R_a}{(K_a \Phi)^2} T \tag{3.4}$$

The first term in equation 3.4 represents the ideal no-load ($T \simeq 0$) speed, which therefore depends on $E_a(\alpha)$. If the motor current is assumed continuous, motor terminal voltage $E_a$ depends only on the firing angle $\alpha$ and is given by equations 3.2 and 3.3 for the semi-converter and the full-converter, respectively. The variations of $E_a$ with $\alpha$ for continuous motor current are shown in Fig. 3.3. These curves also represent the theoretical no-load speed as a function of firing angle. The second term in equation 3.4 represents the decrease in speed as the motor torque increases. Since the armature circuit

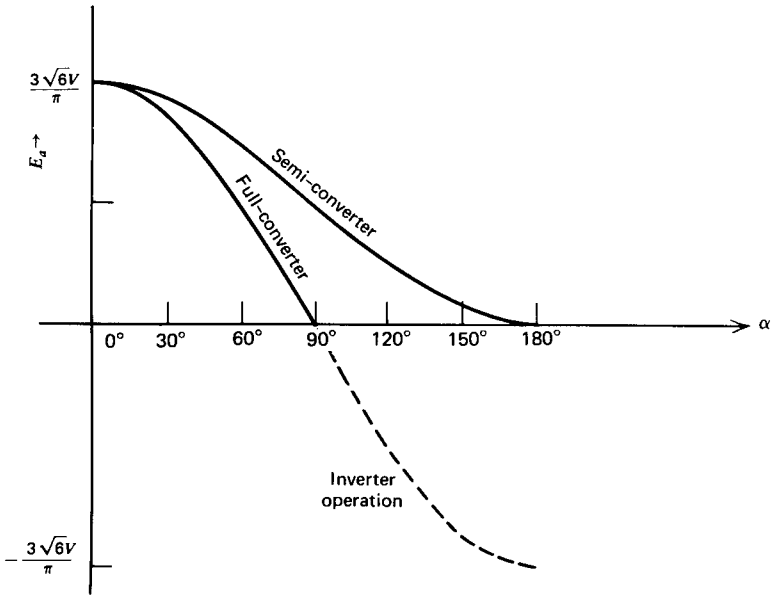


*Fig. 3.3* Average output voltage $E_a$ as a function of firing angle in three-phase converters for continuous motor current.

resistance $R_a$ is small, the decrease in speed is small (i.e., good speed regulation). In large motors, the motor current at no load (i.e., motor idling) is not small, and if a three-phase converter is used the motor current is likely to be continuous even at no-load condition. Therefore, three-phase drives provide better speed regulation and improved performance as compared to single-phase drives.

**Example 3.1**

The speed of a 125 hp, 600 V, 1800 rpm, separately excited dc motor is controlled by a 3$\phi$ (three-phase) full-converter. The converter is operated from a 3$\phi$, 480 V, 60 Hz supply. The rated armature current of the motor is 165 A. The motor parameters are $R_a = 0.0874\ \Omega$, $L_a = 6.5$ mH, and $K_a\Phi = 0.33$ V/rpm. The converter and ac supply are considered to be ideal.

1 Find no-load speeds at firing angles $\alpha = 0°$ and $\alpha = 30°$. Assume that at no load, the armature current is 10% of the rated current and is continuous.
2 Find the firing angle to obtain rated speed of 1800 rpm at rated motor current. Compute the supply power factor.
3 Compute the speed regulation for the firing angle obtained in part 2.

*Solution*

1 **No-Load Condition** The supply phase voltage is

$$V = \frac{480}{\sqrt{3}} = 277 \text{ V}$$

From equation 3.3 the motor terminal voltage is

$$E_a = \frac{3\sqrt{6} \times 277}{\pi} \cos\alpha = 648 \cos\alpha$$

For $\alpha = 0°$

$$E_a = 648 \text{ V}$$

$$E_g = E_a - I_a R_a$$

$$= 648 - (16.5 \times 0.0874)$$

$$= 646.6 \text{ V}$$

No-load speed is

$$N_0 = \frac{E_g}{K_a \Phi} = \frac{646.6}{0.33}$$

$$= 1959 \text{ rpm}$$

For $\alpha = 30°$

$$E_a = 648 \cos 30° = 561.2 \text{ V}$$

$$E_g = 561.2 - (16.5 \times 0.0874) = 559.8 \text{ V}$$

No-load speed is

$$N_0 = \frac{559.8}{0.33} = 1696 \text{ rpm}$$

2 **Full-Load Condition** Motor back emf $E_g$ at 1800 rpm is

$$E_g = 0.33 \times 1800 = 594 \text{ V}$$

Motor terminal voltage at rated current is

$$E_a = 594 + (165 \times 0.0874)$$

$$= 608.4 \text{ V}$$

Therefore,

$$648 \cos \alpha = 608 \text{ V}$$

$$\cos \alpha = \frac{608.4}{648} = 0.94$$

$$\alpha = 20.1°$$

At full-load condition, the ripple in the motor current is negligible. Therefore from Fig. 3.2 the supply current $i_A$ is a square wave of amplitude 165 A and width 120°. The rms value of the supply current is

$$I_A = \left(\frac{1}{\pi} \times 165^2 \times \frac{2\pi}{3}\right)^{1/2}$$

$$= \sqrt{\frac{2}{3}} \times 165$$

$$= 134.64 \text{ A}$$

Supply volt-ampere is

$$U = 3VI_A = 3 \times 277 \times 134.64$$

$$= 111{,}885.8 \text{ VA}$$

Assuming no losses in the converter, power from the supply $P_s$ is the same as the power input to the motor. Hence

$$P_s = E_a I_a = 608.4 \times 165$$

$$= 100{,}386 \text{ W}$$

Therefore, the supply power factor is

$$PF = \frac{P_s}{U} = \frac{100{,}386}{111{,}885.8} = 0.9$$

or, from equation 3.45,

$$PF = 0.9549 \cos 20.1° = 0.9$$

3 **Speed Regulation** At full-load condition motor current is 165 A and speed is 1800 rpm. If the load is thrown off keeping the firing angle the same at $\alpha = 20.1°$, the motor current decreases to 16.5 A. Therefore

$$E_g = 608.4 - (16.5 \times 0.0874)$$

$$= 606.96 \text{ V}$$

and no-load speed is

$$N_0 = \frac{606.96}{0.33} = 1839.3 \text{ rpm}$$

The speed regulation is

$$= \frac{1839.3 - 1800}{1800} \times 100\%$$

$$= 2.18\%$$

## 3.2 SERIES CONNECTED CONVERTERS

For high-voltage dc drives, either thyristors are connected in series in a converter or two converters can be connected in series. The latter arrangement can provide additional advantages in terms of improvement in supply power factor and higher ripple frequency. Three series arrangements of converters are shown in Fig. 3.4. The two secondaries of the transformer are phase-displaced by 30°. This provides higher output ripple frequency and minor improvement in input power factor. One of the converters connected in series can be uncontrolled as shown in Fig. 3.4*a*. This arrangement will result in reduced supply reactive Kilovolt-ampere (k*VAR*) and hence better power factor. In the following sections these series connected converters are described and their properties are investigated.

### 3.2.1 Input Power Factor

An important performance parameter of phase-controlled converter systems is the variation of supply power factor. The power factor is defined as

$$PF = \frac{I_{A_1}}{I_A} \cos\phi_1$$

$$= \mu \cos\phi_1 \tag{3.5}$$

where $I_A$ = rms input current
$I_{A_1}$ = rms fundamental input current
$\phi_1$ = phase angle between input fundamental current and supply voltage
$\mu = \frac{I_{A_1}}{I_A}$ = current distortion factor
$\cos\phi_1$ = displacement factor.

To obtain the power factor, one must determine $I_{A_1}$, $\phi_1$, and $I_A$.

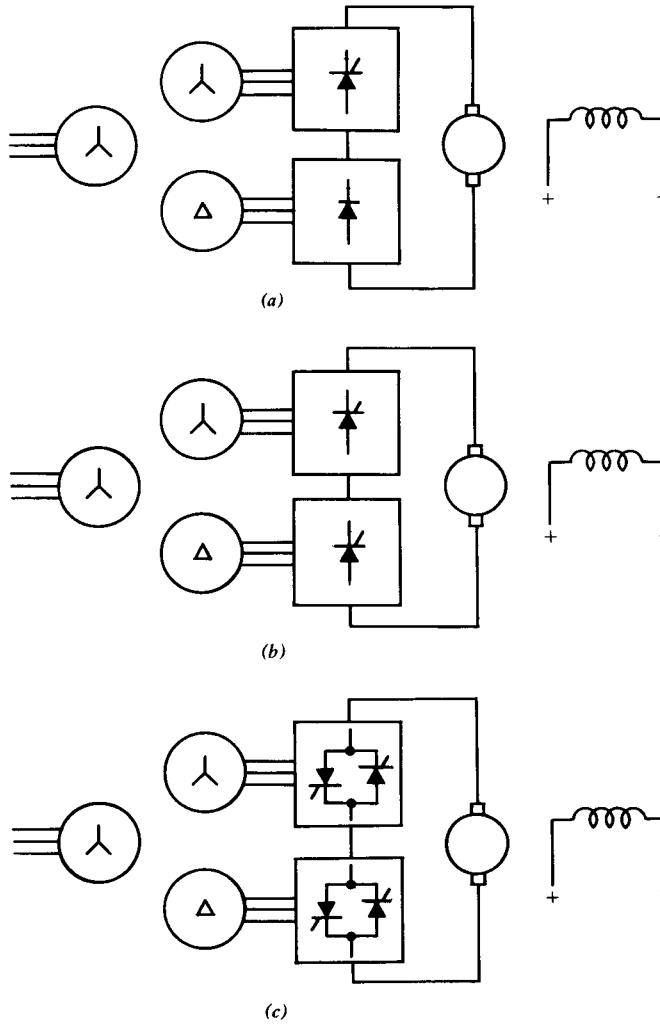


*Fig. 3.4* High-voltage converters. (*a*) Series converters, half controlled. (*b*) Series converters, fully controlled. (*c*) Series dual-converters, fully controlled.

### *Fundamental Current and Displacement Angle, $I_{A_1}$ and $\phi_1$*

The fundamental current $I_{A_1}$ and its phase angle $\phi_1$ can be obtained by finding the fundamental currents for the individual converters (Fig. 3.5*a*) and then adding them as phasor quantities:

$$I_{A_1}\underline{/\phi_1} = I_{s1_1}\underline{/\phi_{11}} + \sqrt{3}\, I_{s2_1}\underline{/\phi_{21}} \tag{3.6}$$

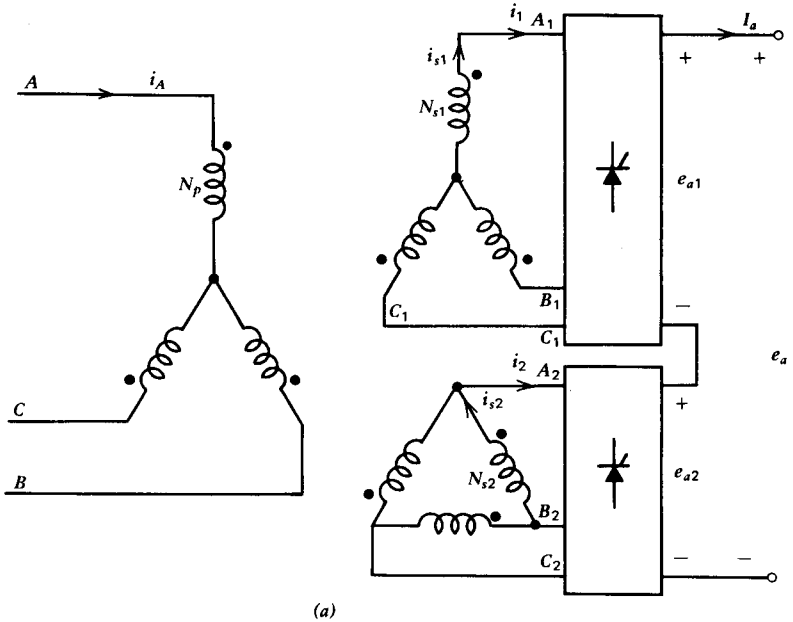


*Fig. 3.5* (*a*) Series converters, fully controlled. $N_{s1}/N_p = 1$; $N_{s2}/N_p = \sqrt{3}$. (*b*) Current division in delta connection.

where $I_{s1_1}\underline{/\phi_{11}}$ = fundamental current in phasor of the star secondary winding

$I_{s2_1}\underline{/\phi_{21}}$ = fundamental current in phasor of the delta secondary winding.

The fundamental current of the secondary winding $i_{sk_1}$ can be described as follows:

$$i_{sk_1} = A_k \sin \omega t + B_k \cos \omega t = C_k \sin(\omega t + \phi_{k1}) \tag{3.7}$$

where $k$ denotes the converter and

$$A_k = \frac{2}{\pi}\int_{\omega t}^{\pi+\omega t} i_{sk} \sin \omega t \, d(\omega t) \tag{3.8}$$

$$B_k = \frac{2}{\pi}\int_{\omega t}^{\pi+\omega t} i_{sk} \cos \omega t \, d(\omega t) \tag{3.9}$$

$$C_k = \sqrt{A_k^2 + B_k^2} \tag{3.10}$$

$$\phi_{k1} = \tan^{-1}\frac{B_k}{A_k} \tag{3.11}$$

$$I_{sk_1} = \frac{C_k}{\sqrt{2}} \tag{3.12}$$

***Rms Current $I_A$***

The rms input current can be determined from the resultant input current waveform as follows:

$$I_A = \left[\frac{1}{\pi}\int_{\omega t}^{\omega t+\pi} i_A^2 \, d(\omega t)\right]^{1/2} \tag{3.13}$$

### 3.2.2 Series Converters, Fully Controlled

The arrangement of two series connected full-converters is shown in Fig. 3.5*a*. The converters are connected to two secondaries of a transformer, the primary of which is connected in star. One secondary is connected in star, the other in delta.

Because of the series connection of the converters, the total output voltage is the sum of the individual converter output voltages.

$$e_a = e_{a1} + e_{a2} \tag{3.14}$$

For the sake of simplicity, assume that the output current $I_a$ is constant or ripple free. Because of series connection, this current will be the same for both converters.

In Fig. 3.6 voltage and current waveforms are drawn for a firing angle of 45°. The supply and transformer are considered ideal. The supply phase voltages (also the phase voltages of the star connected secondary if $n = 1$) are shown in Fig. 3.6*a*. In order to make the voltage output of the converters the same, a turn ratio of $\sqrt{3}$ is necessary between the windings of the delta and star secondaries. The line-to-line voltage of the delta secondary is phase

shifted by 30° with respect to the star secondary of primary as shown in Fig. 3.6*b* and *c*. The firing angle is measured, as before, from the zero crossing of the line-to-line voltage (such as $v_{AC}$). This is also the crossing point of the phase voltage $A$ and phase voltage $C$. The converter output voltages $e_{a1}$ and $e_{a2}$ for a 45° firing angle are shown in Fig. 3.6*b* and *c*, respectively. The total output voltage $e_a$ is shown in Fig. 3.6*d*.

The line current $(i_1, i_2)$ for each converter is a square wave of magnitude $I_a$ and a width of 120°. The line current $i_1$ for the star secondary is the same as its winding current $i_{s1}$, as shown in Fig. 3.6*e*. The three line currents for the delta secondary, each phase shifted from the other by 120°, are shown in Fig. 3.6*f*. The winding current $i_{s2}$ is obtained by considering the transformer secondary as a current divider as shown in Fig. 3.5*b*. Thus,

$$|i_{s2}| = \tfrac{2}{3} I_a \qquad \text{Lines } A_2 \text{ and } B_2 \text{ are both conducting.}$$

$$= \tfrac{1}{3} I_a \qquad \text{Only one of line } A_2 \text{ or } B_2 \text{ is conducting.}$$

This winding current $i_{s2}$ is shown in Fig. 3.6*g*. The primary current (i.e., supply line current) will be the sum of the secondary winding currents times the proper turns ratio. Thus

$$i_A = \left(i_{s1} + \sqrt{3}\, i_{s2}\right) n \tag{3.15}$$

where $n$ is the secondary-to-primary turns ratio of the star connection (i.e., $n = N_{s1}/N_p$). In this particular case $n$ is considered as unity. This line current $i_A$ is shown in Fig. 3.6*h*.

***Fundamental Current:*** $I_{A1} \underline{/ \phi_1}$

The coefficients of the fundamental current for the first converter are obtained by referring to Fig. 3.6*e* as follows. The angles are measured with respect to the primary phase voltage $v_A$.

$$A_1 = \frac{2}{\pi} \int_{\theta}^{\pi+\theta} i_{s1} \sin\theta \, d\theta$$

$$= \frac{2}{\pi} \int_{\pi/6+a}^{5\pi/6+\alpha} I_a \sin\theta \, d\theta$$

$$= \frac{2}{\pi} \sqrt{3} I_a \cos\alpha \tag{3.16}$$

$$B_1 = \frac{2}{\pi} \int_{\pi/6+\alpha}^{5\pi/6+\alpha} I_a \cos\theta \, d\theta$$

$$= -\frac{2}{\pi} \sqrt{3} I_a \sin\alpha \tag{3.17}$$

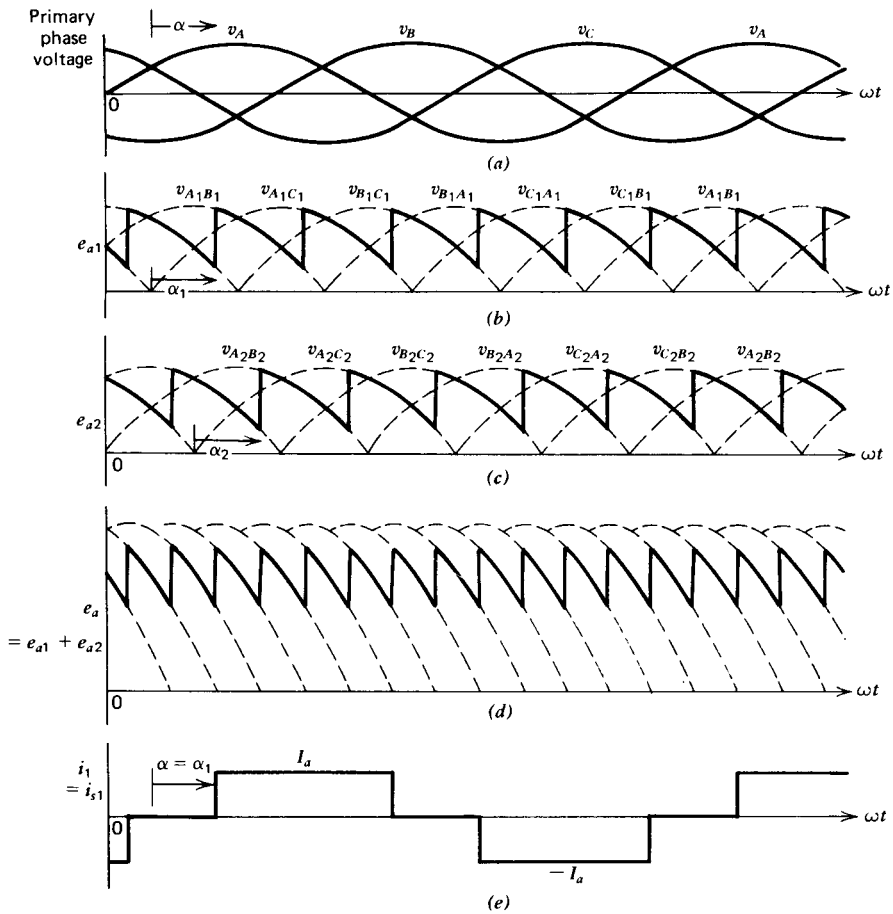


*Fig. 3.6* Waveforms for series converters, fully controlled. $\alpha = \alpha_1 = \alpha_2 = 45°$.

Thus,

$$I_{s1_1} = \frac{\left(A_1^2 + B_1^2\right)^{1/2}}{\sqrt{2}}$$

$$= \frac{\sqrt{6}}{\pi} I_a \tag{3.18}$$

$$\phi_{11} = \tan^{-1}\left(-\frac{\sin\alpha}{\cos\alpha}\right)$$

$$= -\alpha \tag{3.19}$$

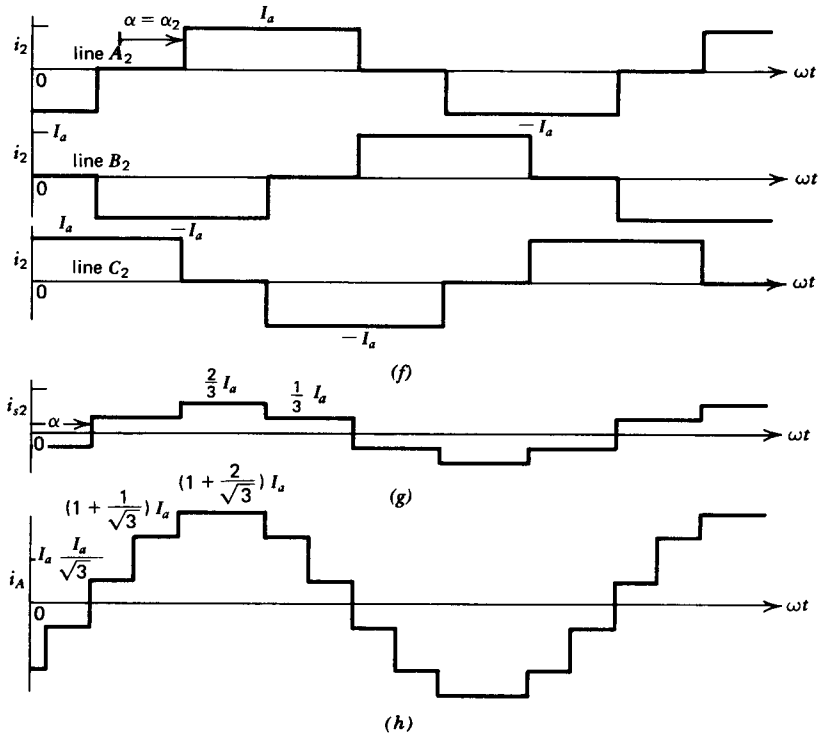


*Fig. 3.6* (*Continued*)

For the second converter, referring to Fig. 3.6*g*,

$$A_2 = \frac{2}{\pi}\left[\int_{\alpha}^{\alpha+\pi/3} \frac{I_a}{3} \sin\theta\, d\theta + \int_{\alpha+\pi/3}^{\alpha+2\pi/3} \frac{2I_a}{3} \sin\theta\, d\theta + \int_{\alpha+2\pi/3}^{\alpha+\pi} \frac{I_a}{3} \sin\theta\, d\theta\right]$$

$$= \frac{2}{\pi} I_a \cos\alpha \tag{3.20}$$

and similarly

$$B_2 = -\frac{2}{\pi} I_a \sin\alpha \tag{3.21}$$

Thus,

$$I_{s2_1} = \frac{\sqrt{2}}{\pi} I_a \tag{3.22}$$

$$\phi_{21} = -\alpha \tag{3.23}$$

The primary fundamental current is then

$$I_{A_1}\underline{/\phi_1} = \frac{\sqrt{6}}{\pi} I_a\underline{/-\alpha} + \sqrt{3}\,\frac{\sqrt{2}}{\pi} I_a\underline{/-\alpha}$$

$$= \frac{2\sqrt{6}}{\pi} I_a\underline{/-\alpha} \tag{3.24}$$

***Rms Supply Current $I_A$***

Note from Fig. 3.6 that as $\alpha$ changes, both $i_{s1}$ and $i_{s2}$ will be phase shifted by the same amount. Their wave shapes will remain unchanged. The supply current $i_A$, which is formed by these two currents, will thus retain its waveform but will be phase shifted as the firing angle $\alpha$ changes. The rms current is then given by

$$I_A = \left(\frac{1}{\pi}\int_{\alpha}^{\alpha+\pi} i_A^2\, d\theta\right)^{1/2} \tag{3.25}$$

Because of the symmetry, integration over a quarter-cycle is sufficient.

$$I_A = \left(\frac{2}{\pi}\int_{\alpha}^{\alpha+\pi/2} i_A^2\, d\theta\right)^{1/2}$$

$$= \left\{\frac{2}{\pi}\left[\int_{\alpha}^{\alpha+\pi/6}\left(\frac{I_a}{\sqrt{3}}\right)^2 d\theta + \int_{\alpha+\pi/6}^{\alpha+\pi/3}\left(1+\frac{1}{\sqrt{3}}\right)^2 I_a^2\, d\theta \right.\right.$$

$$\left.\left. + \int_{\alpha+\pi/3}^{\alpha+\pi/2}\left(1+\frac{2}{\sqrt{3}}\right)^2 I_a^2\, d\theta\right]\right\}^{1/2}$$

$$= \left(\frac{4+2\sqrt{3}}{3}\right)^{1/2} I_a \tag{3.26}$$

***Input Power Factor***

The current distortion factor from equations 3.24 and 3.26 is

$$\mu = \frac{I_{A_1}}{I_A} = 0.9886 \tag{3.27}$$

which is constant and independent of firing angle.

From equation 3.24, $\phi_1 = -\alpha$. Therefore, the input power factor for the fully controlled series converters is

$$PF = \mu\cos\phi_1 = 0.9886\cos\alpha \tag{3.28}$$

### 3.2.3 Series Converters, Half Controlled

The arrangement shown in Fig. 3.7 is similar to that in Fig. 3.5*a* except that a diode bridge replaces one of the SCR bridges. Here the diode converter is considered to be connected to the delta secondary of the transformer.

The voltage and current waveforms are shown in Fig. 3.8 for a firing angle of 45° for the SCR converter. As the firing angle changes, the shape of the output voltage $e_{a1}$ and the phase of the input current $i_1$ of the SCR converter change. However, the output voltage of the diode converter $e_{a2}$ is independent of the firing angle. Besides, the input current of the diode bridge, represented by $i_{s2}$, does not shift in phase with respect to the primary voltage. The operation of the diode converter corresponds to an SCR converter being fired at 0° at all times. The primary or supply current $i_A$ is therefore composed of a current $i_{s2}$ whose phase and shape remain unaltered and a current $i_{s1}$ whose shape remains unaltered but whose phase angle changes with the firing angle of the SCR-converter. The shape of the current $i_A$ therefore changes with the firing angle, whereas it does not change in the case of series connected fully controlled converters.

#### *Fundamental Current $I_{A1}/\phi_I$*

The waveforms of the series-connected controlled converter and diode bridge (Fig. 3.7) are shown in Fig. 3.8. The fundamental current in the controlled

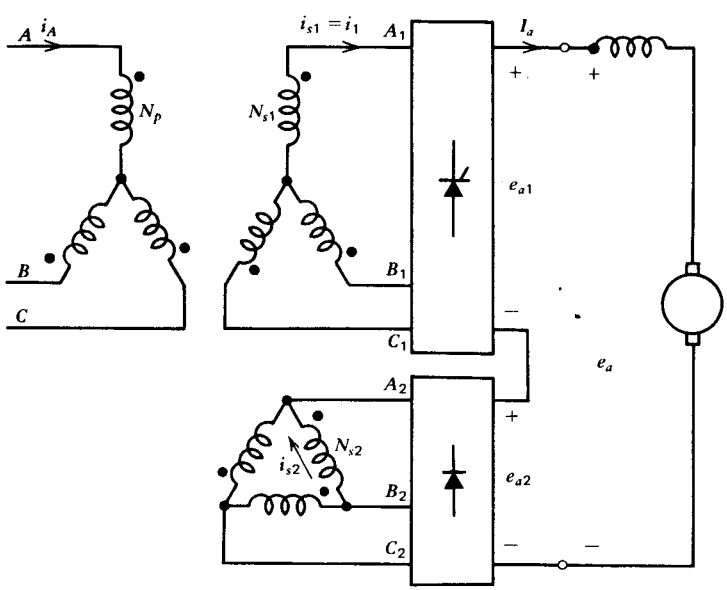


*Fig. 3.7* Series converters, half controlled.

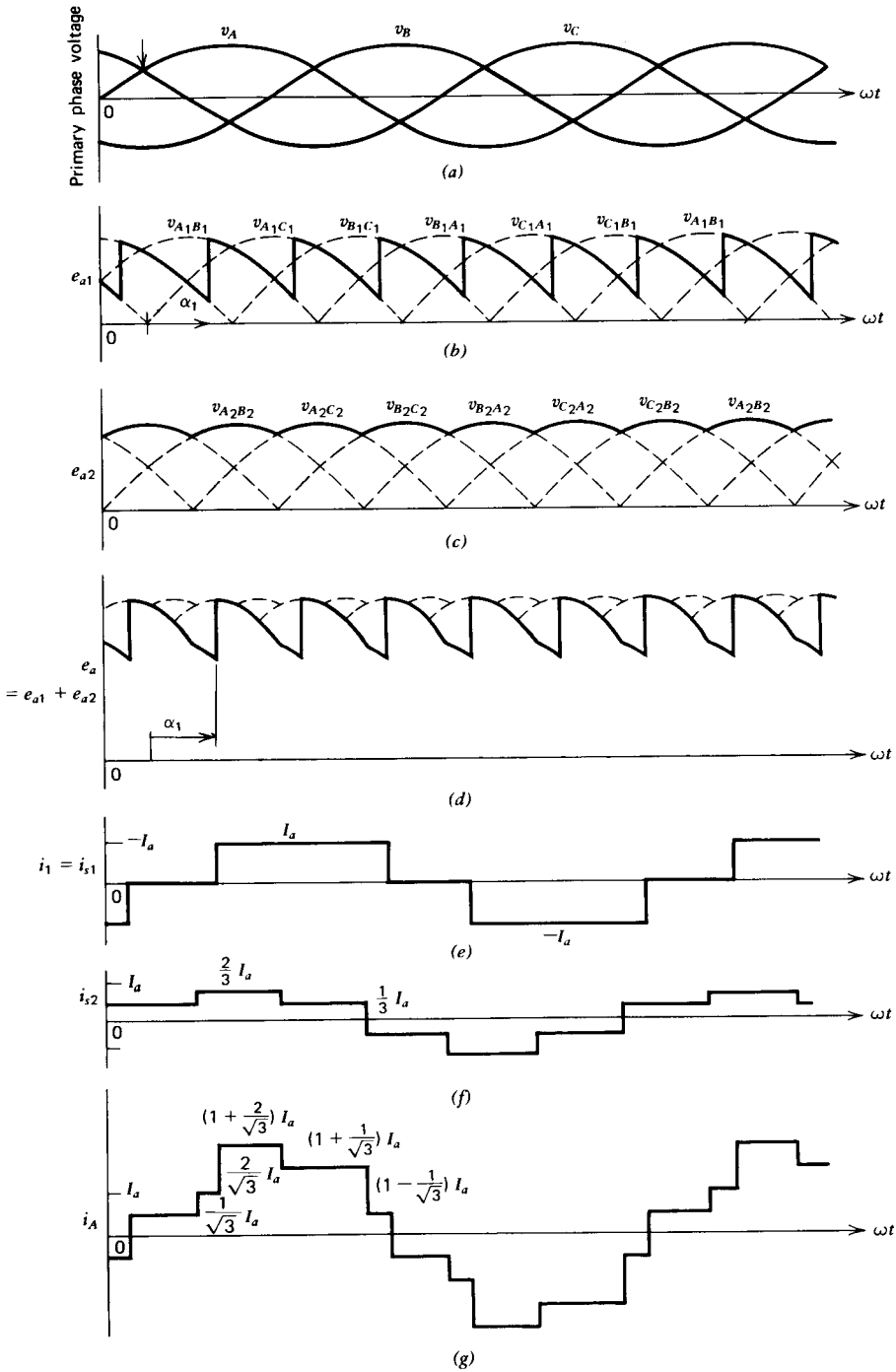


***Fig. 3.8*** Waveforms for series converters, half controlled.

converter will be the same as before, as given by equations 3.18 and 3.19:

$$I_{s1_1} = \frac{\sqrt{6}}{\pi} I_a \tag{3.29}$$

$$\phi_{11} = -\alpha \tag{3.30}$$

In the diode bridge, the current waveform shown in Fig. 3.8*f* does not change in shape and phase. It corresponds to a controlled converter with a zero firing angle. Thus, from equations 3.22 and 3.23

$$I_{s2_1} = \frac{\sqrt{2}}{\pi} I_a \tag{3.31}$$

$$\phi_{21} = 0° \tag{3.32}$$

The primary fundamental current is then

$$I_{A_1}\underline{/\phi_1} = \frac{\sqrt{6}}{\pi} I_a\underline{/-\alpha} + \sqrt{3}\,\frac{\sqrt{2}}{\pi} I_a\underline{/0°}$$

$$= \frac{2\sqrt{6}}{\pi} I_a \cos\frac{\alpha}{2}\underline{/-\frac{\alpha}{2}} \tag{3.33}$$

The fundamental current magnitude therefore changes with the firing angle.

***Rms Current $I_A$***

The waveshape of the primary current $i_A$ as shown in Fig. 3.8*g* changes with the firing angle. Therefore computation of rms input current is not straightforward. However, expressions for rms current can be obtained for different ranges of the firing angle.

**$0 < \alpha < \pi/6$**

The secondary winding currents and the supply current for a firing angle in this range are shown in Fig. 3.9*a*. Note that the total interval during which the resultant current $i_A$ has a given magnitude remains the same. Thus the rms current is constant although the waveshape changes as the firing angle is changed.

From Fig. 3.9*a*,

$$I_A = \left\{ \frac{1}{\pi}\left[ \int_{\pi/3}\left(\frac{I_a}{\sqrt{3}}\right)^2 d\theta + \int_{\pi/3} I_a^2\left(1+\frac{1}{\sqrt{3}}\right)^2 d\theta + \int_{\pi/3} I_a^2\left(1+\frac{2}{\sqrt{3}}\right)^2 d\theta \right]\right\}^{1/2}$$

$$= I_a\left(\frac{4+2\sqrt{3}}{3}\right)^{1/2} \tag{3.34}$$

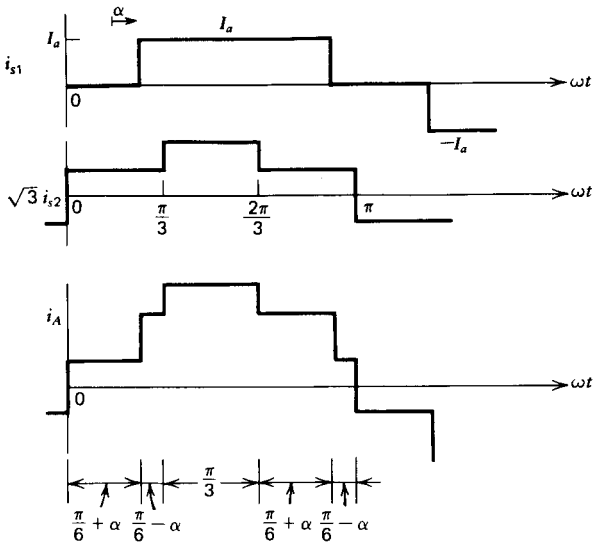


| Magnitude of $i_A$ | Interval |
|---|---|
| $\frac{I_a}{\sqrt{3}}$ | $(\frac{\pi}{6}+\alpha)+(\frac{\pi}{6}-\alpha)=\frac{\pi}{3}$ |
| $I_a\,(1+\frac{1}{\sqrt{3}})$ | $(\frac{\pi}{6}-\alpha)+(\frac{\pi}{6}+\alpha)=\frac{\pi}{3}$ |
| $I_a\,(1+\frac{2}{\sqrt{3}})$ | $\frac{\pi}{3}$ |

(a) $0<\alpha<\frac{\pi}{6}$

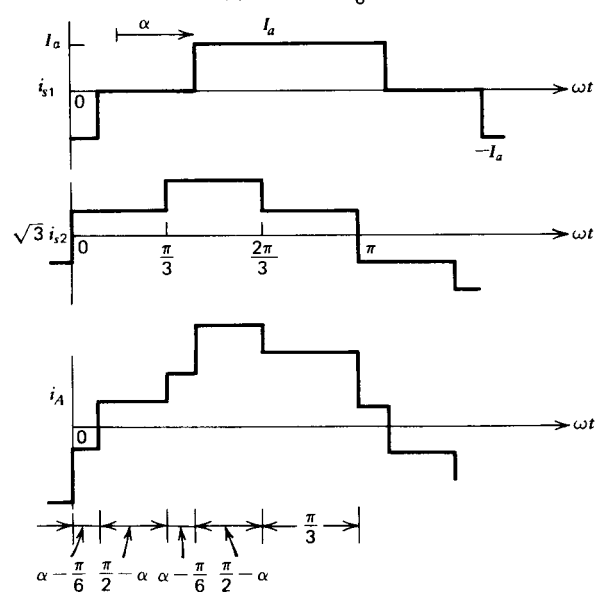


| Magnitude of $i_A$ | Interval |
|---|---|
| $I_a\,(\frac{1}{\sqrt{3}}-1)$ | $\alpha-\frac{\pi}{6}$ |
| $\frac{I_a}{\sqrt{3}}$ | $\frac{\pi}{2}-\alpha$ |
| $I_a\,\frac{2}{\sqrt{3}}$ | $\alpha-\frac{\pi}{6}$ |
| $I_a\,(1+\frac{2}{\sqrt{3}})$ | $\frac{\pi}{2}-\alpha$ |
| $I_a\,(1+\frac{1}{\sqrt{3}})$ | $\frac{\pi}{3}$ |

(b) $\frac{\pi}{6}<\alpha<\frac{\pi}{2}$

***Fig. 3.9*** Current waveforms for different ranges of firing angles in series converters, half controlled.

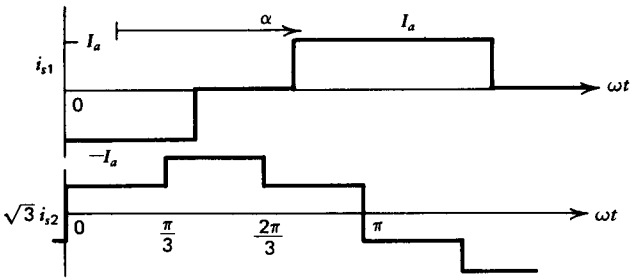


| Magnitude of $i_A$ | Interval |
|---|---|
| $I_a\left(\frac{1}{\sqrt{3}}-1\right)$ | $\frac{\pi}{3}$ |
| $I_a\left(\frac{2}{\sqrt{3}}-1\right)$ | $\alpha-\frac{\pi}{2}$ |
| $I_a\frac{2}{\sqrt{3}}$ | $\frac{5\pi}{6}-\alpha$ |
| $\frac{I_a}{\sqrt{3}}$ | $\alpha-\frac{\pi}{2}$ |
| $I_a\left(1+\frac{1}{\sqrt{3}}\right)$ | $\frac{5\pi}{6}-\alpha$ |

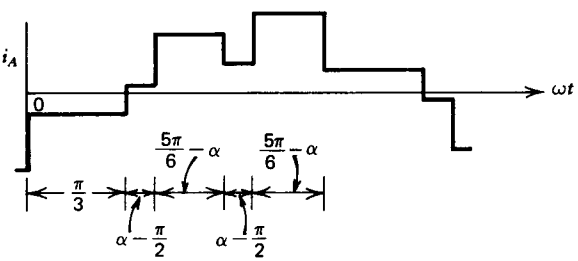


(c) $\frac{\pi}{2}<\alpha<\frac{5\pi}{6}$

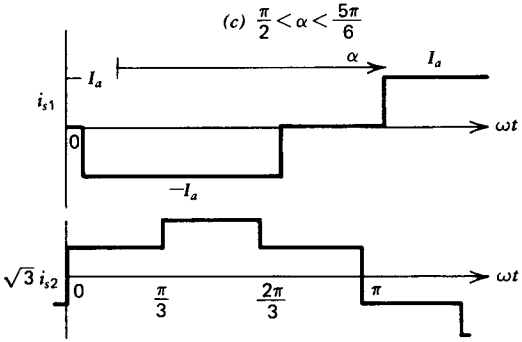


| Magnitude of $i_A$ | Interval |
|---|---|
| $\frac{I_a}{\sqrt{3}}$ | $\alpha-\frac{5\pi}{6}+\frac{7\pi}{6}-\alpha=\frac{\pi}{3}$ |
| $I_a\left(\frac{1}{\sqrt{3}}-1\right)$ | $\frac{7\pi}{6}-\alpha+\alpha-\frac{5\pi}{6}=\frac{\pi}{3}$ |
| $I_a\left(\frac{2}{\sqrt{3}}-1\right)$ | $\frac{\pi}{3}$ |

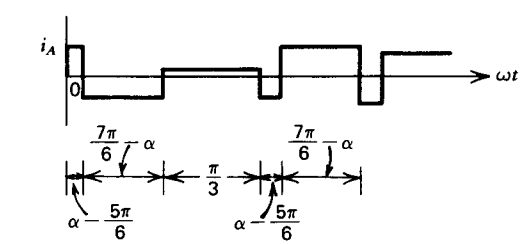


(d) $\frac{5\pi}{6}<\alpha<\pi$

***Fig. 3.9*** ***(Continued)***

This interval ends when the rising edge of $i_{s1}$ coincides with the rising edge of the second step of $i_{s2}$ (i.e., $\omega t = \pi/3$ or $\alpha = \pi/6$).

$$\frac{\pi}{6} < \alpha < \frac{\pi}{2}$$

The supply current waveform for a firing angle in this range is shown in Fig. 3.9*b*. Observe that the interval during which the current has a given magnitude depends on the value of the firing angle. Therefore the rms current also changes with the firing angle. From Fig. 3.9*b*,

$$I_A = \left\{ \frac{1}{\pi} \left[ \int_{\alpha-\pi/6} I_a^2 \left( \frac{1}{\sqrt{3}} - 1 \right)^2 d\theta + \int_{\pi/2-\alpha} \left( \frac{I_a}{\sqrt{3}} \right)^2 d\theta \right.\right.$$

$$+ \int_{\alpha-\pi/6} \left( \frac{2I_a}{\sqrt{3}} \right)^2 d\theta + \int_{\pi/2-\alpha} I_a^2 \left( 1 + \frac{2}{\sqrt{3}} \right)^2 d\theta$$

$$\left.\left. + \int_{\pi/3} I_a^2 \left( 1 + \frac{1}{\sqrt{3}} \right)^2 d\theta \right] \right\}^{1/2}$$

$$= I_a \left[ \frac{4 + 2\sqrt{3}}{3} - \frac{2\sqrt{3}}{\pi} \left( \alpha - \frac{\pi}{6} \right) \right]^{1/2} \tag{3.35}$$

This interval ends when the rising edge of $i_{s1}$ coincides with the falling edge of the second step of $i_{s2}$ (i.e., $\omega t = 2\pi/3$ or $\alpha = \pi/2$).

$$\frac{\pi}{2} < \alpha < \frac{5\pi}{6}$$

Figure 3.9*c* shows the supply current waveform for a firing angle in this region. The rms current is given by

$$I_A = \left\{ \frac{1}{\pi} \left[ \int_{\pi/3} I_a^2 \left( \frac{1}{\sqrt{3}} - 1 \right)^2 d\theta + \int_{\alpha-\pi/2} I_a^2 \left( \frac{2}{\sqrt{3}} - 1 \right)^2 d\theta \right.\right.$$

$$+ \int_{5\pi/6-\alpha} \left( \frac{2I_a}{\sqrt{3}} \right)^2 d\theta + \int_{\alpha-\pi/2} \left( \frac{I_a}{\sqrt{3}} \right)^2 d\theta$$

$$\left.\left. + \int_{5\pi/6-\alpha} I_a^2 \left( 1 + \frac{1}{\sqrt{3}} \right)^2 d\theta \right] \right\}^{1/2}$$

$$= I_a \left[ \frac{4 + 2\sqrt{3}}{3} - \frac{2\sqrt{3}}{\pi} \left( \alpha - \frac{\pi}{6} \right) \right]^{1/2} \tag{3.36}$$

The expression for the rms current is thus the same over the range $\pi/6 < \alpha < 5\pi/6$. The interval ends when the rising edge of $i_{s1}$ coincides with the falling edge of the third step of $i_{s2}$ (i.e., $\omega t = \pi$ or $\alpha = 5\pi/6$).

$$\frac{5\pi}{6} < \alpha < \pi$$

Figure 3.9*d* shows the current waveform for a firing angle in this region. The interval during which the current has a given magnitude is constant. The rms current therefore remains constant.

$$I_A = \left\{\frac{1}{\pi}\left[\left(\frac{I_a}{\sqrt{3}}\right)^2\left(\frac{\pi}{3}\right) + I_a^2\left(\frac{1}{\sqrt{3}} - 1\right)^2\left(\frac{\pi}{3}\right) + I_a^2\left(\frac{2}{\sqrt{3}} - 1\right)^2\left(\frac{\pi}{3}\right)\right]\right\}^{1/2}$$

$$= I_a\left(\frac{4 - 2\sqrt{3}}{3}\right)^{1/2} \tag{3.37}$$

Equation 3.37 can be written in the following form.

$$I_A = I_a\left[\frac{4 + 2\sqrt{3}}{3} - \frac{2\sqrt{3}}{\pi}\left(\frac{2\pi}{3}\right)\right]^{1/2} \tag{3.38}$$

A general equation for the rms supply current can be written from equations 3.34, 3.35, 3.36, and 3.38:

$$I_A = I_a\left(\frac{4 + 2\sqrt{3}}{3} - \frac{2\sqrt{3}}{\pi}\alpha^*\right)^{1/2} \tag{3.39}$$

where $\alpha^* = 0°$ if $0 < \alpha < \frac{\pi}{6}$

$= \alpha - \frac{\pi}{6}$ if $\frac{\pi}{6} < \alpha < \frac{5\pi}{6}$

$= \frac{2\pi}{3}$ if $\frac{5\pi}{6} < \alpha < \pi$

***Power Factor***

From equations 3.33 and 3.39, the current distortion factor is

$$\mu = \frac{\dfrac{2\sqrt{6}}{\pi}\cos\left(\dfrac{\alpha}{2}\right)}{\left(\dfrac{4 + 2\sqrt{3}}{3} - \dfrac{2\sqrt{3}}{\pi}\alpha^*\right)^{1/2}} \tag{3.40}$$

and from equations 3.5 and 3.33, the power factor is

$$PF = \mu \cos\left(\frac{\alpha}{2}\right) \tag{3.41}$$

### 3.2.4 Series Converters with Unshifted Voltage

In the above derivations, the voltages at the input to the series converters are shifted due to the star–delta connection of the secondary windings. This is expected to improve certain aspects of performance. For comparison, fully controlled series converters with unshifted voltage input to the converters are considered in this section. Two types of control, identical control and sequence control, are investigated.

***Identical Control***

In identical control of series connected full-converters, both converters have the same firing angle. This arrangement is therefore equivalent to a single full-converter operating from twice the supply voltage. The fundamental current, from equation 3.18, is

$$I_{A_1} = 2\frac{\sqrt{6}}{\pi} I_a \tag{3.42}$$

The rms current from Fig. 3.6*e* is

$$I_A = \left\{ \frac{1}{\pi}\left[(2I_a)^2\right]\frac{2\pi}{3} \right\}^{1/2} \tag{3.43}$$

The current distortion factor is

$$\mu = \frac{I_{A_1}}{I_A} = 0.9549 \tag{3.44}$$

The power factor is

$$PF = 0.9549 \cos\alpha \tag{3.45}$$

***Sequence Control***

In sequence control[1] of series connected full-converters, one converter is fired at a fully advanced angle (i.e., $\alpha = 0°$) or fully retarded angle (i.e., $\alpha = 180°$), and the firing angle of the other converter is, controlled to provide a variable dc output voltage. In the rectifying (or motoring) mode of operation, the firing angle of one converter, say converter 1 (Fig. 3.10*a*), is kept fully advanced (i.e., $\alpha_1 = 0°$), and the firing angle of converter 2 is controlled in the

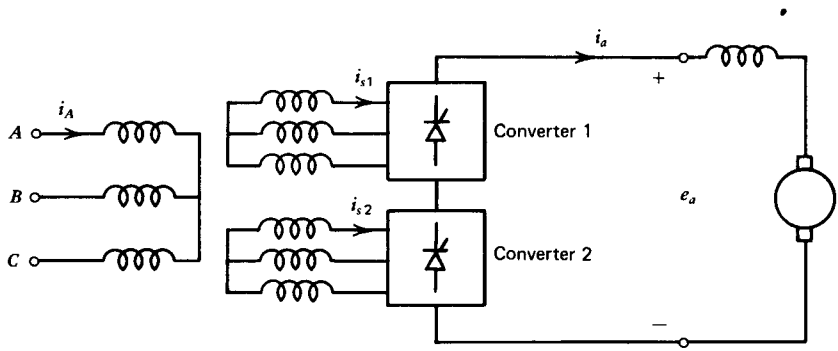


(a)

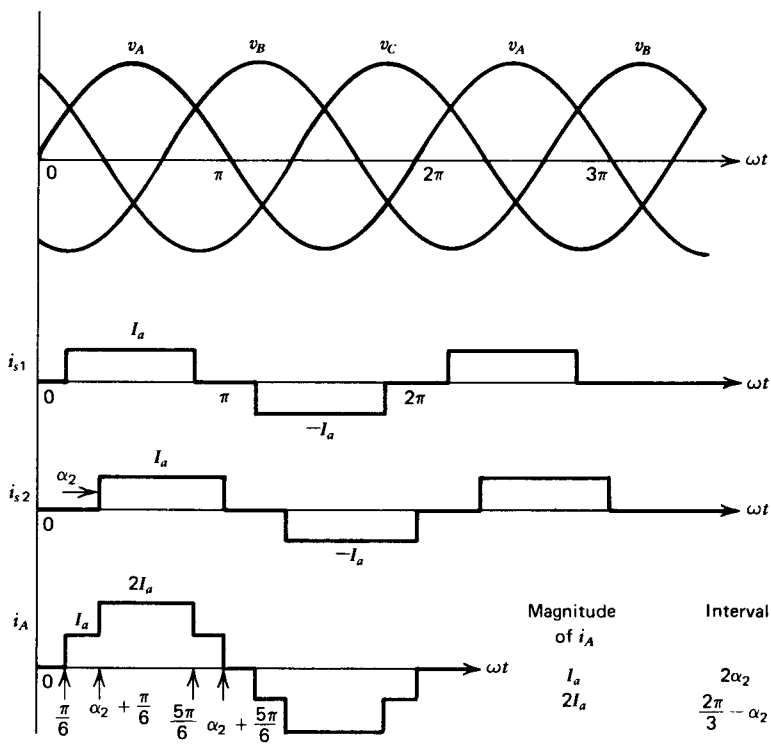


(b) $0 < \alpha_2 < \pi/3$

***Fig. 3.10*** **Sequence control of series converters. (*a*) Power circuit. (*b*)–(*d*) Current waveforms for different ranges of the firing angle.**

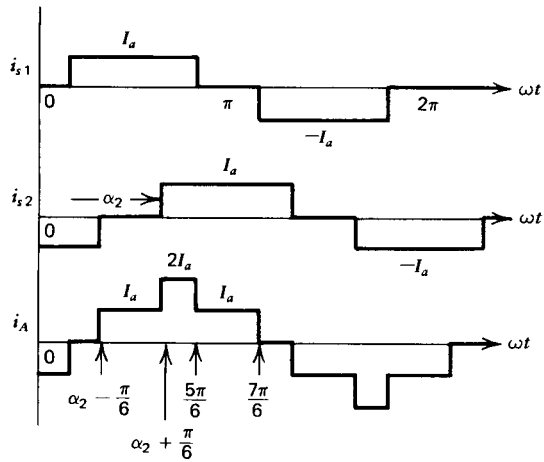


| Magnitude of $i_A$ | Interval |
|---|---|
| $I_a$ | $\frac{2\pi}{3}$ |
| $2I_a$ | $\frac{2\pi}{3} - \alpha_2$ |

(c) $\frac{\pi}{3} < \alpha_2 < \frac{2\pi}{3}$

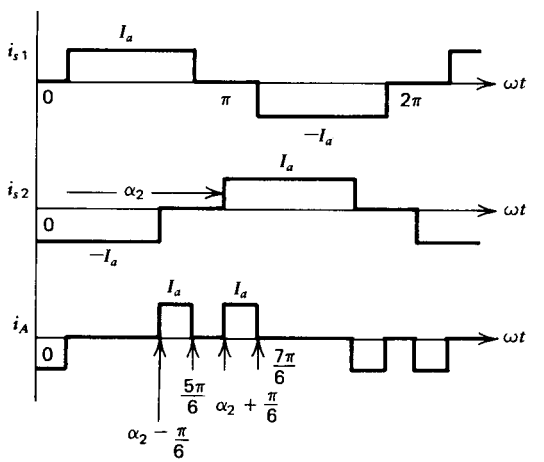


| Magnitude of $i_A$ | Interval |
|---|---|
| $I_a$ | $2\pi - 2\alpha_2$ |

(d) $\frac{2\pi}{3} < \alpha_2 < \pi$

***Fig. 3.10*** *(Continued)*

range $0 < \alpha_2 < 180°$. This produces positive average output voltage. At $\alpha_2 = 0°$, both converters are fully turned on, and the output voltage is maximum. At $\alpha = 180°$, the average output voltages of the two converters cancel each other, and thus the net average output voltage is zero. In the inverting (or regenerating) mode of operation, the firing angle of converter 2 may be kept fully retarded (i.e., $\alpha_2 = 180°$) and that of converter 1 is controlled in the range of $0 < \alpha_1 < 180°$. This produces negative average output voltage.

***Fundamental Current $I_{A_1}$*** If converter 1 is fully advanced (i.e., $\alpha_1 = 0°$), then the fundamental current due to this converter is from equations 3.18 and 3.19,

$$I_{s1_1}\underline{/\phi_{11}} = \frac{\sqrt{6}}{\pi} I_a \underline{/0°} \tag{3.46}$$

The firing angle $\alpha_2$ of converter 2 is changed, and the fundamental current due to converter 2 is

$$I_{s2_1}\underline{/\phi_{21}} = \frac{\sqrt{6}}{\pi} I_a \underline{/-\alpha_2} \tag{3.47}$$

The primary fundamental current, from equations 3.46 and 3.47, is

$$I_{A_1}\underline{/\phi_1} = \frac{\sqrt{6}}{\pi} I_a \underline{/0°} + \frac{\sqrt{6}}{\pi} I_a \underline{/-\alpha_2}$$

$$= \frac{2\sqrt{6}}{\pi} I_a \cos\frac{\alpha_2}{2} \underline{/-\frac{\alpha_2}{2}} \tag{3.48}$$

***Rms Current $I_A$*** The waveforms of the converter currents and the primary line current are also shown in Fig. 3.10. As the firing angle $\alpha_2$ of converter 2 changes, the waveform of the converter currents does not change but that of the primary line current does.

$0 < \alpha < \frac{\pi}{3}$

The current waveforms for a firing angle in this range are shown in Fig. 3.10*b*. The interval during which the supply current has a given magnitude depends on the value of the firing angle $\alpha_2$. The rms current is given by

$$I_A = \left\{ \frac{1}{\pi} \left[ \int_{2\alpha_2} I_a^2 \, d\theta + \int_{2\pi/3-\alpha_2} (2I_a)^2 \, d\theta \right] \right\}^{1/2}$$

$$= I_a \left( \frac{8}{3} - \frac{2\alpha_2}{\pi} \right)^{1/2} \tag{3.49}$$

This interval ends when the falling edge of the positive half-cycle of $i_{s2}$ coincides with the front edge of the negative half-cycle of $i_{s1}$.

$\frac{\pi}{3} < \alpha_2 < \frac{2\pi}{3}$

Figure 3.10*c* shows the current waveforms for a firing angle in this range. The rms line current is

$$I_A = \left\{ \frac{1}{\pi} \left[ \int_{2\pi/3} I_a^2 \, d\theta + \int_{2\pi/3-\alpha_2} (2I_a)^2 \, d\theta \right] \right\}^{1/2}$$

$$= I_a \left( \frac{10}{3} - \frac{4\alpha_2}{\pi} \right)^{1/2} \tag{3.50}$$

This interval ends when the rising edge of $i_{s2}$ coincides with the falling edge of $i_{s1}$.

$\frac{2\pi}{3} < \alpha_2 < \pi$

Figure 3.10*d* shows the current waveforms for a firing angle in this range. The rms line current is

$$I_A = \left( \frac{1}{\pi} \int_{2\pi-2\alpha_2} I_a^2 \, d\theta \right)^{1/2}$$

$$= I_a \left( 2 - \frac{2\alpha_2}{\pi} \right)^{1/2} \tag{3.51}$$

***Power Factor*** From equation 3.48 the supply power factor is given by

$$PF = \frac{I_{A_1}}{I_A} \cos \phi_1$$

$$= \frac{\frac{2\sqrt{6}}{\pi} I_a \cos\left(\frac{\alpha_2}{2}\right)}{I_A} \cos\left(\frac{\alpha_2}{2}\right) \tag{3.52}$$

where $I_A$ is obtained from equations 3.49, 3.50, and 3.51.

### 3.2.5 Power Factor Characteristics

In the previous sections four circuit configurations for series connection of converters have been considered. With shifted converter voltage, power factor as a function of firing angle can be computed from equation 3.28 for fully controlled converters and from equations 3.40 and 3.41 for half-controlled converters. With unshifted converter voltage, power factor can be computed

from equation 3.45 for identical control and from equation 3.52 for sequence control. We are, however, more interested in seeing the variation of power factor with the average output voltage rather than with the firing angle.

***Normalized Output Voltage***

The dc output voltage for identical control of series full-converters with shifted or unshifted converter voltage is given, from equation 3.3, by

$$E_a = 2 \times \frac{3\sqrt{6}}{\pi} V \cos\alpha$$

$$= E_{\max} \cos\alpha \tag{3.53}$$

where

$$E_{\max} = \frac{2 \times 3\sqrt{6}}{\pi} V$$

The normalized output voltage is

$$\frac{E_a}{E_{\max}} = \cos\alpha \tag{3.54}$$

For half-controlled converters with shifted converter voltage or for sequence control of full-converters with unshifted converter voltage, the dc output voltage is

$$E_a = \frac{3\sqrt{6}}{\pi} V \cos 0° + \frac{3\sqrt{6}}{\pi} V \cos\alpha$$

$$= \frac{E_{\max}}{2}(1 + \cos\alpha) \tag{3.55}$$

The normalized output voltage is

$$\frac{E_a}{E_{\max}} = \frac{1 + \cos\alpha}{2} \tag{3.56}$$

***Power Factor Evaluation***

The supply power factor is plotted against the normalized output voltage in Fig. 3.11 for the four circuit configurations studied in this section. It can be seen that half-controlled series converters or sequence control of full-converters provide improved power factor compared with that obtained using identical control (i.e., for the same firing angle) of full-converters. If full regeneration is not required, half-controlled series converters can be used for

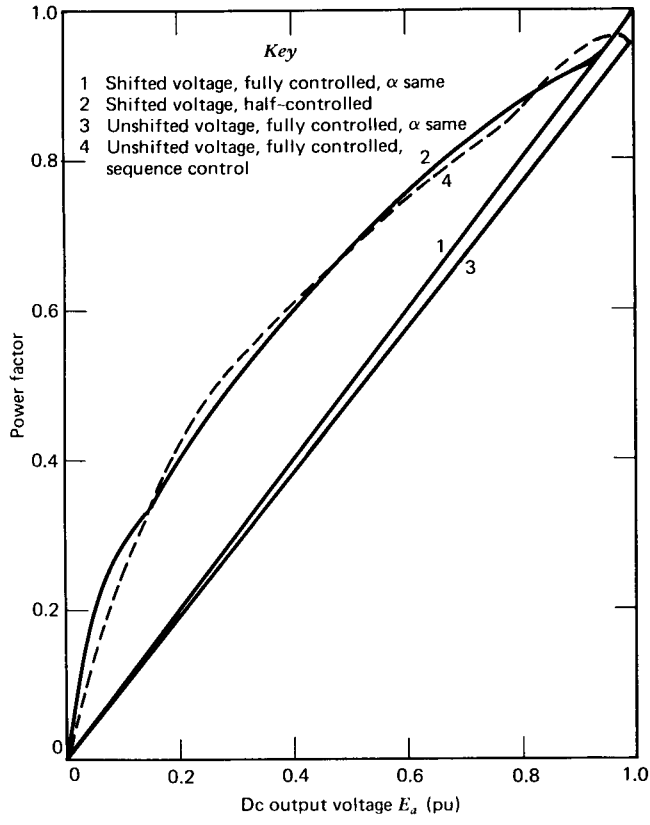


*Fig. 3.11* Supply power factor as a function of dc output voltage in series converters.

the sake of economy. On the other hand, if full regeneration is required, series full-converters with sequence control can be used. These two schemes provide essentially the same power factor. Note further that the voltage shifting has insignificant effects on the power factor. However, voltage shifting for series full-converters makes the ripple frequency 12 times the supply frequency (as shown in Fig. 3.6*d*); whereas the ripple frequency is 6 times the supply frequency (as shown in Fig. 3.8*d*) in the half-controlled series converters. Higher ripple frequency reduces the filtering requirements in the dc output.

## 3.3 DUAL-CONVERTER

A single full-converter provides unidirectional current at the dc terminals, but the voltage of the dc terminals can be reversed. It is thus capable of providing only two-quadrant operation.

If two full-converters are connected back-to-back, both the voltage and

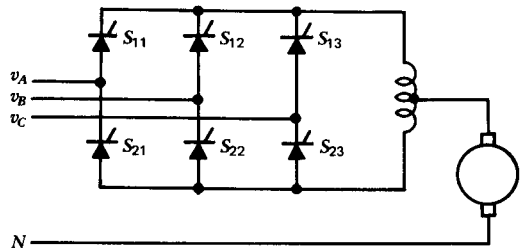


(a) 3-Pulse dual-converter

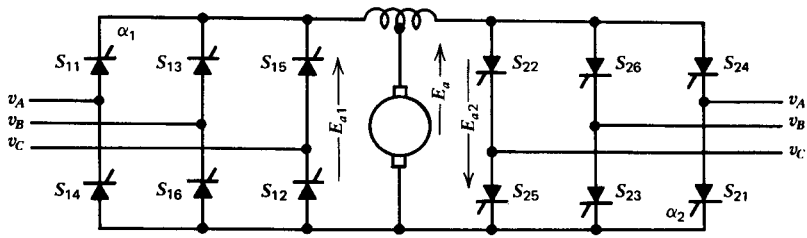


(b) 6-Pulse (bridge) dual-converter

*Fig. 3.12* Dual-converters.

the current at the dc terminals can reverse, and therefore the system will provide four-quadrant operation. Such a system, shown in Fig. 3.12, is called a *dual-converter*. This system is normally used for high-power dc drives, with power levels in the megawatt range, for speed control in both directions. In fact, the dual-converter is the static version of the Ward-Leonard motor-generator set.

### 3.3.1 Ideal Dual-Converter

Assume that the converters are ideal and that they produce pure dc output voltage, that is, there is no ac ripple at the dc output terminals. The magnitude of the dc voltages varies as the cosine of the firing angles of the converters, according to equation 3.3. The converters can be replaced, as shown in Fig. 3.13*a*, by a dc voltage source in series with diodes that represent unidirectional current flow characteristic of the converters.[2]

The firing angles of both converters are regulated by a control voltage $E_c$ so that their dc voltages are always exactly equal and of the same polarity. Thus, both converters produce the same terminal voltage, one converter operating as a rectifier and the other operating as an inverter.

Therefore, from equation 3.3

$$E_{a1} = E_{\max} \cos \alpha_1 \qquad V_{01} = 1.35 V_L \cos\alpha_1 \tag{3.57}$$

DC values

$$E_{a2} = E_{\max} \cos \alpha_2 \qquad V_{02} = 1.35 V_L \cos\alpha_2 \tag{3.58}$$

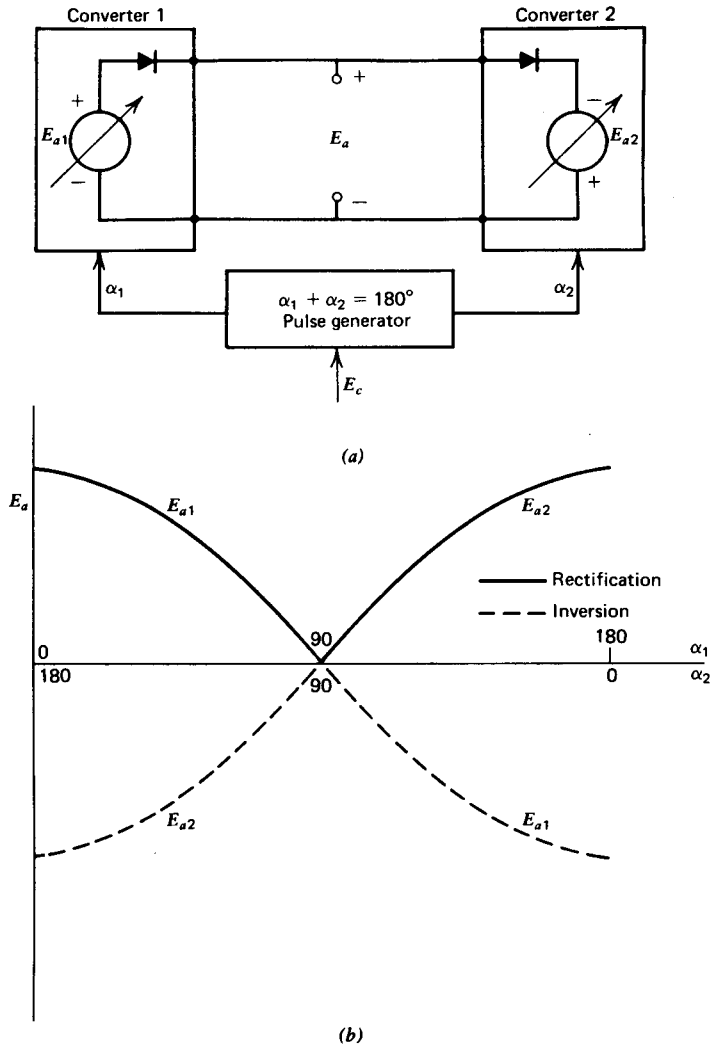


*Fig. 3.13* Ideal dual-converter. (*a*) Equivalent circuit. (*b*) Firing angle versus terminal voltage.

In an ideal dual-converter,

$$E_a = E_{a1} = -E_{a2} \tag{3.59}$$

From equations 3.57, 3.58, and 3.59

$$E_{\max} \cos \alpha_1 = -E_{\max} \cos \alpha_2 \tag{3.60}$$

or

$$\cos \alpha_1 + \cos \alpha_2 = 0 \tag{3.61}$$

Hence,

$$\alpha_1 + \alpha_2 = 180° \tag{3.62}$$

Figure 3.13*b* shows terminal voltage as a function of firing angle for the two converters. A firing control circuit can be evolved such that as the control signal $E_c$ changes, $\alpha_1$ and $\alpha_2$ will change in such a way as to satisfy equation 3.62.

In this ideal dual-converter, the load terminal voltage is the same as the converter voltages, and the current has equal freedom to flow through either converter.

### *Firing Control Scheme*

The basic principle of the firing control scheme is shown in Fig. 3.14. Recall that the references for triggering angles of the thyristors are the crossing points of the phase voltages. For thyristors $S_{11}$ and $S_{21}$ of Fig. 3.12*b*, the reference for the triggering angles $\alpha_1$ and $\alpha_2$ is the instant $t_1$ shown in Fig. 3.14*a*. If the voltage $v_A$ is phase shifted (advanced) by 60° to produce a voltage $e_A$, its peak voltage will coincide with this instant $t_1$. A control voltage $E_c$ can be used to produce triggering pulses for $S_{11}$ at the crossing points with $e_A$. Similarly, a voltage $e'_A$, which is the inverse of $e_A$, can produce triggering pulses for $S_{21}$. If $E_c$ is varied, the relationship $\alpha_1 + \alpha_2 = 180°$ will be maintained. Triggering pulses for two values of the control voltage $E_c$ are shown in Fig. 3.14*c*.

However, phase shifting of the voltage by 60° can be avoided. Figure 3.14*a* shows that, at $t_1$, the voltage $v_B$ is at negative maximum. The trigger pulses generated by comparing the control voltage $E_c$ with $v_B$ and its inverse can be used to trigger $S_{11}$ and $S_{21}$. These two schemes are shown in Fig. 3.15.

Let

$$e_A = K\cos\theta \tag{3.63}$$

$$e'_A = -K\cos\theta \tag{3.64}$$

Thus,

$$E_c = K\cos\alpha_1 \tag{3.65}$$

$$E_c = -K\cos\alpha_2 \tag{3.66}$$

From equations 3.65 and 3.66

$$\cos\alpha_1 + \cos\alpha_2 = 0$$

or $\alpha_1 + \alpha_2 = 180$, which satisfies the desired relationship of equation 3.62.

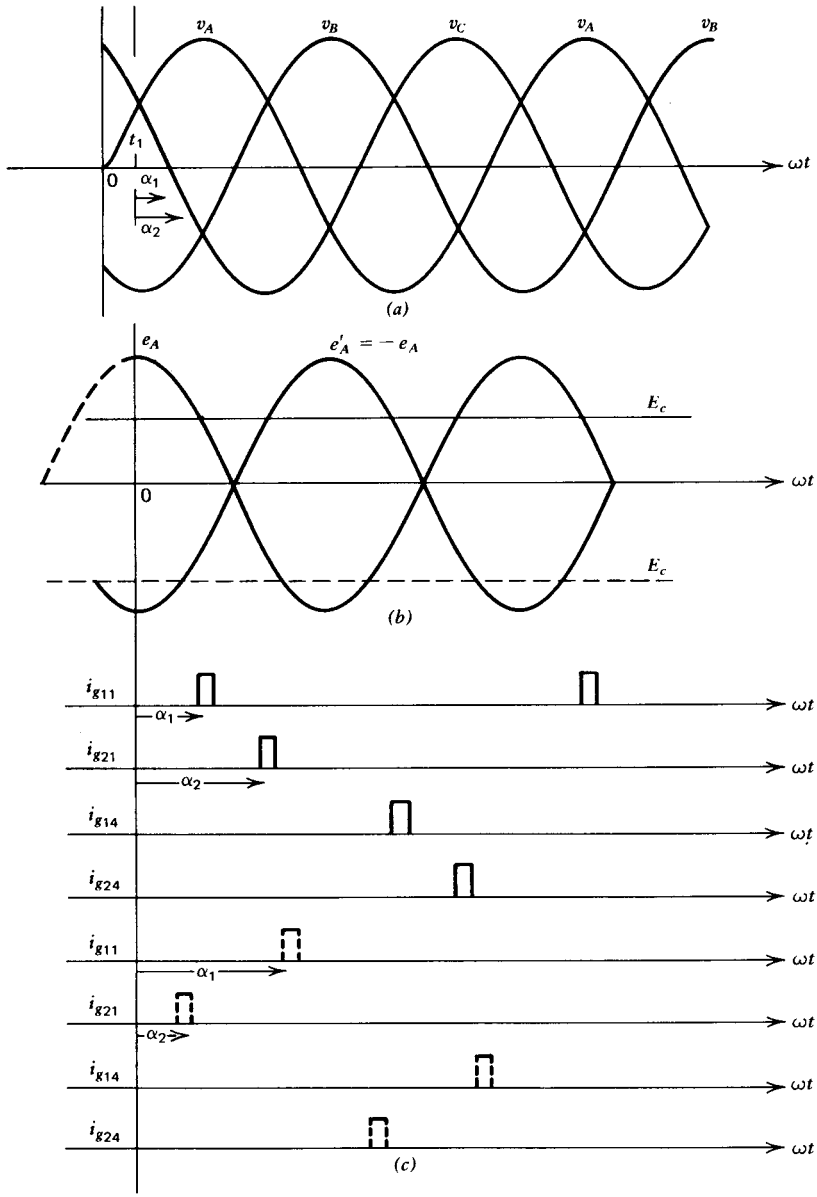


***Fig. 3.14*** Cosine firing scheme. (*a*) Supply phase voltages. (*b*) Phase-shifted supply voltage and control voltage. (*c*) Firing pulses for positive and negative control voltages. (*d*) Voltage transfer characteristic.

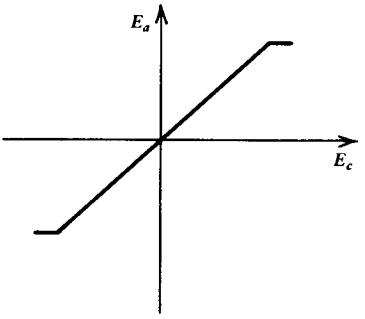


(d) *Fig. 3.14* (*Continued*)

From equations 3.57, 3.58, 3.65, and 3.66

$$E_{a1} = E_{\max} \cos \alpha_1 = E_{\max} \frac{E_c}{K} \tag{3.67}$$

$$E_{a2} = E_{\max} \cos \alpha_2 = -E_{\max} \frac{E_c}{K} \tag{3.68}$$

$$E_a = E_{a1} = -E_{a2} = \frac{E_{\max}}{K} E_c \tag{3.69}$$

The dc terminal voltage of the dual-converter is thus directly proportional to the control voltage $E_c$. The above firing technique, commonly known as the *cosine firing technique*, makes each converter behave essentially as a power amplifier with a linear voltage transfer characteristic, as shown in Fig. 3.14*d*.

### 3.3.2 Nonideal Dual-Converter

If the firing pulses are controlled so that $\alpha_1 + \alpha_2 = 180$, and both converters operate simultaneously, the converters will produce the same average terminal voltages, which will be equal to the average dc terminal voltage. One converter will be in the rectification mode and the other in the inversion mode. However, in a nonideal (i.e., practical) dual-converter, each converter will produce a ripple voltage. These ripple voltages are mostly out of phase. Therefore, if the two converters are solidly connected, the instantaneous voltage difference at the terminals of the two converters will produce enormous circulating current between the two converters that will not flow through the load. It is necessary to control this circulating current by some means. Two methods are commonly used.

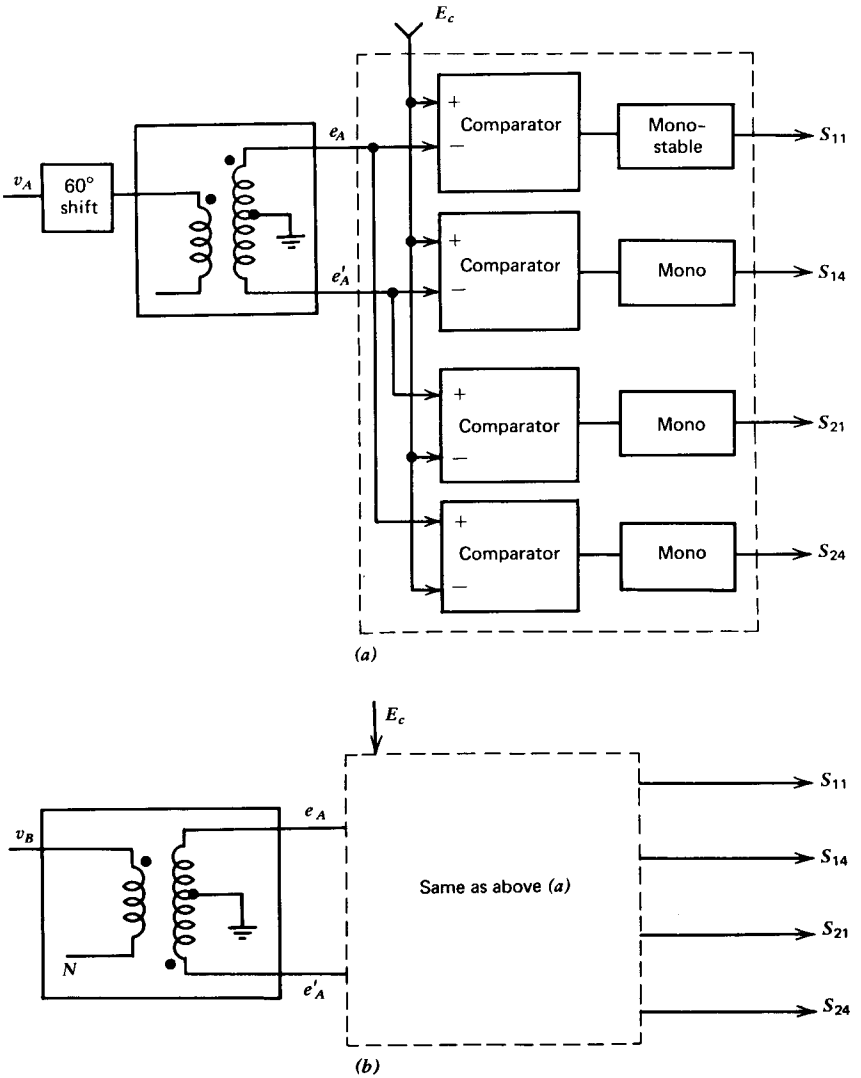


*Fig. 3.15* Schemes to generate firing pulses for a dual-converter. (*a*) Phase-shifted input supply voltage. (*b*) Unshifted input voltage.

1 **Operation without Circulating Current.** The flow of circulating current is completely inhibited by automatic control of the firing pulses. Only one converter operates at a time and carries the load current. The other converter is temporarily blocked.

2 **Operation with Circulating Current.** A controlled amount of circulating current is permitted. The circulating current is limited by means of a circulating current reactor that is connected between the dc terminals of the two converters as shown in Fig. 3.12.

### 3.3.3 Dual-Converter without Circulating Current

There will be no circulating current if one converter carries the load current at any given time and the other converter is blocked from conducting. Normally this condition is achieved by removing completely the firing pulses from the converter that remains idle or blocked. Several control strategies can be evolved, and a few basic schemes are discussed here.

***Control Signal Polarity Selects the Converter***

A simplified block diagram of this scheme is shown in Fig. 3.16. The control signal $E_c$ may represent the speed and direction of rotation of the dc motor in an open-loop control, or it may represent the difference between a set speed and the actual speed in a closed-loop feedback control scheme. The control signal generates firing pulses (represented by their firing angles $\alpha_1$ and $\alpha_2$) for both converters, such that $\alpha_1 + \alpha_2 = 180°$. However, these pulses are "ANDED" with a signal that represents the polarity of the control signal. Therefore only one converter receives firing pulses and the other does not. If

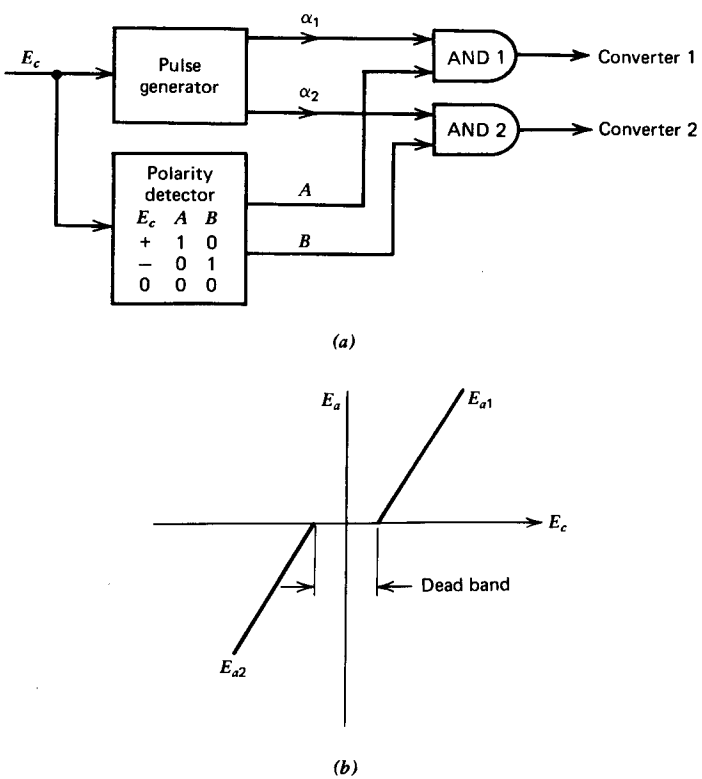


*Fig. 3.16* Converter selection by control signal polarity. (*a*) Basic block diagram. (*b*) Transfer characteristics with dead band to avoid circulating current.

the polarity of $E_c$ is positive, converter 1 receives firing pulses but firing pulses are blocked for converter 2. The motor rotates in the positive direction. If the polarity of $E_c$ is negative, the opposite happens. If $E_c$ is zero, firing pulses are blocked from both converters.

This scheme works satisfactorily in the steady state. However, during switch-over from forward to reverse motion of the motor (i.e., $E_c$ changed from positive to negative), circulating current may flow. When $E_c$ is switched to negative, converter 2 starts conducting. It may happen that conduction in converter 1 has not totally stopped; this results in a circulating current between the converters.

A slow change of $E_c$, or a dead band introduced in the transfer characteristic (as shown in Fig. 3.16*b*), may overcome this problem.

### *Load Current Selects the Converter*

Circulating current can be avoided if load current direction selects the converter. A simplified block diagram of a scheme that produces this result is shown in Fig. 3.17.

Comparator 1 produces an output if the load current $i_a$ is positive, and comparator 2 produces an output if the load current is negative.

Therefore, as long as the current is positive, converter 1 receives the firing

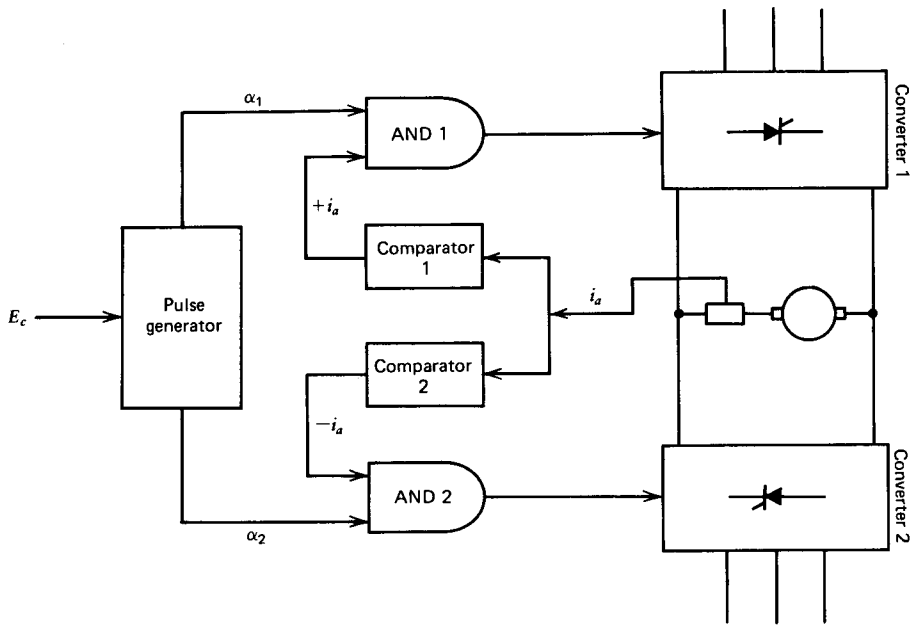


*Fig. 3.17* Converter selection by load current polarity. Basic block diagram.

pulses, and these are blocked from converter 2. If the polarity of the control signal $E_c$ is changed, the current reverses, and firing pulses are applied to converter 2 and blocked from converter 1.

This control scheme operates satisfactorily if the load current is continuous. If $i_a$ is discontinuous, erratic switching of converters, even when $E_c$ is not changed, results in haphazard operation of the system.

### *Both Control Voltage and Load Current Select the Converter*

A combination of the two control schemes discussed above is shown in the simplified block diagram of Fig. 3.18. Both control voltage and load current determine converter selection. If the control signal $E_c$ is zero, both AND gates will block firing pulses, and therefore neither converter receives firing pulses. If $E_c$ is positive and the load current is zero (discontinuous motor current) or positive, converter 1 receives the firing pulses. On the other hand, if $E_c$ is negative and load current is zero or negative, converter 2 receives the firing pulses.

This control scheme apparently works satisfactorily. However, if the load current is discontinuous, there are other problems. These problems are discussed in the following section.

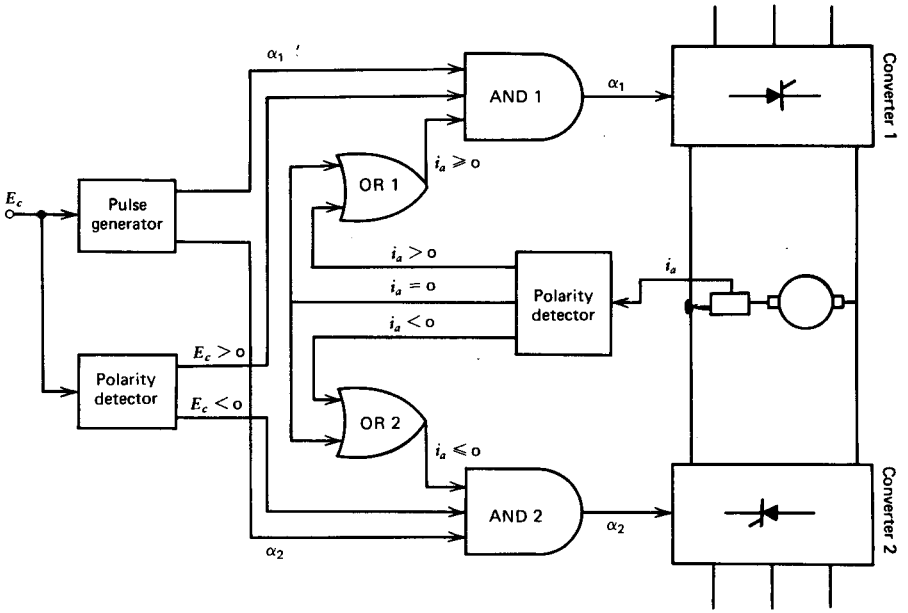


*Fig. 3.18* Converter selection by both control voltage and load current. Basic block diagram.

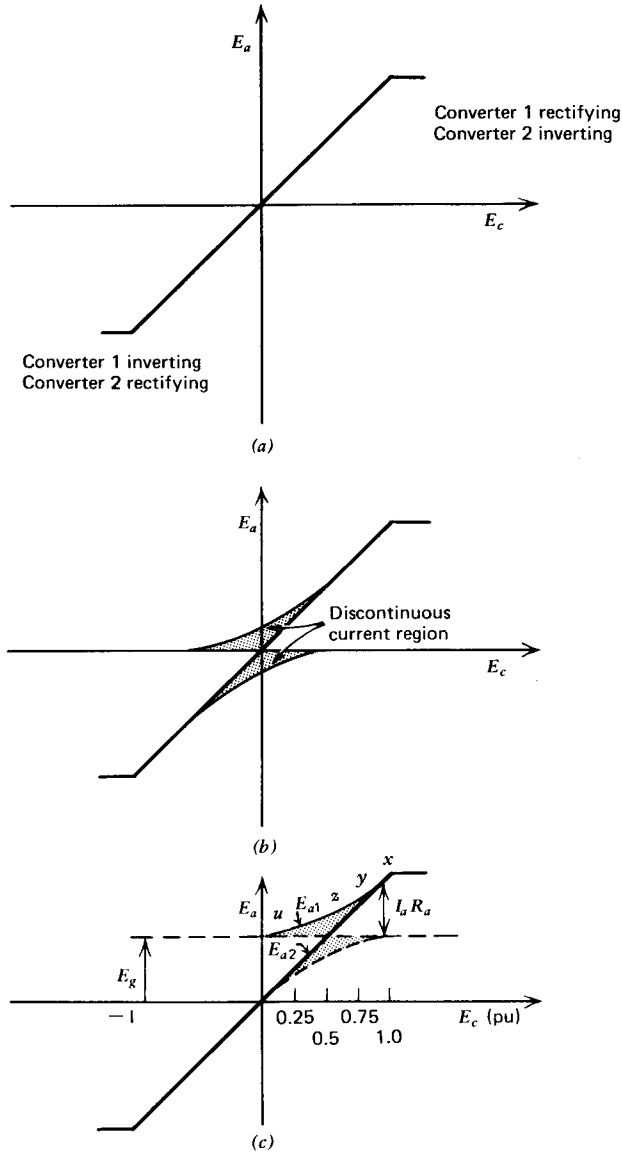


*Fig. 3.19* Dual-converter transfer characteristics. (*a*) Continuous load current. (*b*) Discontinuous load current, motor emf = 0. (*c*) Discontinuous load current, motor emf = $E_g$.

### 3.3.4 Discontinuous Load Current

The transfer characteristic between the control voltage $E_c$ and the dual-converter output voltage $E_a$ is linear (Fig. 3.19*a*) if the load current is continuous. For a discontinuous load current, the transfer characteristic breaks away from the continuous current characteristic as shown in Fig. 3.19*b* and *c*. With a dc motor load, because of back emf, there is a possibility of discontinuous motor current at any output voltage level if load on the motor is light and motor armature inductance is low. The breakaway point with a motor load is centered around the back emf of the motor. Figure 3.19*b* shows the transfer curve for zero back emf (i.e., motor at standstill), and Fig. 3.19*c* shows the curve for the motor in the running condition. To explain the departure from the linear relationship with discontinuous motor current let us assume that the motor back voltage $E_g$ is constant (Fig. 3.19*c*). At the operating point $x$ the motor draws a heavy current ($I_a R_a = E_a - E_g$ is large). At $y$ the motor current is just continuous. At $z$ the motor current is discontinuous, and the converter voltage $E_a$ is higher than the motor back voltage $E_g$ to keep the motor current flowing in the forward direction. At $u$ the converter voltage is the same as the motor back voltage, the motor current is zero, and the motor coasts.

From Fig. 3.19*c*, at $E_c = 0.25$ pu, the motor current is discontinuous. The output voltage $E_{a1}$ of converter 1 is greater than the back emf $E_g$. If the firing pulses are now blocked in converter 1 and released to converter 2, the output voltage $E_{a2}$ of the incoming converter will differ considerably from the motor back voltage. This may result in a catastrophic surge of transient current. This current "surge" at the crossover point can be eliminated in one of the two following ways.

#### *Phase-Back Firing Pulses*

The firing pulses of the incoming converter are initially phase backed, say to 180°, and are subsequently phase advanced by means of a closed-loop control scheme. A smooth crossover can be accomplished. However, a small dead time zone will be introduced during which there is no load current. The system response may be sluggish.

#### *Motor Voltage Feedback*

The motor terminal voltage is sensed and is made to adjust the control voltage, which generates the firing pulses for the idle or incoming converter. This adjustment is effected in such a way that the incoming converter output voltage is preadjusted to the motor terminal voltage. The preadjustment is independent of whether the current in the outgoing converter was previously continuous or discontinuous. This control scheme can provide a smooth changeover without introducing any time delay.

### 3.3.5 Closed-Loop System

The dual-converter is normally operated in a closed-loop feedback control system. Various control strategies[2–4] can be implemented to build a complete system. The following considerations and options are pertinent to such a system.

***Current Limit***

Dc machines have low armature circuit impedances, and it is important that current limit features are incorporated in the system. There are two methods for current limiting, as shown in Fig. 3.20.

***Inner Current-Control Loop*** In the inner current-control loop scheme, the speed error signal is used as a current reference. A limit on the speed error signal provides a limit on the current reference.

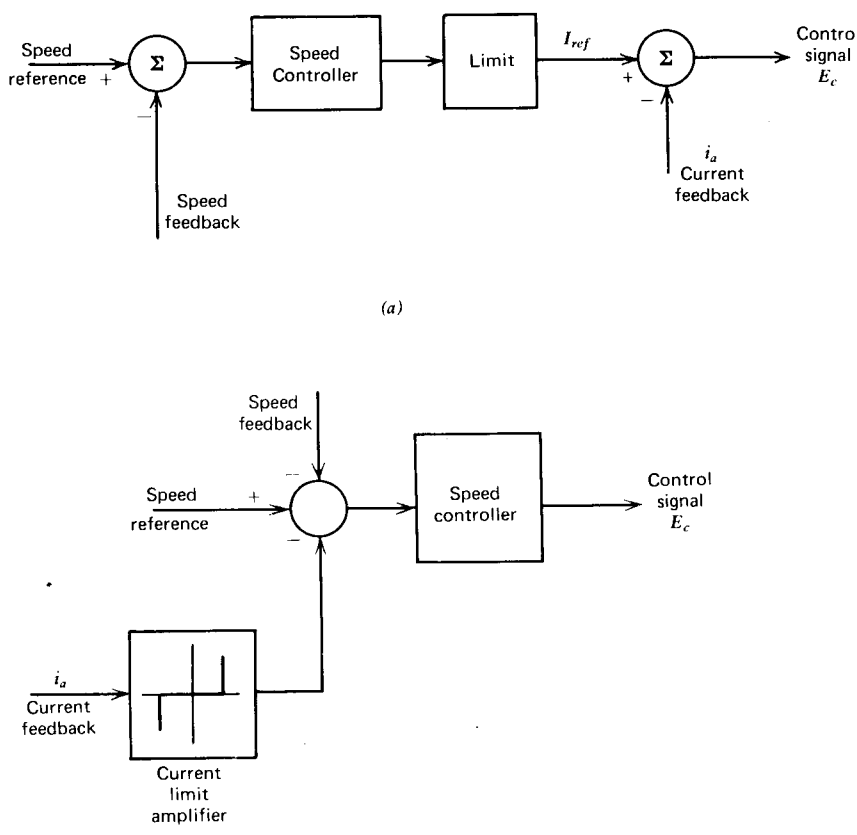


*Fig. 3.20* Current limit strategy. (*a*) Inner current-control loop. (*b*) Outer current-control loop.

The major or outer loop in this scheme is the speed loop. The current loop is in operation all the time and has several advantages. It provides fast response, linearizes the nonlinear gain of the thyristor converter, and overcomes the adverse effects of supply disturbances.

***Outer Current-Control Loop*** In the outer current-control loop scheme, the current feedback signal is compared with a preset threshold reference in a current limit amplifier and fed to the speed controller. The current limit amplifier has zero output as long as the current is below the preset value, and therefore the operation of the speed-control loop remains unaffected. However, if the current exceeds the preset value, the current limit amplifier produces a large output, which overrides the speed control signal and produces an essentially constant current mode of operation. There is only one control loop in this scheme, which is the speed loop. The design is therefore relatively simple. However, some of the advantages of the inner current loop mentioned before are not achieved.

### *Number of Firing Units*

Two separate firing units can be used for the two converters of the dual-converter system. However, in the operation without circulating current mode, only one converter conducts at any given time. It is therefore possible to have only one firing unit and to switch the firing pulses to the appropriate converter.

### *Crossover Philosophy*

To ensure a smooth current transfer in the dual-converter, the incoming converter voltage must be equal to the motor voltage at the instant of switch-over. Otherwise, a large current surge will flow through the converter. A smooth transfer can be achieved either by:

1 Phase-backing the firing pulses or
2 Motor voltage feedback.

A closed-loop control scheme can be designed to provide continuous control of the speed of the drive, both forward and reverse, with automatic regenerative braking and with current limiting. Selection of the control strategies in the design of a closed-loop control system for a dual-converter motor drive depends primarily on the circumstances and requirements of the particular application. The designer, for example, may choose the inner current-control loop, one firing unit, and phase-back crossover philosophy; or outer current-control loop, two separate firing units, and motor-voltage-feedback crossover philosophy.

### 3.3.6 Dual-Converter with Circulating Current

The foregoing study reveals that if a dual-converter is operated without circulating current, several difficulties may arise due to discontinuous load current. Sophisticated control schemes may be necessary to overcome these difficulties. However, these difficulties are avoided if circulating current is allowed to flow in the dual-converter. In this scheme, firing pulses are allowed to trigger thyristors of both converters. The control voltage that generates these firing pulses satisfies equation 3.62. Although both converters produce the same average voltage at their terminals, their instantaneous voltages are different, which will make a circulating current flow in the two converters. This circulating current is limited (or the difference between the instantaneous voltages of the converters is supported) by a circulating current reactor. This scheme has the following advantages:

1 The circulating current keeps both converters in virtually continuous conduction over the whole control range, independent of whether the external load current is continuous or discontinuous, or whether there is any load current at all.
2 A natural mode is provided in the power circuit for the load current to flow in either direction at any time. Thus a reversal of load current is inherently a natural and smooth procedure.
3 The time response is fast if the converters are in continuous conduction.

However, the need for a reactor is a disadvantage. At high power levels the size and cost may be quite significant.

***Operation and Waveforms***

The operation of the dual-converter with circulating current is described below. The following assumptions are considered:

1 The reactor is lossless.
2 The firing angles of the two converters are controlled so that their sum is 180° (i.e., $\alpha_1 + \alpha_2 = 180°$).

As an illustration, the waveforms for $\alpha_1 = 60°$ and $\alpha_2 = 120°$ are shown in Fig. 3.21. Because of the circulating current, both converters are kept in a state of continuous conduction, both at no-load and load conditions. Hence the waveforms of the voltage in the circuit are well defined. The supply voltages are shown in Fig. 3.21*b*, and the converter output voltages are shown in Fig. 3.21*c* and *d*. The instantaneous dc terminal voltage (i.e., output voltage) shown in Fig. 3.21*e* is the average of the instantaneous converter voltages. Note that this output voltage has a shape different from that of either of the converter voltages. However, the average value of the output voltage is the same as the average of each converter voltage.

The instantaneous voltage across the reactor, shown in Fig. 3.21*f*, is the difference between the instantaneous converter voltages. The circulating current, shown in Fig. 3.21*g*, is obtained from the time integral of the voltage across the reactor.

Let the phase voltages be as follows:

$$v_A = \sqrt{2}\, V \sin \omega t \tag{3.70}$$

$$v_B = \sqrt{2}\, V \sin\left(\omega t - \frac{2\pi}{3}\right) \tag{3.71}$$

$$v_C = \sqrt{2}\, V \sin\left(\omega t + \frac{2\pi}{3}\right) \tag{3.72}$$

and

$$v_A + v_B + v_C = 0 \tag{3.73}$$

During the interval $(\pi/6 + \alpha_1) < \omega t < (\pi/6 + \alpha_1 + \pi/3)$,

$$e_{a1} = v_A - v_B = v_{AB} \tag{3.74}$$

$$e_{a2} = -(v_C - v_B) = v_B - v_C = v_{BC} \tag{3.75}$$

$$e_r = e_{a1} - e_{a2} = v_A + v_C - 2v_B \tag{3.76}$$

From equations 3.73 and 3.76

$$e_r = -3v_B \tag{3.77}$$

Therefore the circulating current is given by

$$\begin{aligned} i_c &= \frac{1}{\omega L}\int_{\alpha_1+\pi/6}^{\omega t} e_r\, d(\omega t) \\ &= \frac{1}{\omega L}\int_{\alpha_1+\pi/6}^{\omega t} -3\sqrt{2}\, V \sin\left(\omega t - \frac{2\pi}{3}\right) d(\omega t) \\ &= \frac{3\sqrt{2}\, V}{\omega L}\left[\cos\left(\omega t - \frac{2\pi}{3}\right) - \cos\left(\alpha_1 - \frac{\pi}{2}\right)\right] \end{aligned} \tag{3.78}$$

The circulating current thus depends on the firing angle and is limited by the value of the reactor.

Without a load current, $i_a = 0$ as shown in Fig. 3.21*h*, the converter currents are the same as the circulating current, as shown in Fig. 3.21*i*. The ripple voltage across the reactor thus keeps the converters in a state of just continuous current even though there is no external load current.

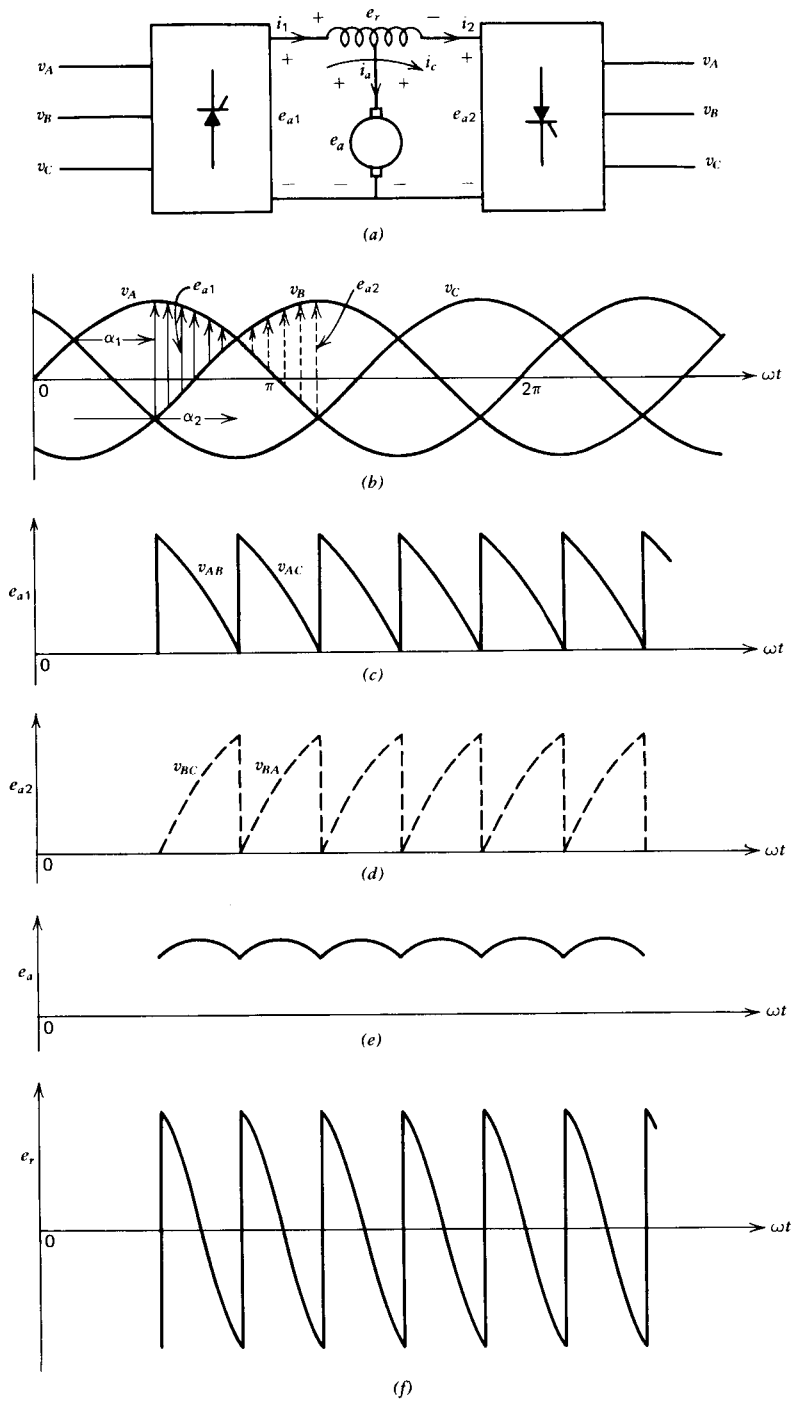


***Fig. 3.21*** Dual-converter waveforms: Firing angle $\alpha_1 = 60°$, $\alpha_2 = 120°$.

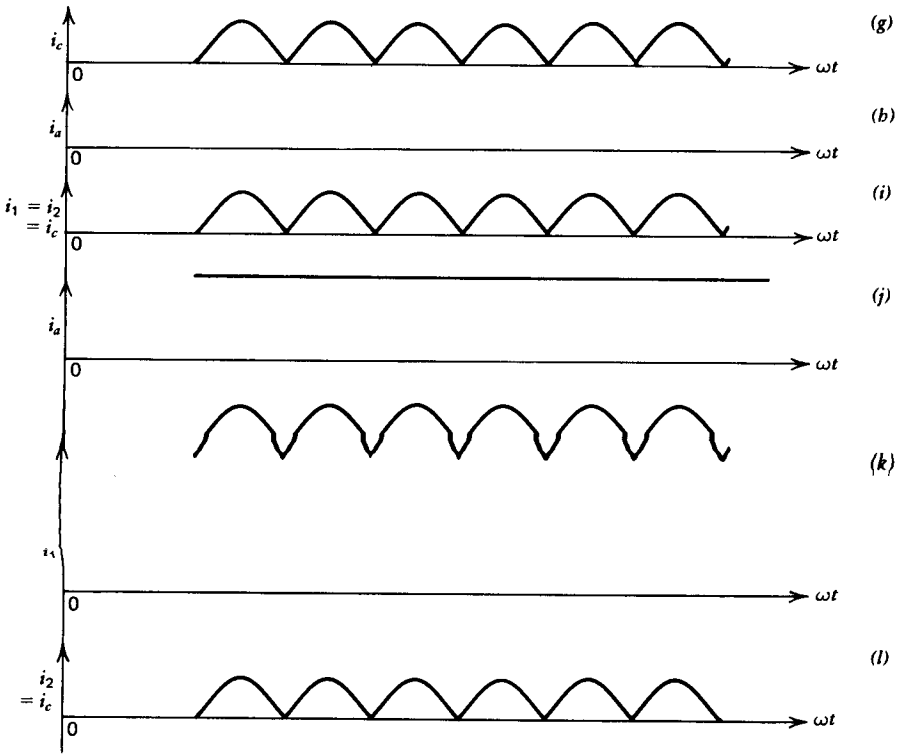


*Fig. 3.21* (*Continued*)

With a smooth load current in the positive direction, as shown in Fig. 2.21*j*, converter 1 carries the load current, and the total current in this converter is the sum of the load current and the circulating current, as shown in Fig. 3.21*k*. Converter 2 simply carries the circulating current, as shown in Fig. 3.21*l*.

**Example 3.2**

For the dual-converter of Fig. 3.21*a*, $V = 120$ V, $\omega = 377$ rad/sec, $L = 10$ mH, $\alpha_1 = 60°$, and $\alpha_2 = 120°$. Calculate the peak value of the circulating current.

*Solution*

From Fig. 3.21*g*, the peak value of the circulating current occurs at $\omega t = \alpha_1 + \pi/6 + \pi/6 = 2\pi/3$. From equation 3.78

$$i_c|_{\text{peak}} = i_c|_{\omega t = 2\pi/3} = \frac{3\sqrt{2}\,V}{\omega L}\left(1 - \cos\frac{\pi}{6}\right)$$

$$= \frac{0.568\,V}{\omega L} = \frac{0.568 \times 120}{377 \times 10 \times 10^{-3}}$$

$$= 18.08 \text{ A}$$

### *Closed-Loop System*

A closed-loop dual-converter system allowing circulating current is shown in Fig. 3.22. Its operation is described as follows.

*Steady State* Assume that the system is in the steady state with a speed setting corresponding to forward motion of the motor. Motor speed is essentially the same as the set speed, and the control signal $E_c$ is positive. Converter 1 operates as a rectifier and carries the load current. Converter 2 carries only the circulating current and is "idle" as far as the load is concerned. This converter is, however, set in the inversion mode.

*Overhauling Load* Suppose the motor is driving a vehicle that is going down a hill. This increases the speed and hence the motor's back emf. The motor current decreases. Because $N > N_r$, the control voltage $E_c$ decreases. Eventually the load current reverses and flows through converter 2. The dc machine now acts as a generator. The machine current increases until equilibrium is reached, at which point the overhauling torque equals the counter torque developed by the dc machine.

*Speed Reversal* To initiate speed reversal, the speed reference voltage is reversed. The speed of the motor cannot change instantaneously; therefore the speed error signal becomes negative. This decreases the control voltage $E_c$. The firing angle $\alpha_1$ of converter 1 is phase-delayed, causing the motor

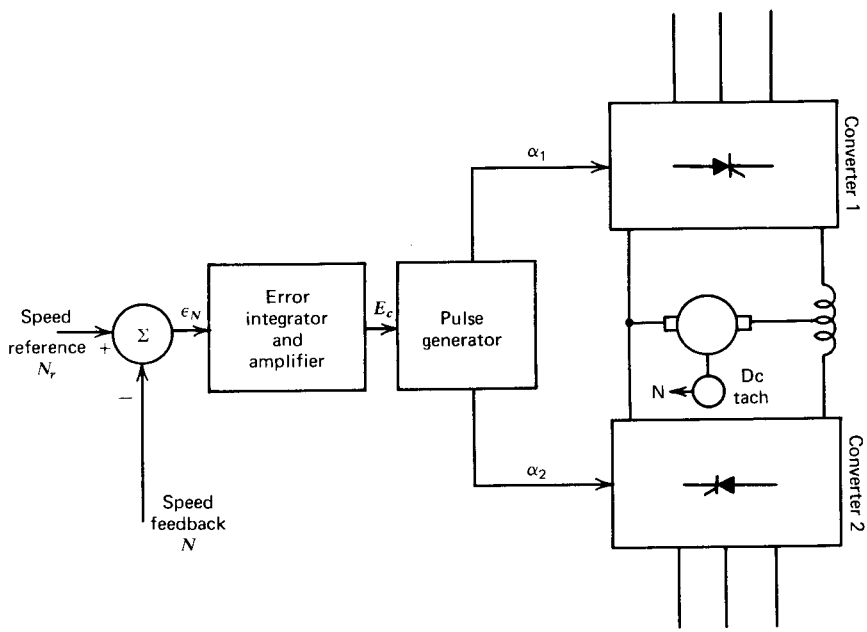


*Fig. 3.22* A closed-loop, circulating-current, dual-converter system. (Current limit not shown.)

current to decrease to zero. The control voltage $E_c$ continues to decrease, and this makes the motor voltage higher than the voltage of converter 2. The current of the dc machine reverses. The machine acts as a generator, and the speed decreases regeneratively to zero. The speed eventually reverses and reaches a steady-state value. During regenerative braking and speed reversal, a current limit control, not shown in Fig. 3.22, keeps the machine current constant.

### 3.3.7 Dual-Mode Dual-Converter

The previous discussion reveals that a dual-converter system can be operated either in the circulating current or noncirculating current modes. The advantages and disadvantages of the two methods of operation are summarized in Table 3.2. It is evident that both systems have merits and demerits.

In the circulating current mode, it is possible that the converters will be loaded to an extent much higher than the maximum load. This makes the presence of the circulating current undesirable. However, it is necessary to operate in the circulating current mode if the load current tends to be

***Table 3.2*** **Advantages and Disadvantages of Dual-Converters with and without Circulating Current**

| With Circulating Current | Without Circulating Current |
|---|---|
| Reactors are needed to limit circulating current. These reactors may be costly | Reactors may be needed to make load current continuous |
| Circulating current increases losses and hence decreases efficiency | Efficiency is higher |
| Converters operate in continuous current mode | Converters may operate in discontinuous current mode |
| Linear transfer characteristics are obtained | Nonlinear transfer characteristics due to discontinuous current are obtained |
| Response is fast due to the continuous current in the converters | Response is sluggish due to the discontinuous current |
| Fault currents between converters due to spurious firing are restricted by the reactor | Faults between converters due to spurious firing results in dead short-circuit conditions |
| The crossover technique is simple | The crossover technique is complex |
| The converter loading is higher than the output load | The converter loading is the same as the output load |

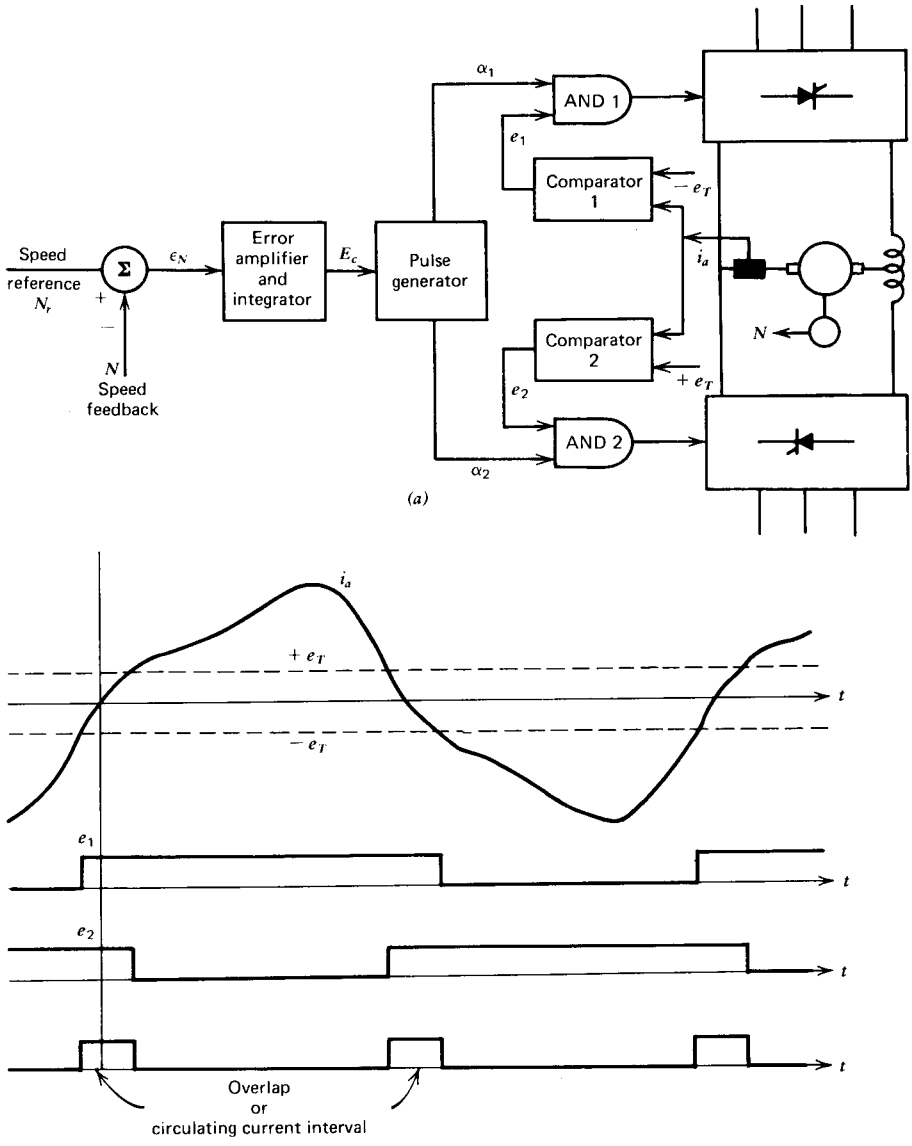


*Fig. 3.23* Dual-mode dual-converter. (*a*) Basic block diagram for dual-mode dual-converter operation. (*b*) Illustrative waveforms.

discontinuous. These contradictory requirements lead to the concept of dual-mode operation in which the dual-converter will operate in both the circulating current and the noncirculating current modes.[2] Figure 3.23 shows a simplified representation of such a control scheme.

In this scheme, the dual-converter is operated mostly in the noncirculating current mode. However, if the load current falls below a "threshold" level, the dual-converter operates in the circulating current mode. It is implied that below the threshold level, there is the possibility of a discontinuous load current.

As shown in Fig. 3.23, the load current is sensed and fed to two comparators. An output $e_1$ is produced at comparator 1 if the load current is greater than a threshold voltage $-e_T$. An output $e_2$ is produced at comparator 2 if the load current is less than the threshold voltage $+e_T$. These outputs $e_1$ and $e_2$ allow the firing pulses to be applied to the converters. Thus when the load current is below the threshold value, both converters receive firing pulses, and circulating current flows through the dual-converter. Otherwise, only one converter receives the firing pulses, and the dual-converter operates in the noncirculating current mode.

In this control scheme, the circulating current flows only when the load current is small. The size of the reactor can thus be small. The core of the reactor can saturate at high load currents when only one converter conducts, and the reactor does not have to perform the circulating current limiting function.

## 3.4 REVERSIBLE DRIVES

In a reversible drive system control of speed is possible in both forward and reverse directions. In some applications speed reversal is required only occasionally, such as reversing a subway car. In other applications, reversing of speed is required frequently. For example, in steelworks, roller tables are driven so that slabs, billets, and strips, can be conveyed from one stage of manufacture to the next. In hot strip mills, a reversible drive makes the hot strip pass through the mill back and forth several times until it is shaped into a desired form and length. In a drive system where speed reversal is frequent, a regenerative drive is desired to allow rapid speed reversal. In a regenerative drive, kinetic energy of the moving mass is recovered while slowing to zero speed, and this results in higher efficiency.

The Ward-Leonard system has been used extensively as a reversible drive. It provides inherent regenerative capability. Although it performs satisfactorily, this system is costly and less efficient because of the two machines required to provide variable dc voltage with reversible polarity for the drive motor. At present thyristor phase-controlled ac/dc converters are being used increasingly in reversible drives. Two systems[3–9] are used. One is referred to

***Table 3.3*** **Thyristor Power Circuits for High Power Regenerative Reversible Drives.**

| Type of reversal | Method of reversal | | Thyristor power circuit | Type of drive | Features |
|---|---|---|---|---|---|
| Armature current reversal | Changeover contactors | | 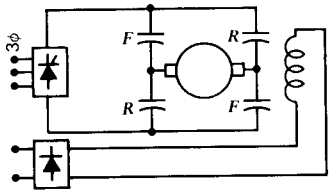  | Drive type 1 | Reasonably good response Moving contactors require maintenance Armature zero-current detection required for contactor changeover |
| | Dual-converter | Circulating current type | 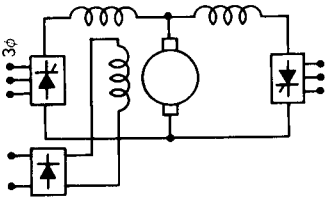  | Drive type 2 | Fastest response Both converters are simultaneously fired Losses in the two converters and reactors to limit circulating current decrease efficiency |
| | | Non-circulating current type | 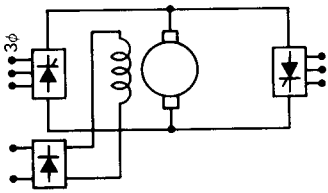  | Drive type 3 | Fast response One converter to be fired at a time Current detection and delay required to prevent firing of both converters together |
| Field current reversal | Dual-converter | | 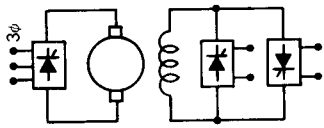  | Drive type 4 | Cheaper Response depends on field forcing |
| | Changeover contactors | | 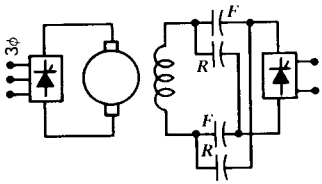  | Drive type 5 | |

as *armature current reversal* and the other as *field current reversal*. In each system, the current is reversed either by a dual-converter or by changeover contactors operated by relays. Typical power circuits[8] used for high-power reversing regenerative drives are shown in Table 3.3. Each system has its own merits and demerits. These are summarized in the Table 3.3. With armature current reversal, the power circuit has to handle the full drive power, whereas with field current reversal, power is controlled at a low level in the field circuit. However, armature current can be reversed faster than field current because of the low time constant of the armature circuit compared to the much larger time constant of the field circuit of the drive motor. In the following sections, the operation and performance of these systems are further discussed.

### 3.4.1 Armature Current Reversal

In the armature current reversal scheme, field current is kept constant during the speed reversal. Motor armature current is reversed to provide a reversing torque, which in turn will reverse the speed. Armature current is reversed by using either:

1 a converter and changeover contactors; or
2 a dual-converter.

The reversing drive system using changeover contactors is cheaper because only one converter is used. The dual-converter system is more expensive because two converters are used. However, if speed reversal is required frequently as in steel mills, the dual-converter system is preferred. If the contactor type system is used it will require frequent maintenance and occasional replacement of the contactors.

#### *Scheme Using Changeover Contactors*

A schematic block diagram of the reversing drive system with changeover contactors (drive type 1) is shown in Fig. 3.24. The "speed set" will determine the forward or reverse speed of the dc motor. The speed controller output will set the current demand. During the reversal process, current demand will be large. However, a limit circuit will keep the armature current constant during speed reversal. The speed controller output will also determine the contactors to be closed. These contactors should be operated when the current is zero; otherwise there will be destructive arcing. The zero current detector circuit will provide this interlock.

In Fig. 3.25 the sequence of events during the speed reversal is described.[5–7] The change in the average currents, voltages, and speed with time is shown for a speed reversal from base speed forward to base speed reverse. It is assumed that the drive motor is unloaded during the speed reversal. During

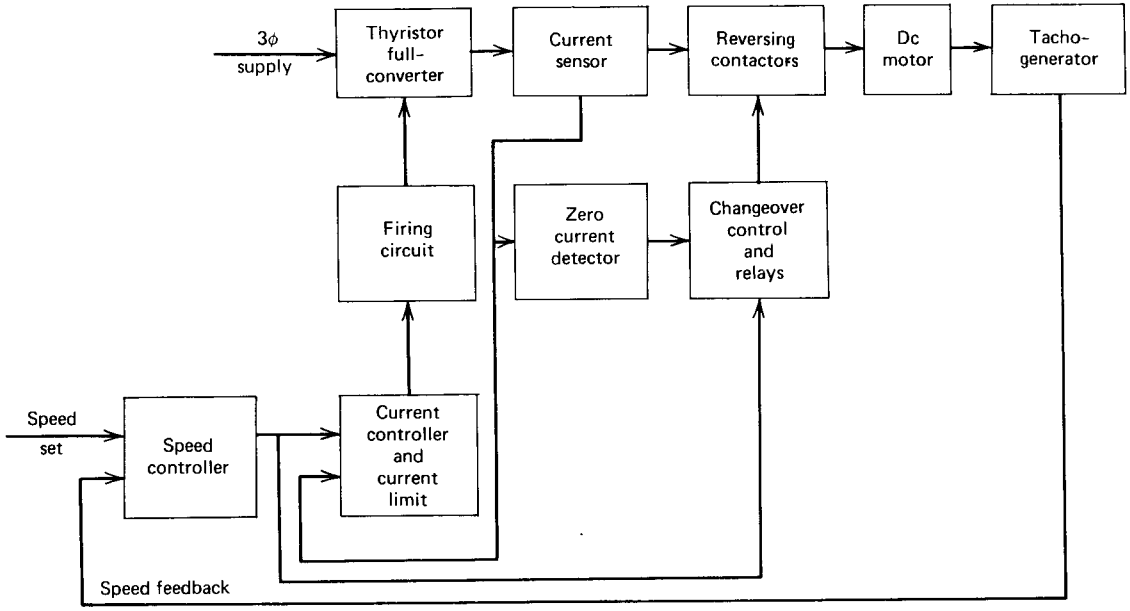


*Fig. 3.24* Schematic block diagram of a reversing drive.

the speed reversal, the motor current will be kept at the set current limit. The reversing torque is therefore constant. If windage and friction losses are neglected during the speed reversal, the motor will decelerate to zero speed and then accelerate to the reverse speed linearly with time. However, if the torque corresponding to windage and friction is considered to be proportional to speed, the speed will change exponentially with time.

The reversing torque is given by

$$T = -KI_a \tag{3.79}$$

The torque balance equation is

$$-KI_a = J\frac{dN}{dt} + BN \tag{3.80}$$

From equation 3.80, the speed as a function of time is

$$N = -\frac{KI_a}{B} + Ae^{-t/\tau_m} \tag{3.81}$$

where $A$ is a constant and
$\tau_m = J/B$ = mechanical time constant of the system.

At the start of the reversing process

$$N(0) = N_b = \text{forward base speed.}$$

Substituting in equation 3.81,

$$N_b = -\frac{KI_a}{B} + A \tag{3.82}$$

from which

$$A = N_b + \frac{KI_a}{B} \tag{3.83}$$

Therefore, from equations 3.81 and 3.83

$$N = -\frac{KI_a}{B} + \left(N_b + \frac{KI_a}{B}\right)e^{-t/\tau_m} \tag{3.84}$$

This represents an exponential change of speed with time during the speed reversal.

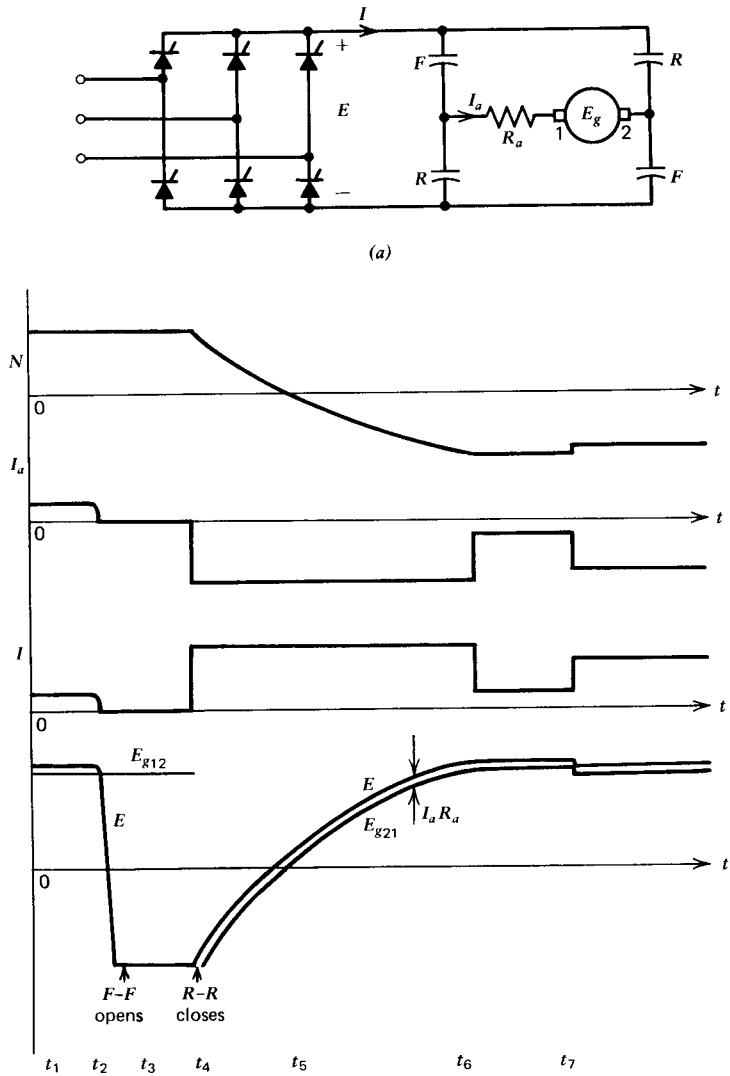


*Fig. 3.25* Armature current reversal using changeover contactors. (*a*) Power circuit. (*b*) Variation of speed, voltages, and currents during a speed reversal.

The sequence of events illustrated by Fig. 3.25 during the motor speed reversal is as follows:

*Steady State in the Forward Direction* At instant $t_1$, the motor is rotating in the forward direction. Contactors *F-F* are closed, and motor current $I_a$ flows through them from the converter. The motor is assumed to be unloaded. Therefore a small motor current flows to provide the windage and friction load.

*Speed Reversal* At instant $t_2$, the reversal cycle is initiated when a reverse speed signal occurs at the "speed set" terminal of Fig. 3.24. The firing pulses are delayed, and the converter is set for inversion. As the converter voltage $E$ falls below the motor back voltage $E_g$, the motor current is blocked. The zero current detector will sense the zero current and will enable the energizing of the relays so that the contactors may change over. The opening of contact *F-F* and closing of contact *R-R* may take 50 to 100 msec. During the interval $t_3$ to $t_4$, the motor is disconnected from the supply and is coasting. Because the rotor has large inertia its speed is assumed to be constant during this coasting interval.

When the $R$ contactors are closed at $t_4$, the motor is again connected to the converter, which is set to invert power. The motor feeds back power to the supply under constant armature current. The motor decelerates to zero speed at instant $t_5$. During the interval $t_4$ to $t_5$, the firing angle continuously adjusts (i.e., advances) so that the motor current stays constant at the current limit. During this interval the system behaves as a regenerative brake. At $t_5$, the motor speed is zero. The converter is operating as a rectifier (i.e., $E$ is positive) to supply the voltage drop due to armature resistance.

The firing angle is being continuously advanced to keep the motor current constant. The converter will continue to operate as a rectifier, and the motor will accelerate in the reverse direction.

At instant $t_6$, the motor reaches its full speed in the reverse direction. The firing angle does not change anymore. Since no accelerating torque is required, the motor current $I_a$ drops to the no-load value.

*Load Applied* If the load is applied at instant $t_7$, the motor current $I_a$ will increase. There will be a slight decrease in speed $N$, in motor back voltage $E_g$, and in converter voltage $E$, due to regulation.

The oscillograms of Fig. 3.26 illustrate the practical operation of this type of reversing scheme. These oscillograms show the change in converter voltage, speed (or motor back voltage), and motor current during a no-load speed reversal. Observe that the current controller keeps the current at the current limit value during the speed reversal. Note also that the total reversal time is due primarily to the mechanical time constant of the system. The time taken by the contactor changeover is insignificant.

This method of speed reversal using changeover contactors is economical in power equipment. The control circuitry is not very complex. The speed reversal is reasonably fast. However, it has the disadvantage of having moving contactors, which may require considerable maintenance.

### *Scheme Using Dual-Converter*

A dual-converter can operate in all four quadrants so that the output current and voltage are both reversible. A dual-converter can be used for speed reversal. This scheme is all static; there are no moving contactors. Both the circulating current and noncirculating current type dual-converters discussed

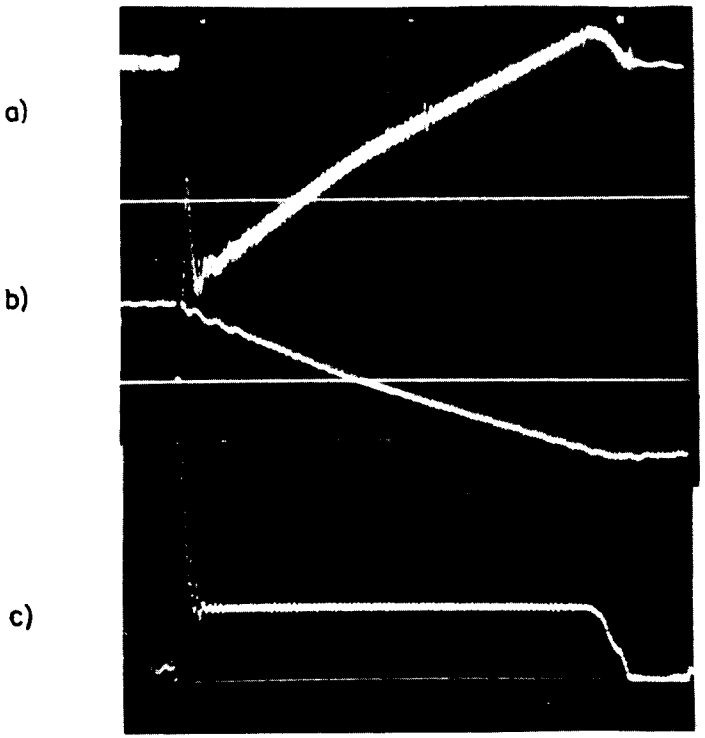


*Fig. 3.26* Typical oscillograms obtained during regenerative speed reversal in Drive Type 1. (*a*) Converter voltage $E$. (*b*) Speed $N$. (*c*) Armature current $I_a$.

earlier can be used. Because no moving contactors are involved, current reversal is very fast.

In the scheme using the circulating current type dual-converter (drive type 2) both converters are fired simultaneously. A small circulating current, less than 20% of the full load current of the drive, is allowed to flow between the converters. Because one converter operates in the rectification mode and the other in the inverting mode, the changeover from motoring to regenerating during speed reversal is almost instantaneous. The sequence of events during a no-load speed reversal in this scheme is described in Fig. 3.27.

At instant $t_1$, the drive motor rotates in the forward direction. Converter 1 operates in the rectification mode and conducts the no-load motor current as well as the circulating current. Converter 2 operates in the inversion mode and carries the circulating current. The amount of circulating current is assumed to be constant throughout the process.

At instant $t_2$, the "speed reverse" command is initiated. Converter voltages will change to keep the motor current constant at the current limit value. The motor current is transferred to converter 2, which now inverts power to

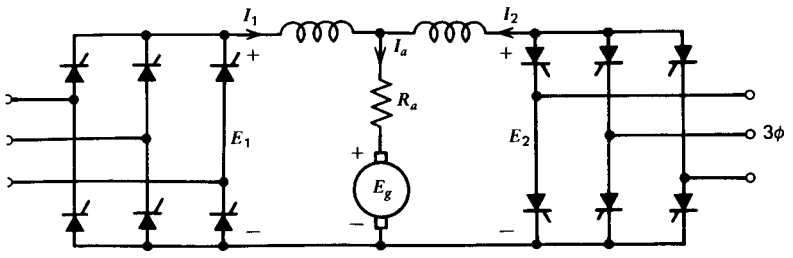


(a)

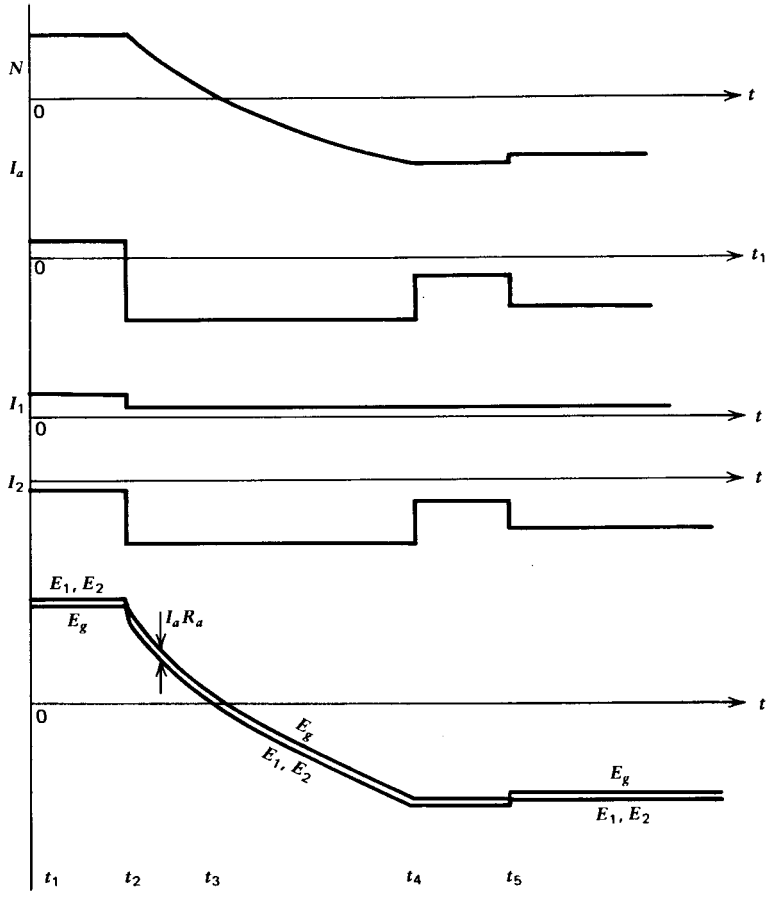


(b)

*Fig. 3.27* Armature current reversal using a circulating current dual-converter. (*a*) Power circuit. (*b*) Variation of speed, voltages, and currents during a speed reversal.

the supply. The motor therefore decelerates regeneratively to zero speed at instant $t_3$.

From $t_3$ onward, converter 2 operates as a rectifier and accelerates the motor in the reverse direction. Converter 1 operates in the inverting mode and carries the circulating current.

At $t_4$, the motor reaches its full speed in the reverse direction. The motor current drops to its no-load value.

At instant $t_5$, the load is applied.

In the scheme using the noncirculating type dual-converter (drive type 3), no reactor is used between the converters to limit the circulating current. Therefore, only one converter can be fired at a time to avoid a short circuit between the converters. As a result, during the changeover of converters, a small time delay of less than 20 msec is incorporated after a current zero is detected for the motor current. This scheme will be further discussed in the following section in connection with field current reversal.

### 3.4.2 Field Current Reversal

To reverse motor speed in the field current reversal scheme the armature current direction is unchanged, and the field current is reversed. The power in the field circuit is much lower than the power in the armature circuit and is never more than a few kilowatts even in a large power drive system. Field current reversal is therefore cheaper compared to armature current reversal. However, during field current reversal, as the filed current changes, it will affect the commutation of the armature current. Besides, the field circuit has a large time constant. For large machines this time constant may be in the order of 1 or 2 sec or more. If the field current has to decay and rise by a natural process, more than 10 sec may be required for the current reversal. To reverse the field current as fast as possible a technique called *field forcing* is used. A higher field voltage, typically 2 to 5 times the normal field voltage, is applied during the field current reversal. The field current changes quickly, and when it reaches its desired reverse value the field voltage is reduced to its normal value. If the field circuit time constant is, say, 2 sec, the field current can be reversed in half a second by using field forcing.

The field current can be reversed either by using a dual-converter (drive type 4) or a single converter with changeover contactors (drive type 5). In order to reverse the field current as rapidly as possible, the current is brought to zero by inversion. The field coil is made to act as a generator and return its magnetic stored energy to the supply through inversion. The field current then reverses to produce reversing torque on the motor. The converter in the armature circuit can be controlled so that it operates in the inverting mode and the motor decelerates regeneratively. The motor will then accelerate to its full speed in the reverse direction.

The sequence of events in a field current reversal scheme using a noncirculating type dual-converter is described in Fig. 3.28.

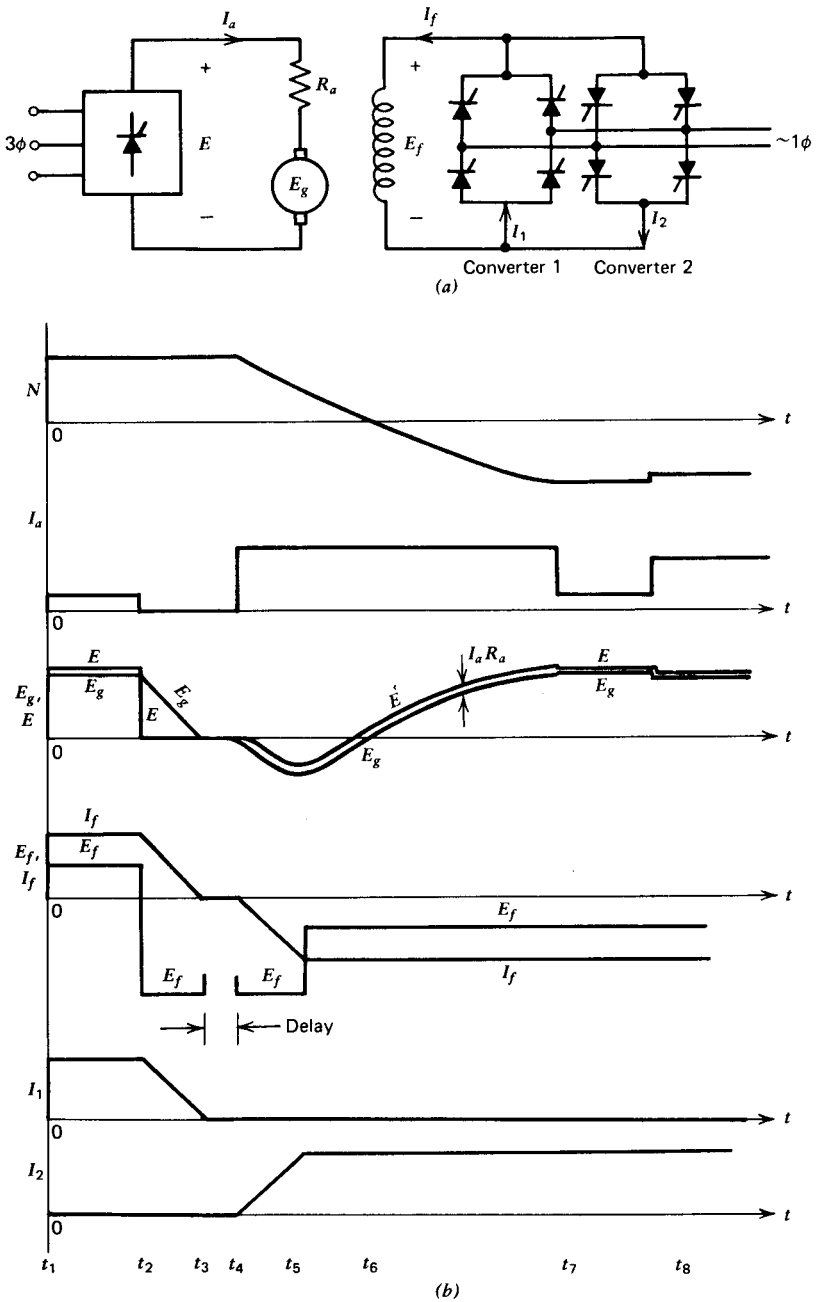


*Fig. 3.28* Field current reversal using a noncirculating type dual-converter. (*a*) Power circuit. (*b*) Variation of speed, voltages, and currents during a speed reversal.

At instant $t_1$, the motor rotates in the forward direction at no load. The field winding has a normal voltage, and the field current is conducted by converter 1. The normal field voltage may correspond to a firing angle of 70°. Therefore $E_f = E_{f_{max}} \cos 70° = 0.34\ E_{f_{max}}$, where $E_{f_{max}}$ is the maximum converter voltage at zero firing angle.

At instant $t_2$, the reversing process is initiated. First, firing of the armature converter is delayed so that $E$ is set to zero. As $E$ becomes less than $E_g$, armature current will drop to zero. Next, the firing of converter 1 is almost fully delayed, say from 70° to 170°. Converter 1 is in the inverting mode, and its voltage is $E_f = E_{f_{max}} \cos 170° = -0.98\ E_{f_{max}}$. This is about 3 times the normal field voltage, and therefore the field current decreases regeneratively under field forcing. As the field current decreases, so does the motor back voltage $E_g$.

At $t_3$, both $I_f$ and $E_g$ are zero. At this instant firing pulses are removed from converter 1. Because a noncirculating type dual-converter is considered, a delay of 10 to 20 msec is allowed before firing pulses are applied to converter 2 at instant $t_4$.

From instant $t_4$ onward, converter 2 builds up the field current in the reverse direction under field forcing. The firing angle is about 10° so that $E_f = -E_{f_{max}} \cos 10° = -0.98\ E_{f_{max}}$. From $t_4$ onward, the motor decelerates regeneratively under constant armature current.

At instant $t_5$, the field current has reached its reverse rated value. The firing angle of converter 2 changes to 70° so that the field winding has its normal voltage and current.

At instant $t_6$, motor speed is zero. From this instant onward, the motor accelerates under constant armature current control.

At instant $t_7$, the motor is at its full reverse speed. The armature current drops to its no-load value.

At $t_8$, the load is applied.

The control circuitry in this scheme, drive type 4, as well as in the scheme using changeover contactors, drive type 5, is relatively complex. In the field current reversal system, even with field forcing, the time response for current reversal cannot be as fast as that in the armature current reversal system. However, the total speed reversal time is primarily influenced by the mechanical time constant of the drive system.

### 3.4.3 Drive Selection

Various regenerative reversing drives have been discussed in the previous sections. If regeneration is not required and speed reversal does not occur frequently, a nonregenerative drive using a semi-converter can be used.

To select a drive system from these alternatives for use in a particular

application, one must consider these factors:

1 Frequency of speed reversal
2 Response time
3 Capital cost
4 Efficiency
5 Maintenance
6 Complexity and reliability

For applications requiring frequent speed reversal, systems using dual-converters are better suited because of minimal maintenance and rapid current reversal. Time response of the current reversal is fast for systems using a dual-converter in the armature circuit. However, overall time response of the complete drive depends on the various time constants. Some typical values of these time constants are shown in Table 3.4. The mechanical time constant greatly influences the time required for speed reversal. If the mechanical time constant is low, armature current reversal becomes advantageous because it will reduce the overall time response. If the mechanical time constant is comparable to the field time constant, it is more economical to select a field reversal drive.

The field reversal system obviously will be less expensive because the power involved is at a low level. A rough idea of the capital cost variation[9] of the various reversing drive systems is shown in Fig. 3.29. The cost for a nonregenerative drive has been considered as a reference. Note that selection of the controller significantly influences the capital cost.

Regenerative drives have efficiencies as high as 95%. However, the circulating type dual-converter system for armature current reversal will have slightly lower efficiency due to losses in the circulating current reactor and losses in both converters, which are in the conduction state at all times.

Reversing systems using changeover contactors require considerable maintenance. A drive with better response time is generally more complex. To obtain faster response, additional components are necessary; these normally

*Table 3.4* **Typical Time Constants of DC Motors**

| Motor (hp) | Mechanical Time Constant (sec) | Armature Time Constant (sec) | Field Time Constant (sec) | Field Current Reversal Using Field Forcing (sec) |
|---|---|---|---|---|
| 10 | 0.75 | 0.025 | 0.5 | 0.2 |
| 50 | 1.25 | 0.075 | 1.0 | 0.35 |
| 500 | 5.0 | 0.100 | 2.0 | 0.5 |

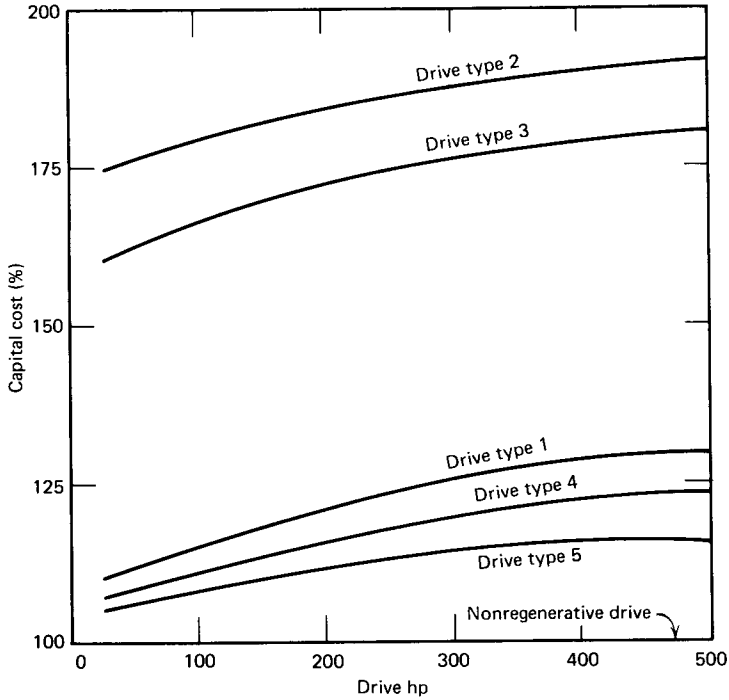


*Fig. 3.29* Capital cost variation of drives. The cost for a nonregenerative drive is considered as a reference (i.e., 100%). Drive type 1: Armature current reversal with changeover contactors. Drive type 2: Armature current reversal with circulating current dual-converter. Drive type 3: Armature current reversal with noncirculating current dual-converter. Drive type 4: Field current reversal with noncirculating current dual-converter. Drive type 5: Field current reversal with changeover contractors.

are either electronic or solid-state in nature. Fortunately, the reliability of electronic equipment is now very high. At present diagnostic features can be incorporated in the control circuitry to monitor fault location. Fault location diagnosis greatly helps in correcting the situation and restoring the drive to operation in a short time.

## REFERENCES

1 W. McMurray, "A Study of Asymmetrical Gating for Phase-Controlled Converters," *IEEE Transactions on Industry Applications*, Vo. IA-8, No. 3, May 1972.

2 B. R. Pelly, *Thyristor Phase-Controlled Converters and Cycloconverters*, Wiley-Interscience, New York, 1971.

3 D. L. Duff and A. Ludbrook, "Reversing Thyristor Armature Dual-Converter with Logic Crossover Control," *IEEE Transactions on Industry and General Applications*, Vol. IGA-1, No. 3, May 1965.

4 T. Krishnan and B. Ramaswami, "A Thyristorized Four Quadrant DC Motor Drive," *IFAC Symposium Proceedings*, Vol. 2, Düsseldorf, October 1974.

5 P. C. Sen and M. L. MacDonald, "Thyristorized DC Drives with Regenerative Braking and Speed Reversal," *IEEE Transactions on Industrial Electronics and Control Instrumentation*, Vol. IECI-25, No. 4, November 1978.

6 F. H. Bouttell, "Thyristor Power Converters for DC Motor Control," Unpublished thesis, Professional Engineers of Ontario (Canada), Toronto, 1969.

7 C. G. Hagensick and E. J. Cham, "Analysis of Ignitron Rectifiers for Reversing Mill Drives," AIEE Winter General Meeting, New York, February, 1958.

8 J. R. G. Schofield, G. A. Smith, and M. G. Whitmore, "The Applications of Thyristors to the Control of DC Machines," IEE Conference Publication, Number 17, London, November 1965.

9 J. G. Milburn, "The Evaluation and Selection of Regenerative Variable Speed DC Drives," IEE Conference Publication, Number 93, London, October 1972.

# 4

# DC Chopper Drives

Many industrial drives and processes take power from dc voltage sources. In most cases, conversion of the dc source voltage to different levels is required. For example, subway cars, trolley buses, or battery-operated vehicles take power from a fixed-voltage dc source. However, their speed control requires conversion of a fixed-voltage dc source to a variable-voltage dc source for the armature of the dc motor. Other industrial applications require dc power converters with ratings that may range from a few watts to thousands of kilowatts. Classically, a variable dc voltage is obtained from a fixed dc voltage by two methods: a resistance controller or a motor-generator set.

**Resistance Control** In this method a variable resistance is used in between the fixed-voltage dc source and the load. This method is still used in the control of traction motors, but it is inefficient because of losses in the resistance.

**Motor-Generator Set** A variable dc output voltage is obtained by controlling the field current of the dc generator. This system is still used in some industrial drives. Three machines of the same power rating are involved, and therefore the system is bulky, costly, slow in response, and less efficient.

In the 1960s high-power thyristor devices became available to make the solid-state dc power converters practical and economically viable for drives powered from dc sources. These converters offer greater efficiency, faster response, smooth operation, minimal maintenance, smaller size, and lower weight and cost. There are two broad types of dc-to-dc thyristor converters, as shown in Fig. 4.1.

***Inverter-Rectifier***

In the inverter-rectifier scheme, the dc is first converted to ac, which is then stepped up or down by a transformer and then rectified back to dc. The conversion is in two stages, dc to ac and ac to dc, and therefore is costly, bulky, and less efficient. However, the transformer provides isolation between load and source.

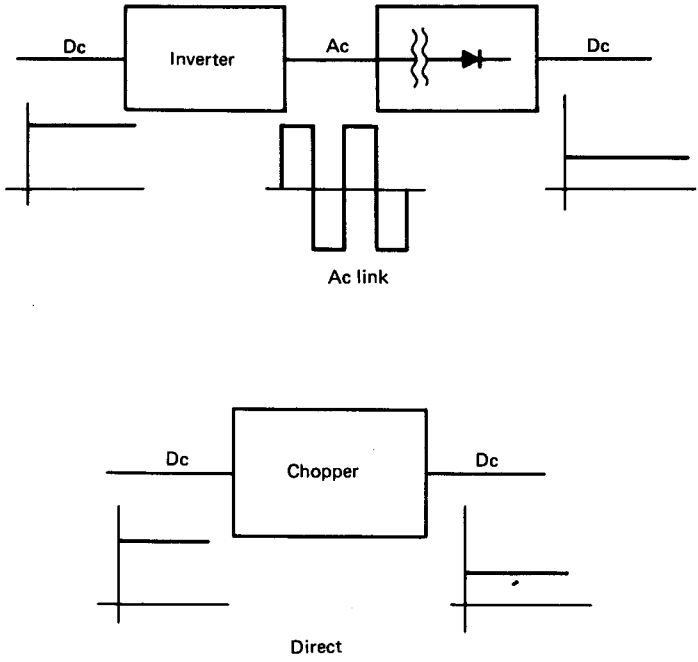


*Fig. 4.1* Dc-to dc thyristor converters.

## *DC Chopper*

The dc chopper converts directly from dc to dc and is a relatively new technology. It may be visualized as a dc equivalent to an ac transformer, because in performing dc-to-dc conversion its behavior is similar to that of a continuously variable turn-ratio transformer.

The chopper can replace the resistor commonly used in series with the armature of dc motors for speed control. Therefore it can be used in battery-operated vehicles where energy saving is a prime consideration. Choppers used in subway cars reduce tunnel heating. Choppers can provide regenerative braking of the motor and return the energy back to the supply. This results in energy saving for transportation systems with frequent stops. Choppers therefore find wide applications in traction systems all over the world. There are several in North America. Choppers are used in the BART (Bay Area Rapid Transit) system in San Francisco and in subway cars in Toronto and Montreal. Choppers also are used in other applications such as interurban and trolley cars, marine hoists, forklifts trucks, and mine-haulers. Choppers will probably be used in future electric automobiles for speed control and braking. A few of the good features of the chopper drives are: smooth control, high efficiency, and fast response and regeneration.

## 4.1 PRINCIPLES OF CHOPPER OPERATION

A chopper is a thyristor on/off switch that connects load to and disconnects it from the supply and produces a chopped load voltage from a constant-input supply voltage. This process is illustrated in Fig. 4.2. The chopper is represented by an SCR inside a dotted square. During the period $t_{ON}$, when the chopper is on, the supply terminals are connected to the load terminals. During the interval $t_{OFF}$, when the chopper is off, load current flows through the free-wheeling diode $D_{FW}$, and the load terminals are shorted. A chopped dc voltage is thus produced at the load terminals. The average load voltage $E_o$ is given by

$$E_o = E\frac{t_{ON}}{t_{ON} + t_{OFF}}$$

$$= E\frac{t_{ON}}{T}$$

$$= \alpha E \tag{4.1}$$

where $t_{ON}$ = on-time
$t_{OFF}$ = off-time
$T = t_{ON} + t_{OFF}$ = chopping period
$\alpha = \frac{t_{ON}}{T}$ = duty cycle.

The load voltage is therefore controlled by the duty cycle of the chopper. It can be varied in one of the following ways.

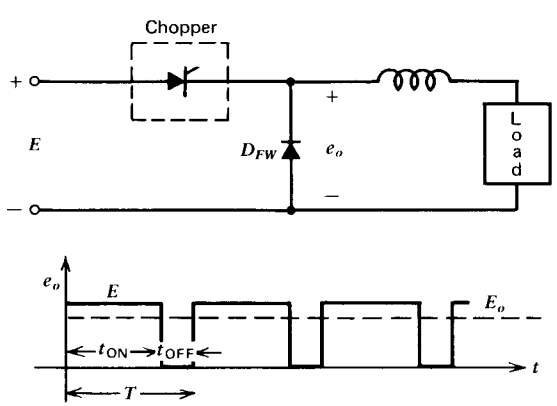


*Fig. 4.2* Basic chopper circuit configuration and operation.

1 **Constant-Frequency System:** $f = 1/T$ The chopping frequency (and hence the chopping period $T$) is kept constant and the on-time $t_{ON}$ is varied. This may be called *pulse-width modulation.*

2 **Variable-Frequency System** The chopping period $T$ is varied, and either (a) on-time $t_{ON}$ is kept constant or (b) off-time $t_{OFF}$ is kept constant. This may be called *frequency modulation.*

Figure 4.3 illustrates the principles of pulse-width modulation and frequency modulation. The latter has the following major disadvantages.

**a** The frequency has to be varied over a wide range to provide the full output voltage range. Filter design for variable-frequency operation is difficult. The possibility of interference with signaling and telephone lines is greater.

**b** The large off-time at low output voltage will make the current of a dc motor load discontinuous.

The constant-frequency system is thus the preferred scheme for chopper drives.

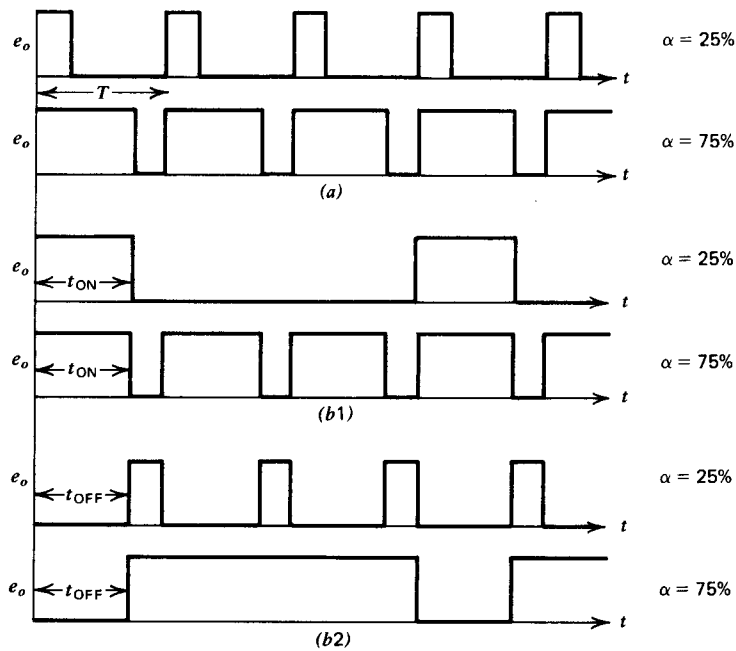


***Fig. 4.3*** Output voltage waveforms for basic chopper. (*a*) Constant-frequency system. (*b*) Variable-frequency system: (1) constant $t_{ON}$; (2) constant $t_{OFF}$.

**Example 4.1**

The speed of a separately excited dc motor is controlled by a chopper as shown in Fig. 4.8*a*. The dc supply voltage is 120 V, armature circuit resistance is $R_a = 0.5\ \Omega$, armature circuit inductance is $L_a = 20$ mH, and motor constant is $K_a\Phi = 0.05$ V/rpm. The motor drives a constant-torque load requiring an average armature current of 20 A. Assume that motor current is continuous.

Determine:

1 the range of speed control;
2 the range of the duty cycle $\alpha$.

*Solution*

Minimum speed is zero at which $E_g = 0$. Therefore from equation 2.17

$$E_a = I_a R_a = 20 \times 0.5 = 10\,\text{V}$$

From equation 4.1

$$10 = 120\alpha$$

$$\alpha = \frac{1}{12}$$

Maximum speed corresponds to $\alpha = 1$ at which $E_a = E = 120$ V.

Therefore

$$E_g = E_a - I_a R_a$$

$$= 120 - (20 \times 0.5)$$

$$= 110\ \text{V}$$

From equation 2.13

$$N = \frac{E_g}{K_a\Phi} = \frac{110}{0.05} = 2200\,\text{rpm}$$

The range of speed is $0 < N < 2200$ rpm, and the range of the duty cycle is $1/12 < \alpha < 1$.

### 4.1.1 Step-Up Choppers

The chopper configuration shown in Fig. 4.2 produces output voltages less than the input voltage (i.e., $E_o < E$). However, a change in the chopper configuration, as shown in Fig. 4.4, provides higher load voltages.

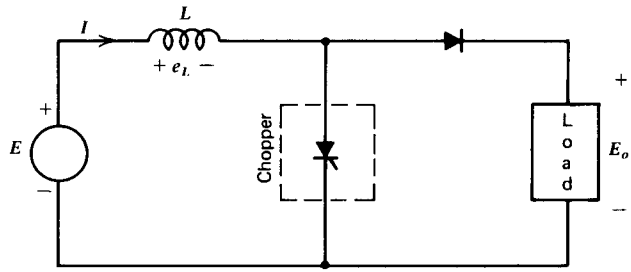


*Fig. 4.4* Step-up chopper configuration.

When the chopper is on, the inductor is connected to the supply $E$, and energy from the supply is stored in it. When the chopper is off, the inductor current is forced to flow through the diode and load. The induced voltage $e_L$ across the inductor is negative. The inductor voltage adds to the source voltage to force the inductor current into the load. Thus, the energy stored in the inductor is released to the load.

If the ripple in the source current is neglected, then during the time the chopper is on the energy input to the inductor from the source is

$$W_i = EIt_{ON} \tag{4.2}$$

During the time the chopper is off, energy released by the inductor to the load is

$$W_o = (E_o - E)It_{OFF} \tag{4.3}$$

For a lossless system, in the steady state, these two energies will be the same.

$$EIt_{ON} = (E_o - E)It_{OFF} \tag{4.4}$$

from which

$$E_o = E\frac{t_{ON} + t_{OFF}}{t_{OFF}}$$

$$= E\frac{T}{T - t_{ON}}$$

$$= \frac{E}{1 - \alpha} \tag{4.5}$$

Thus, for a variation of $\alpha$ in the range $0 < \alpha < 1$, the voltage $E_o$ will vary in the range $E < E_o < \infty$. This principle of operation is utilized in the regenerative braking of a dc motor. In Fig. 4.4, if $E$ represents the armature of the dc

machine and $E_o$ represents the dc supply, power can be fed back from the decreasing motor voltage $E$ to the fixed supply voltage $E_o$ by proper adjustment of the duty cycle.

### 4.1.2 Chopper Configuration

The various chopper configurations and their operation in different quadrants are shown in Table 4.1. In the first quadrant chopper $e_o = E$ when the chopper is on and $e_o = 0$ when the chopper is off. Therefore, both average load voltage $E_o$ and current $I_o$ are positive, and thus power flows from source to load. This configuration is used for motoring operation of a dc motor load.

In the second quadrant, or regenerative, chopper $e_o = 0$ when the chopper is on, and $e_o = E$ when the chopper is off. However, the current flows out from the load. Since $E_o$ is positive and $I_o$ is negative, the power flow is from load to source. This configuration is used for regenerative braking of dc motors.

The above two circuits are combined in the two-quadrant chopper, type $A$. Here $e_o = 0$ if chopper $CH2$ or diode $D_1$ conducts, and $e_o = E$ if chopper $CH1$ or diode $D_2$ conducts. $E_o$ is therefore positive. However, $i_o$ can reverse direction. It is positive if $CH1$ is on or $D_1$ conducts and negative if $CH2$ is on or $D_2$ conducts. Since $E_o$ is positive and $I_o$ is reversible, power flow is reversible. This chopper configuration may be used for both motoring and regenerative braking of a dc motor.

In the two-quadrant chopper, type $B$, $e_o = +E$ if the two choppers are on, and $E_o = -E$ if they are off and diodes $D_1$ and $D_2$ conduct. $E_o$ is positive or negative depending on whether on-time is greater or less than the off-time of the choppers. Since $I_o$ is positive and $E_o$ is reversible, power flow is reversible. This chopper configuration may be used for both motoring and regenerative braking of the dc motor. In the regenerative mode of operation, the motor voltage $E_g$ has to be reversed.

In the four-quadrant chopper both $E_o$ and $I_o$ are reversible. With $CH4$ always on, and $CH3$ always off, operation of choppers $CH1$ and $CH2$ will make $E_o$ positive and $I_o$ reversible. With $CH2$ always on and $CH1$ always off, operation of $CH3$ and $CH4$ will make $E_o$ negative and $I_o$ reversible. This four-quadrant chopper configuration can be used for a reversible regenerative dc drive. However, when a two-quadrant chopper is used, a simple reversal of armature or field terminals of the dc motor will make the drive reversible and regenerative.

## 4.2 CHOPPER DETAILS

We have been considering a chopper as an ideal on-off switch represented by an SCR inside a dotted square. A chopper is, in fact, a main power SCR

***Table 4.1*** **Chopper Configurations**

| Type | Chopper configuration | $E_o - I_o$ characteristics | Function |
|---|---|---|---|
| First-quadrant chopper | 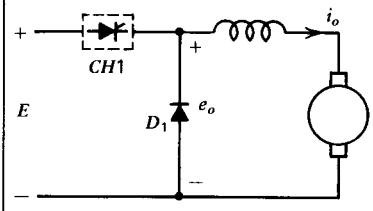 | 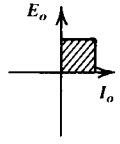 | $e_o = E$, $CH1$ on<br>$= 0$, $CH1$ off<br>$D_1$ on |
| Second-quadrant or regenerative chopper | 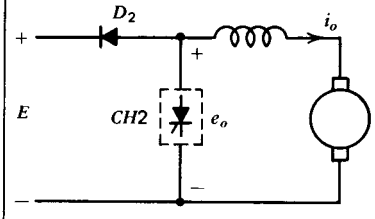 | 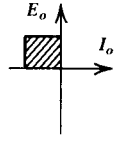 | $e_o = 0$, $CH2$ on<br>$= E$, $CH2$ off<br>$D_2$ on |
| Two-quadrant type *A* chopper | 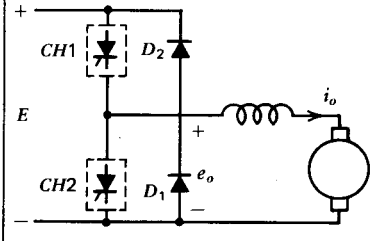 | 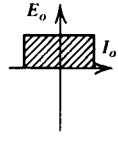 | $e_o = E$, $CH1$ or $D_2$ on<br>$= 0$, $CH2$ or $D_1$ on<br>$i_o$ = Positive<br>$CH1$ or $D_1$ on<br>= Negative<br>$CH2$ or $D_2$ on |
| Two-quadrant type *B* chopper | 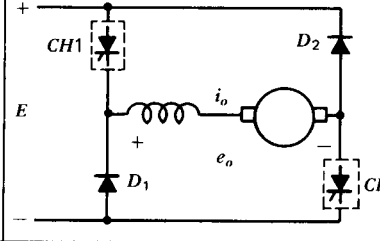 | 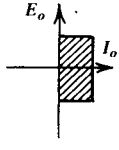 | $e_o = +E$,<br>$CH1$ & $CH2$ on<br>$e_o = -E$,<br>$CH1$ & $CH2$ off<br>$D_1$ & $D_2$ on |
| Four-quadrant chopper | 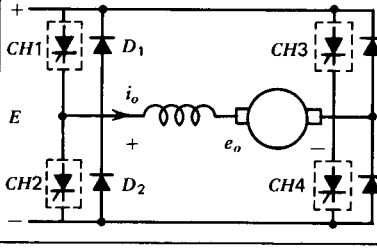 | 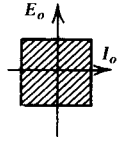 | $CH4$ on & $CH3$ off<br>$CH1$ & $CH2$ Operated<br>$E_o$ = Positive<br>$I_o$ = Reversible<br>$CH2$ on & $CH1$ off<br>$CH3$ & $CH4$ operated<br>$E_o$ = Negative<br>$I_o$ = Reversible |

switch together with the commutation circuitry to turn it off. There are various ways in which an SCR can be turned off. There have been numerous innovations in the commutation circuitry.[1–3] However, commutation circuitry can be broadly divided into two groups:

1 **Load Commutation** In load commutation the load current flowing through the thyristor either becomes zero or is transferred to another device from the conducting thyristor.
2 **Forced Commutation** In forced commutation the current through the SCR is forced to become zero to turn the SCR off. There are two ways in which this can be accomplished.
   a Voltage commutation: In the voltage commutation scheme a charged capacitor momentarily reverse-biases the conducting SCR and turns it off.
   b Current commutation: In the current commutation scheme, a current pulse is made to flow in the reverse direction through the conducting SCR, and when the net SCR current is zero, it is turned off.

Many commutation circuits have been devised. We will describe three circuits to illustrate the above commutation principles.

### 4.2.1 Voltage Commutation of a Chopper

The circuit shown in Fig. 4.5*a* is one of the earliest chopper circuits and has been widely used. The main power switch is the thyristor $S_1$. Its commutation circuitry consists of an auxiliary thyristor $S_2$, diode $D$, inductor $L$, and capacitor $C$.

To start the circuit, the capacitor $C$ is charged with the polarity shown in one of two ways.

1 By closing and then opening the starting switch *sw*. Charging will be through source $E$, capacitor $C$, switch *sw*, and charging resistor $R$.
2 By triggering the auxiliary thyristor $S_2$ first. Charging will be through $E$, $C$, $S_2$, and load. Thyristor $S_2$ will turn off as the charging current decays to zero.

Figure 4.5*b* shows the current and voltage waveforms. The main thyristor $S_1$ is triggered at $t_0$. Current flows in two paths. The load is connected to the supply; therefore load current $i_o$ flows through $S_1$, and commutation current $i_C$ flows through $C$, $S_1$, $L$, and $D$. The charge on $C$ is reversed at $t_1$ and held by the hold-off diode $D$.

To turn off the main thyristor $S_1$, the auxiliary thyristor $S_2$ is triggered at a desired instant $t_2$. The capacitor $C$ is placed across $S_1$, reverse-biases it, and

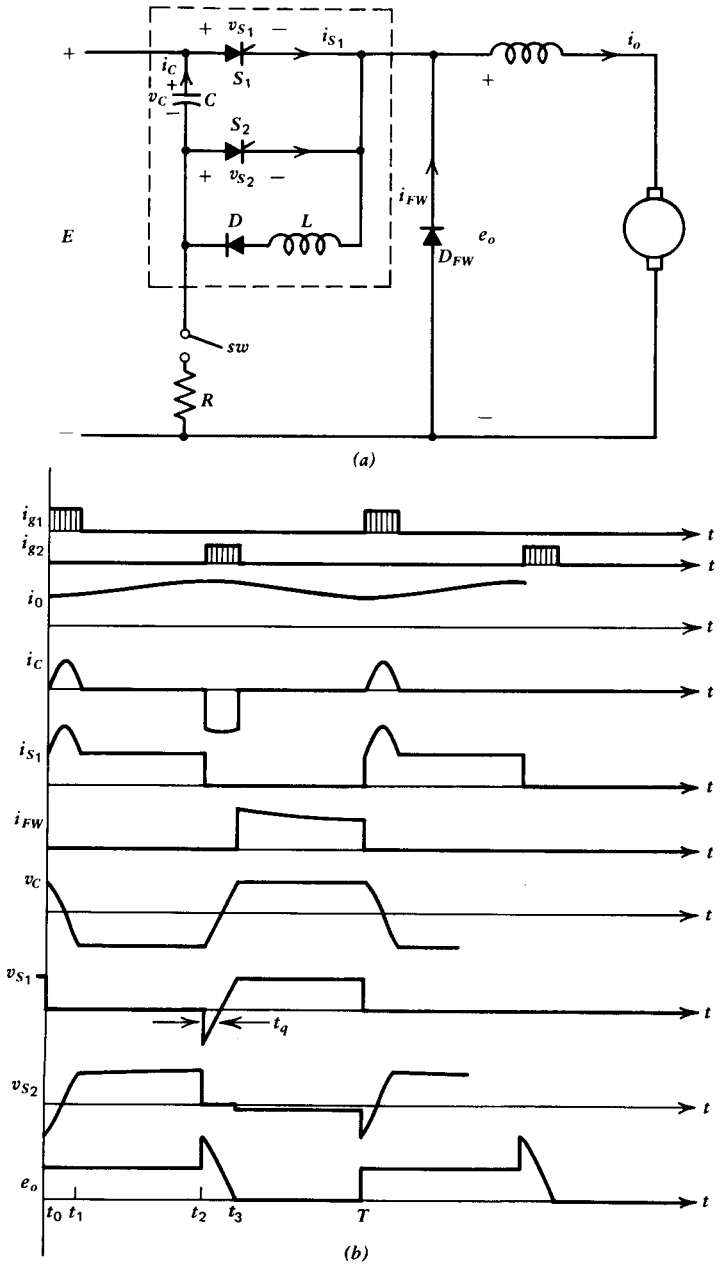


*Fig. 4.5* Voltage-commutated chopper. (*a*) Circuit. (*b*) Waveforms.

turns it off. After the thyristor $S_1$ is turned off, the capacitor provides the load current through $E$, $C$, $S_2$ and load. The thyristor $S_2$ turns off naturally at $t_3$ when the capacitor current decays to zero. This happens when the capacitor voltage equals the supply voltage, making the free-wheeling diode $D_{FW}$ forward-biased. The load current now free-wheels through the free-wheeling diode. At $t = T$, the main thyristor $S_1$ is triggered again, and the cycle repeats.

This is a simple chopper circuit that has been used widely. The auxiliary thyristor $S_2$ is load commutated. This chopper has a few disadvantages. It requires a starting circuit, such as the switch *sw* and resistor $R$, or the logic circuit should be such that thyristor $S_2$ is triggered first. The load voltage jumps to twice the supply voltage when the commutation is initiated.

### *Commutating Capacitor C*

The commutating capacitor can be designed from consideration of the turn-off time $t_q$ available for the thyristor $S_1$. During this time $t_q$, the capacitor voltage rises from $-E$ to zero. Assuming a constant load current $I_{om}$ during commutation,

$$CE = I_{om} t_q \tag{4.6}$$

where $I_{om}$ = maximum load current. From equation 4.6

$$C = \frac{I_{om} t_q}{E} \tag{4.7}$$

For successful commutation, circuit turn-off time $t_q$ must be greater than the thyristor turn-off time $t_{\text{off}}$. Let

$$t_q = t_{\text{off}} + \Delta t \tag{4.8}$$

From equations 4.7 and 4.8

$$C = \frac{I_{om}(t_{\text{off}} + \Delta t)}{E} \tag{4.9}$$

### *Commutating Inductor L*

The commutating inductor $L$ can be designed from a compromise between two requirements: (1) peak value of the capacitor current $i_c$, which flows through $S_1$ when it is fired; (2) the time $t_1 - t_0$ during which the capacitor current pulse lasts. This time is required to reset the capacitor voltage polarity so that the capacitor is ready to commutate $S_1$ when $S_2$ is fired.

The capacitor current $i_c$ when $S_1$ is fired is a current in an $LC$ ringing circuit and is given by

$$i_c = E\left(\frac{C}{L}\right)^{1/2} \sin \omega_r t \tag{4.10}$$

where $\omega_r = (1/LC)^{1/2} = 2\pi/T_r$ is the ringing frequency in radians per second and
$T_r = 2(t_1 - t_0)$.

The peak capacitor current is

$$i_c|_{\text{peak}} = E\left(\frac{C}{L}\right)^{1/2} = \frac{E}{\omega_r L} \tag{4.11}$$

When $S_1$ is turned on, it has to carry the load current and the peak capacitor current. Let this peak capacitor current be equal to or less than the load current so that the peak current through $S_1$ is not unduly large.

$$E\left(\frac{C}{L}\right)^{1/2} \leqslant I_{om} \tag{4.12}$$

or

$$L \geqslant C\left(\frac{E}{I_{om}}\right)^2 \tag{4.13}$$

The resetting time $t_1 - t_0$ can be decreased by selecting a small value of the commutating inductance $L$. However, a small value of $L$ increases the peak value of the capacitor current as can be seen from equation 4.11. On the other hand, if $t_1 - t_0$ is large, the range of load voltage is reduced. The minimum load voltage is given by

$$E_0|_{\min} = \frac{t_1 - t_0}{T} E \tag{4.14}$$

where $T$ is the time period of the chopper.

In order to vary the load voltage over a wide range the minimum value of $E_0$ should be equal to or less than 10% of the supply voltage $E$. Therefore

$$\frac{t_1 - t_0}{T} \leqslant 0.1 \tag{4.15}$$

or

$$\frac{\pi\sqrt{LC}}{T} \leqslant 0.1 \tag{4.16}$$

from which

$$L \leqslant \frac{0.01T^2}{\pi^2 C} \tag{4.17}$$

**Example 4.2**

A battery-powered electric car is controlled by a chopper, as shown in Fig. 4.5*a*. The battery voltage is 100 V; starting current is 100 A; thyristor turn-off time is 20 $\mu$sec; chopper frequency is 400 Hz. Calculate the values of the commutating capacitor $C$ and commutating inductor $L$.

*Solution*

For reliable commutation let $\Delta t = t_{\text{off}} = 20$ $\mu$sec. Therefore, from equation 4.9,

$$C = \frac{100 \times 40 \times 10^{-6}}{100}$$

$$= 40\ \mu\text{F}$$

From equation 4.13

$$L > 40 \times 10^{-6} \times \left(\frac{100}{100}\right)^2 \text{H}$$

$$> 40\ \mu\text{H}$$

Now the chopper period $T = 2.5$ msec. From equation 4.17

$$L < \frac{0.01(2.5 \times 10^{-3})^2}{\pi^2(40 \times 10^{-6})} \text{H}$$

$$< 158.5\ \mu\text{H}$$

The value of the commutating inductor is in the range $40 < L < 158.5$ $\mu$H. A value of $L$ close to 40 $\mu$H will be a good choice because it will allow the minimum load voltage be about 5% of the supply voltage, thereby giving a wider range of variation in the load voltage.

### 4.2.2 Current Commutation of a Chopper

Figure 4.6*a* shows a current-commutated chopper. The main thyristor $S_1$ of the chopper is commutated by a current pulse generated in the commutation circuitry. The sequence of operation is as follows, and various significant waveforms are shown in Fig. 4.6*b*.

The capacitor $C$ is charged through the source $E$, the capacitor $C$, and the charging resistor $R$. The main thyristor is fired at $t = t_0$. The load terminals are connected to the supply, and the load current flows through $S_1$.

At $t = t_1$, commutation of $S_1$ is initiated by firing the auxiliary thyristor $S_2$. An oscillatory current flows in the circuit consisting of $C$, $S_2$, and $L$.

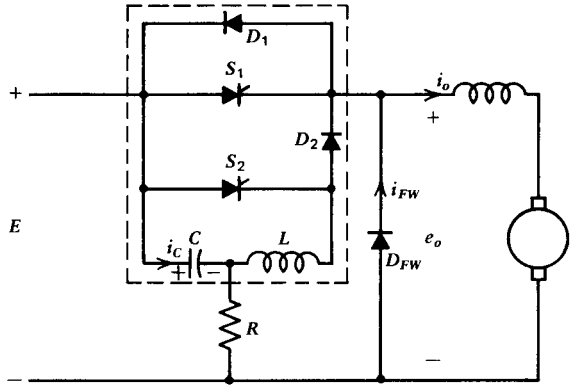


(a)

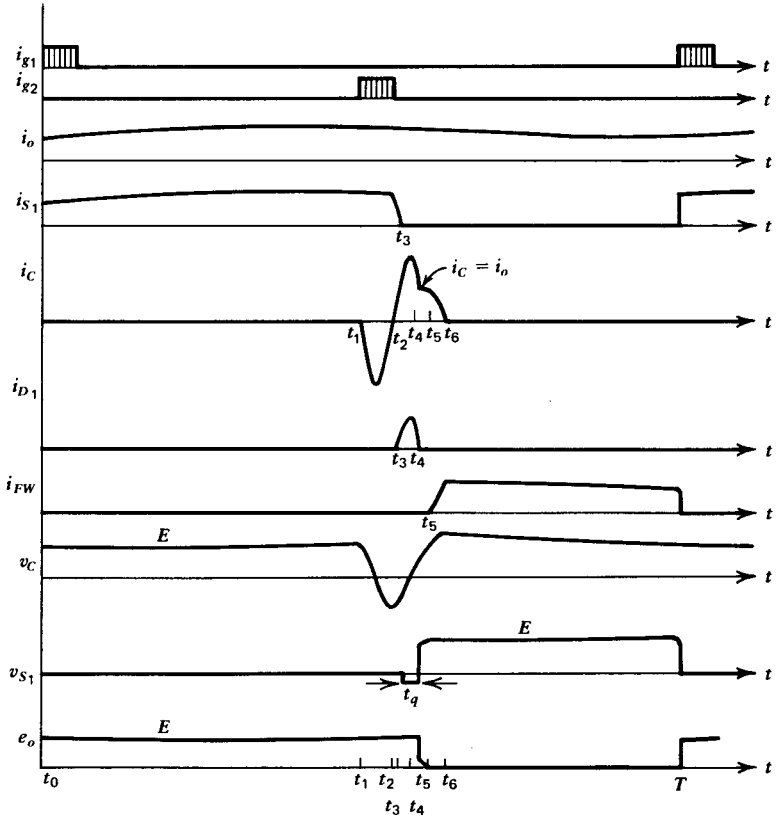


(b)

***Fig. 4.6*** Current-commutated chopper. (*a*) Circuit. (*b*) Waveforms.

When $i_C$ reverses at $t_2$, thyristor $S_2$ turns off (natural commutation), and the oscillatory current $i_C$ flows through $D_2$ and $S_1$. In $S_1$ it flows in the opposite direction and therefore decreases its current $i_{S_1}$. At $t_3$, $i_C = i_{S_1}$ and so the net current through $S_1$ is zero and it turns off. As $i_{S_1}$ reduces to zero, diode $D_1$ begins to conduct the current $i_C - i_o$ and keeps the main thyristor $S_1$ reverse-biased.

At $t_4$, $i_C = i_o$ and $i_{D_1} = 0$. At this instant, if the free-wheeling diode $D_{FW}$ is not forwarded-biased, the load current will flow through $E$, $C$, $L$, $D_2$, and load.

At $t_5$, the free-wheeling diode becomes forward-biased and starts to conduct the load current $i_o$. The oscillatory circuit consisting of $C$ and $L$ is now subjected to new circuit conditions through $E$, $C$, $L$, $D_2$, and $D_{FW}$; and $i_C$ decays to zero at $t_6$ leaving $v_C$ greater than $E$. During $t_5$ to $t_6$, $i_o = i_C + i_{FW}$ and therefore, as $i_C$ decays, $i_{FW}$ builds up. From $t_6$ onward, load current free-wheels through $D_{FW}$ and decays. The capacitor voltage $v_C$ also decays because of discharge through $R$.

At $t = T$, the main thyristor $S_1$ is fired again, and the cycle repeats.

This chopper was developed by the Hitachi Electric Co., Japan, and has been used in traction cars, such as the subway cars in Toronto, Canada.[4] It has the following advantages. Commutation is reliable as long as load current is less than the peak commutation current $i_C$. The capacitor always remains charged with the right polarity. The auxiliary thyristor $S_2$ is naturally commutated as its current passes through zero value.

### *Commutating Components L and C*

The values of the commutating components $L$ and $C$ are selected to satisfy the following conditions.

1 Peak commutating current is larger than maximum anticipated load current to ensure commutation of the load current. Therefore, from equation 4.11,

$$E\left(\frac{C}{L}\right)^{1/2} = xI_{om} \tag{4.18}$$

where $x > 1$ and

$I_{om}$ = maximum load current.

2 Circuit turn-off time $t_q$ is greater than the thyristor turn-off time $t_{\text{off}}$.

$$t_q = t_{\text{off}} + \Delta t$$

From Fig. 4.6*b*, $t_q = t_4 - t_3$.

A good choice of $x$ is 2; that is, the peak value of the commutation current is twice the maximum anticipated load current. At this value of $x$

$$\omega_r t_q = \frac{2\pi}{3} \tag{4.19}$$

or

$$t_q = \frac{2\pi}{3}(LC)^{1/2} = t_{\text{off}} + \Delta t \tag{4.20}$$

and

$$2I_{om} = E\left(\frac{C}{L}\right)^{1/2} \tag{4.21}$$

From equations 4.20 and 4.21

$$L = \frac{3E(t_{\text{off}} + \Delta t)}{4\pi I_{om}} \tag{4.22}$$

$$C = \frac{3I_{om}(t_{\text{off}} + \Delta t)}{\pi E} \tag{4.23}$$

**Example 4.3**

In example 4.2, if the chopper used is a current-commutated chopper, as shown in Fig. 4.6*a*, calculate the values of the commutating components $L$ and $C$.

*Solution*

From equation 4.22

$$L = \frac{3 \times 100 \times 40 \times 10^{-6}}{4 \times 3.14 \times 100}\ \text{H}$$

$$= 9.55\ \mu\text{H}$$

From equation 4.23

$$C = \frac{3 \times 100 \times 40 \times 10^{-6}}{3.14 \times 100}\ \text{F}$$

$$= 38.22\ \mu\text{F}$$

### 4.2.3 Load Commutation of a Chopper

Figure 4.7*a* shows a load-commutated chopper.[3] The chopper has four thyristors that function both as main and commutation thyristors. Thyristor pairs $S_1$, $S_2$ and $S_3$, $S_4$ alternately conduct the load current.

The sequence of operation is as follows, and some important waveforms are shown in Figure 4.7*b*.

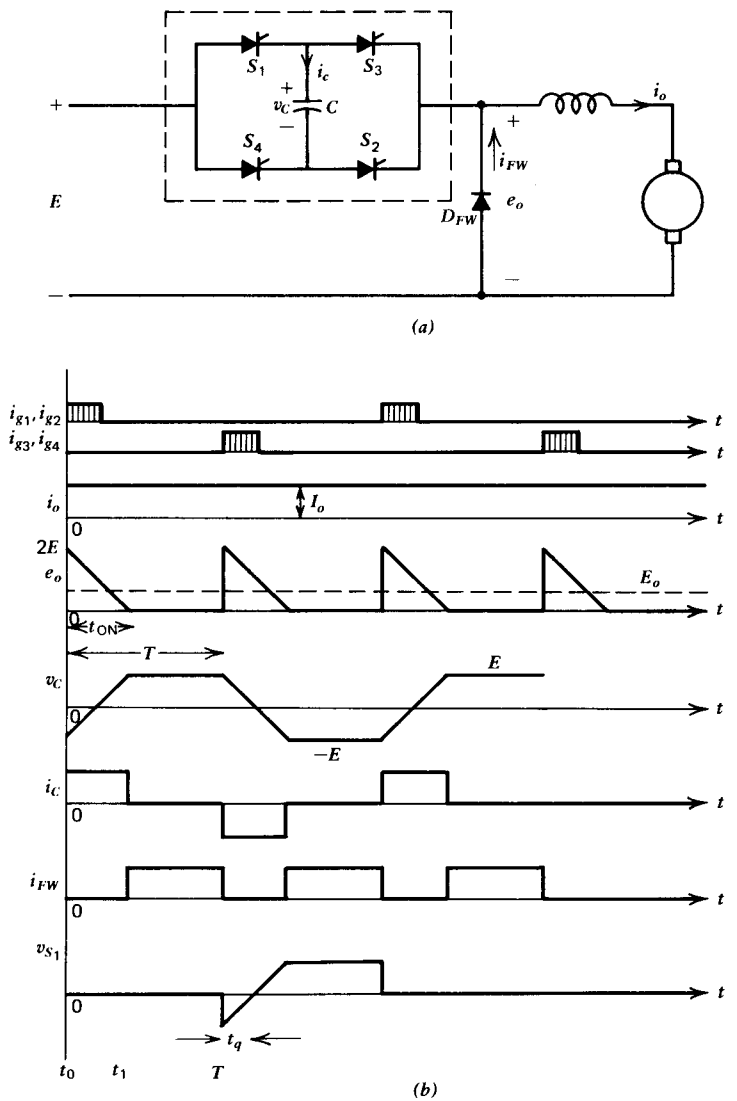


*Fig. 4.7* Load-commutated chopper. (*a*) Circuit. (*b*) Waveforms.

At $t = t_0$, thyristors $S_1$ and $S_2$ are triggered. Prior to this instant, the capacitor voltage was negative ($v_C = -E$) due to conduction by $S_3$ and $S_4$. The load voltage $e_o = E - v_C$ therefore jumps to $2E$. The load current now flows through $E$, $S_1$, $C$, $S_2$, and the load. The load current flowing through $C$ charges it, and at $t_1$ the capacitor voltage becomes $+E$. The free-wheeling diode $D_{FW}$ becomes forward-biased, and the load current is transferred from $S_1$ and $S_2$ to $D_{FW}$.

From $t_1$ onward, the free-wheeling diode $D_{FW}$ conducts the load current. At $t = T$, the other pair of thyristors $S_3$ and $S_4$ are triggered. This places the capacitor across $S_1$ and $S_2$, reverse-biases them, and turns them off. The cycle repeats.

The output voltage in this chopper is varied by changing the chopper frequency. It is therefore a frequency-modulated chopper. For a constant load current $I_o$ the on-time of the chopper is

$$t_{\text{ON}} = \frac{2EC}{I_o} \tag{4.24}$$

The output voltage is

$$\begin{aligned} E_o &= E\frac{t_{\text{ON}}}{T} \\ &= Et_{\text{ON}}f \\ &= \frac{2E^2Cf}{I_o} \end{aligned} \tag{4.25}$$

where $f$ = frequency of the chopper.

At the maximum chopper frequency of $f = f_{\max}$

$$E_o|_{f_{\max}} = E \tag{4.26}$$

From equations 4.25 and 4.26

$$E = \frac{2E^2C}{I_o} f_{\max} \tag{4.27}$$

or

$$f_{\max} = \frac{I_o}{2EC} \tag{4.28}$$

The value of the capacitor is chosen for maximum load current $I_{om}$. From equation 4.28 this value is

$$C = \frac{I_{om}}{2Ef_{\max}} \tag{4.29}$$

This chopper has several minor disadvantages. The peak load voltage is twice the supply voltage. Some load filtering may reduce this peak voltage. For high-power applications efficiency may become low because of higher switching losses at high frequencies and losses in the two conducting thyristors in series with the load. The free-wheeling diode must be a fast-recovery type, because $2E$ appears across it in a short time. A logic circuit must insure that one pair of thyristors is not turned on until the current in the other pair is commutated. This timing can be easily realized by sensing the capacitor current that is alternating. The commutating capacitor has to carry the load current at a frequency half the chopper frequency.

However, this chopper has some very good features. It is capable of commutating any amount of current. It does not require a commutating inductor that is normally costly and noisy. It can operate at high frequencies in the order of kilocycles, and therefore filtering requirements to smooth out motor current are minimal.

**Example 4.4**

In example 4.2, if the chopper used is a load-commutated chopper as shown in Fig. 4.7*a* and maximum chopper frequency is 5 kHz, calculate the value of the commutating capacitor $C$.

*Solution*

From equation 4.29

$$C = \frac{100}{2 \times 100 \times 5000} \quad \text{F}$$

$$= 100 \quad \mu\text{F}$$

The capacitor carries an alternating current, and therefore low-loss paper-type capacitors should be used. It also carries the load current. If a single capacitor of 100 $\mu$F and 100 A rating is not available; ten capacitors, each of 10 $\mu$F, or five capacitors, each of 20 $\mu$F, may have to be used, depending on the current rating of the capacitors available.

## 4.3 CHOPPER-FED DC MOTORS

The most important applications of choppers are in the speed control of dc motors used in industrial or traction drives. In this section chopper-controlled dc motors are analyzed. The performance characteristics of series dc motors and separately excited dc motors are obtained and discussed.

### 4.3.1 Analysis

Figure 4.8 shows the basic circuit and relevant waveforms for a chopper-driven series dc motor. Assume that the motor current $i_a$ is continuous as shown in Fig. 4.8*b* and that the speed is constant. The governing equations[2,5] are

$$E = R_a i_a + L_a \frac{di_a}{dt} + K_{af} i_a N + K_{res} N \qquad 0 < t < t_{ON} \tag{4.30}$$

$$0 = R_a i_a + L_a \frac{di_a}{dt} + K_{af} i_a N + K_{res} N \qquad t_{ON} < t < T \tag{4.31}$$

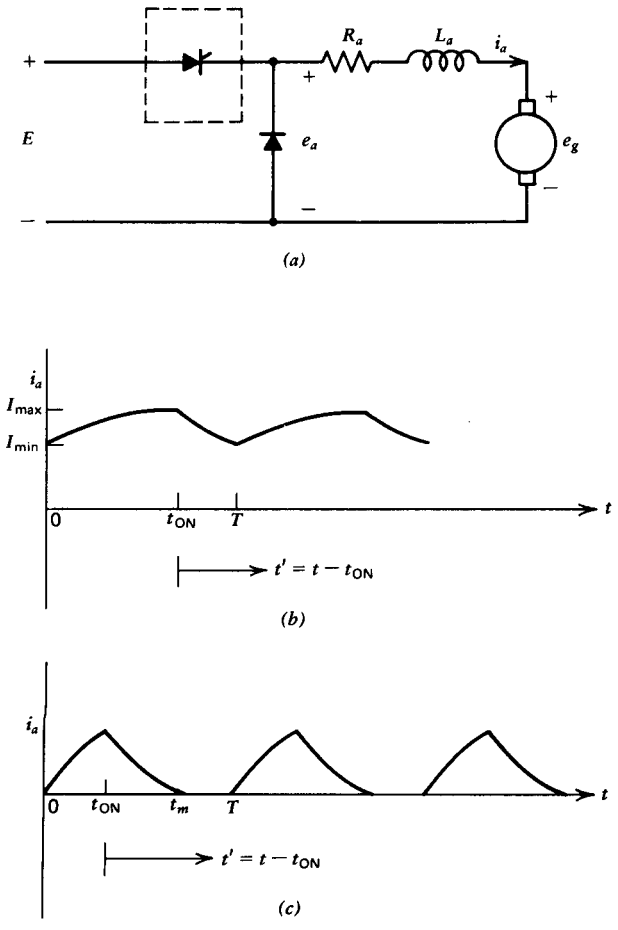


***Fig. 4.8*** Chopper-fed dc motor. (*a*) Basic circuit. (*b*) Continuous motor current. (*c*) Discontinuous motor current.

In the steady state, the current will be minimum at the instant the chopper is turned on and maximum at the instant the chopper is turned off, that is, $i_a(0) = I_{min}$ and $i_a(t_{ON}) = I_{max}$. The solutions for $i_a$ are

$$i_a = \frac{E - K_{res}N}{R_a + K_{af}N}(1 - e^{-t/\tau}) + I_{min}e^{-t/\tau} \qquad 0 < t < t_{ON} \tag{4.32}$$

$$i_a = \frac{-K_{res}N}{R_a + K_{af}N}(1 - e^{-t'/\tau}) + I_{max}e^{-t'/\tau} \qquad t_{ON} < t < T \tag{4.33}$$

where $t' = t - t_{ON}$ and
$\tau = L_a/(R_a + K_{af}N)$

From equation 4.32

$$I_{max} = i_a(t_{ON}) = \frac{E - K_{res}N}{R_a + K_{af}N}(1 - e^{-t_{ON}/\tau}) + (I_{min}e^{-t_{ON}/\tau}) \tag{4.34}$$

Now $i_a(0) = i_a(T) = i_a(t' = T - t_{ON})$. Therefore, from 4.33,

$$I_{min} = i_a(t' = T - t_{ON}) = \frac{-K_{res}N}{R_a + K_{af}N}(1 - e^{-(T - t_{ON})/\tau})$$

$$+ I_{max}e^{-(T - t_{ON})/\tau} \tag{4.35}$$

From equations 4.34 and 4.35

$$I_{min} = \frac{E}{R_a + K_{af}N}\frac{(e^{t_{ON}/\tau} - 1)}{(e^{T/\tau} - 1)} - \frac{K_{res}N}{R_a + K_{af}N} \tag{4.36}$$

$$I_{max} = \frac{E}{R_a + K_{af}N}\frac{(1 - e^{-t_{ON}/\tau})}{(1 - e^{-T/\tau})} - \frac{K_{res}N}{R_a + K_{af}N} \tag{4.37}$$

In the case of discontinuous armature current, as shown in Fig. 4.8*c*,

$$I_{min} = 0$$

From equation 4.34

$$I_{max} = \frac{E - K_{res}N}{R_a + K_{af}N}(1 - e^{-t_{ON}/\tau}) \tag{4.38}$$

To find the instant $t = t_m$ or $t' = t_m - t_{ON}$ at which the current becomes zero, the value of $I_{max}$ obtained from equation 4.38 is substituted in equation

4.33 and $i_a$ is made zero. Therefore

$$0 = \frac{-K_{res}N}{R_a + K_{af}N}(1 - e^{-(t_m - t_{ON}/\tau)}) + \frac{E - K_{res}N}{R_a + K_{af}N}(1 - e^{-t_{ON}/\tau})(e^{-(t_m - t_{ON}/\tau)}) \tag{4.39}$$

From equation 4.39

$$t_m = \tau \ln \left\{ e^{t_{ON}/\tau}\left[1 + \frac{E - K_{res}N}{K_{res}N}(1 - e^{-t_{ON}/\tau})\right]\right\} \tag{4.40}$$

The continuity of the motor current can be determined from equation 4.40. Once the nature of the current is known, the motor current is given by equation 4.32 when the chopper is on, and by equation 4.33 when the chopper is off. Equation 4.33 is valid for $t_{ON} < t < T$ for continuous motor current and $t_{ON} < t < t_m$ for discontinuous motor current.

To study the performance characteristics of the motor, expressions for average and rms motor current and average motor voltage have to be determined. These are obtained as follows.

***Average Motor Current: $I_a$***

$$I_a = \frac{1}{T}\left[\int_0^{t_{ON}} i_a(t)\,dt + \int_{t_{ON}}^{t_m} i_a(t)\,dt\right] \tag{4.41}$$

Let

$$I_1 = \frac{E - K_{res}N}{R_a + K_{af}N} \tag{4.42}$$

$$I_2 = \frac{-K_{res}N}{R_a + K_{af}N} \tag{4.43}$$

From equations 4.32, 4.33, 4.41, 4.42, and 4.43

$$I_a = \frac{1}{T}\left[I_1 t_{ON} + \tau(I_{min} - I_1)(1 - e^{-t_{ON}/\tau}) - I_2(t_m - t_{ON}) + \tau(I_{max} + I_2)(1 - e^{-(t_m - t_{ON})/\tau})\right] \tag{4.44}$$

Equation 4.44 is an expression for average motor current in closed form.

***RMS Motor Current: $I_{ar}$***

$$I_{ar} = \left\{ \frac{1}{T} \left[ \int_0^{t_{ON}} i_a^2(t)\,dt + \int_{t_{ON}}^{t_m} i_a^2(t)\,dt \right] \right\}^{1/2} \tag{4.45}$$

$$= \left\{ \frac{1}{T} \left[ I_1^2 t_{ON} + 2\tau I_1 (I_{min} - I_1)(1 - e^{-t_{ON}/\tau}) \right.\right.$$

$$+ \frac{\tau}{2}(I_{min} - I_1)^2 (1 - e^{-2t_{ON}/\tau}) + I_2^2 (t_m - t_{ON})$$

$$- 2\tau I_2 (I_{max} + I_2)(1 - e^{-(t_m - t_{ON})/\tau})$$

$$\left.\left. + \frac{\tau}{2}(I_{max} + I_2)^2 (1 - e^{-2(t_m - t_{ON}/\tau)}) \right] \right\}^{1/2} \tag{4.46}$$

Equation 4.46 is also in closed form.

***Torque***

The average motor torque is given by

$$T = K_{af} I_{ar}^2 \tag{4.47}$$

***Average Motor Voltage***

For continuous current

$$E_a = E\alpha \tag{4.48}$$

and $t_m = T$. For discontinuous current

$$E_a = E\alpha + K_{res} N \frac{(T - t_m)}{T} \tag{4.49}$$

and $t_m < T$.

***Separately Excited DC Motor***

The above analysis is also valid for separately excited dc motors with the following exceptions.

1 The term $K_{af}N$ is not present.
2 $K_{res}N$ is replaced by a back emf $K_a \Phi N$.

Therefore

$$I_1 = \frac{E - K_a \Phi N}{R_a} \tag{4.50}$$

$$I_2 = \frac{-K_a \Phi N}{R_a} \tag{4.51}$$

3 $T = K_a \Phi I_a$ (4.52)

### 4.3.2 Performance Characteristics

The operating characteristics of the chopper-controlled dc motors can be evaluated by using the expressions for current in closed form obtained in the previous section. The flowchart for a computer program for the evaluation of the operating characteristics is shown in Fig. 4.9. For a particular duty cycle and assumed speed, the continuity of the motor current is first determined, and then appropriate expressions are used to determine the performance parameters.

***Separately Excited DC Motor Performance***

The performance characteristics of a laboratory-size separately excited dc motor (110 V, 1800 rpm, 2.5 hp) are obtained and discussed here.

The torque-speed characteristics for a chopping frequency of 120 Hz are shown in Fig. 4.10. This frequency is chosen so that results can be compared with those of the single-phase phase-controlled motors in which the frequency of turning on a thyristor is also 120 Hz.

The *T-N* characteristics (Figs. 4.10 and 2.9) for both chopper control and phase control are drooping in nature. However, the drop in speed is less for chopper control than for phase control, primarily because of the nature of the supply voltage, which does not change with time. The region of discontinuous motor current operation can be reduced with the chopper control by increasing the chopping frequency or time constant of the motor circuit (i.e., adding an inductor in the motor circuit). This is shown in Fig. 4.11. The *T-N* characteristics will be essentially the same if the motor circuit inductance is increased or if the chopper frequency is increased by the same factor.

The variation of peak-to-average and rms-to-average motor current as a function of speed is shown in Figs. 4.12 and 4.13, respectively. These are compared with characteristics obtained with phase control for the same motor armature inductance. Chopper control shows improved performance in the region of higher speed. An increase in chopper frequency to 600 Hz, with $\tau_a$ kept at 10 msec, substantially improves the performance of the chopper control scheme. The significant reduction in peak motor current increases the commutating capability of the motor. The decrease in the rms current with chopper control decreases the heating of the motor.

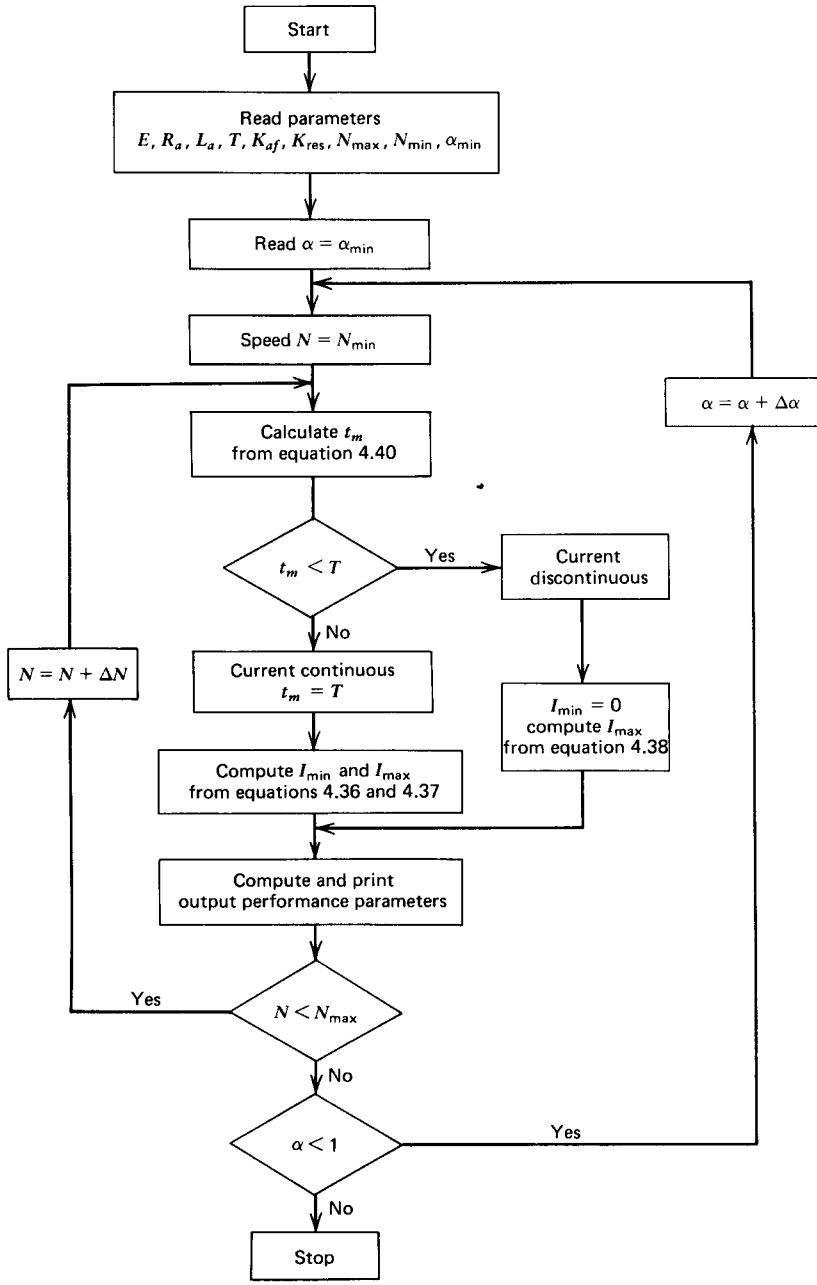


*Fig. 4.9* Computer flowchart to determine the performance characteristics of chopper-controlled dc motors.

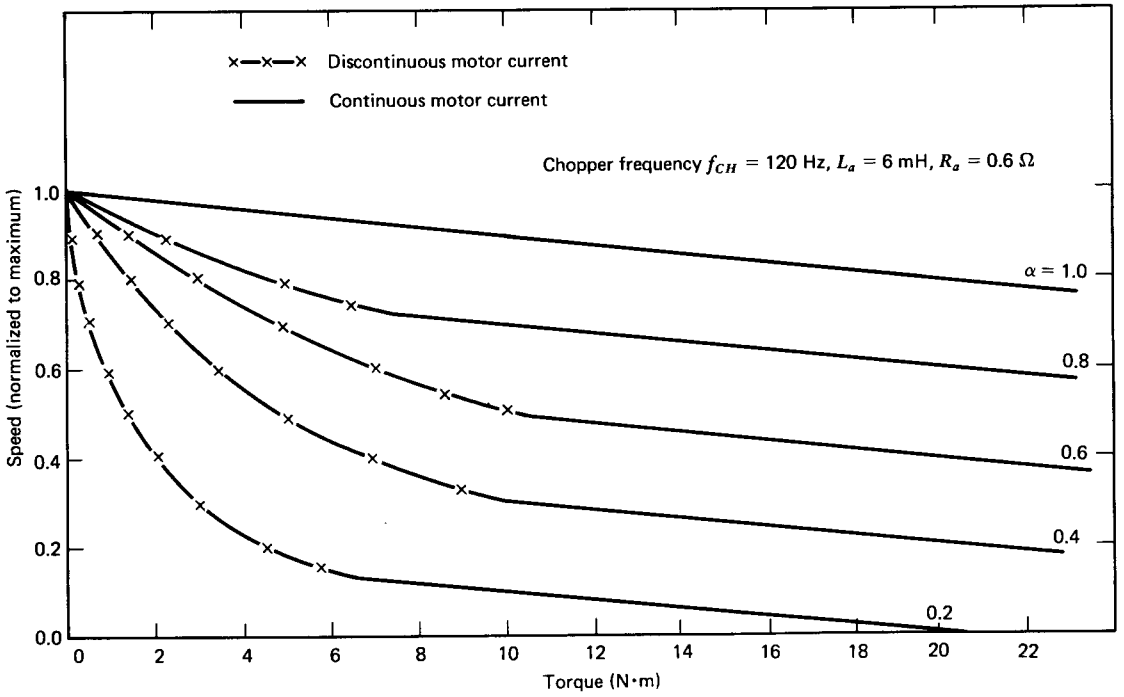


***Fig. 4.10*** Torque-speed characteristics for a chopper-fed separately excited dc motor.

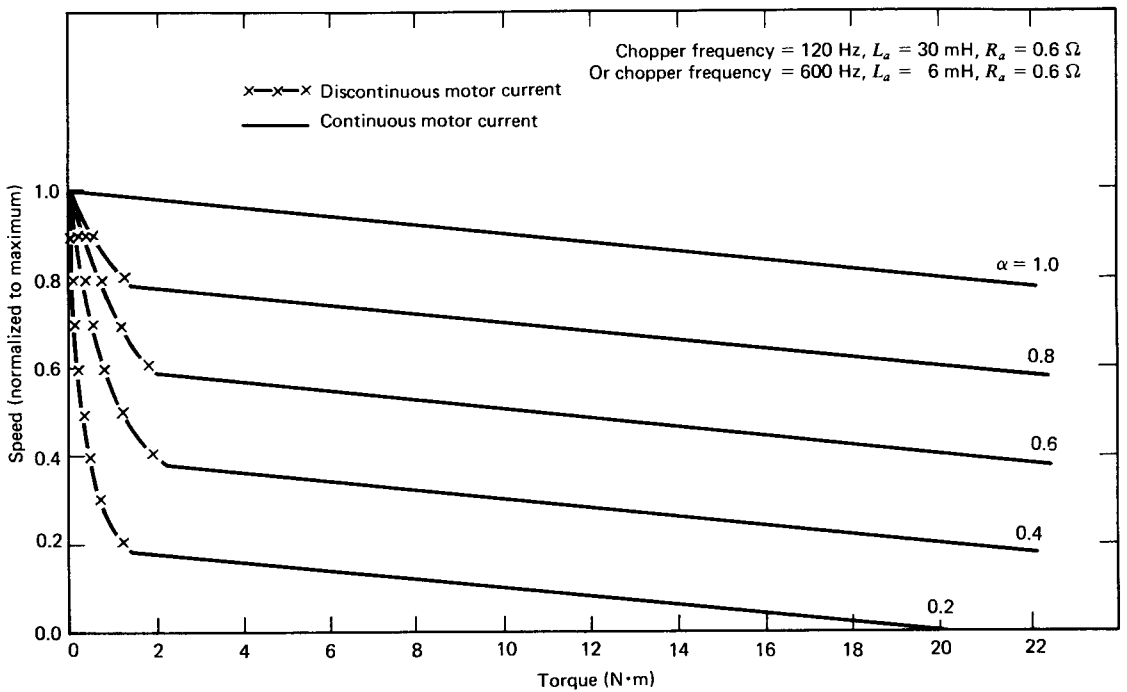


*Fig. 4.11* Effects of chopping frequency or armature inductance on continuity of motor current and on torque-speed characteristics of a separately excited dc motor controlled by a chopper.

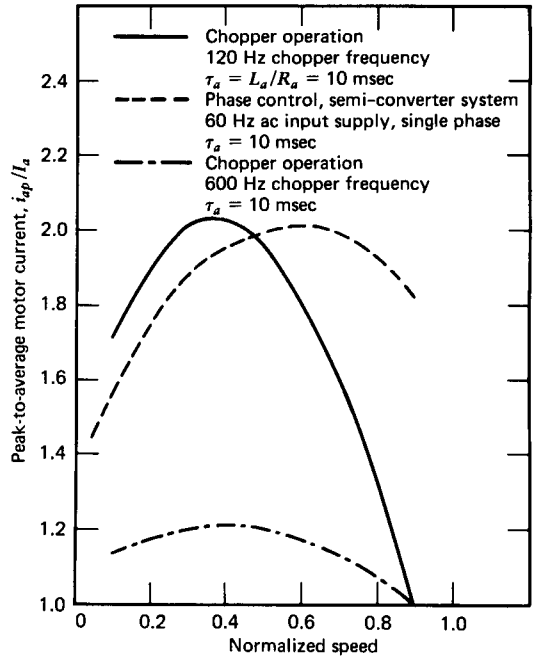


*Fig. 4.12* Variation of peak-to-average motor current ratio with speed. The separately excited dc motor operates at a constant torque (10 N·m) of rated value.

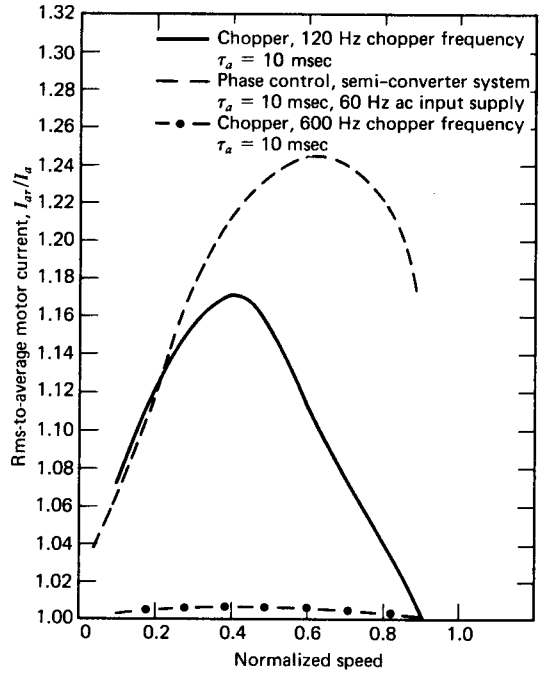


*Fig. 4.13* Variation of rms-to-average motor current ratio with speed. The separately excited dc motor operates at the rated torque (10 N·m).

### *Series Motor Performance*

The torque-speed characteristics for chopping frequencies of 120 Hz and 300 Hz are shown in Figures 4.14, and 4.15, respectively. With the higher chopping frequency the discontinuous current operation is almost eliminated.

The peak-to-average and rms-to-average motor currents as a function of speed are shown in Figs. 4.16 and 4.17, respectively. For comparison the results obtained with the phase-control scheme are also shown. Evidently chopper control provides improved performance, and an increase in chopping frequency greatly improves the performance.

### *Discussion*

In this study typical laboratory-size dc motors (2–2.5 hp) are considered. The results represent the general behavior of dc motors controlled by thyristor choppers. The performance characteristics obtained in this study are typical of the first-order effects expected of chopper control of dc motors.

For the same power rating, choppers will be costlier than phase-controlled converters because commutation circuitry is required in choppers to turn off the main thyristor. However, motor performance is better with chopper control than with phase control. With phase control, if sufficient inductance

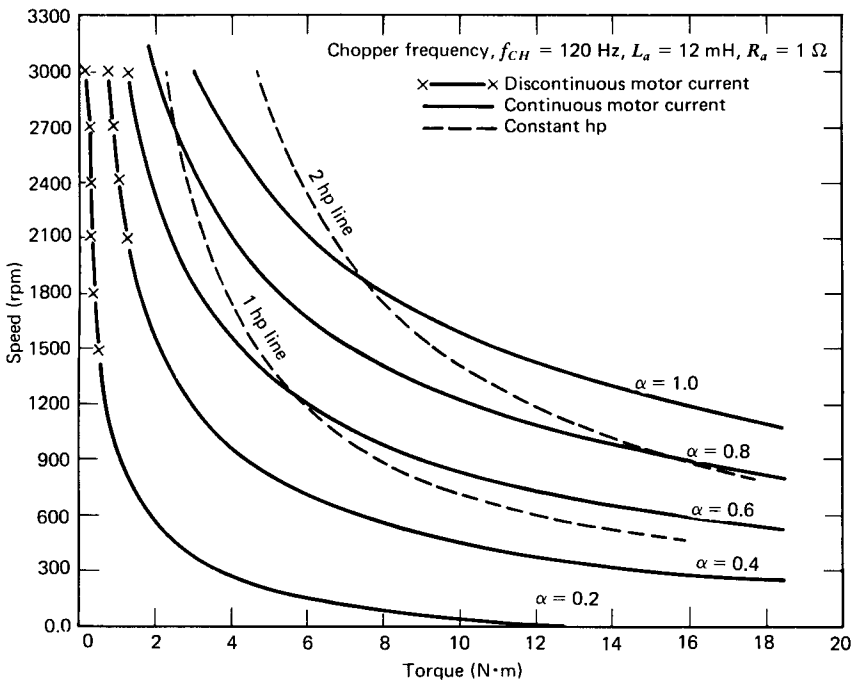


*Fig. 4.14* Torque-speed characteristics for a chopper-fed dc series motor.

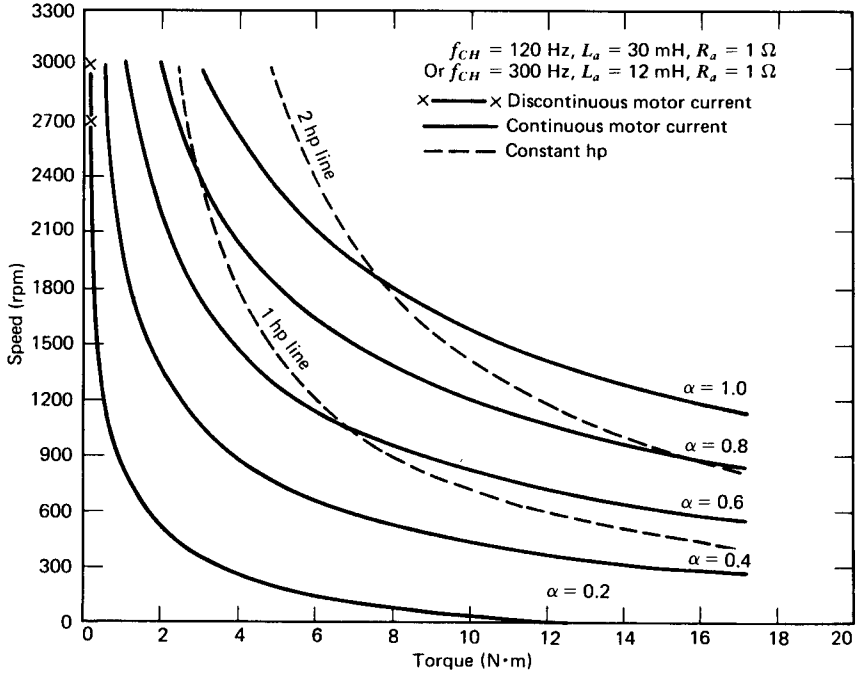


*Fig. 4.15* Effects of chopper frequency or armature inductance on continuity of motor current and on torque-speed characteristics of a dc series motor controlled by a chopper.

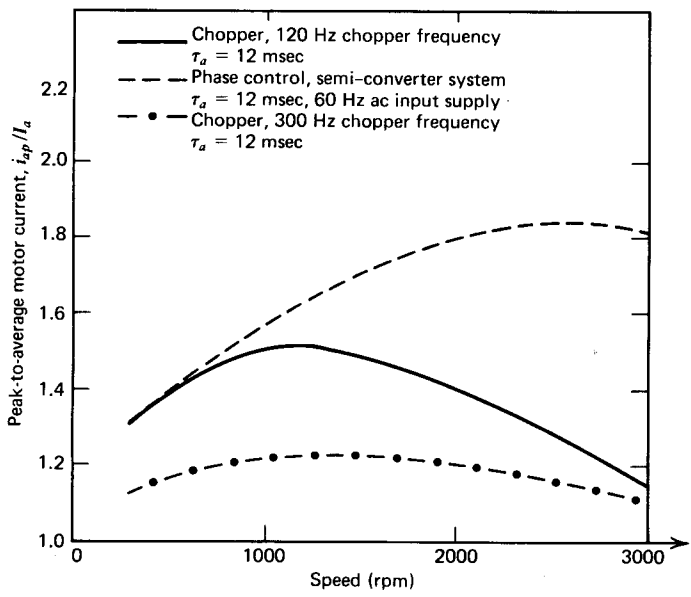


*Fig. 4.16* Variation of motor peak-to-average current ratio with speed. The dc series motor operates at a constant horsepower (1 hp) mode.

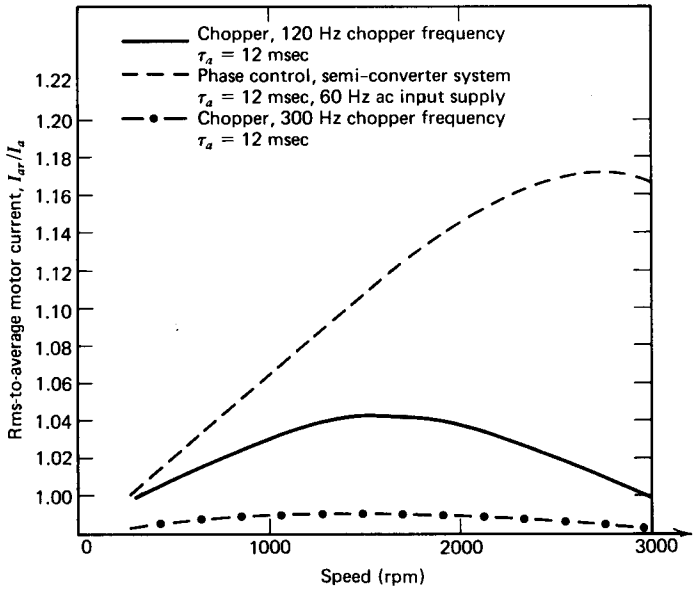


*Fig. 4.17* Variation of motor rms-to-average current ratio with speed. The dc series motor operates at 1 hp.

is not added to the armature circuit, the current pulsation becomes large, resulting in high peak current and increased heating. Special motor design will be necessary. With chopper control, if the chopping frequency is high, in the range of say $300 < f_{CH} < 600$ Hz, motor performance will be satisfactory even without additional inductance in the armature circuit. Special motor design will not be necessary. In the Toronto (Canada) subway transit system series dc motors are controlled by classical resistance control. In recent years, chopper control (using the chopper shown in Fig. 4.6*a*) has been implemented in some cars.[4] With no change in the series dc motors practically no deterioration in the motor performance has been found. The chopping frequency is about 200 Hz, and a smoothing reactor is used in the armature circuit. Higher chopping frequencies could have been used, and smoothing reactors could have been avoided. However, high chopping frequencies limit the range of variation of the output voltage, because commutation time becomes a significant portion of the chopping period.

## 4.4 INPUT FILTER

The chopper is an on-off switch. When it is on, supply current and motor current are the same. When the chopper is off, motor current flows through the free-wheeling diode, and the supply current is zero. The chopper therefore produces chopped current for the supply. This is shown in Fig. 4.18. The load

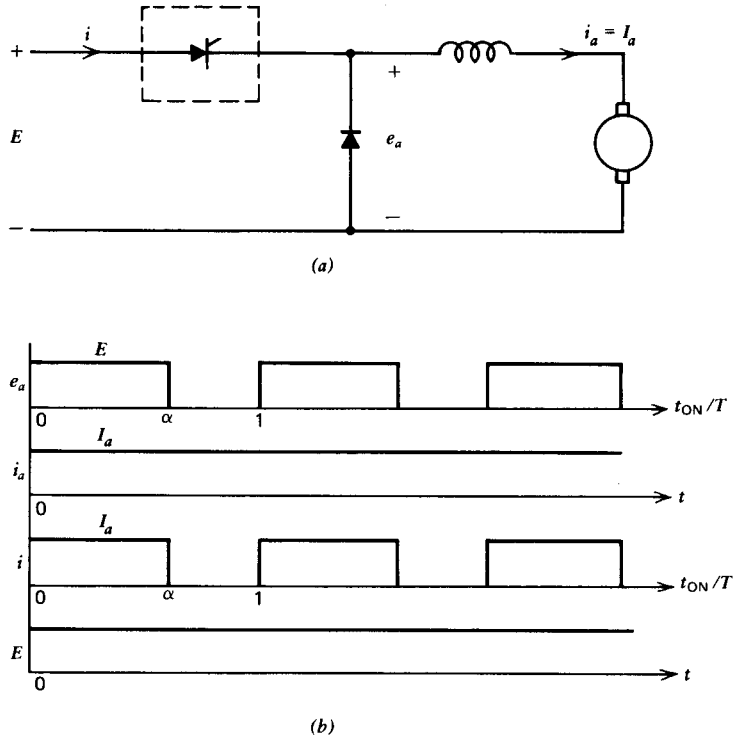


*Fig. 4.18* Basic chopper. (*a*) Circuit. (*b*) Waveforms.

inductance is assumed large, so that the motor current is considered to be ripple free. The following observations can be made:

1 The average power from the supply and to the load is the same, assuming a lossless system.

$$EI_0 = \alpha EI_a \tag{4.53}$$

$$I_0 = \alpha I_a \tag{4.54}$$

where $I_0$ = average value of the supply current. If the duty cycle is less than one, $\alpha < 1$, the average supply current is less than the average motor current.

2 When the chopper is on, the instantaneous supply current is the same as the instantaneous motor current. This makes the peak input power demand high.

The supply current therefore has harmonics that will produce undesirable effects, such as source voltage fluctuation, signal interference, supply distortion, additional heating, and so on. A simple capacitor filter, as shown in Fig.

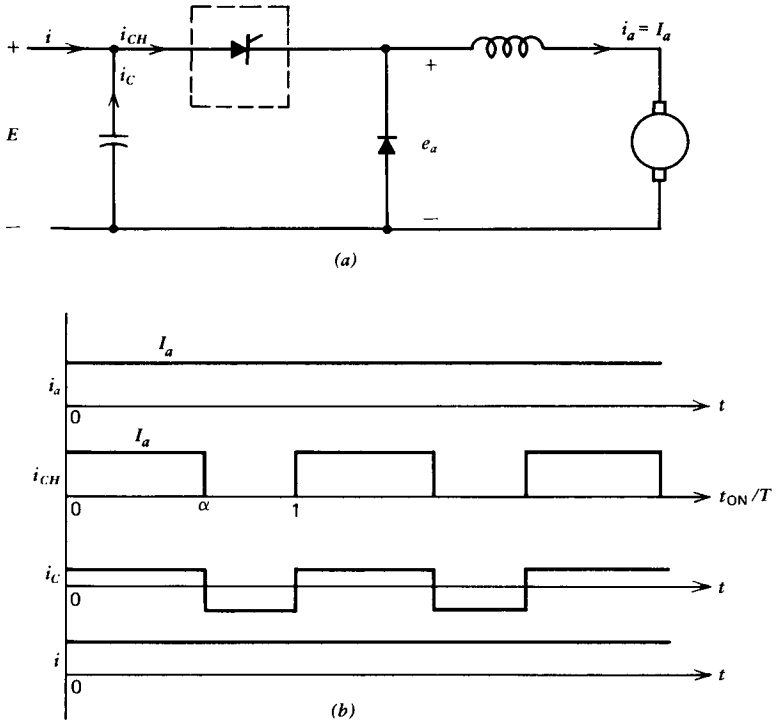


*Fig. 4.19* Basic chopper with input capacitor filter. (*a*) Circuit. (*b*) Waveforms.

4.19, will reduce ripple from the supply current. The capacitor will provide the ripple current of the chopper, and only the average current is drawn from the supply. The high peak power demand from the supply is thus eliminated.

In order to approach the idealized waveforms of Fig. 4.19, the capacitor has to be infinitely large. In practice, however, instead of using only a large capacitor filter, an *L-C* filter (Fig. 4.20) is used to reduce the size of the capacitor. The filter inductor has the additional function of providing transient isolation between supply and load during a short-circuit condition.

In Fig. 4.20*b*, the *n*th harmonic current in the supply is given by

$$I_n = \frac{X_C/n}{(nX_L) - (X_C/n)} I_{CH_n} \tag{4.55}$$

where $X_L = 2\pi f_{CH} L$ (4.56)

$$X_C = \frac{1}{2\pi f_{CH} C} \tag{4.57}$$

$n$ = order of harmonic.

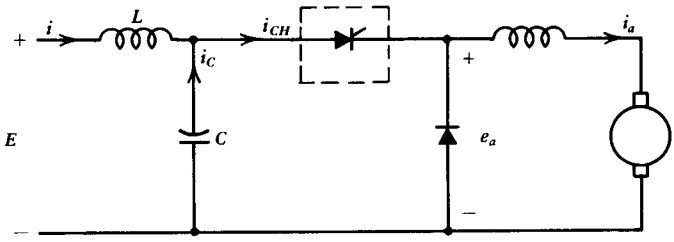


(a)

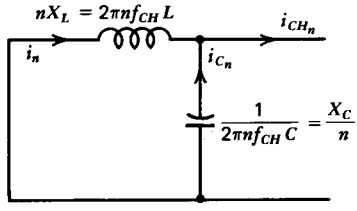


(b)

***Fig. 4.20*** **Basic chopper circuit with input *L-C* filter. (*a*) Circuit. (*b*) Equivalent circuit for *n*th harmonic.**

From equations 4.55, 4.56, and 4.57

$$I_n = \frac{1}{4\pi n^2 f_{CH}^2 LC - 1} I_{CH_n}$$

$$= \frac{1}{\left(n\frac{f_{CH}}{f_r}\right)^2 - 1} I_{CH_n} \tag{4.58}$$

where $I_n$ = rms $n$th harmonic of the supply current
$I_{CH_n}$ = rms $n$th harmonic of the chopper current
$f_{CH}$ = chopper frequency
$f_r$ = resonant frequency of $L$ and $C = 1/2\pi\sqrt{LC}$ .

These two frequencies $f_{CH}$ and $f_r$ should be different; otherwise resonance occurs, resulting in large voltage oscillation of supply voltage. Normally $f_{CH}$ is 2 or 3 times $f_r$ to avoid this resonance phenomena.[6] The supply harmonic current is thus approximately given by

$$I_n \simeq \left(\frac{f_r}{nf_{CH}}\right)^2 I_{CH_n} \tag{4.59}$$

The supply harmonic can thus be reduced

1 for the same filter elements by increasing the chopper frequency;
2 for the same chopper frequency by decreasing $f_r$ (i.e., increasing the values of $L$ and/or $C$);
3 by lessening ripple amplitude of the chopper current, which will reduce $I_{CH_n}$.

**Example 4.5**

A chopper is used to control the speed of a dc motor as shown in Fig. 4.20*a*. The motor is accelerated under current control (i.e., constant torque). Assume that the armature current remains constant at $I_a$ amperes during start-up.

1 Show that the maximum rms ripple current in the chopper current $i_{CH}$ occurs at a duty cycle of one-half, that is, at $\alpha = 0.5$.
2 For the duty cycle $\alpha = 0.5$, determine the values of the input filter components $L$ and $C$ for the following conditions: Supply voltage = 120 V. Chopper frequency $f_{CH} = 400$ Hz. Start-up motor current $I_a = 100$ A. Rms fundamental current to be allowed in the supply is 10% of the dc component of the source current. Electrolytic capacitor of rating 1000 $\mu$F and 300 V dc can take 5 A rms ripple current. For the design $f_{CH} \geqslant 2f_r$.
3 For the values of $L$ and $C$ obtained in part 2, determine the average and first three harmonic currents (in rms) in the supply.

*Solution*

1 The chopper current $i_{CH}$ is in the form of square pulses of magnitude $I_a$ and width $\alpha$ as shown in Fig. 4.21. Therefore, the dc component $I_{CH_{dc}}$, rms current $I_{rms}$, and ripple current $I_{ripple}$ are as follows:

$$I_{CH_{dc}} = I_a\alpha$$

$$I_{rms} = \left(\int_0^{\alpha} I_a^2\, d\alpha\right)^{1/2} = I_a\sqrt{\alpha}$$

$$I_{ripple} = \left[\left(I_a\sqrt{\alpha}\right)^2 - (I_a\alpha)^2\right]^{1/2}$$

$$= I_a(\alpha - \alpha^2)^{1/2}$$

For maximum ripple current

$$\frac{dI_{ripple}}{d\alpha} = 0$$

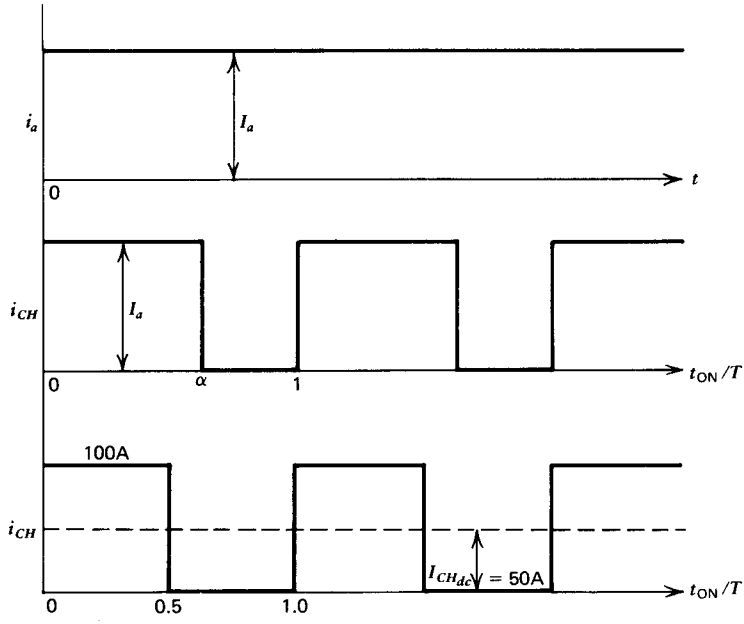


*Fig. 4.21* Example 4.5

or

$$\frac{I_a(1-2\alpha)}{2(\alpha-\alpha^2)^{1/2}} = 0$$

from which

$$\alpha = 0.5$$

2 The *L-C* filter should be selected for the worst case, which corresponds to $\alpha = 0.5$. At this duty cycle (bottom wave form in Fig. 4.21) the Fourier series for the chopper current is

$$i_{CH} = I_{CH_{dc}} + \frac{4}{\pi}\frac{I_a}{2n}(\sin\omega t + \sin 3\omega t + \sin 5\omega t + \cdots)$$

Now,

$$I_{CH_{dc}} = \frac{100}{2} = 50 \text{ A}$$

The fundamental, third, and fifth harmonic currents in the chopper are

$$I_{CH_1} = \frac{4 \times 100}{\sqrt{2} \times \pi \times 2} = 45 \text{ A}$$

$$I_{CH_3} = 15 \text{ A}$$

$$I_{CH_5} = 9 \text{ A}$$

The dc component of the chopper current comes from the supply only. The capacitor cannot provide a dc current. Therefore, the dc component $I_0$ of the supply current is

$$I_0 = I_{CH_{dc}} = 50 \text{ A}$$

If the fundamental supply current $I_1$ is not to exceed 10% of the dc current $I_0$, then

$$I_1 = 5 \text{ A}$$

From equation 4.55

$$I_1 = \frac{X_C}{X_L - X_C} I_{CH_1}$$

$$5 = \frac{X_C}{X_L - X_C} \times 45$$

or

$$X_L = 10X_C$$

Fundamental capacitor current $I_{C_1}$ is

$$I_{C_1} = \frac{X_L}{X_L - X_C} I_{CH_1}$$

$$= \frac{10X_C}{10X_C - X_C} \times 45$$

$$= 50 \text{ A}$$

Each electrolytic capacitor can take 5 A of current. Therefore 10 capaci-

tors connected in parallel are required.

$$C = 10{,}000\ \mu\text{F}$$

$$X_C = \frac{1}{2\pi 400 \times 10^4 \times 10^{-6}}\ \Omega = 3.98 \times 10^{-2}\ \Omega$$

$$X_L = 10X_C = 3.98 \times 10^{-1}\ \Omega$$

$$L = \frac{0.398}{2\pi 400} = 158\ \mu\text{H}$$

$$f_r = \frac{1}{2\pi\sqrt{LC}} = 127\ \text{Hz}$$

which makes

$$f_{CH} = \frac{400}{127} f_r = 3.15 f_r$$

3 From equation 4.58

$$I_1 = \frac{45}{(3.15)^2 - 1} = 5.0\ \text{A}$$

$$I_3 = \frac{15}{(3 \times 3.15)^2 - 1} = 0.17\ \text{A}$$

$$I_5 = \frac{9}{(5 \times 3.15)^2 - 1} = 0.036\ \text{A}$$

and

$$I_0 = 50\ \text{A}$$

## 4.5 MULTIPHASE CHOPPER

If two or more choppers are operated in parallel and phase shifted from each other, the ripple amplitude decreases and the ripple frequency increases. As a result, the supply harmonic current is effectively reduced.

A two-chopper arrangement is shown in Fig. 4.22*a*. The supply currents, without filter, are shown in Fig. 4.22*b* for in-phase operation and phase-shift operation for a duty cycle of $\alpha = 40\%$. The frequency of the supply ripple

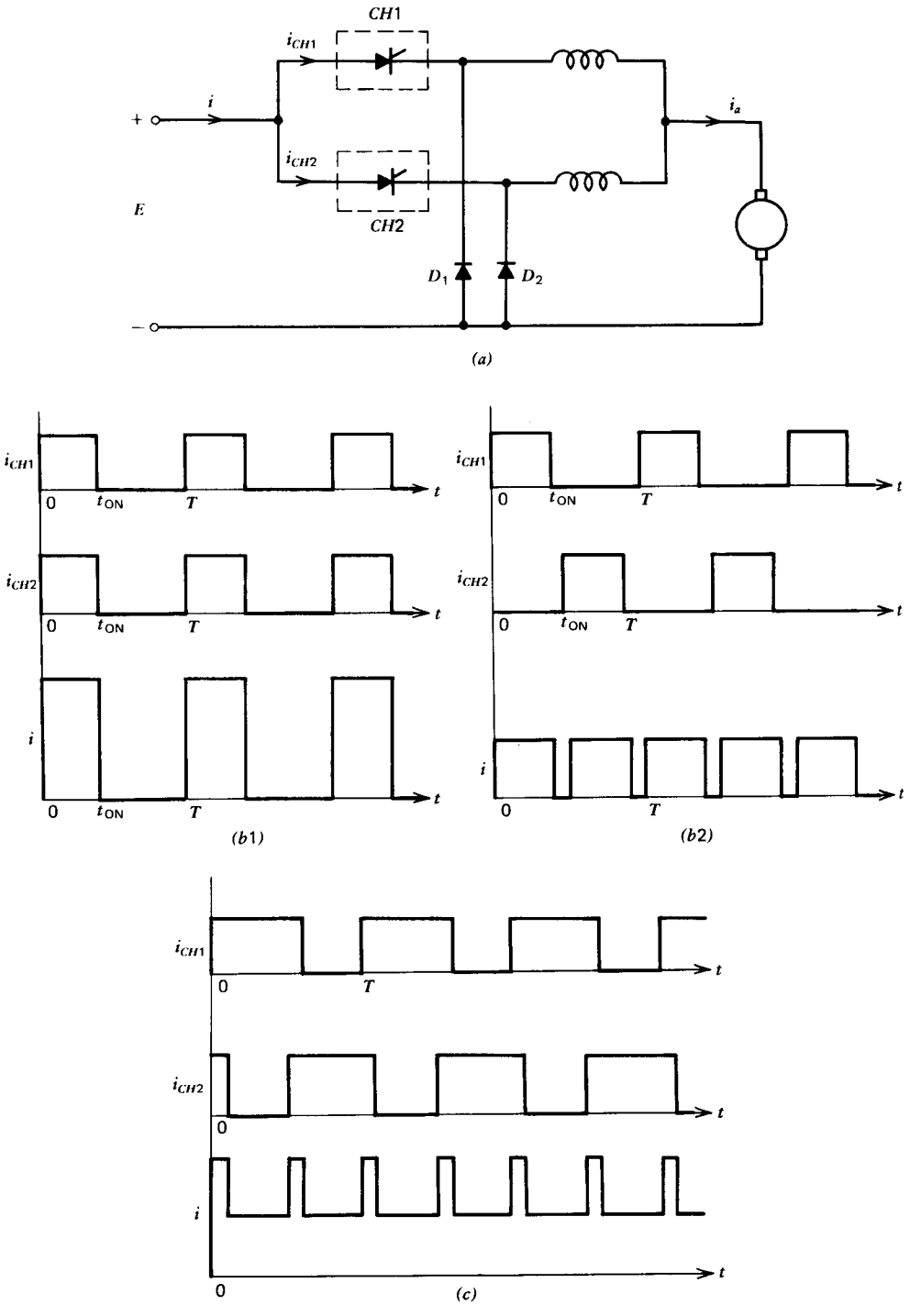


*Fig. 4.22* Multiphase chopper. (*a*) Basic circuit. (*b*) Waveforms for $\alpha = 40\%$. (1) In-phase operation; (2) Phase-shift operation. (*c*) Phase-shift operation, $\alpha = 60\%$.

current is doubled, and the amplitude of the ripple current is halved in the phase-shift operation compared to the in-phase operation. The in-phase operation corresponds to the case of single-chopper operation.

For 50% duty cycle in the phase-shifted multiphase chopper system, supply current is continuous and ripple-free for this idealized current waveform. The supply current will be half of the motor current. A 100 A motor current will thus appear as a 50 A source current. If the duty cycle is increased, the supply current will be continuous having half of the motor current as amplitude and containing a pedestal of half the motor current, as shown in Fig. 4.22*c*, for a duty cycle of 60%.

Multiphase chopper operation[7–9] may be advantageous for larger drives, particularly if the load current requirement is large. Use of a single chopper in such a case will involve the task of matching the static and dynamic conduction characteristics of the devices connected in parallel. In a multiphase chopper system, separate inductors provide an effective means for paralleling. The disadvantages of multiphase chopper systems are the need for additional motor connections, additional external inductors, additional commutating components, and additional complexity in the control logic.

## REFERENCES


1 General Electric Co., *General Electric SCR Manual*, Fifth Edition, Electronics Park, Syracuse, NY, 1977.

2 S. B. Dewan and A. Straughen, *Power Semiconductor Circuits*, Wiley-Interscience, New York, 1975.

3 S. B. Dewan and G. S. Dang, "A Fast Response DC Chopper," *IEEE Conference Record*, IAS-75, New York, 1975.

4 F. W. Roberts, "A Report on Regenerative Chopper Controls for Toronto Subway Cars," Toronto Transit Commission, Toronto, September 1973.

5 S. R. Doradla, "Control Schemes for Solid State DC Series Motor Drives," Unpublished Ph.D Thesis, Queen's University, Kingston, Canada, 1975.

6 R. A. Van Eck, "The Separately Excited DC Traction Motor Applied to DC and Single Phase AC Rapid Transit Systems and Electrified Railroads, Part II—Application," *IEEE Transactions on Industry and General Applications*, Vol. IGA-7, No. 5, New York, September 1971.

7 E. Reimers, "Design Analysis of Multi-phase DC-chopper Motor Drive," *IEEE Conference Record*, IGA-70, New York, 1970.

8 C. J. Amoto, "Latent Losses in 'Lectric Lizzies," *IEEE Transactions on Industry and General Application*, Vol. IGA-5, No. 5, New York, September 1969.

9 K. Tachibana, T. Tsuboi, and S. Kariya, "Harmonic Currents in Catenary Systems from Chopper Control," *IEEE Transactions on Industry Applications*, Vol. IA-8, No. 2, New York, March 1972.

# 5

# Braking

In previous chapters the speed control of motors in the driving mode has been extensively discussed. To stop the drive motor, a braking mechanism is necessary. Classically, a motor is stopped by applying *friction* (mechanical) *brakes*. The amount of braking is normally controlled pneumatically by air pressure. Friction brakes have been very reliable and have been used extensively over the years. However, the brake shoes are subject to considerable wear and tear. If braking is required frequently, as in transit vehicles, frequent maintenance and ultimate replacement of the brake shoes may make this type of braking uneconomic and undesirable.

Fortunately, a motor can also be operated as a generator. As a result there are two other types of braking: *dynamic braking* and *regenerative braking*. In both cases, the kinetic energy of the drive system is converted to electrical energy. In this process, the motor operates as a generator, experiences a torque opposing its motion, and therefore slows down. At lower speeds, friction brakes are normally used. However, use of friction brakes is reduced.

In dynamic braking, electrical energy is dissipated in a stack of braking resistors. The scheme is simple, but if it is used in subway cars, it may produce considerable tunnel heating. In regenerative braking electrical energy is fed back to the supply. The scheme is complex; however, it saves energy. In modern rapid transit systems, the higher vehicle speeds make the energy saving worthwhile. It is possible to recover as much as 40% of the energy supplied to the vehicle. In battery-operated cars, where energy is limited, regenerative braking should be a prime consideration. When regeneration fades out at lower speeds friction brakes can be blended with the fading electrical braking.

In the following sections, dynamic braking and regenerative braking are discussed further. Application of electrical braking in transit systems is considered as an example because of its growing importance.

## 5.1 DYNAMIC BRAKING

In dynamic braking, the motor is made to act as a generator. The armature is disconnected from the supply, but it continues to rotate and generate a voltage. The polarity of the generated voltage remains unchanged if the direction of field excitation is unaltered. But if a resistance is connected across the coasting motor, the direction of the armature current is reversed, because the armature represents a source of power rather than a load. Thus a braking torque is developed, exactly as in a generator, tending to oppose the motion. The braking torque can be controlled by the field excitation and armature current. Note that the motor operation is primarily limited by its commutation capability and thermal heating and to a lesser degree by its voltage rating. Therefore, at high speed, the armature current should be maintained constant at rated value. In the motoring mode, the maximum speed, which is about 2 to 3 times the base speed, is obtained by field weakening. In the braking mode at high speed, if the field current is increased to rated value to obtain the same braking torque as the acceleration torque, then the armature voltage will be 2 to 3 times the rated value. In dynamic braking, this overvoltage is permitted because the armature is disconnected from the supply. This implies that the braking power, which is the product of armature voltage and current, can be high in dynamic braking. When the field current is increased to its maximum value, and a constant deceleration rate is desired as in transit systems, the braking resistor can be reduced to keep armature current constant and hence braking torque at its full value. In an industrial drive a constant braking torque may not be necessary. In this

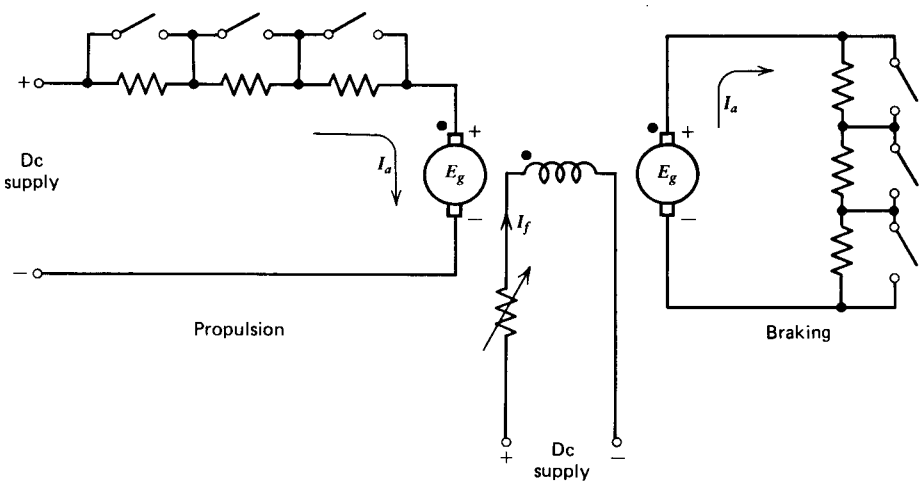


*Fig. 5.1* Schematic of classical control.

case, the braking resistance may be kept constant, and the braking torque drops linearly down to zero speed.

In classical control, resistances are used in series with the armature for control in propulsion as well as braking. A simplified schematic diagram is shown in Fig. 5.1. The resistances are shorted out to regulate the armature current. In some applications, the same set of resistances is used for both propulsion and dynamic braking. In others, separate sets of resistances are used for propulsion and braking to provide a desired torque profile during acceleration and deceleration.

### 5.1.1 Phase-Controlled Drives

The schematic diagram of a phase-controlled drive using a separately excited dc machine is shown in Fig. 5.2. In the propulsion mode, the motor is accelerated with full field current and at constant armature current. The armature current is regulated by controlling the firing angle of the ac-dc converter in a closed-loop control system. When the output voltage of the ac-dc converter is maximum, further increase in speed is achieved through field weakening (i.e., by reduction in the field current).

For dynamic braking the armature of the dc motor is disconnected from the ac-dc converter and connected across the braking resistor. If a constant braking torque is required, the field current can be increased first. When the field current reaches its maximum value, the brake resistance can be decreased. Ideally, braking torque can be maintained constant down to zero speed. In practice, however, friction brakes are applied in the lower-speed region (Fig. 5.2*b*).

For dynamic braking in a series dc motor drive, the motor can be used as a series generator or separately excited generator, as shown in Fig. 5.3. The contactors *M* in Fig. 5.3*a* are closed for operation in the drive mode. In order to switch to dynamic braking using the motor as series generator, contactors *M* are opened and contactors *B* are closed. This arrangement makes the series field flux unidirectional, whereas current through the armature is reversed to produce braking torque. Note that the shape of the magnetization curve is important for the generating action of a series generator connected to a resistance load. If the motor is used as a separately excited generator, as shown in Fig. 5.3*b*, the series field winding is connected to a low-voltage, high-current ac-dc converter. Because of separate excitation, the shape of the magnetization curve is not important.

### 5.1.2 Chopper Drives

For dynamic braking in chopper drives the same chopper that controls motor torque in the drive mode can also be used to control the effective value of the braking resistor to provide a desired braking torque profile. A schematic

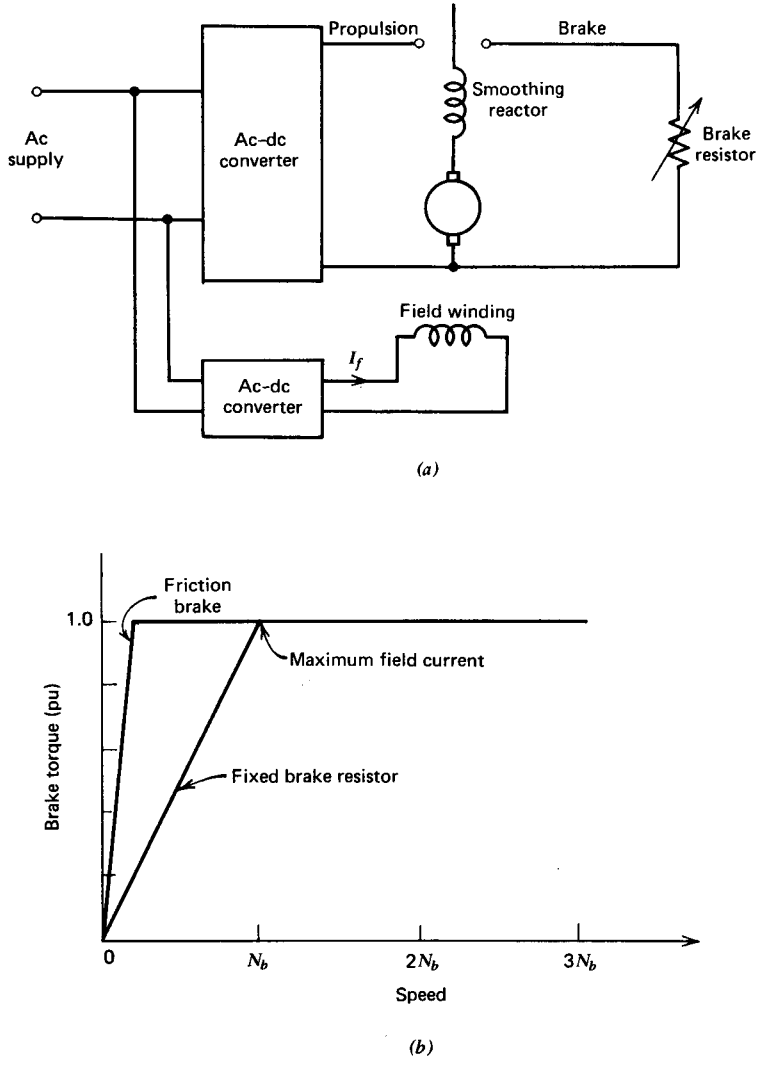


*Fig. 5.2* Phase-controlled drive using separately excited dc motor. (*a*) Circuit configuration in propulsion and dynamic braking modes. (*b*) Brake torque versus speed. Rated torque = 1 pu.

diagram of the scheme is shown in Fig. 5.4. If high braking power is required, as in traction applications, the maximum voltage generated in the armature during dynamic braking can be 2 to 3 times the rated value. In such a case, the chopper should be connected across a portion $R_1$ of the brake resistor. This arrangement reduces the voltage rating of the chopper and hence is economic. The other portion $R_2$ of the braking resistor can be shorted out as soon as the speed is low enough.

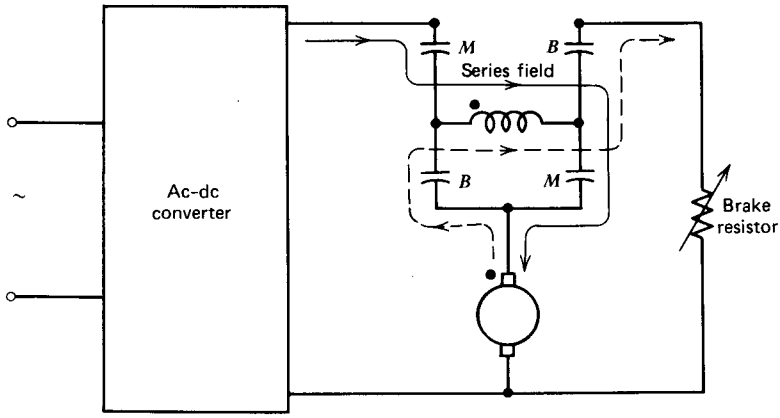


(a)

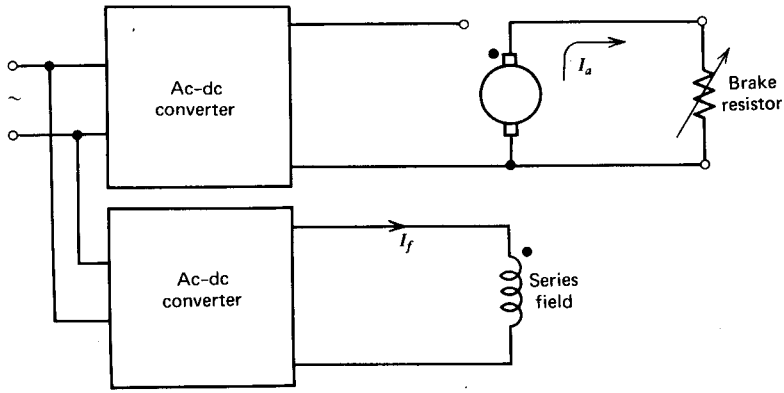


(b)

*Fig. 5.3* Phase-controlled drive using series motor. (*a*) Series generator during dynamic braking. (*b*) Separately excited generator during dynamic braking.

Any level of braking torque can be obtained by controlling the field excitation and the effective value of the braking resistor. At high speed, the chopper is kept off, and field control is employed to provide the desired braking torque. When the field current reaches its maximum value, the chopper is operated to reduce the effective value of the braking resistor. Because of separate field excitation, the level of braking torque can be maintained down to very low speed. A braking torque profile such as the one shown in Fig. 5.2*b* can be obtained if desired.

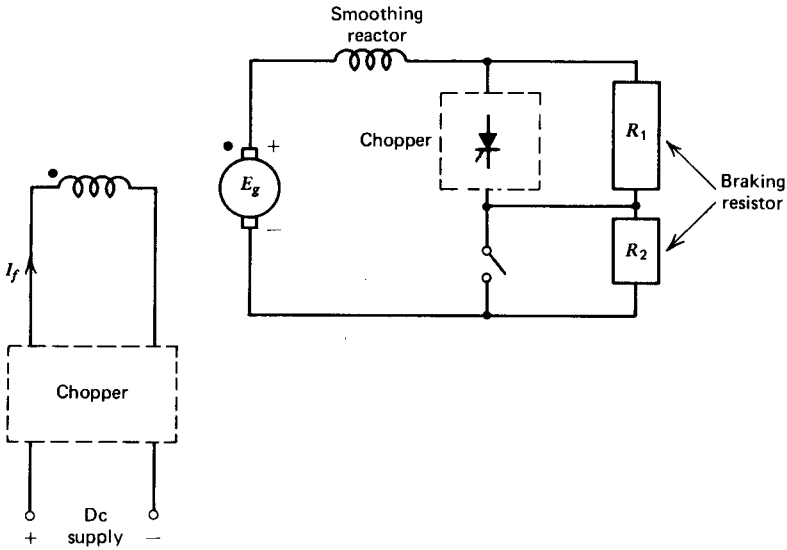


*Fig. 5.4* Schematic of a chopper drive in dynamic braking operation.

## 5.2 REGENERATIVE BRAKING

In dynamic braking the kinetic energy converted to electrical energy is lost in the braking resistor. Why waste the energy? Why not return the energy to the supply? In regenerative braking the generated power, instead of being wasted in a resistor, is returned to the supply. The scheme may be relatively complex; however, it saves energy and is desirable in applications where stopping is frequent.

The motor acts as a generator during regenerative braking. However, unlike dynamic braking, the motor is not disconnected from the supply. The maximum generated voltage in the motor armature is thus limited to rated voltage. Recall that in dynamic braking, because the motor is disconnected from the supply, the generated armature voltage can be increased to 2 to 3 times the rated voltage. As a consequence, at high speed the braking power in regenerative braking is far less than the braking power in dynamic braking. However, if a resistance is inserted between the armature and the supply during regenerative braking, the armature voltage can be increased beyond the supply voltage. The added resistance absorbs the additional voltage drop. This modification results in higher braking torque at high speed, but at the cost of less energy recovery due to loss in the resistance. As the speed slows down, the additional armature resistance can be shorted out. Figure 5.5 shows the brake torque profile with and without additional armature resistance during regenerative braking.

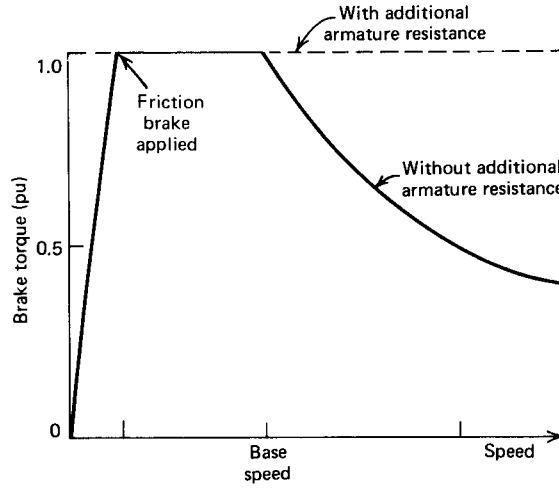


*Fig. 5.5* Regenerative braking operation. Brake torque versus speed with and without added resistance in the armature circuit. Rated torque = 1 pu.

### 5.2.1 Phase-Controlled Drives

The schematic diagram of a phase-controlled drive using a separately excited dc machine is shown in Fig. 5.6. The converter is a full ac-dc converter so that it can operate in the rectification mode for motoring and in the inversion mode for regenerative braking. To invert power from the motor armature to the ac supply through the ac-dc converter, the polarity of the armature voltage has to be changed. This can be done by reversing the field current or by using a changeover contactor switch for the armature as discussed in Chapter 3. During regenerative braking, the armature current is kept constant to a limiting value through a closed-loop control system. As the speed decreases due to braking torque and release of kinetic energy, the generated armature voltage decreases. However, the closed-loop control system continuously changes the firing angle of the converter to keep the armature current constant. The oscillograms of speed and armature current in Fig. 5.6*b* are typical for regenerative braking at constant armature current.

It is known that in a series generator an increase in the armature current increases the generated voltage, which in turn further increases the armature current. This leads to unstable operation of a series generator connected to a source. Therefore, if a series motor is used, it should be operated as a separately excited generator during regenerative braking.

### 5.2.2 Chopper Drives

The chopper that controls the motor power in the driving mode can be used to control regenerative power in the regenerative braking mode. The positions

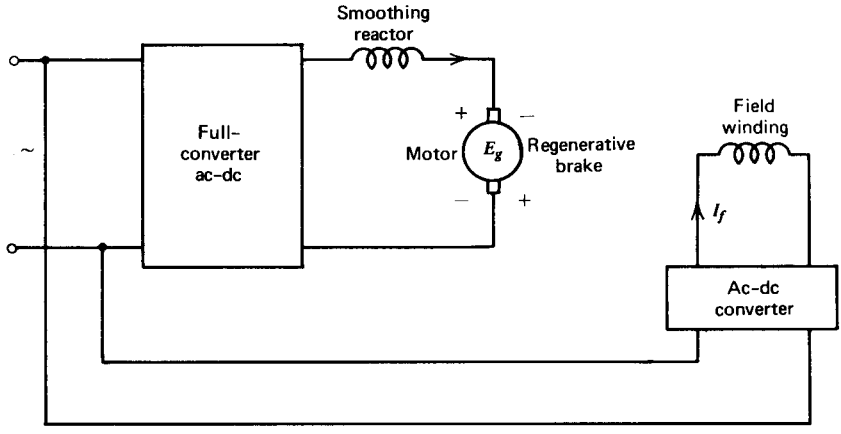


(a)

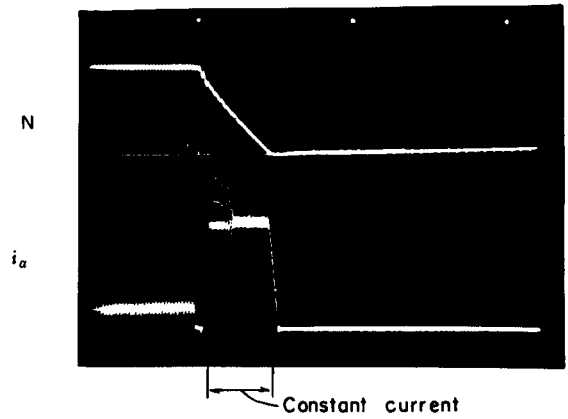


(b)

*Fig. 5.6* Regenerative braking operation of phase-controlled drives. (*a*) Schematic circuit diagram. (*b*) Oscillograms of speed $N$ and armature current $i_a$ during regenerative braking.

of the chopper and the free-wheeling diode are interchanged as shown in Fig. 5.7*a* and *b*. The function of the chopper in motoring and braking is the same. The on-off ratio of the chopper is regulated in a closed-loop control system to maintain the desired braking current. In regenerative braking when the chopper is on the motor terminals are shorted. The armature current builds up, and energy is stored in the reactor connected in series with the armature. When the chopper is off armature current is forced into the supply. Energy stored in the reactor from the armature is thus released to the supply.

If a series motor is used, an additional reactor in series with the armature may not be necessary. The series field winding stores energy during the

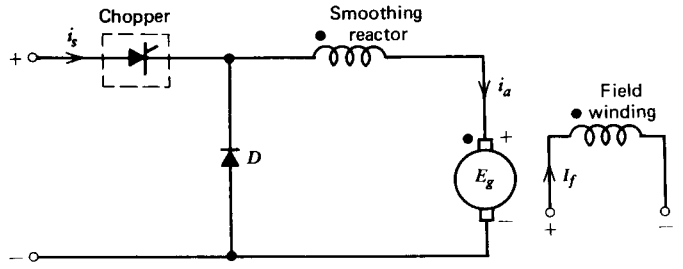


(a)

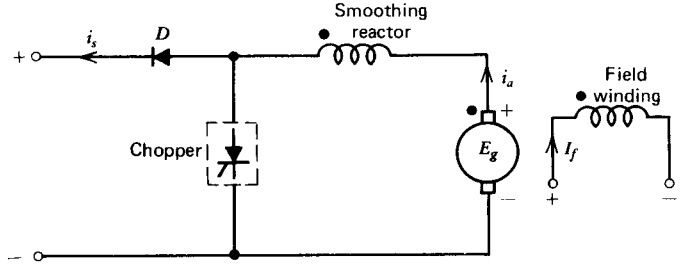


(b)

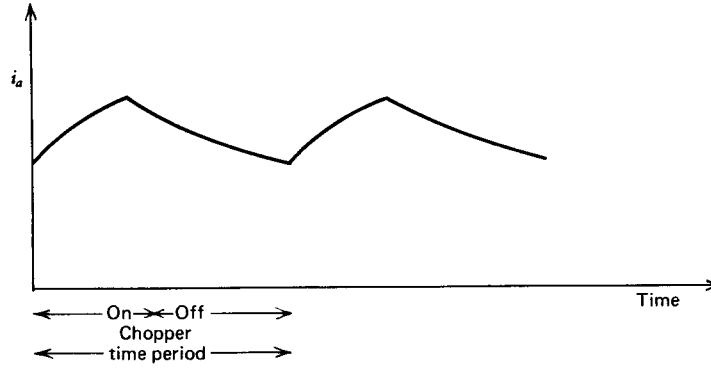


(c)

*Fig. 5.7* Chopper drives. (*a*) Schematic for motoring operation. (*b*) Schematic for regenerative braking operation. (*c*) Armature current waveform during regenerative braking. (*d*) Series field connection for unidirectional field.

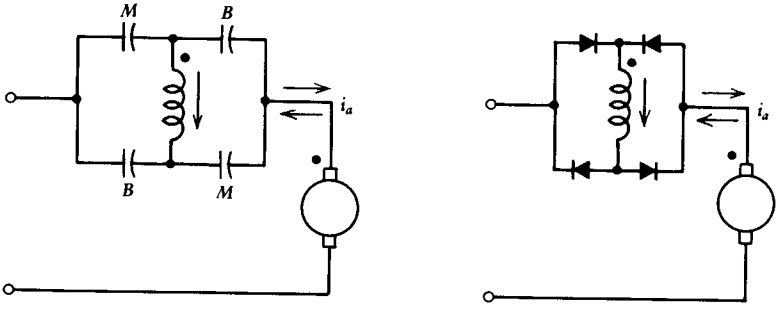


(d)

*Fig. 5.7 (Continued)*

chopper on interval and releases energy to the source during the chopper off interval. However, the series field should remain unidirectional during motoring and regenerative braking operation.

The scheme shown in Fig. 5.7 requires a single one-quadrant chopper and a mechanical switching arrangement. The chopper operates in the first quadrant in the driving mode, with positive average armature voltage and positive average armature current. It operates in the second quadrant in the regenerative braking mode, with positive average armature voltage and negative average armature current. Motoring and regenerative braking also can be obtained if a two-quadrant chopper is used. This eliminates the mechanical switching arrangement. However, it requires two choppers in one unit. This scheme is shown in Fig. 5.8. Chopper $CH_1$ and diode $D_1$ conduct during the motoring operation, and chopper $CH_2$ and diode $D_2$ conduct during regenerative braking. During motoring the motor draws current from the supply, whereas during regenerative braking the motor, acting as a generator, delivers current to the source. The average motor current $I_a$ can be maintained constant in a closed-loop control system by regulating the on-off ratio of the chopper. In regenerative braking, as the speed slows down, the generated voltage $E_g$ decreases. This requires a longer on interval for the chopper $CH_2$ to build the armature current, as illustrated in the last timing diagram in Fig. 5.8*c*.

### *Nonreceptive Line*

Where does the energy go that is fed back during the regenerative braking? Normally there are other accelerating motors or equipments served by the supply bus. The energy returned during regenerative braking is used by these loads. However, if the line is nonreceptive during regenerative braking, the line voltage increases. Up to a 20% increase in line voltage can be tolerated.

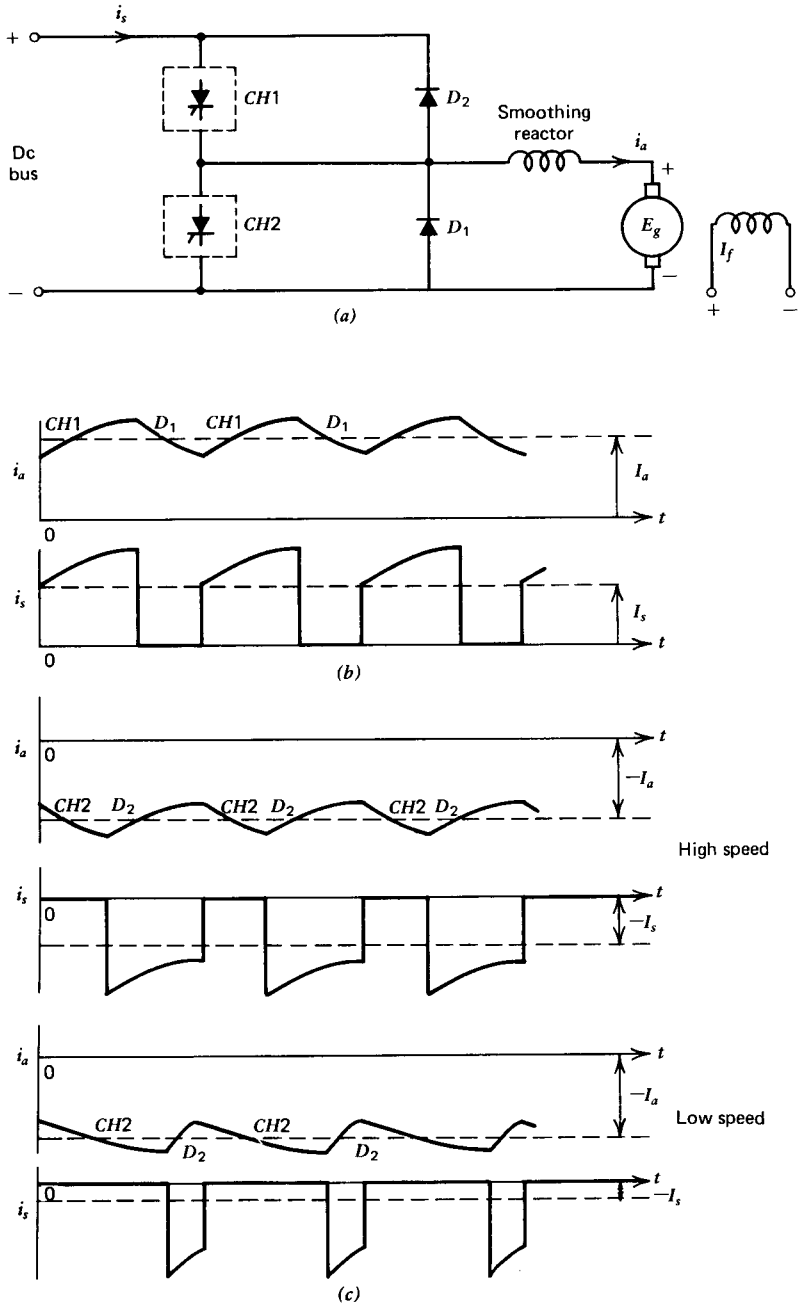


*Fig. 5.8* A chopper drive using two quadrant chopper for motoring and regenerative braking. (*a*) Circuit schematic. (*b*) Motoring. (*c*) Regenerative braking.

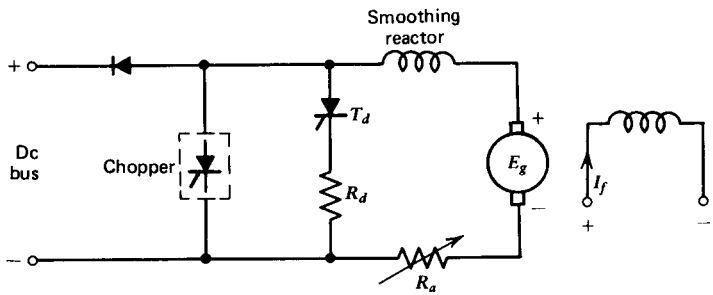


*Fig. 5.9* Schematic diagram to implement dynamic braking with regenerative braking.

During regenerative braking, therefore, the line voltage should be sensed. If it exceeds a certain preset value, the regenerative braking is removed, and either friction braking or dynamic braking is applied.[1-4]

Figure 5.9 shows a scheme in which dynamic braking is blended with regenerative braking. It allows an almost instantaneous shift from regenerative to dynamic braking if the line is not receptive. At the time of each gating pulse for the chopper, the logic circuit determines the receptivity of the line. If it is nonreceptive, thyristor $T_d$ will be gated to divert the motor current through resistor $R_d$. Only when the line becomes receptive is the chopper gated to provide regenerative braking.

As discussed earlier, the resistance $R_a$ in Fig. 5.9 can be inserted in series with the armature so that the generated voltage $E_g$ can rise to 2 to 3 times the supply voltage at high speed for higher braking power.

## 5.3 TRANSIT SYSTEMS

The transit industry, especially urban rapid transit systems, is in a major evolutionary process all over the world.[1-6] Advanced technologies are being tried in transit systems to move passengers at moderately high speed (100–150 km/h). In North America, the BART (Bay Area Rapid Transit) system[1] in the United States and the Toronto subway[2] and Montreal Metro systems in Canada, all use advanced solid-state technology and have been operating satisfactorily. The trend worldwide is to use dc motors equipped with thyristor chopper control. Both series motors and separately excited motors are being used. The preferred line voltage is either 600 V or 1000 V. All three types of braking—friction, dynamic, and regenerative—are being employed. In this section, some of the significant requirements and implementations in transit systems are examined.

In transit systems, the vehicle should accelerate and decelerate at a

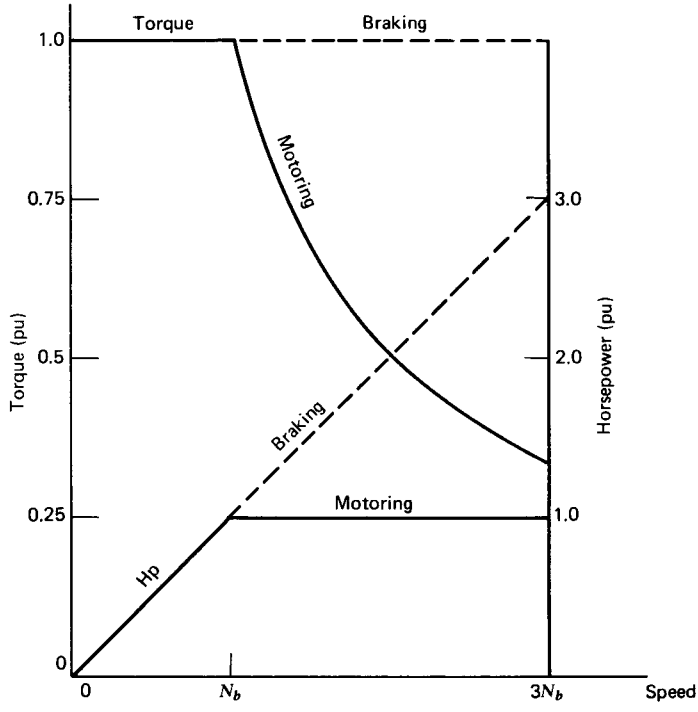


*Fig. 5.10* Typical torque and power profiles in transit systems. Rated torque = 1 PU, rated horsepower = 1 PU.

constant rate for passenger comfort. This requires constant accelerating and decelerating torque. Typical torque and power versus speed profiles[4] in transit systems are shown in Fig. 5.10. In the motoring operation, the vehicle is accelerated under full torque and full field flux up to a base speed $N_b$. This base speed $N_b$ is defined as the speed of the motor when its armature voltage attains the rated voltage under full field flux. To operate above base speed, the armature voltage is kept constant at the rated value, and the field is gradually weakened by a field controller. In transit systems the typical top speed is about 3 times the base speed. Below the base speed the horsepower increases linearly with speed. The control system can regulate the field current so that for operation beyond base speed the horsepower remains constant. At higher speed, therefore, horsepower, armature voltage, and armature current remain constant.

For satisfactory braking the decelerating torque is approximately equal to the initial accelerating torque. This condition can be achieved by one of the following methods.

1 The field current is raised to its full value, and the armature current is kept constant at the level required during acceleration. If the top speed is $k$ times the base speed, increasing the field current to its rated value increases the armature generated voltage to $k$ times the rated value. In dynamic braking, this increase is permissible because the armature is disconnected from the supply. In regenerative braking resistances are inserted in series with the armature to absorb the voltage difference between armature voltage and line voltage. In this method part of the generated power is therefore lost in the resistors. An alternative method is to make the rated armature voltage $1/k$ times the line voltage. Therefore at the top speed, if full field is applied, the armature voltage rises to the line voltage, which is $k$ times the rated armature voltage. In this method all of the generated power is recovered. Because the rated armature voltage is $1/k$ times the line voltage, the rated current is $k$ times the rated current of the former method for the same rated horsepower rating. In both methods, however, the chopper and motor must be designed to handle the peak braking power, which is $k$ times the rated power. In a typical transit car, the peak power is 3 times the rated power.

2 Armature current is maintained at the rated value, and the field current is controlled in such a way that the armature voltage does not exceed the line voltage. This method, in a regenerative braking scheme, provides an electrical braking-torque profile the same as the motoring-torque profile. Additional torque in the high-speed region (i.e., from top speed to base speed) is provided by friction brakes.

**Example 5.1**

In a transit system, the dc bus voltage is 600 V, and each car is driven by four series motors each of rating 300 V and 330 A. The circuit configuration during regenerative braking is shown in Fig. 5.11*a*. Field windings $F_1$–$F_4$ are cross-connected for equal torque sharing. The braking-torque profile is shown in Fig. 5.11*b*. Regenerative braking and friction braking are applied from top speed down to base speed. The regenerative braking is removed at 20% of the base speed. The area under the solid line represents regenerative braking, and the hatched area represents friction braking. Determine the percentage of initial energy returned to the supply by regenerative braking. Neglect road friction and aerodynamic drag.

*Solution*

Total braking torque remains constant during deceleration of speed. Therefore the speed changes linearly with time.

$$N \propto t$$

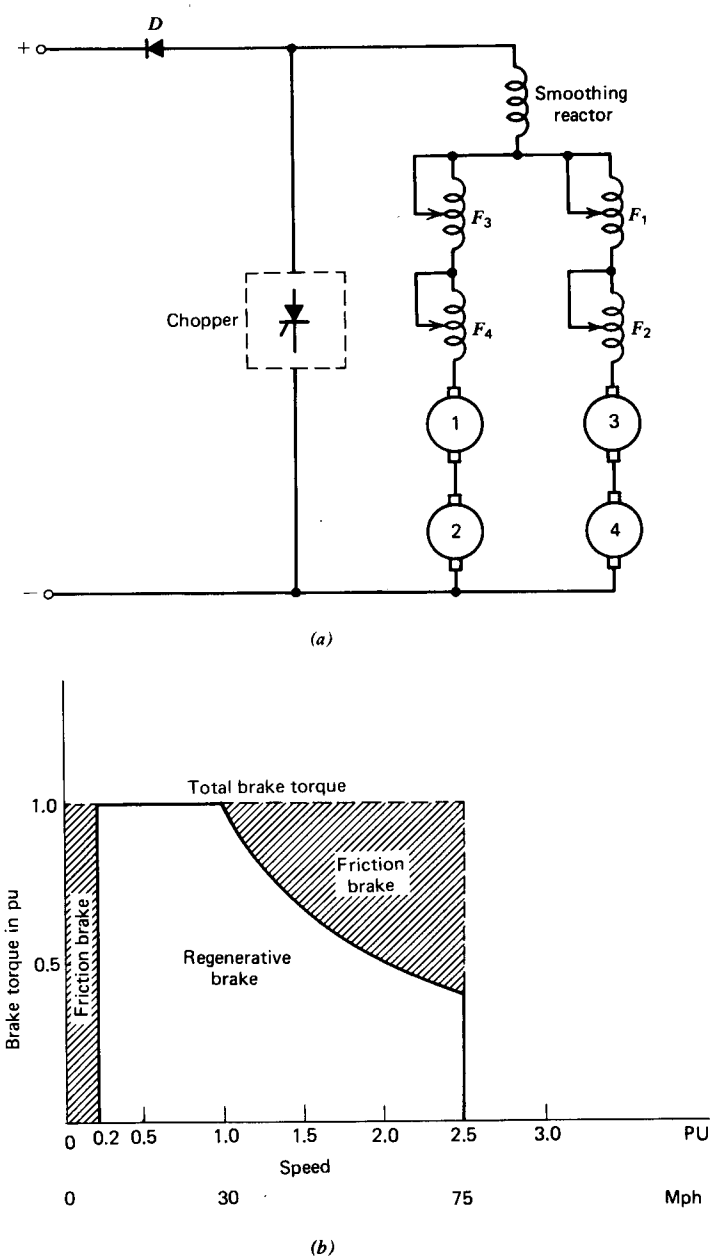


*Fig. 5.11* Example 5.1 (*a*) Circuit during regenerative braking. (*b*) Braking-torque profile.

The total energy of the system is

$$\propto \int_0^{2.5} (\text{torque})(\text{speed})\,(dt)$$

$$\propto \int_0^{2.5} TN\,dN$$

$$\propto \int_0^{2.5} 1N\,dN$$

$$\propto \frac{N^2}{2}\Big|_0^{2.5}$$

$$\propto 3.125$$

From top speed to base speed the electrical braking torque is inversely proportional to speed. Therefore the energy recovered due to regeneration is

$$\propto \int_{0.2}^{2.5} TN\,dN$$

$$\propto \int_{0.2}^{1} 1N\,dN + \int_1^{2.5} \frac{1}{N} N\,dN$$

$$\propto \frac{N^2}{2}\Big|_{0.2}^{1} + N\Big|_1^{2.5}$$

$$\propto 1.98$$

Hence the percentage of the initial energy returned to the supply by regenerative braking is

$$= \frac{1.98}{3.125} \times 100\%$$

$$= 63.4\%$$

The energy lost due to friction braking is 36.6%.

## REFERENCES


1 B. J. Krings, "Alternate Converter Systems for Traction Applications," *IEEE Conference Record*, ISPCC-72, New York, 1972.

2 F. W. Roberts, "A Report on Regenerative Chopper Controls for Toronto Subway Cars," Toronto Transit Commission, Toronto, September 1973.

3 R. M. Romano, "Series Chopper Control System for Rapid Transit Cars," *IEEE Conference Record*, ISPCC-72, New York, 1972.

4 B. Berman and G. H. Gelb, "Requirement and Implementation of Regenerative Train Control," *IEEE Conference Record*, IA-73, New York, 1973.

5 R. A. Van Eck, "The Application of the DC-DC Chopper in Traction Service," *IEEE Conference Record*, IA-74, New York, 1974.

6 R. A. Van Eck, "The Separately Excited DC Traction Motor Applied to DC and Single Phase AC Rapid Transit Systems and Electrified Railroads, Part I and II," *IEEE Transactions on Industry and General Applications*, Vol. IGA-7, No. 5, September 1971.

# 6

# Closed-Loop Control

Dc motors are widely used in many speed-control drives. Open-loop operation of dc motors may not be satisfactory in many applications. For example, the torque-speed characteristics shown in Fig. 2.10 indicate that the speed changes if the firing angle is kept constant and the torque applied to the dc motor is increased. However, if the drive requires constant-speed operation the firing angle has to change to maintain a constant speed. This can be achieved in a closed-loop control system. The basic block diagram of such a system is shown in Fig. 6.1. If the motor speed decreases due to application of additional load torque, the speed error $\varepsilon_N$ increases, which increases the control signal $E_c$. This in turn changes the firing angle of the converter, and thus increases the motor armature voltage $E_a$. An increase in the motor voltage develops more torque to restore the speed of the drive system. The system thus passes through a transient period until the developed torque matches the applied torque.

A closed-loop system generally has the advantages of greater accuracy, improved dynamic response, and reduced effects of disturbances such as loading. When the drive requirements include rapid acceleration and deceleration, closed-loop control is necessary. In a closed-loop system even the drive characteristics can be modified. Thus, the system can be made to operate at constant torque or constant horsepower over a certain speed range, a requirement in traction systems. Circuit protection can be provided in a closed-loop control system. In fact, most industrial drive systems operate as closed-loop feedback systems.

The response of a closed-loop system can be studied by using transfer function techniques. In the following sections, a systematic development of the transfer function of the various blocks as well as the whole system is presented. The necessity and significance of the various control loops and different parameters in an actual closed-loop control system are shown. An illustrative design procedure is outlined. For simplicity and ease of understanding, the system is reduced to the lowest possible order. Modern control techniques such as phase-locked-loop control and microcomputer control are discussed.

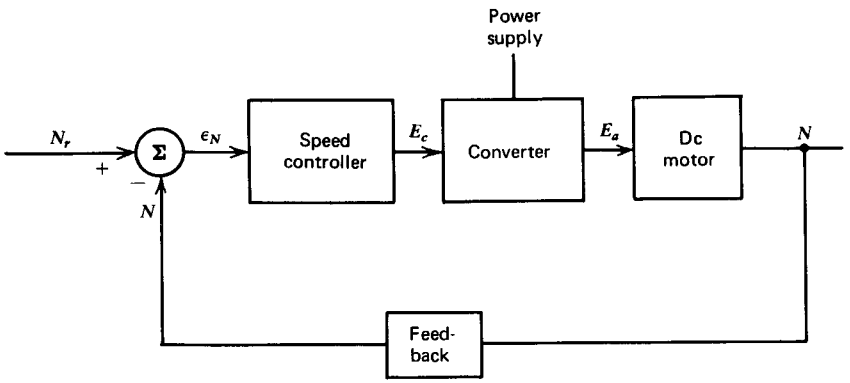


*Fig. 6.1* Basic block diagram of a closed-loop speed-control system.

## 6.1 SEPARATELY EXCITED DC MOTOR DRIVES

Separate excitation in a separately excited dc motor makes the speed control of the motor relatively easy. In most applications the armature voltage of the motor is controlled in a closed-loop feedback system, as shown in Fig. 6.1. Other protective features, such as current limiting, are incorporated in the closed-loop control system. The response of a closed-loop speed-control system is studied[1] in the following sections. The transfer functions of the motor and its associated control components and of the overall system are derived to assess the dynamic response of the drive.

### 6.1.1 Motor Transfer Function

Consider a separately excited dc motor with armature voltage control, as shown in Fig. 6.2*a*. The voltage loop equation is

$$e_a = e_g + R_a i_a + L_a \frac{di_a}{dt} \tag{6.1}$$

where

$$e_g = K_a \Phi n \tag{6.2}$$

The torque balance equation is

$$t = T_L + Bn + J\frac{dn}{dt} \tag{6.3}$$

where

$$t = K_a \Phi i_a \tag{6.4}$$

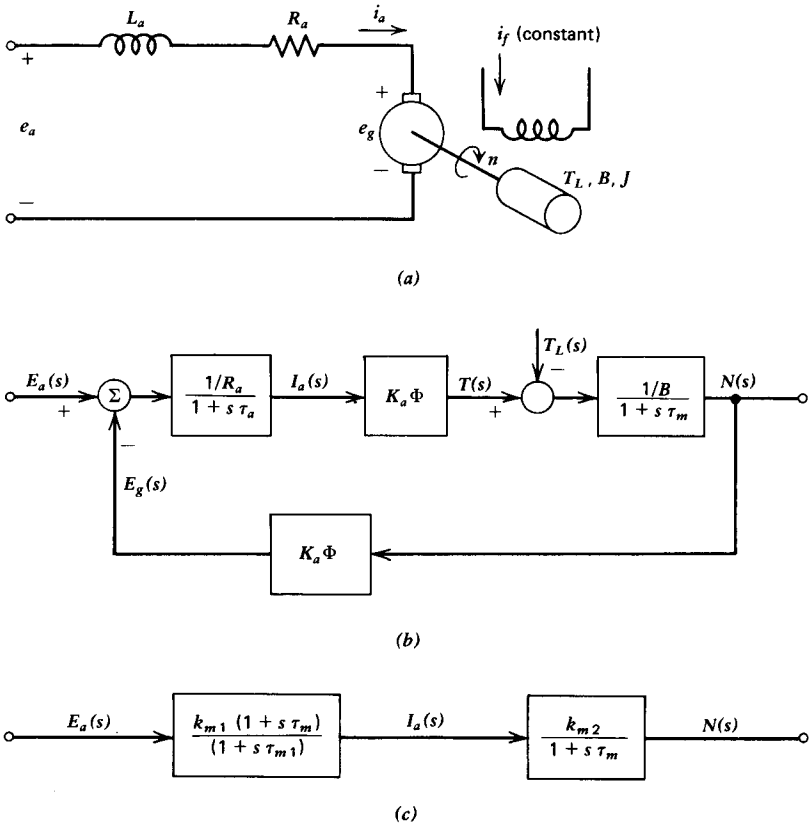


*Fig. 6.2* Development of motor transfer function. (*a*) Separately excited dc motor model. (*b*) Functional block diagram. (*c*) Simplified functional block diagram.

In the Laplace domain, equations 6.1 through 6.4 can be written as

$$E_a(s) = E_g(s) + R_a I_a(s) + L_a s I_a(s) \tag{6.5}$$

$$E_g(s) = K_a \Phi N(s) \tag{6.6}$$

$$T(s) = T_L(s) + BN(s) + JsN(s) \tag{6.7}$$

$$T(s) = K_a \Phi I_a(s) \tag{6.8}$$

Thus, from equation 6.5

$$I_a(s) = \frac{E_a(s) - E_g(s)}{R_a + sL_a} = \frac{[E_a(s) - E_g(s)]1/R_a}{1 + \tau_a s} \tag{6.9}$$

where $\tau_a = L_a / R_a$ = electrical time constant of the motor armature circuit.

From equation 6.7

$$N(s) = \frac{T(s) - T_L(s)}{B + Js} = \frac{[T(s) - T_L(s)]1/B}{1 + \tau_m s} \tag{6.10}$$

where $\tau_m = J/B =$ mechanical time constant of the motor.

These relationships are shown in block diagram form in Fig. 6.2*b*. Notice the feedback loop present in the form of the back emf. This back emf provides the moderate speed regulation inherent in the separately excited dc motor.

From Fig. 6.2*b* an expression can be obtained for the change in speed $N(s)$ due to disturbances in applied voltage $E_a(s)$ and load torque $T_L(s)$.

$$N(s) = \frac{G_1(s)}{1 + G_1(s)H_1(s)} E_a(s) + \frac{G_2(s)}{1 + G_2(s)H_2(s)} T_L(s) \tag{6.11}$$

where

$$G_1(s) = \frac{(1/R_a)}{1 + s\tau_a}(k_a\Phi)\frac{(1/B)}{1 + s\tau_m} \tag{6.11a}$$

$$H_1(s) = K_a\Phi \tag{6.11b}$$

$$G_2(s) = \frac{-(1/B)}{1 + s\tau_m} \tag{6.11c}$$

$$H_2(s) = \frac{-(K_a\Phi)^2/R_a}{1 + s\tau_a} \tag{6.11d}$$

If we neglect the load torque term for now, from equations 6.11, 6.11*a*, and 6.11*b*

$$\frac{N(s)}{E_a(s)} = \frac{K_a\Phi}{(K_a\Phi)^2 + R_a B(1 + s\tau_a)(1 + s\tau_m)} \tag{6.12}$$

If $\tau_a \ll \tau_m$ (which is almost always the case), then $\tau_a$ can be neglected, and the expression simplifies to

$$\frac{N(s)}{E_a(s)} = \frac{K_a\Phi}{(K_a\Phi)^2 + R_a B + sR_a B\tau_m} = \frac{k_m}{1 + s\tau_{m1}} \tag{6.12a}$$

where

$$\tau_{m1} = \frac{R_a B}{(K_a\Phi)^2 + R_a B}\tau_m \tag{6.12b}$$

$$k_m = \frac{K_a\Phi}{(K_a\Phi)^2 + R_a B} \tag{6.12c}$$

$$\tau_{m1} < \tau_m \tag{6.12d}$$

From Fig. 6.2*b*

$$\frac{N(s)}{I_a(s)} = \frac{K_a\Phi/B}{1 + s\tau_m} = \frac{k_{m2}}{1 + s\tau_m} \tag{6.13}$$

Therefore, from equations 6.12a and 6.13

$$\frac{I_a(s)}{E_a(s)} = \frac{N(s)}{E_a(s)} \times \frac{I_a(s)}{N(s)}$$

$$= \frac{k_m B(1 + s\tau_m)}{K_a\Phi(1 + s\tau_{m1})} = \frac{k_{m1}(1 + s\tau_m)}{1 + s\tau_{m1}} \tag{6.14}$$

Thus the motor can be represented, for the purpose of analyzing it for voltage control, as two blocks as shown in Fig. 6.2*c*. The gain constants $k_{m1}$, $k_{m2}$ and $k_m$ shown in Fig. 6.2*c* are as follows.

$$k_{m1} = \frac{B}{(K_a\Phi)^2 + R_a B} = \frac{k_m}{K_a\Phi/B} \tag{6.14a}$$

$$k_{m2} = \frac{K_a\Phi}{B} \tag{6.14b}$$

$$k_m = k_{m1}k_{m2} \tag{6.14c}$$

### 6.1.2 Closed-Loop Speed Control

If a dc tachogenerator is attached to the motor shaft, a speed signal can be fed back and the error $\varepsilon_N(s)$ used to control the armature voltage. This scheme is shown in Fig. 6.3.

The applied armature voltage is controlled by a three-phase full-converter. Using a cosine firing scheme, a linear relationship between the control voltage

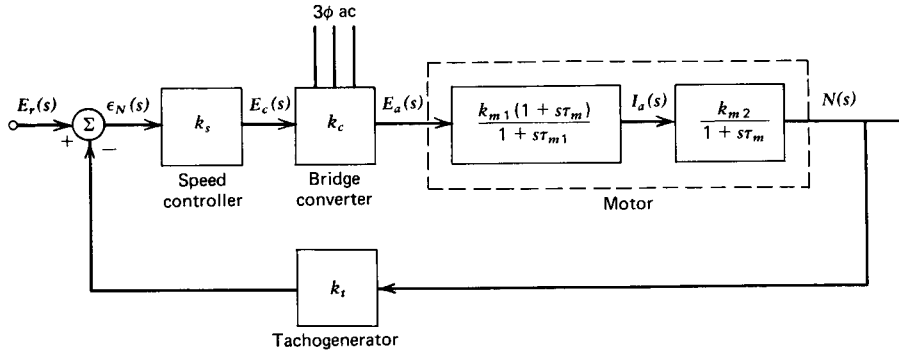


*Fig. 6.3* Speed-control loop.

$E_c$ and the armature voltage $E_a$ can be obtained. If the small time delay associated with the converter is neglected then

$$\frac{E_a(s)}{E_c(s)} = k_c = \frac{3\sqrt{2}\, V_{LL}}{\pi \hat{E}_c}$$

where $\hat{E}_c$ corresponds to 0° firing angle and $V_{LL}$ is the ac line to line rms voltage.

### *Proportional (P) Controller*

Several types of speed controllers[2] are possible. Two of the more common ones are proportional ($P$) and proportional-integral ($PI$). First, a $P$ controller is considered.

From Fig. 6.3

$$\frac{N(s)}{E_r(s)} = \frac{G(s)}{1 + G(s)H(s)} \tag{6.15}$$

where

$$G(s) = \frac{k_s k_c k_{m1} k_{m2}}{1 + s\tau_{m1}} \tag{6.15a}$$

$$H(s) = k_t \tag{6.15b}$$

From equations 6.15, 6.15a, and 6.15b

$$\frac{N(s)}{E_r(s)} = \frac{k_1}{1 + s\tau_1} \tag{6.16}$$

where

$$k_1 = \frac{k_s k_c k_{m1} k_{m2}}{k_s k_c k_{m1} k_{m2} k_t + 1} \tag{6.16a}$$

$$\tau_1 = \frac{\tau_{m1}}{k_s k_c k_{m1} k_{m2} k_t + 1} \tag{6.16b}$$

If $k_s k_c k_{m1} k_{m2} k_t \gg 1$, then

$$k_1 \simeq \frac{1}{k_t} \tag{6.16c}$$

$$\tau_1 \simeq \frac{\tau_{m1}}{k_s k_c k_{m1} k_{m2} k_t} \tag{6.16d}$$

From equations 6.16 and 6.13

$$\frac{I_a(s)}{E_r(s)} = \left[\frac{N(s)}{E_r(s)}\right]\left[\frac{I_a(s)}{N(s)}\right] = \frac{k_1}{k_{m2}} \frac{(1+\tau_m s)}{(1+\tau_1 s)} \tag{6.17}$$

The current response to a step change in input $E_r$ is

$$I_a(s) = \frac{k_1 E_r}{k_{m2} s} \frac{(1+\tau_m s)}{(1+\tau_1 s)}$$

$$= \frac{A_1}{s} + \frac{A_2}{s + 1/\tau_1} \tag{6.18}$$

where

$$A_1 = \frac{k_1 E_r}{k_{m2}} \tag{6.18a}$$

$$A_2 = \frac{k_1 E_r}{k_{m2}}\left(\frac{\tau_m}{\tau_1} - 1\right) \tag{6.18b}$$

From equations 6.18, 6.18a, and 6.18b, in the time domain, the current $I_a(t)$ is

$$I_a(t) = \frac{E_r k_1}{k_{m2}}\left[1 + \frac{(\tau_m - \tau_1)}{\tau_1} e^{-t/\tau_1}\right] \tag{6.19}$$

Since $\tau_m \gg \tau_1$, $\tau_1$ can be neglected. Normalizing the current with respect to the steady-state change $I_a(\propto)$,

$$\frac{I_a(t)}{I_a(\propto)} \simeq 1 + \frac{\tau_m}{\tau_1} e^{-t/\tau_1} \tag{6.20}$$

Equation 6.20 shows that an input change in $E_r$ results in a large sudden change in current that decays slowly. This transient overcurrent is undesirable from the standpoint of converter rating and protection. This is particularly the case for starting or other large changes.

### 6.1.3 Current Control

The previous analysis reveals that it would be beneficial to limit the current to some maximum allowable value. This objective cannot be achieved by using the configuration of Fig. 6.3 where the motor voltage is controlled by the speed error. Any attempt to clamp this speed error will limit the motor voltage. If armature losses are neglected, clamping the speed error will limit the speed, but not the current. However, a current limit can be implemented if we first construct an inner current-control loop using the clamped speed error as the current reference. Both *P* controller and *PI* controller for the current-control loop are discussed here.

***P Controller***

The inner current-control loop is shown in Fig. 6.4. In this Figure $k_r$ is the gain of the current transducer, which may be simply a sampling resistor in the armature circuit. The gain of the current controller is $k_I$, which here is assumed to be a proportional controller.

From Fig. 6.4 the transfer function is

$$\frac{I_a(s)}{E_I(s)} = \frac{k_I k_c k_{m1} \dfrac{1+\tau_m s}{1+\tau_{m1} s}}{1 + k_r k_I k_c k_{m1} \dfrac{(1+\tau_m s)}{(1+\tau_{m1} s)}}$$

$$= k_{IC} \frac{(1+\tau_m s)}{(1+\tau_{m2} s)} \tag{6.21}$$

where

$$K_{IC} = \frac{k_I k_c k_{m1}}{1 + k_r k_I k_c k_{m1}} \tag{6.21a}$$

$$\tau_{m2} = \frac{\tau_m k_r k_I k_c k_{m1} + \tau_{m1}}{1 + k_r k_I k_c k_{m1}} \tag{6.21b}$$

Since $k_r k_I k_c k_{m1} \gg 1$

$$k_{IC} \simeq \frac{1}{k_r} \tag{6.22}$$

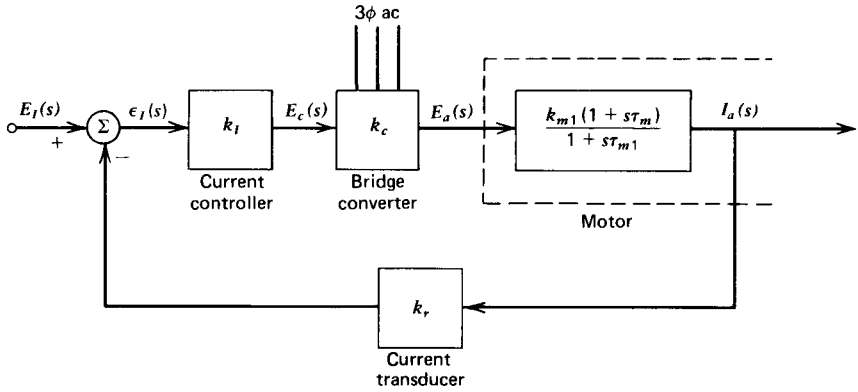


*Fig. 6.4* Current-control loop.

and

$$\tau_{m2} \simeq \tau_m + \frac{\tau_{m1}}{k_r k_I k_c k_{m1}} \tag{6.22a}$$

Also $\tau_m \gg \tau_{m1}$, therefore

$$\tau_{m2} \simeq \tau_m \tag{6.22b}$$

From equations 6.21 and 6.22*b*, it appears that a pole zero cancellation is possible, resulting in no overshoot or time delay. In practice there will be a delay due to the armature-circuit electrical time constant and the converter delay. Both these are usually sufficiently small to be neglected as done here. Therefore

$$\frac{I_a(s)}{E_1(s)} = k_{IC} \simeq \frac{1}{k_r} \tag{6.23}$$

Because $I_a$ is directly related to $E_I$, a limit on $E_I$ will effectively limit the current. This inner loop can now be incorporated within the speed-control loop, using the clamped speed error as the current reference $E_I$. The implementation of this scheme is shown in the block diagram of Fig. 6.5*a*. The block diagram can be simplified, by using expression 6.23 and by neglecting the nonlinear clamping, to the diagram in Fig. 6.5*b*.

Now, referring to Fig. 6.5*b*,

$$\frac{N(s)}{E_r(s)} = \frac{k_s k_{m2} k_{IC} \dfrac{1}{1+\tau_m s}}{1 + \dfrac{k_t k_s k_{m2} k_{IC}}{1+\tau_m s}}$$

$$= \frac{k_2}{1+\tau_2 s} \tag{6.24}$$

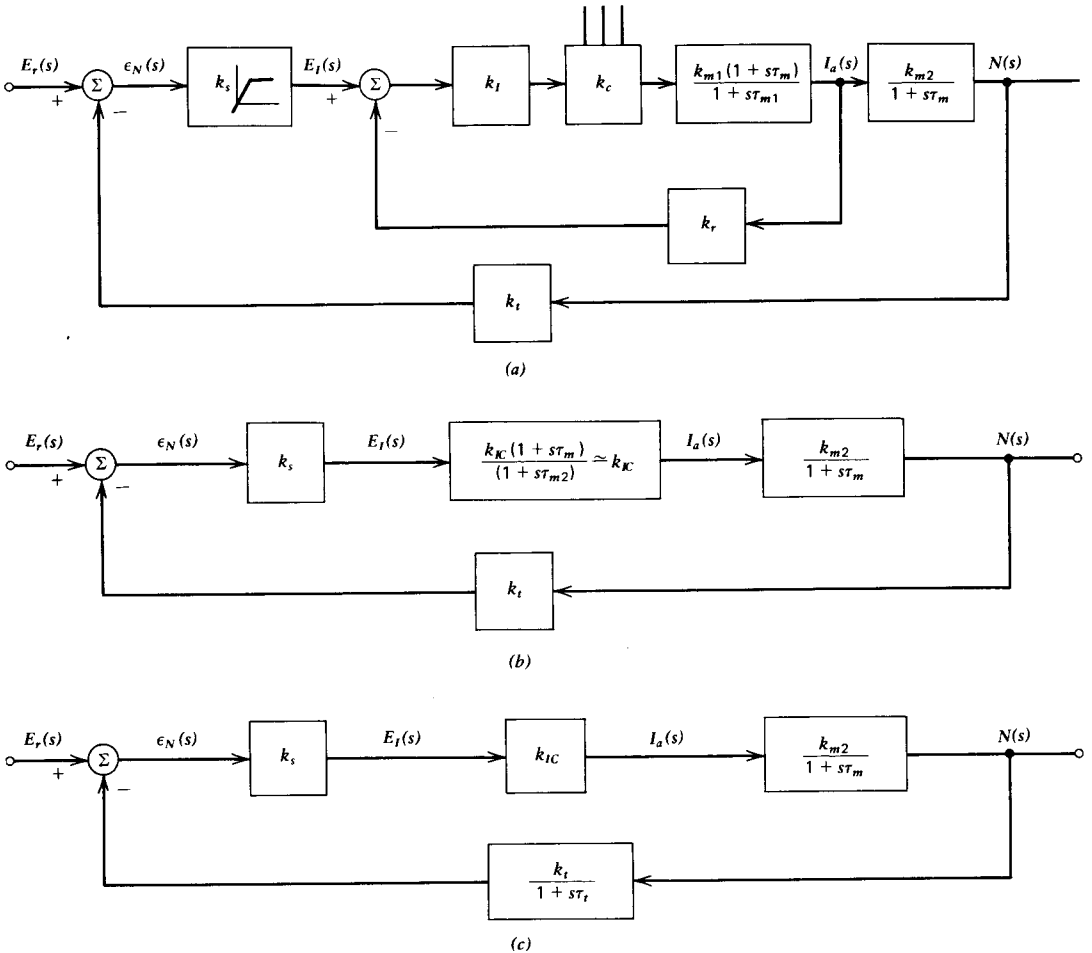


*Fig. 6.5* Proportional speed control with inner current-control loop. (*a*) Functional block diagram. (*b*) Simplified functional block diagram. (*c*) Functional block diagrams with added tachogenerator filter.

where

$$k_2 = \frac{k_s k_{m2} k_{IC}}{1 + k_t k_s k_{m2} k_{IC}} \tag{6.24a}$$

$$\tau_2 = \frac{\tau_m}{1 + k_t k_s k_{m2} k_{IC}} \tag{6.24b}$$

For $k_t k_s k_{IC} k_{m2} \gg 1$,

$$k_2 \simeq \frac{1}{k_t} = k_1 \qquad \text{(from equation 6.16c)} \tag{6.24c}$$

and

$$\tau_2 \simeq \frac{\tau_m}{k_t k_s k_{m2} k_{IC}}$$

Also, from equations 6.24 and 6.13

$$\frac{I_a(s)}{E_r(s)} = \left[\frac{N(s)}{E_r(s)}\right]\left[\frac{I_a(s)}{N(s)}\right] = \frac{k_2}{k_{m2}} \frac{(1 + \tau_m s)}{(1 + \tau_2 s)} \tag{6.25}$$

While equation 6.25 is not very different from equation 6.17, the expression in the former equation is only true while $I_a$ is less than the limiting value. If, during acceleration or load changes, the speed error is large such that $E_I$ is clamped at the maximum value $\hat{E}_I$, the current is limited to a maximum value $\hat{I}_a = k_{IC}\hat{E}_I$. From Fig. 6.5*b*, the speed is then described by

$$N(s) = I_a(s) \frac{k_{m2}}{(1 + \tau_m s)}$$

$$= \frac{I_a}{s} \frac{k_{m2}}{(1 + \tau_m s)} \tag{6.26}$$

where $I_a$ is the change in current from its initial value to the maximum value.

Sometimes a filter is required to reduce the ripple in the tachogenerator output, as shown in Fig. 6.5*c*. The resulting transfer function is

$$\frac{N(s)}{E_r(s)} = \frac{k_s k_{IC} k_{m2}}{1 + k_s k_{IC} k_{m2} k_t} \frac{(1 + s\tau_t)}{1 + s\dfrac{(\tau_m + \tau_t)}{k^1} + \dfrac{s^2 \tau_m \tau_t}{k^1}} \tag{6.27}$$

where $\tau_t$ = tachogenerator filter time constant and

$$k^1 = (1 + k_s k_{IC} k_{m2} k_t) \tag{6.27a}$$

$$\simeq k_s K_{IC} k_{m2} k_t \tag{6.27b}$$

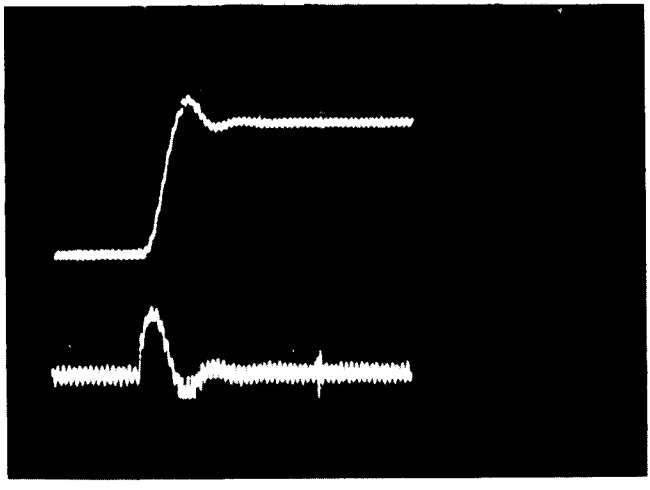


*Fig. 6.6* Response of proportional control (with tach. filter) to step change in speed reference. (*a*) Speed response. (*b*) Current response.

Also, from equations 6.27 and 6.13

$$\frac{I_a(s)}{E_r(s)} = \left[\frac{N(s)}{E_r(s)}\right]\left[\frac{I_a(s)}{N(s)}\right]$$

$$= \frac{k_s k_{IC}}{1 + k_s k_{IC} k_{m2} k_t} \frac{(1 + s\tau_t)(1 + s\tau_m)}{\left(1 + s\dfrac{\tau_m + \tau_t}{k^1} + \dfrac{s^2 \tau_m \tau_t}{k^1}\right)} \tag{6.27c}$$

The second-order response given by equations 6.27 and 6.27c can be verified by referring to Fig. 6.6, which is a photograph of the response to a step change in the speed reference.

### *Proportional-Integral (PI) Controller*

The addition of integral feedback can be used to eliminate the steady-state error and to reduce the forward gain required. To obtain this integral component, the proportional speed controller is replaced by a proportional-integral (*PI*) type controller. The new controller transfer function is $(1 + \tau_s s)/\tau_s s$. The resulting block diagram is presented in Fig. 6.7.

The overall transfer function becomes

$$\frac{N(s)}{E_r(s)} = \frac{k_s k_{IC} k_{m2} \dfrac{(1 + \tau_s s)}{(\tau_s s)(1 + \tau_m s)}}{1 + \dfrac{k_t k_s k_{IC} k_{m2}(1 + \tau_s s)}{(\tau_s s)(1 + \tau_m s)}} \tag{6.28}$$

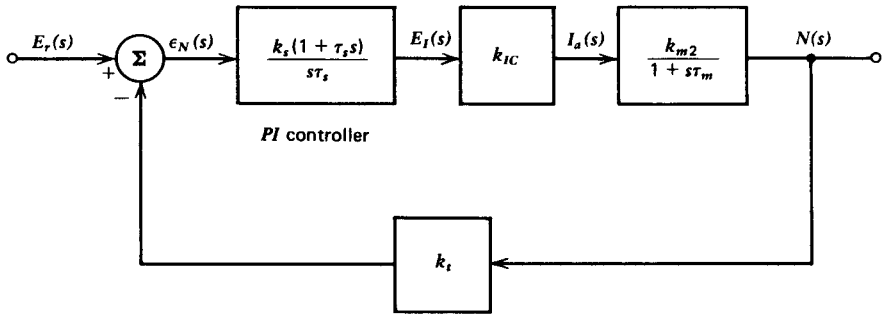


*Fig. 6.7* Speed-control loop with PI controller.

For $k_t k_s k_{IC} k_{m2} \gg 1$

$$\frac{N(s)}{E_r(s)} = \frac{1}{k_t} \frac{(1+\tau_s s)}{1+\tau_s s+\tau_s \tau_2 s^2} \tag{6.29}$$

where

$$\tau_2 = \frac{\tau_m}{k_t k_s k_{IC} k_{m2}} \tag{6.29a}$$

and from equations 6.29 and 6.13

$$\frac{I_a(s)}{E_r(s)} = \frac{N(s)}{E_r(s)} \cdot \frac{I_a(s)}{N(s)} = \left(\frac{1}{k_t k_{m2}}\right) \frac{(1+\tau_s s)(1+s\tau_m)}{1+\tau_s s+\tau_s \tau_2 s^2} \tag{6.30}$$

a)

b)

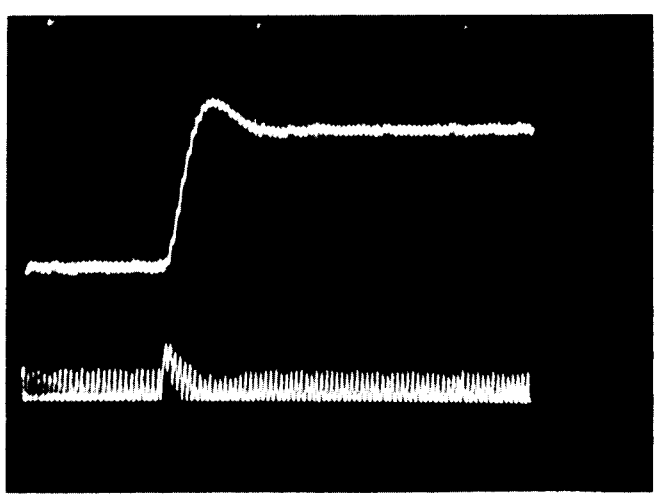

*Fig. 6.8* Response of proportional-integral control to step change in speed reference. (*a*) Speed response. (*b*) Current response.

The second-order response given by equations 6.29 and 6.30 is shown in the photograph of Fig. 6.8.

### 6.1.4 Load Torque Disturbance

In some applications a load is suddenly applied to the motor. The effect of such load torque distrubances is studied in this section.

***P Controller***

The complete block diagram, using a proportional controller for the speed loop, is shown in Fig. 6.9*a*. If changes in the speed reference $E_r$ are neglected, an expression for the current can be written in terms of the speed change $N(s)$.

From Fig. 6.9*a*

$$I_a(s) = \frac{1}{R_a}\left\{-K_a\Phi N(s) + k_I k_c\left[-k_r I_a(s) + k_s\left(\frac{-k_t N(s)}{1+s\tau_t}\right)\right]\right\} \tag{6.31}$$

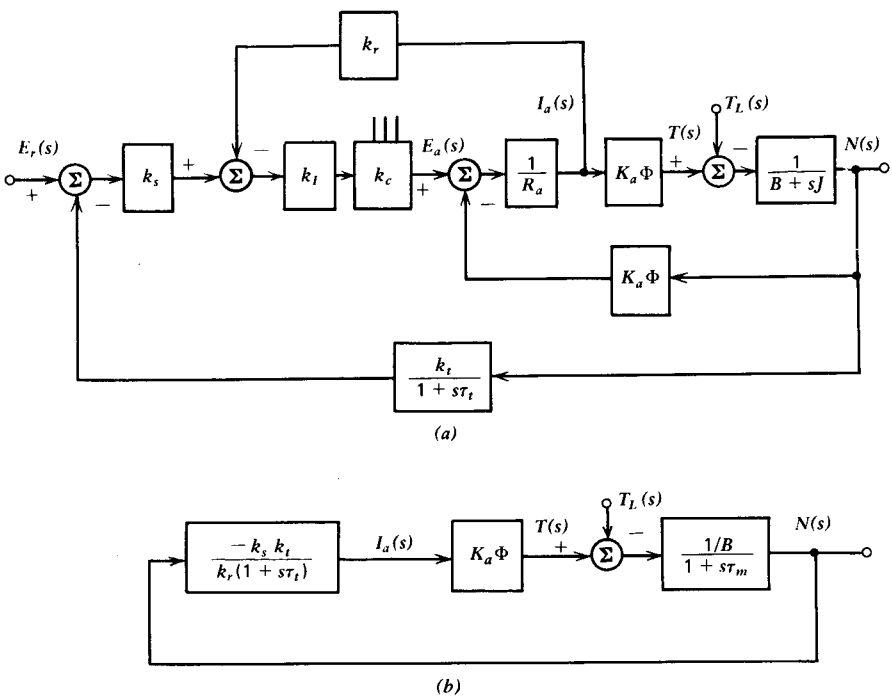


***Fig. 6.9*** **Effect of load torque disturbances. (*a*) Functional block diagram. (*b*) Simplified functional block diagram.**

$$I_a(s) = -\left[\frac{K_a\Phi + \dfrac{k_I k_c k_s k_t}{1+s\tau_t}}{R_a + k_I k_c k_r}\right] N(s) \tag{6.32}$$

Since $k_I k_c k_s k_t \gg K_a\Phi$ and $k_I k_c k_r \gg R_a$,

$$I_a(s) \simeq -\frac{k_s k_t}{k_r(1+s\tau_t)} N(s) \tag{6.33}$$

The block diagram then simplifies to that shown in Fig. 6.9*b*. Thus

$$\frac{N(s)}{T_L(s)} = \frac{-\dfrac{1}{B+sJ}}{1+\dfrac{K_a\Phi k_s k_t}{k_r(1+s\tau_t)}\left(\dfrac{1}{B+sJ}\right)}$$

$$= \frac{-\dfrac{1}{B}(1+s\tau_t)}{\left\{1+\dfrac{K_a\Phi k_s k_t}{k_r B}\right\}\left[1+s\dfrac{(\tau_m+\tau_t)}{k^1}+s^2\dfrac{\tau_m\tau_t}{k^1}\right]} \tag{6.34}$$

where

$$k^1 = 1 + \frac{K_a\Phi k_s k_t}{k_r B}$$

Because $K_a\Phi/B = k_{m2}$ and $k_r \simeq 1/k_{IC}$

$$k^1 = 1 + k_s k_t k_{IC} k_{m2}$$

Since

$$\frac{K_a\Phi k_s k_t}{k_r B} \gg 1,$$

$$\frac{N(s)}{T_L(s)} \simeq \frac{-1}{\dfrac{K_a\Phi k_s k_t}{k_r}} \frac{1+s\tau_t}{1+s\left(\dfrac{\tau_m+\tau_t}{k^1}\right)+s^2\left(\dfrac{\tau_m\tau_t}{k^1}\right)} \tag{6.35}$$

Equation 6.35 is identical to equation 6.27 except for a change in gain. Therefore the poles will be the same as in equation 6.27. Second-order response in both cases, step change in torque and speed reference, is evident in the oscillograms of Figs. 6.10 and 6.6.

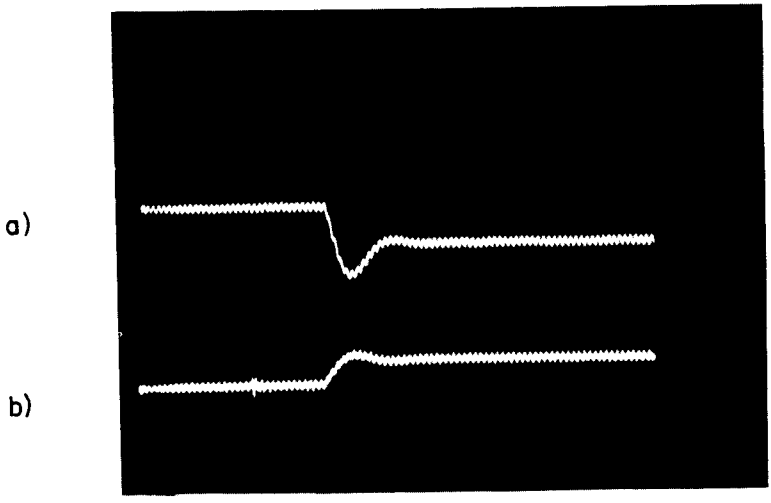


*Fig. 6.10* Response to step increase in load torque with proportional control. (*a*) Speed. (*b*) Current.

The current response from equations 6.33 and 6.35 is

$$\frac{I_a(s)}{T_L(s)} = \frac{I_a(s)}{N(s)} \cdot \frac{N(s)}{T_L(s)}$$

$$= \frac{1}{K_a\Phi\left(1 + s\left(\frac{\tau_m + \tau_t}{k^1}\right) + s^2\frac{\tau_m\tau_1}{k^1}\right)} \tag{6.36}$$

which also shows a similar second-order response.

***PI Controller***

With proportional-integral control, the controller block designated by $k_s$ in Fig. 6.9*a* is replaced by the *PI* transfer function $k_s[(1 + \tau_s s)/\tau_s s]$. Because the *PI* controller provides filtering, a filter may not be necessary for the tachogenerator output. Therefore neglecting $\tau_t$, from Fig. 6.9*b* for the *PI* controller,

$$\frac{N(s)}{T_L(s)} = \frac{-\dfrac{1}{B + Js}}{1 + \left(\dfrac{K_a\Phi k_s k_t}{k_r}\right)\left(\dfrac{1 + \tau_s s}{\tau_s s}\right)\left(\dfrac{1}{B + Js}\right)}$$

$$= \frac{-\tau_s k_r}{K_a\Phi k_s k_t} \frac{s}{1 + \tau_s\left(1 + \dfrac{Bk_r}{K_a\Phi k_s k_t}\right)s + \dfrac{\tau_s\tau_m Bk_r}{K_a\Phi k_s k_t}s^2} \tag{6.37}$$

Because

$$\frac{K_a \Phi k_s k_t}{B k_r} \gg 1$$

then

$$\frac{N(s)}{T_L(s)} \simeq \frac{-\tau_s k_r}{K_a \Phi k_s k_t} \frac{s}{1 + \tau_s s + \tau_s \tau_2 s^2} \tag{6.38}$$

where

$$\tau_2 = \frac{\tau_m k_r B}{K_a \Phi k_s k_t}$$

Substitution of $k_r \simeq 1/k_{IC}$ and $B/K_a\Phi \simeq 1/k_{m2}$ yields

$$\tau_2 = \frac{\tau_m}{k_{IC} k_{m2} k_s k_t}$$

From Fig. 6.9*b*, for the *PI* controller, neglecting $\tau_t$,

$$\frac{I_a(s)}{N(s)} = \frac{-k_s k_t (1 + \tau_s s)}{k_r s \tau_s} \tag{6.39}$$

Now, from equations 6.38 and 6.39,

$$\frac{I_a(s)}{T_L(s)} = \left[\frac{I_a(s)}{N(s)}\right]\left[\frac{N(s)}{T_L(s)}\right] \tag{6.40}$$

$$= \frac{1}{k_a \Phi} \frac{(1 + \tau_s s)}{(1 + \tau_s s + \tau_s \tau_2 s^2)} \tag{6.41}$$

The poles of equations 6.38 and 6.41, for a step change in torque, are the same as those of equations 6.29 and 6.30 for a step change in speed. Because the poles are the same the responses will be the same. This is expected, because poles are characteristics of a system and not of input signals. The response due to a step change in torque is shown in Fig. 6.11 for a *PI* controller. The transfer function in equation 6.38 has a zero at the origin. Therefore, for a step change in torque, there will be a no steady-state speed change. This is shown in the oscillogram of Fig. 6.11*a*.

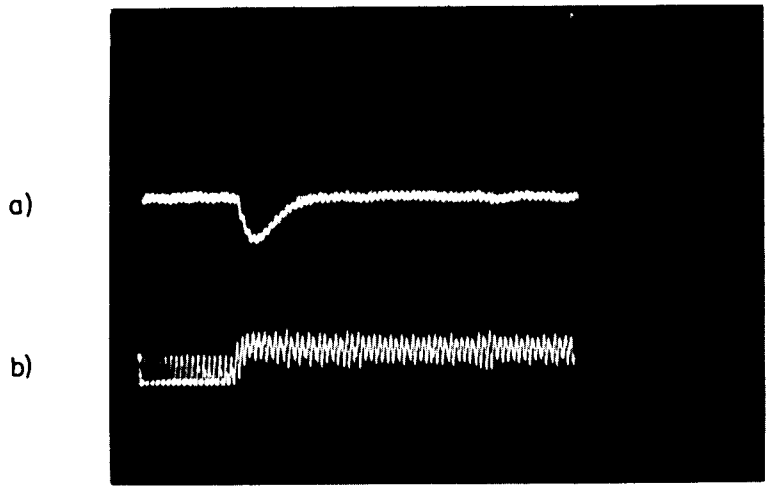


*Fig. 6.11* Response to step increase in load torque with proportional-integral control. (*a*) Speed. (*b*) Current.

### *Current Limiting*

Current limiting is a major feature of this drive. It could not be considered in the linear system analysis as set forth in the preceding sections. Current limiting is obtained using a current controller as explained earlier. The resulting effect can be seen in Fig. 6.12, which is a photograph of the start-up current and speed. After an initial overshoot caused by controller time lag,

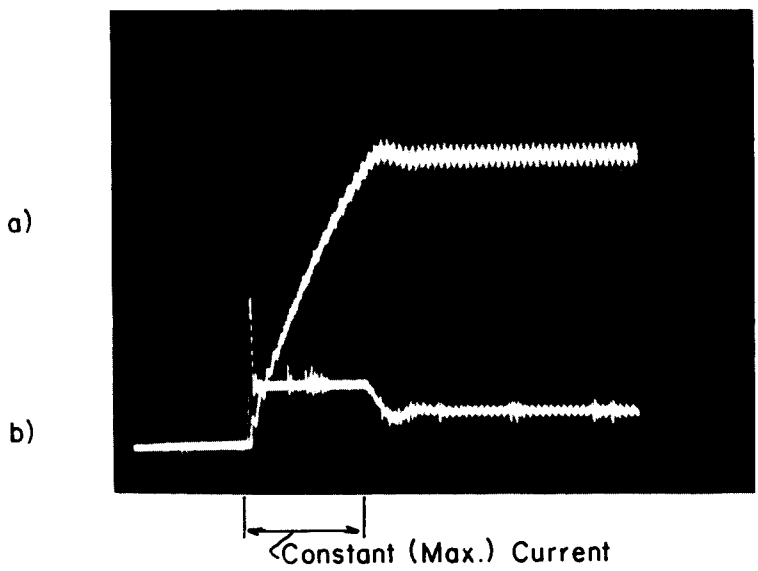


*Fig. 6.12* Effect of current limiting during start-up. (*a*) Speed. (*b*) Current.

the current is held at a constant value. Once the desired speed is reached, the speed error is smaller than the clamping value, and the system behaves as analyzed previously.

While the current is limited, the speed response is governed by equation 6.26. Thus during starting, the speed is described by

$$N(s) = \frac{\hat{I}_a k_{m2}}{s(1 + \tau_m s)} \tag{6.42}$$

$$N(t) = \hat{I}_a k_{m2}(1 - e^{-t/\tau_m}) \tag{6.43}$$

This result also can be derived from the basic torque balance equations 6.3 and 6.4. Considering a no-load start up,

$$K_a \Phi \hat{I}_a = J\frac{dN}{dt} + BN \tag{6.44}$$

$$N(t) = \frac{K_a \Phi \hat{I}_a}{B}(1 - e^{-t/\tau_m})$$

$$= \hat{I}_a k_{m2}(1 - e^{-t/\tau_m}) \tag{6.45}$$

If $B$ is very small,

$$K_a \Phi I_a = J\frac{dN}{dt} \tag{6.46}$$

$$N(t) = \left(\frac{K_a \Phi I_a}{J}\right)t \tag{6.47}$$

Equation 6.47 shows a linear change in speed with time. The oscillogram of Fig. 6.12 indicates an essentially linear increase in speed.

Because the current is limited, the thyristors are inherently protected. The normally large starting and transient currents, which can damage the converter and possibly the motor, have been eliminated in this closed-loop control system having this current limit feature.

### 6.1.5 Design Procedure

A design procedure is discussed here for a closed-loop speed-control system using a 110 V, 2.5 hp, 1800 rpm separately excited dc motor. The parameters and constants describing an experimental system are presented in Table 6.1.

Assuming that the feedback gains $k_t$ and $k_r$ are fixed at the values given in Table 6.1, only the gains $k_I$ and $k_S$ are left to be determined. The clamping value of $E_I$ also must be chosen.

***Table 6.1*** **Parameters and Constants of a Closed-Loop Control System for a Separately Excited Dc Motor Drive**
The experimental set-up used two identical machines, one as a drive motor and the other for loading.

| | | |
|---|---|---|
| DC motor: 110 $V$, 2.5 hp, 1800 rpm | $R_a = 1\ \Omega$ | Armature circuit resistance, including a 0.4 Ω resistor externally connected in series with the drive motor |
| | $L_a = 46$ mH | Armature circuit inductance, including a 40 mH inductor externally connected in series with the drive motor |
| | $J = 0.093$ kg − m$^2$ | For the two machines mechanically connected together |
| | $B = 0.008$ N·m·sec/rad | For the two machines |
| | $I_a = 20$ A | Rated motor current |
| | $k_a\Phi = 0.55$ V·sec/rad | Back emf and torque constant |
| Parameters and constants | $\tau_a = L_a/R_a = 46$ msec | |
| | $\tau_m = J/B = 11.63$ sec | |
| | $\tau_t = 0.1$ sec | |
| | $\tau_{m1} = \dfrac{\tau_m R_a B}{(K_a\Phi)^2 + R_a B} = 0.3$ sec | |
| | $k_{m1} = \dfrac{B}{(K_a\Phi)^2 + R_a B} = 0.0258$ A/V | |
| | $k_{m2} = \dfrac{K_a\Phi}{B} = 68.75$ rad/sec·A | |
| | $k_t = 0.057$ V·sec/rad | |
| | $k_r = 0.5$ V/A | |
| | $k_c = \dfrac{E_a}{E_c} = \dfrac{(3\sqrt{2}/\pi) \times 120}{6.55} = 25$ | |
| | $k_{IC} \simeq 1/k_r = 2$ | |

### *Current Controller Gain, $k_I$*

The gains can be chosen on the basis of steady-state error considerations, where

$$\varepsilon_I(\propto) = \left.\frac{1}{1 + G(s)H(s)}\right|_{s=0} \tag{6.48}$$

For the current-control loop, from Fig. 6.4,

$$G(s)|_{s=0} = k_I k_c k_{m1} \tag{6.49}$$

and

$$H(s)|_{s=0} = k_r \tag{6.50}$$

Therefore

$$\varepsilon_I(\propto) = \frac{1}{1 + k_I k_c k_{m1} k_r} \tag{6.51}$$

or

$$k_I = \frac{\dfrac{1}{\varepsilon_I(\propto)} - 1}{k_c k_{m1} k_r} \tag{6.52}$$

where $\varepsilon_I(\propto)$ is the desired steady-state error. While the current error is not critical, it must not be too large. A practical value might be 10%. For $\varepsilon_I(\propto) = 0.1$

$$k_I = \frac{10 - 1}{(25)(0.0258)(0.5)}$$

$$\simeq 28$$

***Current Limit Reference, $\hat{E}_I$***

From equation 6.23, the current will be clamped at

$$\hat{I}_a = \frac{\hat{E}_I}{k_r}$$

For a current limit of 25 A,

$$\hat{E}_I = \hat{I}_a k_r$$

$$= 12.5\text{V} \tag{6.53}$$

***Speed Controller Gain, $k_s$***

The speed controller gain $k_s$ can be chosen in the same manner as the current controller gain $k_I$.

$$\varepsilon_N(\propto) = \left.\frac{1}{1 + G(s)H(s)}\right|_{s=0} \tag{6.54}$$

***P Controller***

From Fig. 6.5*c*

$$G(s)|_{s=0} = k_s k_{IC} k_{m2} \tag{6.55}$$

$$H(s)|_{s=0} = k_t \tag{6.56}$$

Thus

$$\varepsilon_N(\propto) = \frac{1}{1 + k_s k_{IC} k_{m2} k_t} \tag{6.57}$$

Therefore

$$k_s = \frac{\dfrac{1}{\varepsilon_N(\propto)} - 1}{k_{IC} k_{m2} k_t} \tag{6.58}$$

where $\varepsilon_N(\propto)$ is the desired steady-state error. From equation 6.57, this error can be reduced by increasing the controller gain $k_s$. For 0.25% steady-state error in speed,

$$k_s = \frac{400 - 1}{(2)(68.75)(.057)}$$

$$\simeq 51$$

***PI Controller***

For the *PI* controller, the steady-state error is ideally zero. The controller gain $k_s$ and its pole $(1/\tau_s)$ can thus be designed from the consideration of damping and natural frequency.

The characteristic equation of the system, from equation 6.29, is

$$1 + s\tau_s + s^2\tau_s\tau_2 = 0 \tag{6.59}$$

The poles are

$$s = \frac{1}{2\tau_2}\left[-1 \pm j\sqrt{\frac{4\tau_2}{\tau_s} - 1}\right] \tag{6.60}$$

A commonly accepted damping ratio is $1/\sqrt{2}$, and for this damping ratio

$$\tau_s = 2\tau_2 \tag{6.61}$$

The natural frequency is then

$$\omega_n = \frac{1}{\sqrt{2}\,\tau_2} \tag{6.62}$$

The controller gain from equation 6.29a is

$$k_s = \frac{\tau_m}{k_t k_{IC} k_{m2} \tau_2} \tag{6.63}$$

Suppose a natural frequency of $\omega_n = 10$ rad/sec is chosen. Then from equations 6.62 and 6.61

$$\tau_2 = \frac{1}{(\sqrt{2})10} = 0.071 \text{ sec}$$

and

$$\tau_s = 0.142 \text{ sec}$$

Also, from equation 6.63,

$$k_s \simeq 21$$

The various gains and parameters calculated here are used in the experimental set-up. The oscillograms of speed response and current response shown in Figs. 6.6 and 6.8 are obtained for proportional and proportional-integral control, respectively. Second-order response and good damping, predicted in the theory and the design procedure, are apparent in these oscillograms.

In this section the concept of closed-loop control has been developed systematically. The analysis presented here will help the reader to understand the complexity of a closed-loop drive system. The design procedure outlined here for closed-loop control of a 2.5 hp motor drive system is not rigorous. However, it provides a basis and guide for selecting gains and parameters in designing other complex drive systems.

## 6.2 SERIES DC MOTOR MODEL

Dc series motors are best suited for certain applications, such as vehicle, crane, hoist, and similar drives where large starting torques at low speeds are desired. At low-speed regions, the motor draws a large current, and if sufficient iron is not used to reduce weight the magnetic circuit is saturated, and the flux per pole remains essentially constant. The behavior of the motor is similar to a separately excited dc motor. Thus the analysis of Section 6.1 is

applicable to a system where the dc series motor is operated in the saturated mode.

However, when the vehicle is running above base speed carrying less current or when a crane or hoist, for example, operates at a light load, the magnetic circuit may not saturate. If sufficient iron is used, the magnetic circuit may not saturate even at a high current. Analysis of the system performance under such conditions becomes complex, because of nonlinearities in equations such as 6.64 and 6.65 that describe the operation of the dc series motors. Numerical analysis[3] or state space analysis[4] may be used in an open-loop control. Application of these methods in a closed-loop system is difficult.

### 6.2.1 Linearized Model

A linear model or transfer function for the series motor can be derived by applying small signal perturbation techniques.[5,6] This model can then be used in the analysis of a closed-loop system incorporating the series motor. The analysis is valid for small disturbances around a given steady-state operating point.

In this method of deriving a linear model, the system is assumed to operate in the steady state, and the defining equations are linearized for a small signal perturbation.

The differential equations governing the performance of the dc series motors are

$$e_a = R_a i_a + L_a \frac{di_a}{dt} + K_{af} i_a n + K_{res} n \tag{6.64}$$

$$K_{af} i_a^2 = J \frac{dn}{dt} + Bn + T_L \tag{6.65}$$

These equations are valid for both transient and steady-state conditions. They are nonlinear because of the product and square terms involving the variables. In addition, variation of the parameters, such as $R_a$, $L_a$, $K_{af}$, and $B$, will make the equations nonlinear. To derive a linearized model or transfer function, the following assumptions are made.

1 The parameters remain constant for a small perturbation.
2 During the transient period after the disturbance, the transient behavior is considered in terms of time variation of average values of current and speed, rather than their instantaneous values; that is, the system passes through quasi steady-state operating conditions during the disturbance.
3 Average and rms currents are essentially the same.

The current being unidirectional, the average voltage across the inductance is zero over a cycle. In terms of average values, the defining equations are

$$E_a = I_a R_a + K_{af} I_a N + K_{res} N \tag{6.66}$$

$$K_{af} I_a^2 = J\frac{dN}{dt} + BN + T_L \tag{6.67}$$

Small signal linearization around an operating point gives

$$\Delta E_a = \Delta I_a(R_a + K_{af} N_o) + \Delta N(K_{res} + K_{af} I_{ao}) \tag{6.68}$$

$$2K_{af} I_{ao}\,\Delta I_a = Jp\,\Delta N + B\,\Delta N + \Delta T_L \tag{6.69}$$

where $p = d/dt$
$I_{ao}$ = motor current at the operating point
$N_o$ = motor speed at the operating point.

In the Laplace domain, these equations can be rewritten as follows:

$$\Delta I_a(s) = \frac{\Delta E_a(s) - \Delta N(s)(K_{res} + K_{af} I_{ao})}{R_a + K_{af} N_o} \tag{6.70}$$

$$\Delta N(s) = \frac{2K_{af} I_{ao}\,\Delta I_a(s) - \Delta T_L(s)}{B + Js} \tag{6.71}$$

These equations in block diagram representation are shown in Fig. 6.13*a*.

***Step Change in Motor Voltage***

If only the response due to changes in motor voltage is considered, the block diagram simplifies to that shown in Fig. 6.13*b*. The transfer function relevant to speed changes is given by

$$\frac{\Delta N(s)}{\Delta E_a(s)} = \frac{G_E(s)}{1 + G_E(s) H_E(s)} \tag{6.72}$$

where

$$G_E(s) = \frac{2K_{af} I_{ao}}{R_a + K_{af} N_o}\,\frac{1}{B + sJ} \tag{6.73}$$

$$H_E(s) = K_{res} + K_{af} I_{ao} \tag{6.74}$$

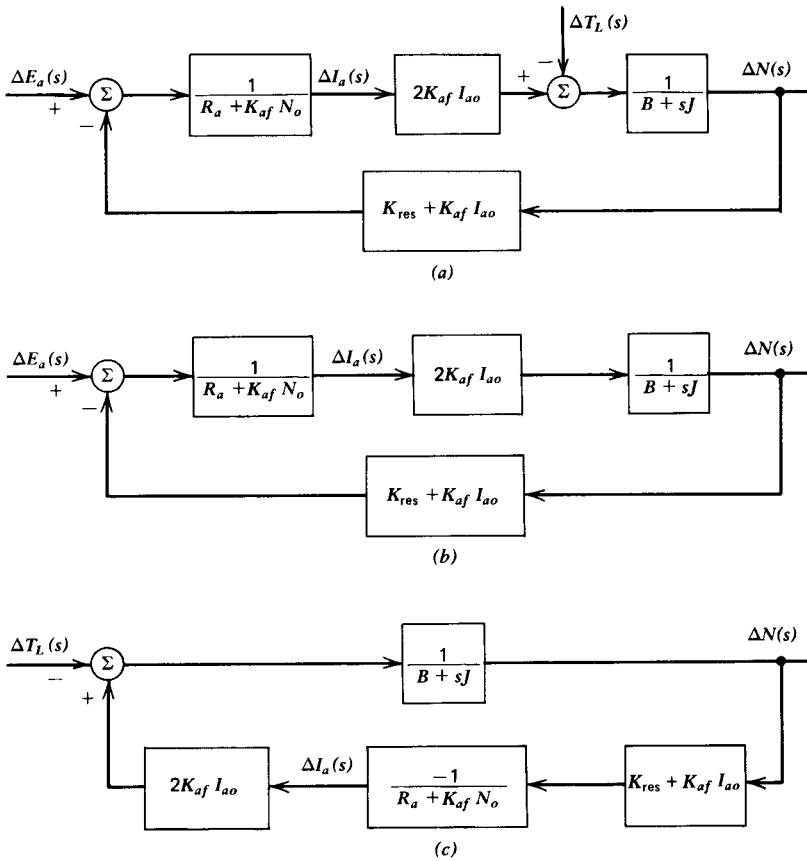


***Fig. 6.13*** Transfer function model for a dc series motor.

From equations 6.72, 6.73, and 6.74

$$\frac{\Delta N(s)}{\Delta E_a(s)} = \frac{2K_{af}I_{ao}}{R_a + K_{af}N_o} \frac{1}{B + \dfrac{2K_{af}I_{ao}(K_{res} + K_{af}I_{ao})}{R_a + K_{af}N_o} + sJ}$$

$$= k_{EN}\frac{1}{1 + s\tau_o} \tag{6.75}$$

where

$$B_o = B + \frac{2K_{af}I_{ao}(K_{res} + K_{af}I_{ao})}{R_a + K_{af}N_o} \tag{6.76}$$

$$\tau_o = \frac{J}{B_o} \tag{6.77}$$

$$k_{EN} = \frac{2K_{af}I_{ao}}{B_o(R_a + K_{af}N_o)} \tag{6.78}$$

The transfer function for current changes is given by

$$\frac{\Delta I_a(s)}{\Delta E_a(s)} = \frac{\Delta I_a(s)}{\Delta N(s)} \cdot \frac{\Delta N(s)}{\Delta E_a(s)} \tag{6.79}$$

$$= \frac{B + sJ}{2K_{af}I_{ao}} \cdot k_{EN} \frac{1}{1 + s\tau_o}$$

$$= k_{EI} \frac{1 + s\tau_m}{1 + s\tau_o} \tag{6.80}$$

where

$$k_{EI} = \frac{B}{2K_{af}I_{ao}} k_{EN} \tag{6.81}$$

***Step Change in Load Torque***

If only the effect of load torque changes is of interest, the block diagram in Fig. 6.13*c* applies. The transfer function for the speed response is

$$\frac{\Delta N(s)}{\Delta T_L(s)} = \frac{-G_T(s)}{1 - G_T(s)H_T(s)} \tag{6.82}$$

where

$$G_T(s) = \frac{1}{B + sJ} \tag{6.83}$$

$$H_T(s) = -\frac{(2K_{af}I_{ao})(K_{res} + K_{af}I_{ao})}{R_a + K_{af}N_o} \tag{6.84}$$

From equations 6.82, 6.83, 6.84, and 6.76

$$\frac{N(s)}{T_L(s)} = \left(-\frac{1}{B_o}\right)\frac{1}{1 + s\tau_o} \tag{6.85}$$

$$= k_{TN} \frac{1}{1 + s\tau_o} \tag{6.86}$$

The transfer function for current changes is given by

$$\frac{\Delta I_a(s)}{\Delta T_L(s)} = \frac{\Delta I_a(s)}{\Delta N(s)} \cdot \frac{\Delta N(s)}{\Delta T_L(s)} \tag{6.87}$$

$$= \left( \frac{K_{res} + K_{af} I_{ao}}{R_a + K_{af} N_o} \frac{1}{B_o} \right) \frac{1}{1 + s\tau_o} \tag{6.88}$$

$$= k_{TI} \frac{1}{1 + s\tau_o} \tag{6.89}$$

### 6.2.2 Numerical Analysis and the Linearized Model—A Comparison

The motor behavior can be more accurately determined by solving the nonlinear differential equations 6.64 and 6.65 numerically on a digital computer. In the numerical method solutions are obtained for instantaneous variations of motor speed and current. Any change in the parameters can be incorporated in the program. This method is therefore rigorous and valid for small as well as large disturbances. A flowchart is shown in Fig. 6.14. The defining equations are rewritten as follows:

$$pi_a = \frac{e_a - R_a i_a - K_{af} i_a n - K_{res} n}{L_a}$$

$$= f_1(n, i_a) \tag{6.90}$$

$$pn = \frac{K_{af} i_a^2 - Bn - T_L}{J}$$

$$= f_2(n, i_a) \tag{6.91}$$

Equations 6.90 and 6.91 are two first-order differential equations and can be solved numerically by the Runge-Kutta fourth-order approximation method.[3] The flowchart of Fig. 6.14 allows determination of both transient behavior and steady-state behavior. The latter can be obtained by considering the motor to be at standstill to start with.

In this section, the validity of the linearized model derived in Section 6.2.1 is assessed by comparing the transient behavior predicted from the linearized models and that obtained from the numerical solution. The time variations of speed and current for a step change in motor voltage or torque are derived as follows.

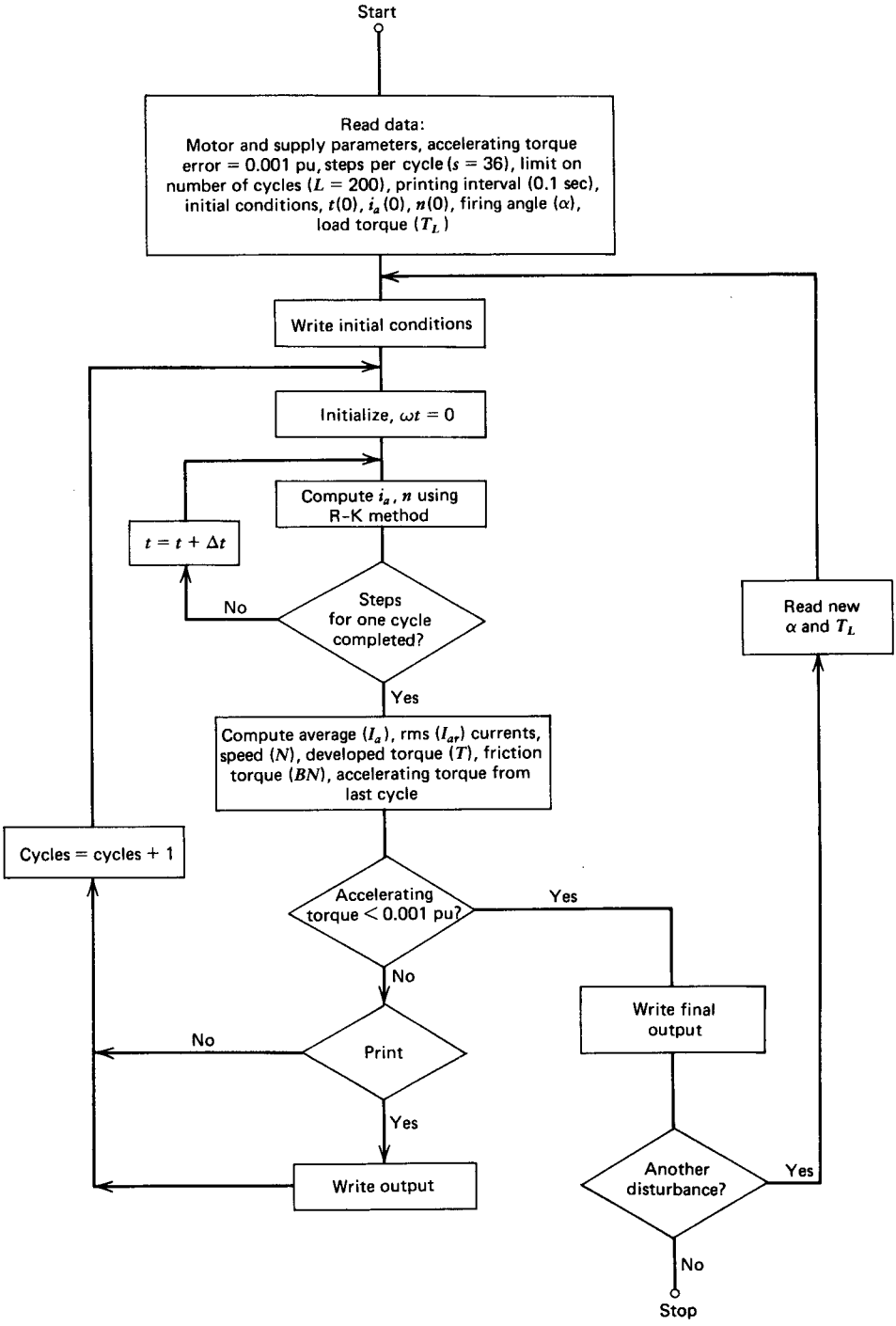


*Fig. 6.14* Computer flowchart for study of steady-state or dynamic behavior of dc motors by numerical method.

***Step Change in Motor Voltage***

From equation 6.75

$$\Delta N(s) = \Delta E_a(s) \cdot k_{EN} \frac{1}{1 + s\tau_o}$$

$$= k_{EN} \frac{\Delta E_a}{s} \cdot \frac{1}{1 + s\tau_o} \tag{6.92}$$

$$\Delta N(t) = k_{EN} \Delta E_a \cdot (1 - e^{-t/\tau_o}) \tag{6.93}$$

From equation 6.80

$$\Delta I_a(s) = k_{EI} \frac{\Delta E_a}{s} \frac{1 + s\tau_m}{1 + s\tau_o} \tag{6.94}$$

$$\Delta I_a(s) = k_{EI} \Delta E \left( \frac{1}{s} - \frac{\tau_o - \tau_m}{1 + s\tau_o} \right) \tag{6.95}$$

$$\Delta I_a(t) = k_{EI} \Delta E \left[ 1 - \left( 1 - \frac{\tau_m}{\tau_o} \right) e^{-t/\tau_o} \right] \tag{6.96}$$

***Step Change in Load Torque***

From equation 6.86

$$\Delta N(s) = k_{TN} \frac{\Delta T}{s} \frac{1}{1 + s\tau_o} \tag{6.97}$$

$$\Delta N(t) = k_{TN} \Delta T (1 - e^{-t/\tau_o}) \tag{6.98}$$

From equation 6.89

$$\Delta I_a(s) = k_{TI} \frac{\Delta T}{s} \frac{1}{1 + s\tau_o} \tag{6.99}$$

$$\Delta I_a(t) = k_{TI} \Delta T (1 - e^{-t/\tau_o}) \tag{6.100}$$

***Response Study***

The steady-state operating condition is obtained by the numerical method, the flowchart for which is shown in Fig. 6.14. The variation of average speed and current during the start-up of the series motor from standstill is shown in Fig. 6.15. This provides a steady-state operating condition. Disturbances are then applied around the operating point. The responses to such changes are

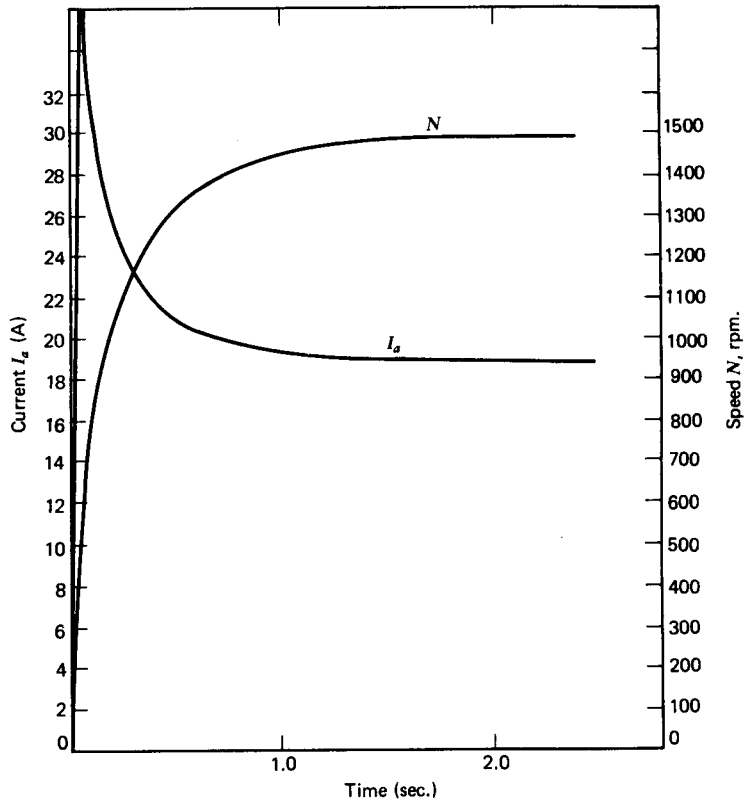


*Fig. 6.15* Speed and current variation during start-up of a series motor (numerical method).

obtained by the numerical method as well as from the linearized transfer functions given by equations 6.93, 6.96, 6.98, and 6.100. The results are compared in Figs. 6.16 and 6.17 for a 5% armature voltage change and a 10% torque change, respectively. The various parameter values and constants are shown in Table 6.2.

The results in Figs. 6.16 and 6.17 indicate that the linearized models for the series motor predict the response with fair accuracy.

## 6.3 PHASE-LOCKED-LOOP (PLL) CONTROL

The degree of speed control required in industrial drives depends on the application. In some applications open-loop regulation of the drive motor may be adequate. In others closed-loop feedback control is required for precise speed control and fast response. Conventionally, this is achieved by an analog servo feedback system in which any change in speed is sensed by a

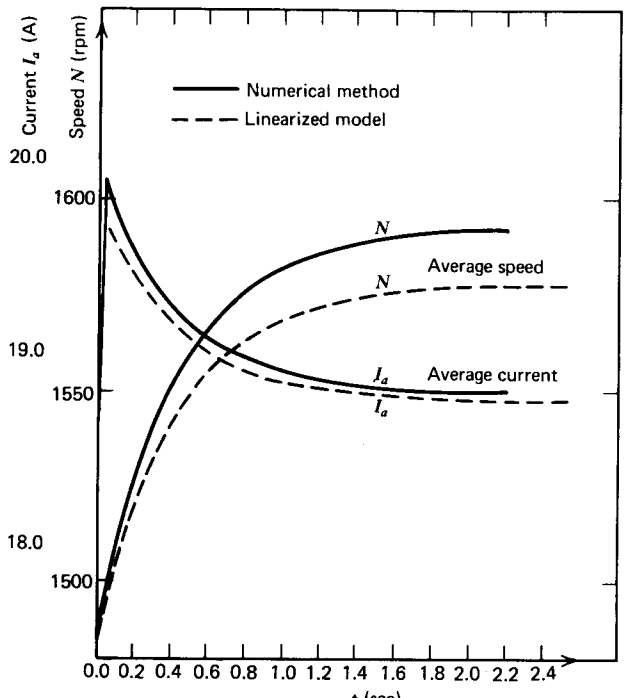


*Fig. 6.16* Transient response due to change in firing angle from $\alpha = 25°$ to $\alpha = 0°$. Dc series motor is supplied by a single-phase semi-converter.

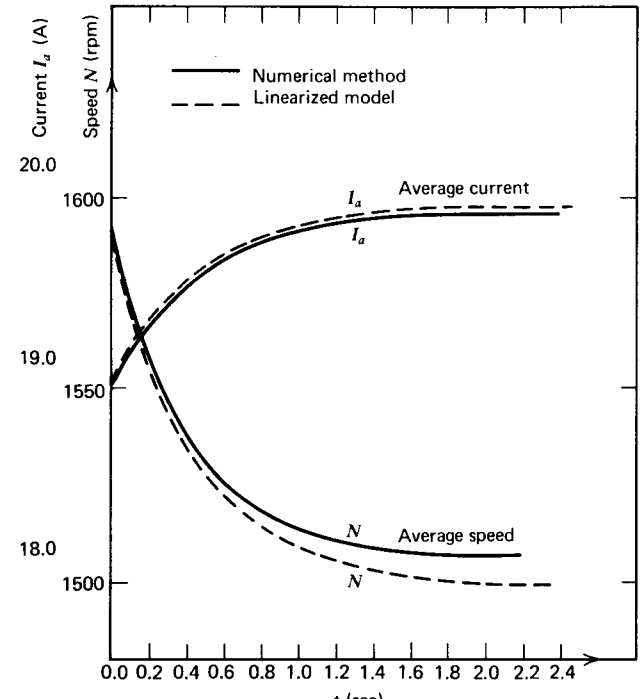


*Fig. 6.17* Transient response due to 10% change in load torque. Dc series motor is supplied by a single-phase semi-converter.

*Table 6.2* **Parameters and Constants for the Series Motor Model Study**

| | | | |
|---|---|---|---|
| Supply | | $1\phi$, 120 V, 60 Hz | |
| Converter | | Semi-converter | |
| Motor parameters | $K_{af}$ | $= 0.027$ H | |
| | $K_{res}$ | $= 0.0273$ V·sec/rad | |
| | $R_a$ | $= 1\Omega$ | |
| | $L_a$ | $= 32$ mH (includes added inductance of 20 mH in the armature circuit) | |
| | J | $= 0.0465$ kg-m$^2$ | |
| | B | $= 0.004$ N·m·sec/rad | |
| Disturbance | $\Delta E_a$ | $= 5.4$ V | $\Delta T = 1$ N·m |
| | | $= \frac{5.4}{102.6} \times 100$ | $\simeq 10\%$ |
| | | $\simeq 5\%$ | |
| | ($\alpha$ changed from 25.8° to 0°) | | ($T_L$ changed from 9 N·m to 10 N·m) |
| Steady-state operating point | $\alpha$ | $= 25.8°$ | $\alpha = 0°$ |
| | $E_a$ | $= 102.62$ V | $E_a = 108.02$ V |
| | $N_o$ | $= 1485$ rpm | $N_o = 1592.8$ rpm |
| | $I_{ao}$ | $= 18.72$ A | $I_{ao} = 18.8$ A |
| | $T_L$ | $= 9$ N·m | $T_L = 9$ N·m |
| Constants | $B_o$ | $= 0.108$ | $B_o = 0.102$ |
| | $\tau_o$ | $= 0.432$ | $\tau_o = 0.457$ |
| | $\tau_m$ | $= 11.625$ | $\tau_m = 11.625$ |
| | $k_{EN}$ | $= 1.807$ | $k_{TN} = -9.818$ |
| | $k_{EI}$ | $= 0.007$ | $k_{TI} = 0.954$ |

tachometer and compared with a fixed reference voltage to generate a correction signal. However, this analog feedback system is not satisfactory in some applications where excellent speed regulation and fast dynamic response are required. A *PI* (proportional-integral) controller ideally should provide perfect speed regulation and fast response. However, because the devices that sense the speed are not ideal and because other analog devices used in the feedback circuit are less than ideal, speed regulation is not perfect. At best 0.2% speed regulation can be achieved in an analog feedback control system. Figure 6.11 shows that when a torque is applied or changed, there is a transient speed dip. In addition, the steady-state speed is reached after a certain time interval. This type of operation may not be satisfactory in certain drives where high-quality products are desired.

These shortcomings of analog feedback control systems can be overcome by using a digital phase-locked-loop control system. In the phase-locked-loop method, the motor speed is converted to a digital pulse train, which is

synchronized with a reference digital pulse train. In this way, by locking onto a reference frequency, precise control of speed is achieved. The phase-locked-loop control system is desirable where several motors must be synchronized to each other, as in a conveyer for materials handling, or where a digital clock has to coordinate the motor speed, as in computer peripherals, or where high-quality product is required, as in paper or textile mills.

Phase-locked-loop techniques have been used primarily in communication systems to synchronize signals. Phase-locked-loops (PLL) are now available as inexpensive digital integrated circuits. With the development of both integrated circuits and solid-state power circuits, the use of PLL techniques in motor speed control has generated considerable interest recently.[7–11] In the following sections the operation of a basic phase-lock-loop is described, and the analysis of a dc drive system using a PLL control system is presented.

### 6.3.1 The Phase-Locked-Loop (PLL)

The basic phase-locked-loop circuit is presented in schematic form in Fig. 6.18*a*. The heart of the PLL circuit is a digital integrated circuit known as a *phase detector* (or *comparator*), which takes two pulse trains ($f_i$ and $f$) at the input and produces a pulse-width modulated output $E_e$, the pulse-width being proportional to the difference in phase between the input pulse trains. If the two pulse trains have the same frequency and are exactly coincident in time, the phase detector output is zero; otherwise the detector produces an error signal as shown in the waveforms of Fig. 6.18. Since $E_e$ is in a pulse-width form, a loop filter is necessary to convert the pulse train $E_e$ to a dc level $E_c$ representing the phase error. This is fed to a voltage-controlled oscillator (VCO) whose output frequency $f$ changes in response to the input voltage $E_c$. Thus any phase error in $f_i$ and $f$ tends to be self-correcting, that is, the phase-locked-loop acts to maintain $f$ equal to $f_i$. When the two frequencies are equal the system is said to be phase-locked. It is this equality of $f$ and $f_i$ that is important in the precise control of motor speed.

For motor speed control the equivalent of the VCO of Fig. 6.18*a* is a power converter circuit, a motor and a pulse-speed encoder, as shown in Fig. 6.19*a*. The output from the loop filter controls the motor power supply and hence its speed. A speed-dependent pulse train is generated, which is compared with the reference pulse train that represents the desired speed. Any tendency of the motor speed to change will be detected immediately in the phase detector circuit and corrected. The detection is almost instantaneous, and hence the response is fast. As long as the two frequencies stay locked, the steady-state motor speed remains unaffected, thereby providing perfect speed regulation. It is difficult to measure the speed regulation accurately enough to verify zero speed regulation. One method of determining speed is to measure the encoder output frequency. This method may indicate that the speed regulation is as low as 0.002%, which represents about a hundredfold improvement over the conventional analog speed-control system.

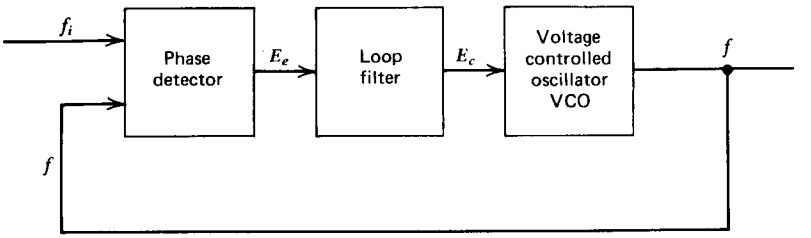


(a)

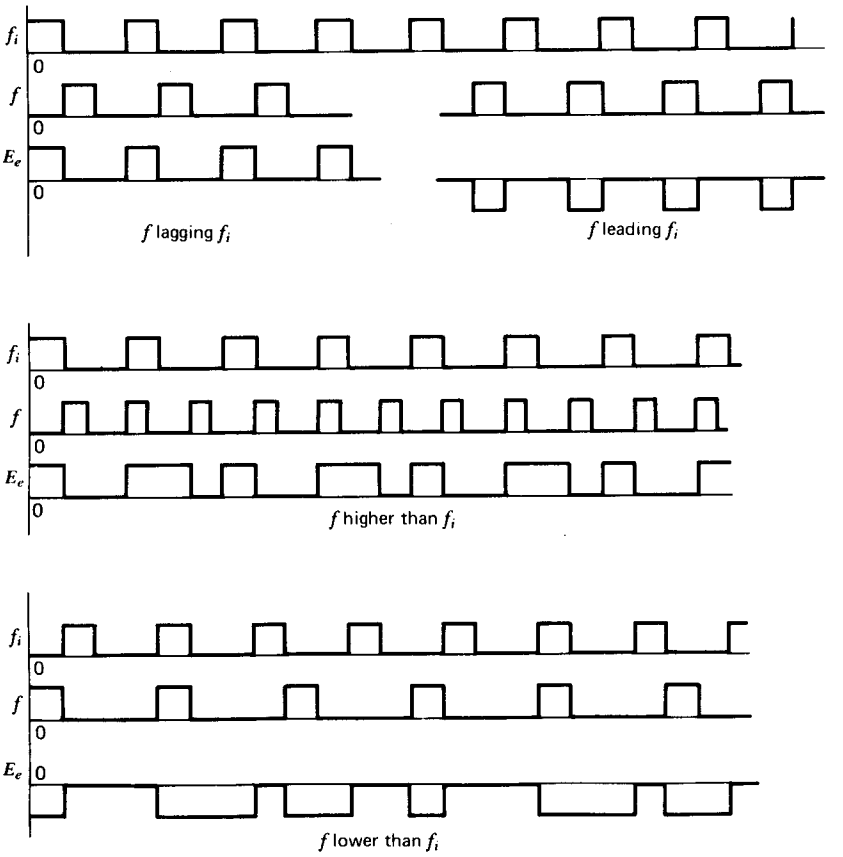


(b)

***Fig. 6.18*** **Basic phase-locked-loop (PLL) operation. (*a*) PLL in block diagram. (*b*) Waveforms to illustrate operation of the phase detector.**

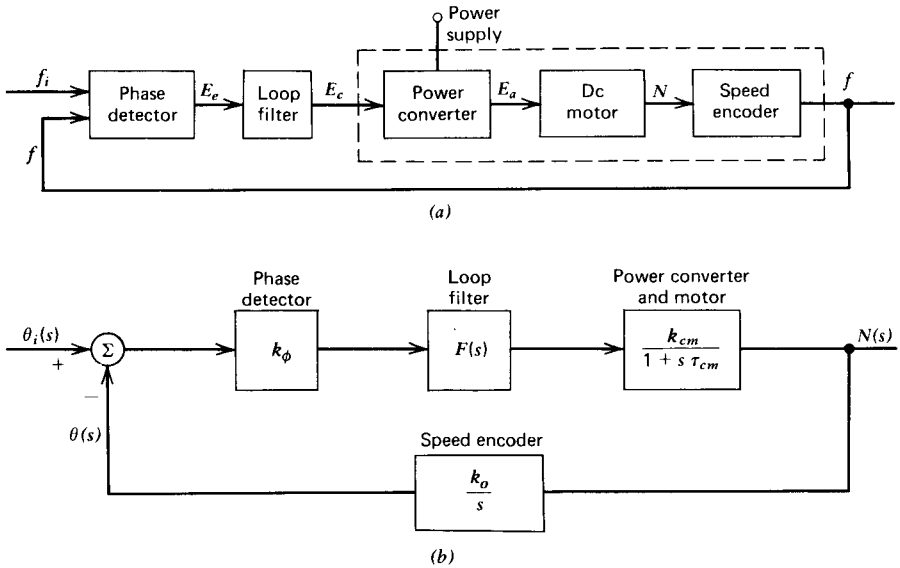


*Fig. 6.19* Phase-locked-loop (PLL) control system. (*a*) Motor speed control using PLL technique. (*b*) Transfer function model.

### 6.3.2 Analysis and System Simulation

The system behavior such as speed regulation, dynamic response, and stability can be studied by using the root locus technique.[8] This is a convenient analytical tool and requires a knowledge of open-loop poles and zeros of the system. This approach develops a "feel" for the system without a large amount of computation.

In order to use root locus analysis, a transfer function of the system is developed for the block diagram of Fig. 6.19*a*. The detector circuitry can be represented by a gain $k_\phi$ volt/radian, as shown in Fig. 6.19*b*. The filter is represented by a general transfer function $F(s)$. The poles and zeros of the filter will greatly influence the system performance. The power converter and the motor can be modeled by a gain $k_{cm}$ and a time contant $\tau_{cm}$. Their values will depend on whether or not a current-control loop is present in the power converter.

Depending on the size of the motor, the power converter may or may not have a current-control loop. For a small fractional-horsepower motor, a current-control loop may not be necessary. However, for an integral horsepower motor, a current limit must be incorporated. The electrical time constant is negligible compared to the mechanical time constant for most motors. If there is a current-control loop from Fig. 6.5*c*, $k_{cm} \simeq k_{IC} k_{m2}$ and $\tau_{cm} \simeq \tau_m$. If there is no current-control loop from Fig. 6.3, $k_{cm} = k_c k_m$ and

$\tau_{cm} \simeq \tau_{m1}$. Both gain and time constant are large in the former case and small in the latter.

The speed encoder transforms the speed into a frequency so that phase is compared with a reference by the loop. Since phase is the time integral of frequency, the encoder is modeled by a pole at the origin.

This development of the transfer function for the various control blocks is shown in Fig. 6.19*b*. The closed-loop transfer function of the system is written as follows:

$$\frac{N(s)}{\theta_i(s)} = \frac{G(s)}{1 + G(s)H(s)} \tag{6.101}$$

where $$G(s) = \frac{k_\Phi k_{cm} F(s)}{1 + s\tau_{cm}} \tag{6.101a}$$

$$H(s) = \frac{k_o}{s} \tag{6.101b}$$

The closed-loop poles, and hence stability and system behavior, will be determined by the poles and zeros of the open-loop transfer function $G(s)H(s)$.

$$G(s)H(s) = k_\Phi k_{cm} k_o \frac{F(s)}{s(1 + s\tau_{cm})}$$

$$= k \frac{F(s)}{s(1 + s\tau_{cm})} \tag{6.102}$$

where $k = k_\Phi k_{cm} k_o$.

There are two open-loop poles, at 0 and $1/\tau_{cm}$, plus whatever poles are associated with $F(s)$. The filter transfer function can also contribute zeros. As the loop gain is increased, the closed-loop poles move from the open-loop poles toward the open-loop zeros. Thus $F(s)$ and the loop gains are the two variables available for pole adjustment.

### *Filter Transfer Function F(s)*

A great variety of filters can be used. The system response and stability will be affected by the type of filter used. The pole introduced by the converter-motor transfer function will significantly influence the closed-loop poles as the gain increases. Root locus plots are therefore presented in Fig. 6.20 for both small and large values of time constant $\tau_{cm}$ corresponding to the converter-motor combination.

Some possible filter transfer functions are now considered.

1 $F(s) = 1/(1 + s\tau_1)$ Because the phase detector output is in pulse-width form, it must usually be filtered. The root locus plot using such a filter is shown in Fig. 6.20*a*. Because the filter introduces an additional pole, there are altogether three poles. If the motor time constant is large the system will become unstable at a much smaller gain than if the time constant is small.

2 $F(s) = 1/s$ Because an integrator is a common filter in phase-locked-loops, it is also considered here. Fig. 6.20*b* indicates that, as the gain increases, the two poles at zero migrate towards the right half plane. Therefore phase integral control is unstable or oscillatory for all gains.

3 $F(s) = (1 + s\tau_1)/s$, ***PI* Controller** This filter adds a zero to the system. Addition of zeros makes the poles migrate towards them as the gain increases, thereby giving a leftward swing to the poles, which make the system stable. However, Fig. 6.20*c* shows that the situation is not improved if the motor time constant is large. If the motor time constant is small, the two poles at the origin experience a leftward swing as the gain increases, thereby making the system stable.

4 $F(s) = (1 + s\tau_1)/(1 + s\tau_2)$ A filter consisting of a pole and a zero is now considered. The resulting pole position depends mainly on the relative position of the open-loop pole and zero. In Fig. 6.20*d*1 the zero is to the left of the added pole, in which case the root locus is not much different from the low-pass filter case as shown in Fig. 6.20*a*. In Fig. 6.20*d*2 the zero is to the right of the filter pole. For a motor with a large time constant, this results in a leftward swing of the two dominant poles, which is a desirable effect. In order to obtain this improvement in a system using a large motor, $\tau_1$ must be greater than $\tau_2$, which gives a differential characteristic over the frequency range $1/\tau_2$ to $1/\tau_1$. This type of characteristic corresponds to what is sometimes called phase-lead compensation. From the improved root locus, it can be predicted that the addition of derivative feedback will be beneficial, for a motor having a large time constant.

5 $F(s) = s$ Derivative control alone results in a zero at the origin. If the pole-zero created at the origin is cancelled, then the result is the same as with an analog speed control. The behavior is stable with respect to speed as can be seen for Fig. 6.20*e*. However, the input is now a speed signal or a frequency proportional to speed. With respect to phase, a closed-loop pole remains at zero, and the system is unstable. The system does not remain phase locked.

6 $F(s) = 1 + s\tau_1$ Phase error plus its derivative produce a zero at $-1/\tau_1$, and the corresponding root locus is shown in Fig. 6.20*f*. With increasing gain, the closed-loop poles are drawn to the left quite effectively.

| $F(s)$ | Root locus plot: Small motor $\tau_{cm}$ small | Root locus plot: Large motor $\tau_{cm}$ large |
|---|---|---|
| (a) $\dfrac{1}{1+s\tau_1}$ | 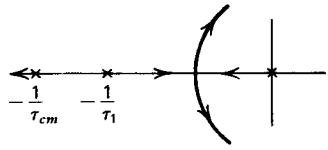  | 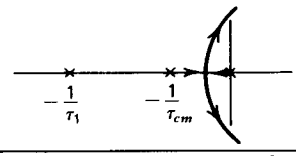  |
| (b) $\dfrac{1}{s}$ | 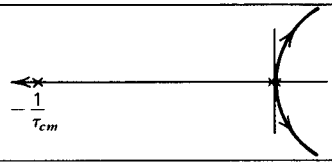  | 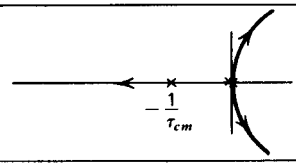  |
| (c) $\dfrac{1+s\tau_1}{s}$ | 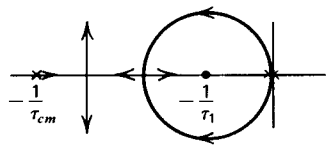  | 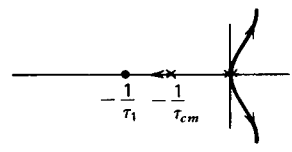  |
| (d1) $\dfrac{1+s\tau_1}{1+s\tau_2}$ $\tau_1 < \tau_2$ | 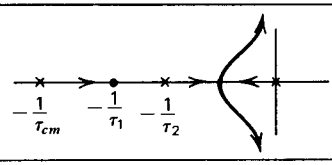  | 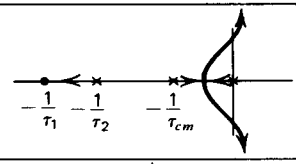  |
| (d2) $\dfrac{1+s\tau_1}{1+s\tau_2}$ $\tau_1 > \tau_2$ | 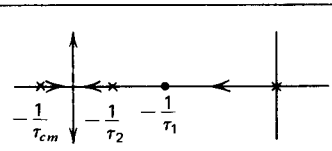  | 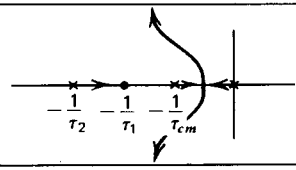  |
| (e) $s$ | 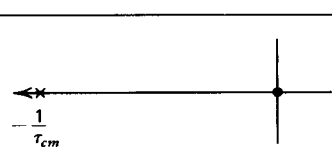  | 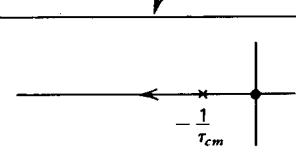  |
| (f) $1+s\tau_1$ | 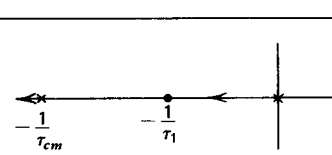  | 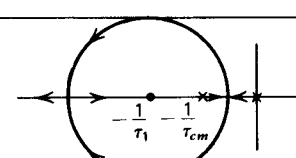  |

***Fig. 6.20*** **Root locus plots for PLL drive system.**

### *Motor Size*

A large motor has a large time constant. The root locus plots of Fig. 6.20 indicate that a small motor having a small time constant can be satisfactorily used in a phase-locked-loop control system if the filter has a pole at the origin and a zero (i.e., *PI* controller) at some other point in the left half plane. However, if the motor is large, a filter having proportional and derivative characteristics is required to make the system stable and to make it stay phase locked.

With derivative feedback a major problem is noise susceptibility. It is therefore necessary to implement derivative feedback in such a way that the

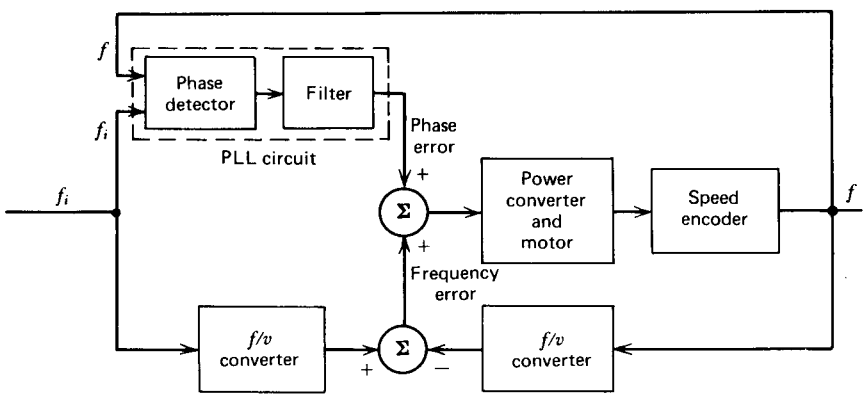


(a)

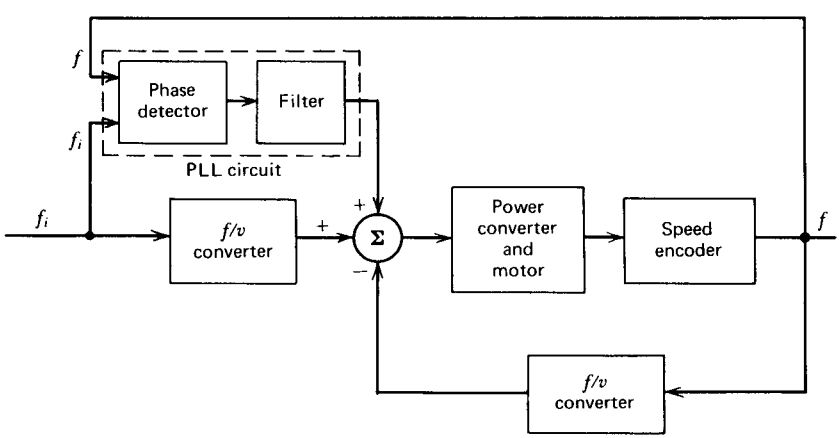


(b)

*Fig. 6.21* PLL drive for stable operation. (*a*) Block diagram. (*b*) Simplified block diagram.

noise susceptibility is reduced. Because the derivative of phase is frequency, the derivative of phase error is frequency error. This frequency error signal can be obtained with less noise problem than attempting to differentiate the phase error signal. The speed encoder output frequency and the reference frequency can each be converted to a voltage by a precision $f/v$ (frequency to voltage) converter. The difference between the two voltages provides the derivative feedback signal.

The circuit implementation of this scheme in block diagram form is shown in Fig. 6.21*a*. The filter output is proportional to phase error, and the difference between the outputs of the $f/v$ converters is proportional to frequency error (the derivative of phase error). In practical implementation of this scheme both the phase error filter and the $f/v$ converters will have filters to provide smoothed-out signal. All three filters will have approximately the same time constant because they are all dealing with the same fundamental frequency ($f$ or $f_i$). For fast response more pulses are required per revolution of the motor shaft, which will allow the use of a small time constant for the filters. Of course, a very large number of pulses per revolution of the motor shaft results in a high loop gain, which may create a stability problem. Pulses in the range of 36 to 120 per revolution have been used in some applications.[7–9] Note that if filters are added to the phase-locked-loop circuit and to the $f/v$ converters the implementation represents the case shown in Fig. 6.20*d*2. However, if the filter time constant $\tau_2$ is very small, the case illustrated in Fig. 6.20*f* is essentially the same as the case illustrated in Fig. 6.20*d*2.

Figure 6.21*a* can be redrawn by merging the summing points into one as shown in Fig. 6.21*b*. This permits the system to be seen from a different perspective. Without the PLL circuit, the system is a conventional analog feedback system. The PLL is added to trim the speed command. This addition compensates for feedback and converter errors to give, theoretically, zero speed regulation. This hybrid control scheme improves the performance achievable by either an analog control system or a simple phase-locked-loop control system.

### 6.3.3 PLL Drives

Dc motors using the phase-locked-loop (PLL) control technique run in exact synchronism with an ac reference frequency. The motors therefore appear to behave as synchronous motors operating from a variable-frequency ac supply. In general, a dc motor with a PLL control system will cost substantially less than a synchronous motor controlled by a thyristor inverter.

Several dc motors each having its own PLL control can be governed by a common master speed command. The motors can run at the same speed or at preset speed ratios. Figure 6.22 shows a system block diagram of a multimotor system in which each motor runs at a preset ratio of the master speed command.[12] The PLL control system is therefore capable of providing precise

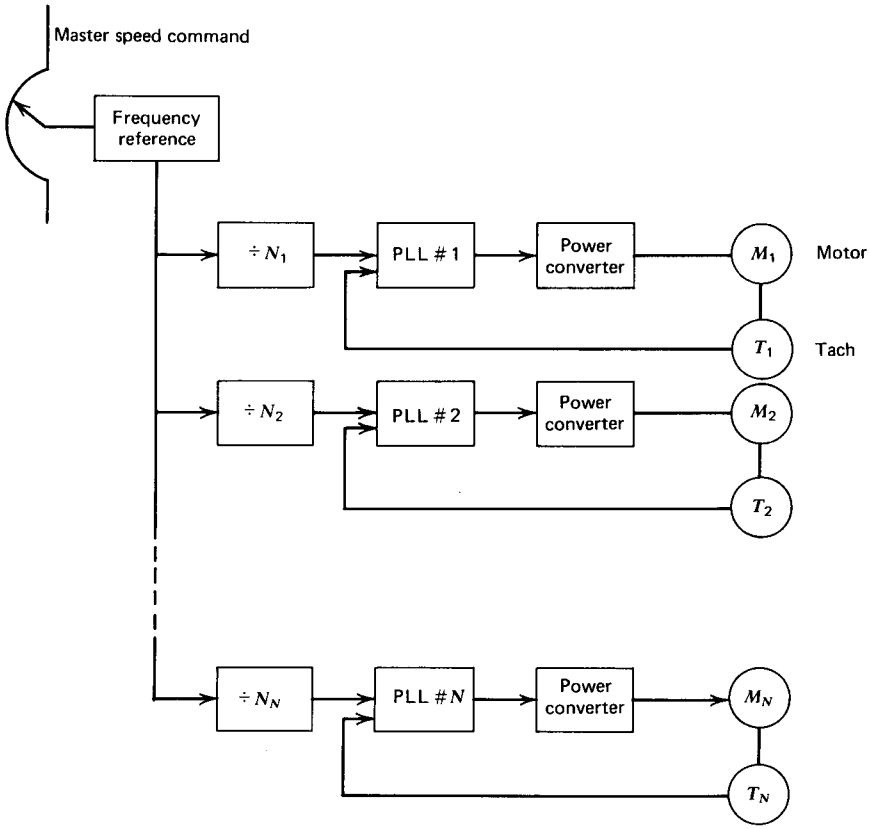


*Fig. 6.22* Multimotor system with PLL control providing preset speed ratios for speed-coordinated sequential operation.

speed ratios between successive stands in a process line such as are found in textile mills, paper mills, printing mills, and similar applications.

## 6.4 MICROCOMPUTER CONTROL

A conventional analog control scheme implemented in dc drives consists of an outer speed-control loop and an inner current-control loop. The concept and the significance of these loops have been discussed earlier in Section 6.1. Figure 6.23 shows a block diagram representation of a reversing dc drive using analog speed regulation. The analog control method has several disadvantages, such as nonlinearity in the analog speed transducer, difficulty in accurately transmitting the analog signal, errors due to temperature, component aging, drift and offset of the analog components, extraneous disturbances, and so on.

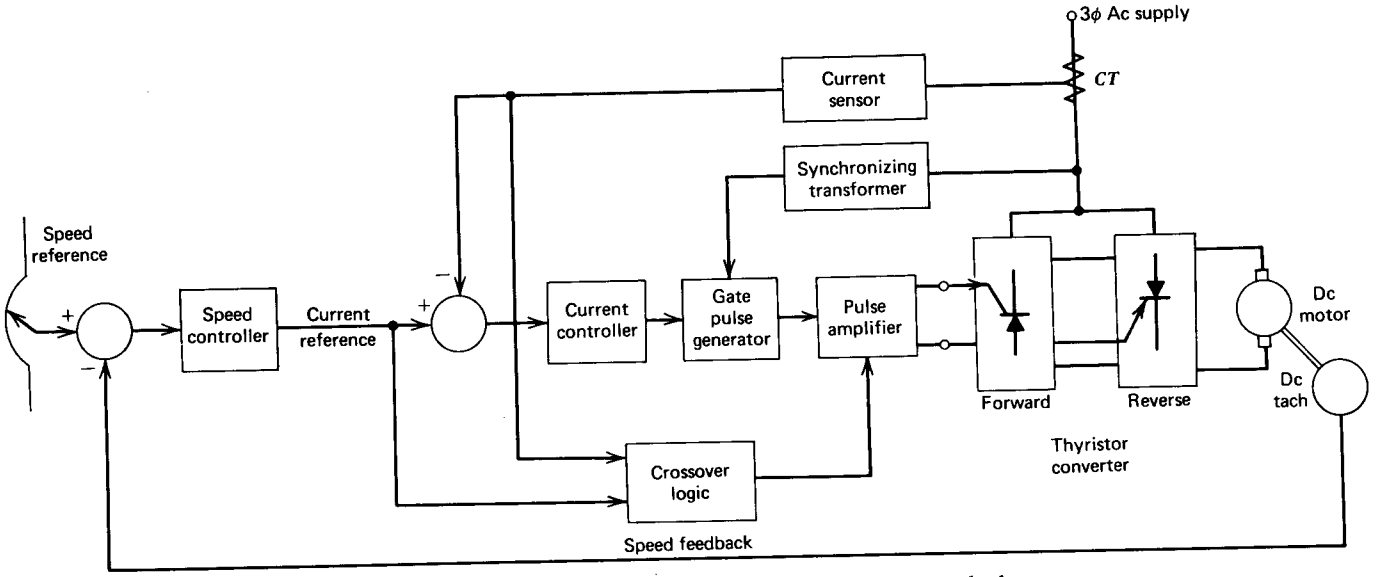


*Fig. 6.23* Block diagram of a reversing dc drive using analog control scheme.

A digital control system, on the other hand, is free from these disadvantages. The control blocks shown in Fig. 6.23 can be implemented by digital circuits. For example, in analog implementation of the speed controller, the speed reference is set by a potentiometer, and the speed controller is a *P* (proportional) or *PI* (proportional-integral) controller using operational amplifiers. In digital implementation, a digital tachometer produces a pulse train whose frequency is proportional to the motor speed. The pulse train is fed into a digital counter so that the speed is available as a digital count. The reference speed may also be represented by a pulse train from an oscillator and converted to a digital count. The two speeds are then compared in a gated comparator. The comparator output is fed to an up/down counter, which is driven up or down by an amount proportional to the speed difference. The proportionality constant determines the gain of the digital speed controller and has an important effect on system response.

The control circuitry is conventionally made of hardwired logic circuits. This is satisfactory if the control requirement is simple. However, if the control system becomes very complex and if flexibility of operation is required, hardwired logic circuits may not meet the performance requirements. For example, a battery-powered electric vehicle may require sophisticated and complex controls such as optimum control of torque, blending of regenerative and friction braking for energy conservation and passenger comfort, programmed battery charging, fault monitoring, diagnostics, and so on. High-performance industrial drives, such as rolling mills and paper mills, require high accuracy, good speed resolution, and fast response. These tasks can be performed better by using a microcomputer-based control system rather than hardwired logic circuitry. In the following sections, the basics of microcomputer control in drive systems are discussed.

### 6.4.1 Basics of Microprocessors and Microcomputers

A microcomputer is a bus-oriented control unit interconnecting several LSI (large-scale integration) chips. Figure 6.24 shows the basic blocks in a microcomputer structure.

#### *Microprocessor ($\mu P$)*[13]

The heart of the microcomputer is the microprocessor, which performs calculations and controls various functions. This central chip is also known as the central processing unit (CPU) or microprocessing unit (MPU). The microprocessor is the most important development the electronics industry has seen in recent years. This chip was introduced to meet the need for a universal large-scale integrated (LSI) circuit. Before the microprocessor, the LSI chip became more dedicated to a particular application.

The microprocessor has the ability to perform a wide variety of functions. It carries out an operation by executing a sequence of instructions (called a

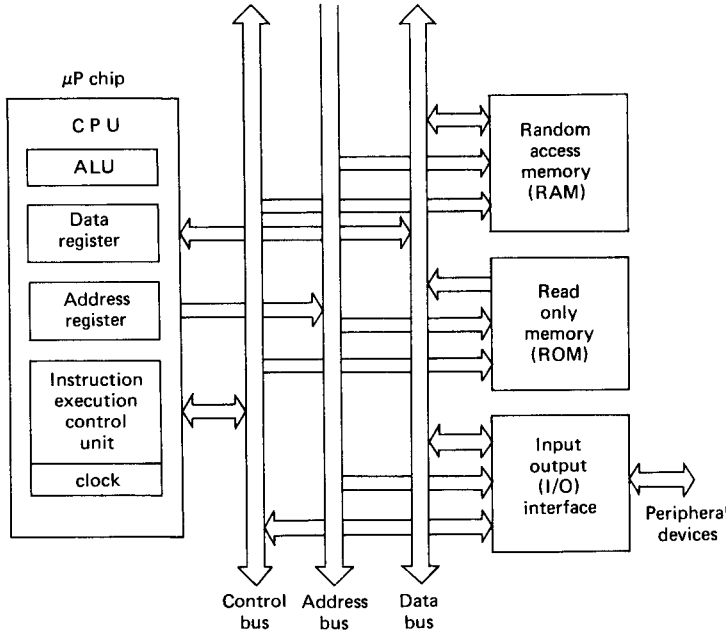


*Fig. 6.24* Microcomputer basic architecture.

software program) that are stored in a memory connected to the microprocessor.

The various components within the microprocessor are shown in the simplified block diagram of a μP chip in Fig. 6.24. The arithmetic logic unit (ALU) is the processing unit where all logical and arithmetic operations such as addition, subtraction, and bit manipulation are performed. The data registers are used for intermediate data manipulation and storage, thereby cutting down the number of transfers to and from the memory. They also receive and transfer data into and out of the CPU. The address registers are used for storing memory addresses and are used in conjunction with the data registers for data transfer to and from the memory of the input/output interface. The control unit controls and supervises the correct execution of instructions. The clock, or CPU timebase generator, is contained in the control unit. The clock frequency determines the basic operating speed of the microprocessor.

### *Memory: ROM and RAM*

The memory is a unit where instructions and data are stored. The memory contains a large number of locations or cells. The size of the memory is equal to the number of locations in the memory.

In the ROM (read only memory) instructions are stored permanently. They can only be read and cannot be destroyed. Most microcomputers are

used for only one purpose. This dedicated use means that only a limited number of programs (i.e., sets of instructions) need to be stored in the memory. Therefore, most microcomputers store their program in a nonvolatile ROM, as the list of instructions never changes. The actual program is "burned in" during manufacturing. Data constants, such as look-up tables, are also stored in ROMs.

In the RAM (random access memory) information can be written (i.e., stored) as well as read. Data or variable information can be stored in the RAM. The CPU, under program control, can read or alter the contents of a RAM location as desired.

A microcomputer system can have both ROMs and RAMs. Constants, look-up tables, and permanent programs can be stored in ROMs, while RAMs may contain problem variables and the portions of the program that may change in future.

### *Input-Output (I/O) Interface*

The input-output interfaces permit communication between the CPU and the outside world. These interface circuits transfer data between the CPU and external devices. Apart from providing this link between the CPU and peripheral units, the interface circuits also convert the external data into a form usable by the microcomputer.

### *Data Bus, Address Bus, and Control Bus*

Microcomputers are bus-oriented control units. Information is communicated among various parts of the system through the data bus, the address bus, and the control bus. In a microcomputer system using 8-bit microprocessors, there are typically 8 lines for the data bus, 16 lines for the address bus, and 6 lines for the control bus.

### *Program or Computer Software*

The microprocessor can carry out various tasks only if it is provided with a set of instructions, called a *program*. The microprocessor, however, understands only binary codes and operates on binary instructions of "ones" and "zeros." Writing a program in binary codes is very tedious and prone to error. A programmer, therefore, uses a convenient language to write the instructions. The most basic of the languages for a microprocessor is called *assembly language* in which symbolic (or mnemonic) codes are used. Every microprocessor has its own assembly language. In this symbolic coding system, an instruction is represented by a group of three or four letters chosen so as to suggest the function of the instruction. For example, for the MC6800 microprocessor ADD is used to signify the operation of additions, and LDAB to imply "Load Accumulator B". The symbolic coding of instructions cannot be understood by the microprocessor, which acts only on binary information. A program, called an *assembler program*, converts the *symbolic program* (also

called the source-program) into a *binary program* (also called the object-program), which the microprocessor can execute.

If the program is changeable and reloadable, it is called *software*. The program that is not changeable by the user and is held in ROM is known as *firmware*. The electronics and circuitry of the microcomputer system are called *hardware*. The greatest advantage of microcomputer control of a drive system is the flexibility. The drive characteristics can be changed or new functions can be added in the future simply by changing the computer software (or firmware) with practically no change or minimal change to the hardware.

### 6.4.2 Microcomputer Control of Reversing Drives

The basic structure of a microcomputer control unit has been described in the previous sections. A detailed presentation of this subject matter is beyond the scope of this book. In recent years, numerous books have been published on this subject.[14–16] In this section the application of microcomputer control in a reversing drive system is discussed briefly.

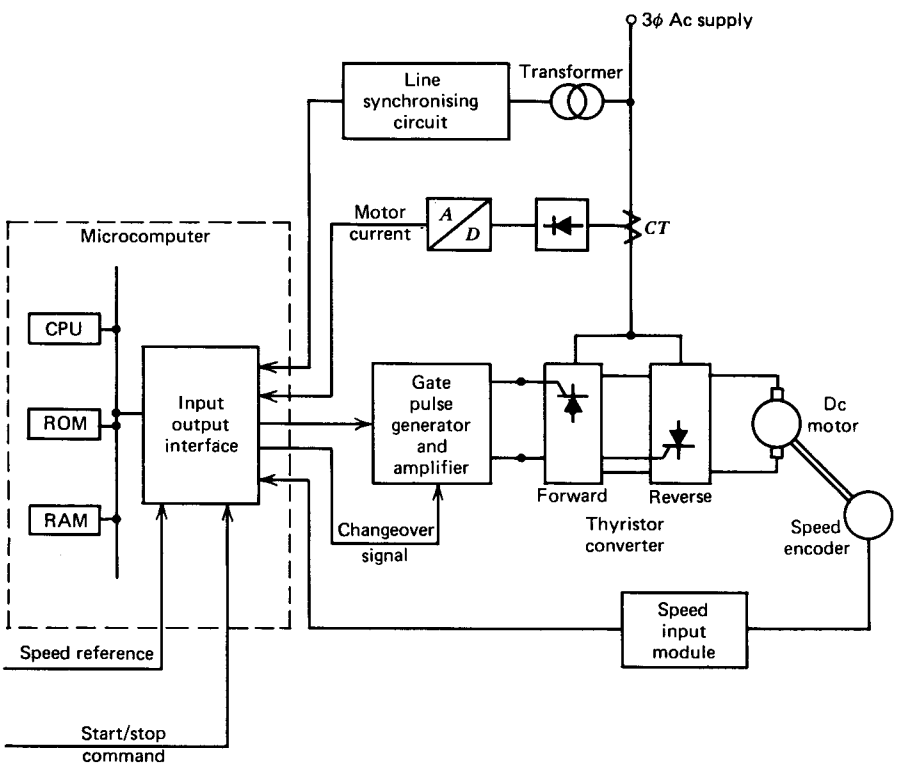


*Fig. 6.25* Block diagram of a reversing dc drive using microcomputer control system.

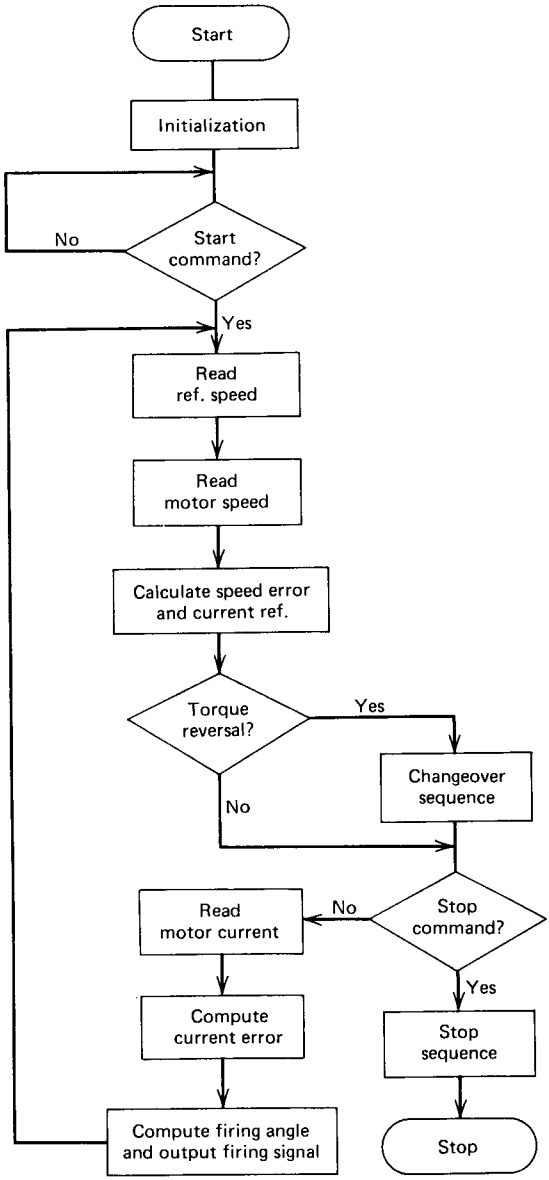


*Fig. 6.26* **Program flowchart for a reversing drive using microcomputer control system.**

High-performance industrial drives, such as the reversing drive used for rolling mills, require high precision, fast response, and other complex control. The analog control scheme shown in Fig. 6.23 has been generally used in such drives with a fair degree of success. However, microcomputer control promises flexibility, improved performance, and economic viability. Figure 6.25 shows a simplified block diagram representation of a reversing dc drive using a microcomputer control system.

The speed information can be fed into the microcomputer using either a dc tachometer and an $A/D$ (analog to digital) converter or by a digital tachometer and a digital counter. The motor current data is usually fed into the computer through a fast $A/D$ converter. A synchronizing circuit interface is required so that the microprocessor can synchronize the generation of the firing pulse data with the supply line frequency. The gate pulse generator is shown as receiving a firing signal from the microcomputer. This generator could be incorporated as part of the microcomputer with gate pulse amplifiers as the only external elements. However, at present most microprocessors are not fast enough to allow the generation of gate pulses timed by software. Instead, data representing a required firing angle is fed to an external logic circuit, which generates the firing pulses in the proper sequence.

A set of instructions (i.e., a program) is stored in the memory, and those instructions are executed by the microprocessor for proper functioning of the drive. A typical program flowchart for this drive system is shown in Fig. 6.26. When the program starts, the first operation is to initialize the internal registers and the interface circuits. The microprocessor is now ready to receive the starting command. After receiving the start signal, it begins executing the program in a continuous cyclic manner. The sequence of instructions allows the computer to process data for speed regulation, current regulation, and changeover reversal operation.

The stability of the system depends partly on the operating speed of the microprocessor, but mainly on how the standard analog controller scheme (i.e., proportional or proportional-integral) is implemented in terms of software. Once the input-output hardware has been designed, a desired response can be obtained by simply changing the constants in the software representation of the system control equations.

### 6.4.3 State of the Art

In 1972 Intel first announced the availability of microprocessors. Since then several semiconductor manufacturers have entered the competitive market. The most generally used microprocessors are 8-bit microprocessors such as Intel 8080, Motorola 6800, Fairchild F-8, Texas Instruments 9980, RCA 1802, Rockwell RPS-8, Signetics 2650, Zilog Z80, and so on.

The clock frequency of these microprocessors, which determines the speed of a microprocessor, varies in the range 0.1 to 10 MHz. The number of cycles required to execute an instruction varies with microprocessors, and the total

time to execute an instruction is not necessarily the same in all microprocessors.

Microprocessors were first applied to data acquisition systems. However, they are rapidly penetrating new application frontiers. In recent years, a great deal of interest has been generated in the application of microprocessors in industrial drives.[17–22] A microprocessor-based control system for motor drives promises several distinct advantages. Foremost among these is the flexibility. The control scheme is implemented in the software. Therefore, to change the control scheme in order to obtain a different drive characteristic or add a new control function, only the software needs to be modified, with minimal or no change in the hardware. Thus controllers can be standardized. Microprocessor control can be completely digitized, with its sensitivity to external influence thereby decreased. A microprocessor-based control system requires fewer discrete components and less wiring, which will improve reliability. Microprocessor-based drives can have built-in fault-finding programs. These diagnostic programs will allow the isolation of malfunctioning circuit boards. Nonlinear functions, which are difficult to implement using hardwired logic circuitry, can be implemented easily in a microprocessor-based control system by storing the nonlinear function as a look-up table in the computer memory. A microprocessor-based drive is expected to give high accuracy, better time response, and better speed regulation. The drive can be conveniently monitored from a supervisory central computer, because data is transmitted digitally at high speed.

As the price of microprocessors and their associated peripherals continues to fall, microprocessor-based control systems will become cost competitive. In the near future, microprocessors will be incorporated in industrial drives that require high levels of performance, or in drives that receive commands from central computers, or both.

## REFERENCES


1 P. C. Sen and M. L. MacDonald, "Thyristorized DC Drives with Regenerative Braking and Speed Reversal," *IEEE Transactions on Industrial Electronics and Control Instrumentations*, Vol IECI-25, No. 4, November 1978. [Figures 6.2 to 6.12 are adapted from this source.]

2 K. Ogata, *Modern Control Engineering*, Prentice-Hall, Englewood Cliffs, NJ, 1970.

3 D. G. Moursund and C. S. Duris, *Elementary Theory and Application of Numerical Analysis*, McGraw-Hill Book Company, New York, 1967.

4 K. Ogata, *State Space Analysis of Control Systems*, Prentice-Hall, Englewood Cliffs, NJ, 1967.

5 N. Minorsky, *Theory of Nonlinear Control Systems*, McGraw-Hill Book Company, New York, 1969.

6 M. Ramamoorty and B. Ilango, "The Transient Response of a Thyristor-Controlled Series Motor," *IEEE Transactions on Power Apparatus and Systems*, Vol. PAS-90, No. 1, January 1971.

7 A. W. Moore, "Phase-locked-loops for Motor Speed Control," *IEEE Spectrum*, Vol. 10, No. 4, April 1973.

8 P. C. Sen and M. L. MacDonald, "Stability Analysis of Induction Motor Drives Using Phase-locked-loop Control System," *IEEE Conference Record*, IAS-78, New York, 1978.

9 R. H. Osman and R. Krukowski, "A High Performance Tow Tank Drive Using Phase-locked-loop Techniques," *IEEE Conference Record*, ISPCC-77, New York, 1977.

10 W. L. Kenly and B. K. Bose, "Triac Speed Control of Three Phase Induction Motor with Phase-locked-loop Regulation," *IEEE Conference Record*, IAS-75, New York, 1975.

11 D. H. Smithgall, "A Phase-locked-loop Motor Control System," *IEEE Transactions on Industrial Electronics and Control Instrumentation*, Vol. IECI-22, No. 4, November 1975.

12 Robicon Corporation, *Accessories: DC Motor Control, Phase-locked-loops*, catalog 7.02, Pittsburgh, 1976.

13 Motorola Semiconductors, *Understanding Microprocessors*, 1976.

14 L. Leventhal, *Introduction to Microporcessors: Software, Hardware, Programming*, Prentice-Hall, Englewood Cliffs, NJ, 1978.

15 John Peatman, *Microcomputer-Based Design*, McGraw-Hill Book Company, New York, 1978.

16 Samuel Lee, *Microcomputer Design and Applications*, Academic Press, New York, 1977.

17 A. Kusko, "Application of Microprocessors to AC and DC Electric Motor Drive Systems," *IEEE Conference Record*, IAS-77, New York, 1977.

18 P. C. Sen, J. Trezise, and M. Sack, "Microprocessor Control of an Induction Motor with Flux Regulation," *IEEE Conference Record*, IAS-78, New York, 1978.

19 T. Konishi, K. Kamiyama, Y. Miyahara, T. Ohmae, and N. Sugimoto, "An Application Technology of Microprocessor to Adjustable Speed Motor Drives," *IEEE Conference Record*, IAS-78, New York, 1978.

20 T. Izumi, M. Yamazoe, and T. Nakano, "A Microprocessor-Based Control System of Thyristor Converter Fed DC Motor Drives," *IEEE Conference Record*, IECI-79, New York, 1979.

21 B. K. Bose and H. A. Sutherland, "A Microcomputer Based Real Time Feedback Controller for an Electric Vehicle Drive System," *IEEE Conference Record*, IAS-79, New York, 1979.

22 S. J. Lukus, "Microprocessor Control of a DC Drive," *IEEE Conference Record*, IAS-79, New York, 1979.

# Appendix A

# Thyristors, Transistors, and Diodes

The circuits described in this book consist of controlled switching devices and diodes. Although thyristors or silicon-controlled rectifiers (SCRs) have been shown as the controlled switching devices, power transistors can be used instead. In this appendix, external electrical characteristics of thyristors (or SCRs), power transistors, and diodes are discussed briefly. No attempt is made to describe the physics of operation and methods of fabrication of these devices, which are well covered in the literature.

## A.1 THYRISTOR (OR SCR)

The term *thyristor* refers to a family of four-layer *p-n-p-n* semiconductor switching devices. These devices operate in two stable states: on or off. The silicon-controlled rectifier (SCR) is the most important member of the thyristor family. This device has been widely used and has revolutionized the art of solid-state power control. The SCR considered throughout this book has been almost universally referred to as the thyristor, although this name is not strictly correct.

### A.1.1 Static Terminal Characteristics

The structure and symbol of the thyristor (SCR) are shown in Fig. A.1. It is a four-layer *p-n-p-n* switching device, having three junctions $J_1$, $J_2$, and $J_3$. It has three external terminals, referred to as anode $A$, cathode $K$, and gate $G$. The anode and cathode are connected to the main power circuit. The gate terminal carries a low-level gate current in the direction gate to cathode.

The terminal anode-cathode characteristic[1,2] of the SCR is shown in Fig. A.2. The three regions of operation are described below.

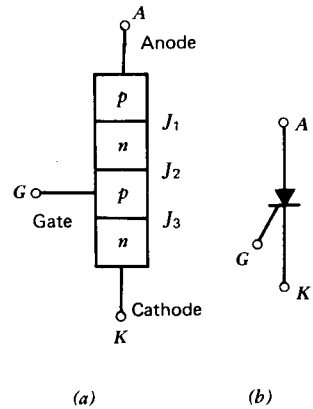


*Fig. A.1* SCR. (*a*) Structure. (*b*) Symbol.

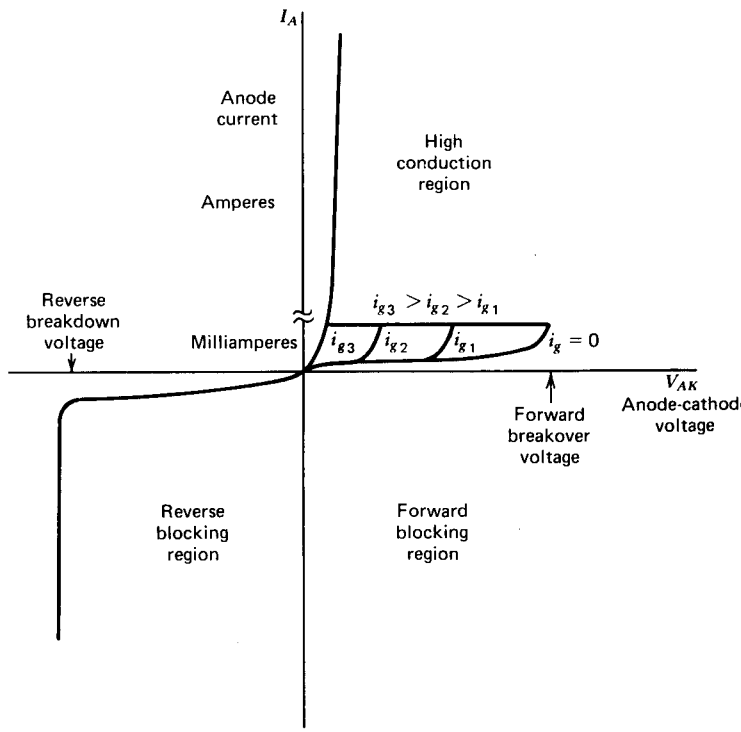


*Fig. A.2* Static anode-cathode characteristics of an SCR.

### *Reverse Blocking Region*

In this region the thyristor exhibits a blocking characteristic similar to that of a diode. If a reverse voltage is applied across the device (i.e., anode negative with respect to cathode), the outer junctions $J_1$ and $J_3$ are reverse biased and the central junction $J_2$ is forward biased. Therefore only a small leakage current (in milliamperes) flows. If the reverse voltage is increased, then at a critical breakdown level an avalanche will occur at $J_1$ and $J_3$, and the current will increase sharply. If this current is not limited to a safe value, power dissipation will increase to a dangerous level that will destroy the device. If the reverse voltage applied across the device is below this critical value, the device will behave as a high-impedance device (i.e., essentially open) in the reverse direction.

### *Forward Blocking Region*

In this region, the anode is made positive with respect to the cathode, and therefore junctions $J_1$ and $J_3$ are forward biased while junction $J_2$ remains reverse biased. Hence the anode current is a small forward leakage current.

### *High Conduction Region*

As the anode to cathode forward voltage is increased, avalanche breakdown occurs at junction $J_2$ at a critical forward breakover voltage, and the SCR switches into a low-impedance condition (high-conduction mode). The anode-cathode voltage drops from, say, several hundred volts to 1 V to 2 V, depending on the rating of the SCR. In the high-conduction mode, the anode current is determined essentially by the external load impedance. Therefore when the thyristor conducts forward current it can be regarded as a closed switch.

If gate currents are applied, the forward breakover voltage is reduced. The voltage at which the device switches to high-conduction modes depends on the amount of gate current. For a sufficiently high gate current, the entire forward blocking region is removed, and the device switches to the high-conduction mode at an essentially zero anode-cathode voltage.

Thyristors used in a practical circuit are selected so that the reverse and forward voltages applied across the device are less than the reverse breakdown voltage and forward breakover voltage, respectively. At a desired instant, when the device is forward biased, the SCR is triggered by a gate pulse to switch it into the high-conduction mode. The current of the gate pulse is normally in excess of the minimum gate current required to turn on the SCR. A typical gate pulse current is in the order of 20 to 200 mA.

Once the SCR is conducting a forward current that is greater than a small minimum value, called the *latching* current, the gate signal is no longer required to maintain the device in its on state. Removal of the gate current does not affect the conduction of the anode current. The SCR will return to

its original forward blocking state if the anode current falls below a low level, called the *holding* current, which for all practical purposes is essentially zero.

### A.1.2 Turn-On Characteristics

The thyristor turns on when it is triggered by a gate pulse. However, the transition from forward voltage blocking to final "full on" is not instantaneous. This is illustrated in Fig. A.3. The total turn-on time $t_{on}$ can be divided into two periods, called the *delay time* $t_d$ and the *rise time* $t_r$. These time periods are defined in Fig. A.3 in terms of anode voltage and current waveforms.

**Delay Time $t_d$** This is the time between the instant at which the gate current reaches 90% of its final value and the instant at which the anode current reaches 10% of its final value.

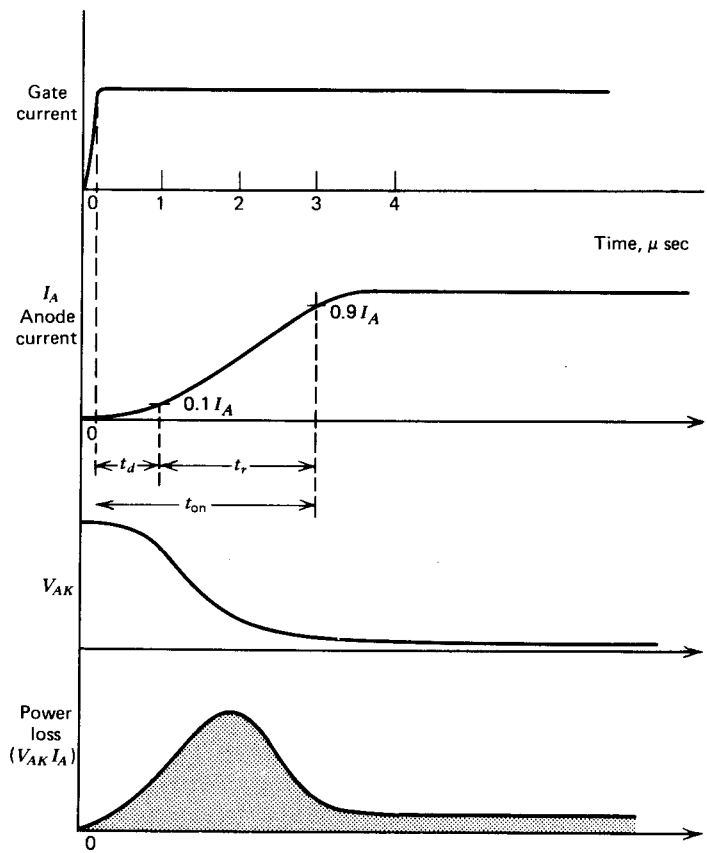


*Fig. A.3* Waveforms during SCR turn-on. Resistive anode load is considered.

**Rise Time $t_r$** This is the time required for the anode current to rise from 10 to 90% of its final value.

**Turn-On Time $t_{on}$** This is the sum of the delay time and the rise time. This can be typically in the order of 1 to 4 $\mu$sec. The width of the firing pulse should therefore be more than 10 $\mu$sec, preferably in the range 20 to 100 $\mu$sec. The amplitude of the gate pulse should be 3 to 5 times the minimum gate current required to trigger the SCR.

Note from Fig. A.3 that during the rise time the SCR carries a large forward current and supports an appreciable forward voltage. This may result in high instantaneous power dissipation creating local internal "hot spots," which could destroy the device. It is therefore necessary to limit the rate of rise of current. This subject will be further discussed below in the section "*di/dt* Protection."

The hatched area under the power curve in Fig. A.3 represents the "switching loss" of the device. This loss may be significant in high-frequency applications.

### A.1.3 Turn-Off Characteristics

Once the SCR starts conducting an appreciable forward current, the gate has no control of it. The SCR will turn off if the anode current becomes zero, called *natural commutation*, or is forced to become zero, called *forced commutation*. However, if a forward voltage is applied immediately after the anode current is reduced to zero, it will not block the forward voltage and will start conducting again although it is not triggered by a gate pulse. It is therefore necessary to keep the device reverse biased for a finite period before a forward anode voltage can be reapplied.

The turn-off time of the thyristor is defined as the minimum time interval between the instant the anode current becomes zero and the instant the device is capable of blocking the forward voltage. The turn-off time is illustrated by the waveforms shown in Fig. A.4. The total turn-off time $t_{off}$ is divided into two time intervals, the reverse recovery time $t_{rr}$ and the gate recovery time $t_{gr}$. At instant $t_1$, the anode forward current becomes zero. During the reverse recovery time, $t_1$ to $t_3$, the anode current flows in the reverse direction. At instant $t_2$, a reverse anode voltage is developed, and the reverse recovery current continues to decrease. At instant $t_3$, junctions $J_1$ and $J_3$ are able to block a reverse voltage. However, the thyristor is not yet able to block a forward voltage because carriers, called *trapped charges*, are still present at junction $J_2$. During the interval $t_3$ to $t_4$ these carriers recombine. At instant $t_4$, the recombination is complete, and therefore a forward voltage can be reapplied at this instant. The SCR turn-off time is the interval between $t_4$ and $t_1$. In an SCR, this time varies in the range 10 to 100 $\mu$sec.

In practical applications, the turn-off time provided to the SCR by the

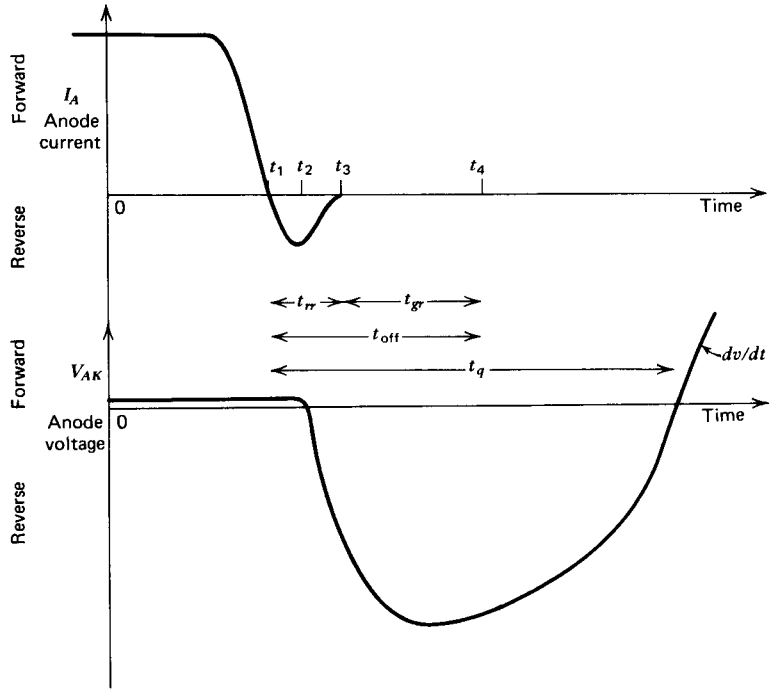


*Fig. A.4* Waveforms during SCR turn-off.

circuit, called the *circuit turn-off time* $t_q$, must be greater than the device turn-off time $t_{off}$ by a suitable safety margin; otherwise the device will turn on at an undesired instant, a process known as *commutation failure*. Thyristors having large turn-off time (50–100 μsec) are called *slow-switching* or *phase-control type* thyristors, and those having low turn-off time (10–50 μsec) are called *fast-switching* or *inverter-type* thyristors. In high-frequency applications, the required circuit turn-off time becomes an appreciable portion of the total cycle time, and therefore inverter-type thyristors must be used.

### A.1.4 Protection

One of the several advantages of SCRs is that they are small in size. However, from the standpoint of protection, small size is a disadvantage. SCRs have low mass and surface area and therefore low thermal time constants. They are very delicate devices, so protection is necessary. Various failure modes and protection techniques are discussed here.

#### *di/dt Protection*

When an SCR is forward biased and it is triggered by a gate pulse, conduction of the anode current starts in the immediate vicinity of the gate

connection. The current thereafter spreads across the whole area of the junction. If the rate of rise of the anode current is large, local "hot spots" will be created near the gate connection due to high current density. This localized heating may burn out the SCR. Therefore, the rate of rise of the anode current ($di/dt$) at switch-on must not exceed a specified limiting value. Normally, a small inductor, called a *di/dt inductor*, is inserted in the anode circuit to limit the $di/dt$ of the anode current. A typical $di/dt$ limit in SCRs is in the range 20 to 500 A/$\mu$sec.

***dv/dt Protection***

When a forward voltage is applied across the thyristor, the two outer junctions $J_1$ and $J_3$ (Fig. A.1*a*) are forward biased, and the central junction $J_2$ is reverse biased. A reverse-biased *p-n* junction has the characteristic of a capacitor. Therefore, when a forward voltage is applied, a charging current flows:

$$i = C_j \frac{dV_{AK}}{dt}$$

where $C_j$ is the junction capacitor.

If the rate of application of the forward voltage is high, the charging current can be so high that the SCR will turn on without a gate pulse. This phenomenon, known as *dv/dt turn-on*, will lead to improper operation in a circuit.

For proper operation in a circuit, the rate of rise of the forward voltage ($dv/dt$) must be less than a specified limit, which is typically in the range 20 to 500 V/$\mu$sec.

To protect against $dv/dt$ turn-on of an SCR, a snubber circuit, which is a *R-C* series circuit in its simplest form, is used across the thyristor.

**Example A.1**

The SCR in Fig. A.5*a* is used to control power in a resistance $R$. The supply is 400 V, and the maximum allowable $di/dt$ and $dv/dt$ for the SCR are 50 A/$\mu$sec and 200 V/$\mu$sec, respectively. Determine the values of the $di/dt$ inductor and the snubber circuit components $R_s$ and $C_s$.

*Solution*

The voltage across the capacitor cannot change instantaneously. Moreover, the SCR in its forward blocking state is equivalent to a high impedance. Therefore, immediately after closing the switch "sw", the equivalent circuit is that shown in Fig. A.5*b*. The voltage equation is

$$V = R_s i + L\frac{di}{dt} + Ri \tag{A.1}$$

$$\frac{di}{dt} = \frac{V - (R_s + R)i}{L} \tag{A.2}$$

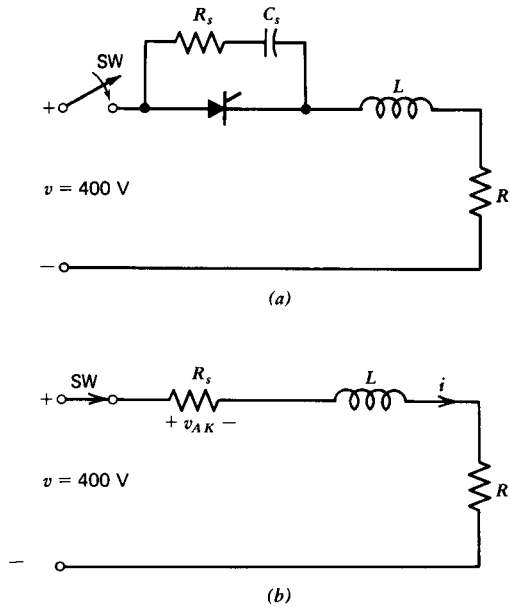


***Fig. A.5*** (*a*) Thyristor circuit with $di/dt$ and $dv/dt$ protection. (*b*) Equivalent circuit at the instant the switch "sw" is closed.

The $di/dt$ is maximum at $i = 0$. Therefore

$$\left(\frac{di}{dt}\right)_{\max} = \frac{V}{L} \tag{A.3}$$

$$L = \frac{V}{(di/dt)_{\max}}$$

$$= \frac{400}{50}\ \mu\text{H}$$

$$= 8\ \mu\text{H}$$

The voltage across the SCR is

$$V_{AK} = R_s i \tag{A.4}$$

Taking the derivative with respect to time,

$$\frac{dV_{AK}}{dt} = R_s \frac{di}{dt} \tag{A.5}$$

Therefore

$$\left(\frac{dV_{AK}}{dt}\right)_{\max} = R_s\left(\frac{di}{dt}\right)_{\max} \tag{A.6}$$

From equations (A.3) and (A.6)

$$\left(\frac{dV_{AK}}{dt}\right)_{\max} = R_s\frac{V}{L} \tag{A.7}$$

Thus

$$R_s = \frac{L}{V}\left(\frac{dV_{AK}}{dt}\right)_{\max}$$

$$= \frac{8 \times 200}{400}\,\Omega$$

$$= 4\ \Omega$$

If $R_s$ is small, the energy lost in it will be high. Figure A.5*a* shows that when the supply is connected to the circuit the capacitor $C_s$ will be charged to the supply voltage before the SCR is triggered. Therefore when the device is turned on, the capacitor $C_s$ will provide a step increase in current through the SCR. If $R_s$ is small, this current spike will be large. The value of $R_s$ is thus normally greater than what is required to limit $dv/dt$. The capacitor $C_s$ is small so that discharge through the SCR when it is turned on does not harm the device. Typical values of $R_s$ and $C_s$ are 10 Ω and 0.1 μF, respectively. If this value of $R_s$ is used, the value of $L$ has to increase to limit $dv/dt$ to the specified value.

From equation (A.7)

$$L = \frac{(VR_s)}{\left(\frac{dv}{dt}\right)_{\max}}$$

$$= \frac{400 \times 10}{200}\ \mu\text{H}$$

$$= 20\ \mu\text{H}$$

This inductor value is not too high, and it is more than is required for $di/dt$ protection.

### *Heat Sink*

When a thyristor is conducting, the anode-to-cathode resistance is very low but not zero. The voltage across the device is in the range 1 to 2 V. A large

anode current flowing through the device may produce sufficient heat to destroy the device. Therefore thyristors are invariably mounted on heat sinks so that heat is conducted from the device to the heat sink, and from there it is radiated and conducted to the atmosphere.

### *Over-Voltage Protection*

A thyristor may be subjected to over-voltage due to bad commutation, short circuit, transients due to switching operation, lightning stroke, and so on. The thyristor is protected against these over-voltages by shunt-connected nonlinear resistance devices. These protective devices have falling resistance characteristics with increasing voltage. If a high voltage surge appears, the nonlinear device produces a virtual short circuit across the thyristor. Selenium thyrector diodes or metal oxide varistors (GE—MOV) are some of the common nonlinear devices used for over-voltage protection.

### *Over-Current Protection*

The thermal capacity of a semiconductor device is small. Therefore continuous overloading, surge currents of long duration, or large surge currents of short duration may increase the junction temperature beyond the permissible limit and destroy the device. Over-current protection is provided by a circuit breaker and a fast-acting fuse in series with the thyristor. The circuit breaker is used to protect the thyristor against continuous overloads or surge currents of long duration. The fast-acting fuse is used to protect the thyristor against large surge currents of very short duration. The tripping time of the circuit breaker, the fusing time of the fast-acting fuse, and the rating of the device have to be properly coordinated. The $I^2t$ rating of the fuse must be less than the corresponding value for the device provided by the manufacturer.

The circuit breaker or the fuse must open the circuit before the thyristor can be damaged by a large current of any nature. The circuit breaker is used for the whole circuit, and fuses may be used for individual devices.

### *Gate Protection*

Gate protection is required for over-voltage and over-current. Because of the low power level of the control circuitry, this protection can be provided by simple means. The gate can be protected against over-voltage by connecting a zener diode across the gate and against over-current by connecting a series resistance.

A common problem encountered in the SCR circuitry is *spurious* (*or noise*) *firing* of the device. Trigger pulses may be induced at the gates due to turn-on or turn-off of a neighboring SCR or transients in the power circuit. These undesirable trigger pulses may turn on the device, thus causing improper operation of the circuit. Gates are protected against such spurious firing by using shielded cables or twisted gate lead connections. Most often a capacitor and a resistor are connected across the gate-to-cathode to bypass the noise pulses.

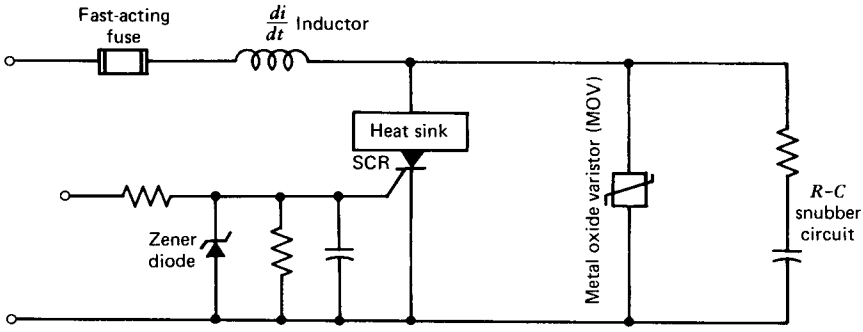


(a)

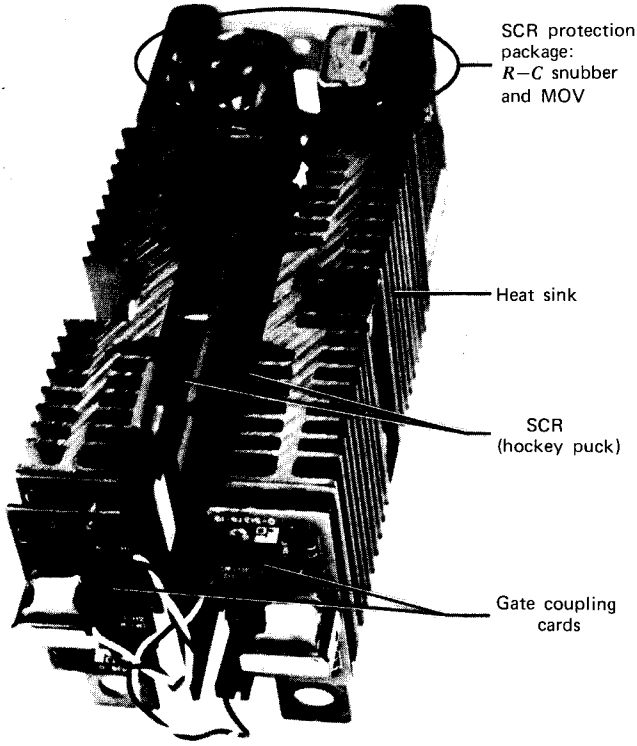


(b)

*Fig. A.6* Thyristor protection. (*a*) Circuit showing components for protection. (*b*) Picture of an SCR module. (Courtesy of Reliance Electric Co.)

*Table A.1* **Thyristor Data Sheet**

| | Phase-Control Type (Slow Switching) | Inverter Type (Fast Switching) |
|---|---|---|
| | G.E. C150 Series | G.E. C158 Series |
| Repetitive peak forward and reverse voltages | 500 V (C150E)<br>800 V (C150N)<br>1000 V (C150P) | 500 (C158E)<br>800 (C158N)<br>1000 (C158P) |
| Reverse and forward leakage current | 10-20 mA | 10-15 mA |
| Holding current | 20 mA | 100 mA |
| RMS current | 100 A | 110 A |
| Forward voltage drop | 1.2–2 V | 1.2–2 V |
| Peak one-cycle surge (60Hz) | 1500 A | 1600 A |
| $I^2t$ for fusing | 7000 amp$^2$-sec | 5200 amp$^2$-sec |
| $dv/dt$ | 200–500 V/$\mu$sec | 200–500 V/$\mu$sec |
| $di/dt$ | 500 A/$\mu$sec | 500 A/$\mu$sec |
| Gate trigger voltage | 1.5–3 V | 3–5 V |
| Gate trigger current | 50–200 mA | 80–300 mA |
| Turn-on time | 3 $\mu$sec | 2 $\mu$sec |
| Turn-off time | 100 $\mu$sec | 20 $\mu$sec |

Figure A.6*a* shows the various components used to protect a thyristor. Figure A.6*b* shows an SCR module with components for protection. Table A.1 summarizes a typical data sheet for two types of thyristors. Manufacturers can provide more detailed information on request.

### *Circuit Protection*

It is not desirable that every time a fault occurs the semiconductor fuse should blow. It is possible to provide protection for the circuit so that the fault condition is removed. One scheme, known as *gate blocking*, is described in Appendix B as shown in Fig. B.7. Whenever over-current is detected, pulses are blocked from appearing at the gates of the thyristor. There are other schemes that can be implemented. For example, as soon as fault current is detected, it can be shunted away by turning on a parallel thyristor until the circuit breaker interrupts the fault current. This scheme is known as *electronic crowbar*.[2]

Another scheme, which may be called *protection by ringing*, can be implemented if two thyristors turn on simultaneously, producing a short circuit on the supply. In a two-quadrant type *A* chopper shown in Table 4.1, circuit protection by ringing can be implemented. A small commutating capacitor is connected at the input to the two-quadrant chopper after an input filter inductor. If the main thyristors of choppers 1 and 2 are on simultaneously due to commutation failure, the capacitor will ring with the

"$di/dt$ inductor" used in the choppers. The negative half-cycle of the ringing current will turn off the thyristors of the choppers. The capacitor and the "$di/dt$ inductor" should be so designed that the peak value of the ringing current is less than the one-cycle surge current of the thyristors. Of course the semiconductor fuse rating, if a fuse is used, should be coordinated so that it does not blow due to this one-cycle ringing current. This kind of ringing circuit may also be used as a commutation circuit[3] for some applications.

## A.2 TRANSISTOR

A transistor is a three-layer *p-n-p* or *n-p-n* semiconductor device. The structure and symbol of an *n-p-n* transistor are shown in Fig. A.7. The three terminals of the device are called collector $C$, base $B$, and emitter $E$. The collector and emitter terminals are connected to the main power circuit, and the base terminal is connected to a control signal.

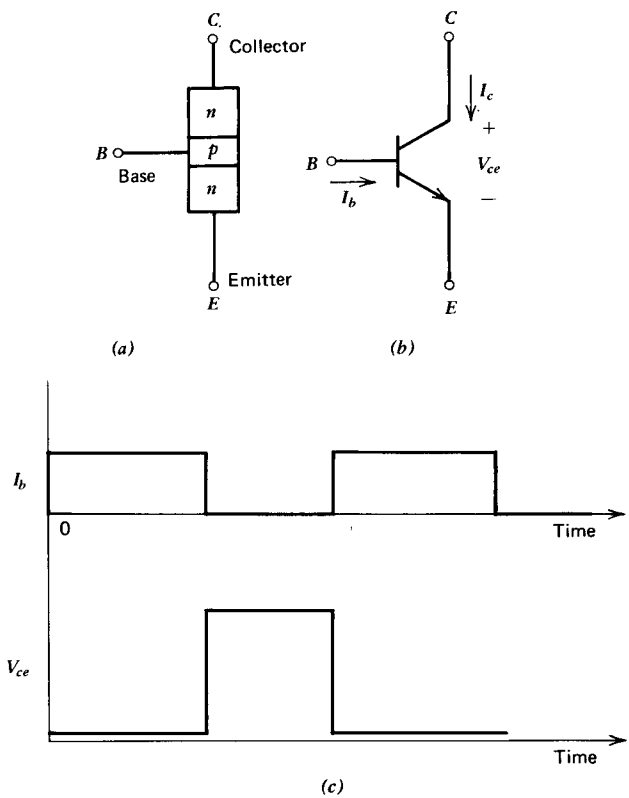


*Fig. A.7* Transistor. (*a*) Structure. (*b*) Symbol. (*c*) Switching operation of a transistor.

Transistors have been used for many years in low-power amplifier circuits. As an amplifier, a signal at the base is made to control the collector current. The signal at the base appears amplified at the collector.

Like thyristors, transistors can also be operated in the switching mode. If the base current $I_b$ is zero, the transistor is in an off state and behaves as an open switch. On the other hand, if the base is driven hard, that is, base current $I_b$ is sufficient to drive the transistor into saturation, then the transistor behaves as a closed switch. This is illustrated in Fig. A.7*c*.

### A.2.1 Power Transistor

In recent years transistors have become available in high voltage and high current rating. These transistors, called *power transistors*, are mostly used in the switching mode. In fact, their applications in motor control circuits are becoming increasingly popular. Power transistors are becoming a viable alternative to thyristors. When power transistors conduct an appreciable current, the forward voltage drop (collector-emitter saturation voltage) is in the order of 0.3 to 0.8 V as compared to 1.2 to 2 V for thyristors. Therefore the power loss in a power transistor is lower than that in a thyristor of similar power rating. Power transistors switch on faster than SCRs, and turn-off problems are practically nonexistent. Commutation circuitry, which is costly and bulky, is not required. If the base current is removed, the transistor turns off. Therefore, power transistors can be used in very high frequency applications (100 KHz).

However, the voltage and current ratings of power transistors available at present are not as high as those of thyristors. The maximum rating of a single power transistor device that can be reliably used is 300 V and 100 A, or 300 A and 100 V. Power transistors have no surge current capacity and can withstand only a low rate of change of current.

To keep a power transistor in the conducting state, a continuous base current is required. In a high-current device, the base-to-collector current gain is as low as 10, and therefore a base current of several amperes is required to keep the device in the "on" condition. The power loss in the base circuit may be appreciable.

If the base current is reduced to zero, the power transistor will turn off. However, the turn-off will be slow. For faster turn-on, excess base current is applied. For faster turn-off, the excess charge in the base region must be removed quickly. This can be achieved by reverse biasing the base during turn-off.

### A.2.2 Power Darlington

A Darlington-connected transistor pair is shown in Fig. A.8. The pair can be fabricated in one chip, or two discrete transistors can be physically connected as a Darlington-transistor.[4] The major advantage of the Darlington device is

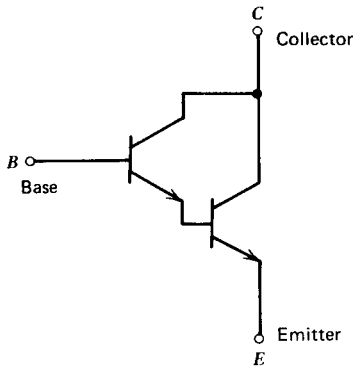


*Fig. A.8* Darlington transistor.

its high current gain. High-power Darlington amplifiers are now becoming available. Recently, large devices with rating as high as 500 V and 200 A have been developed. Current gains in hundreds have been obtained at these high current levels. At these high current gains, the forward on-state voltage drop is high causing high power loss.

Circuits using power transistors or Darlington transistors will be smaller in size and less costly compared to circuits using thyristors. However, there has been little operating experience in high-power applications of transistors. Power transistors or Darlington pairs are more susceptible to failure. Thyristor circuits, on the other hand, have a proven record of many years of reliable operation.

## A.3 DIODE

A diode is a two-layer *p-n* semiconductor device. The structure and symbol of a diode are shown in Fig. A.9. High-power diodes are silicon rectifiers that can operate at high junction temperatures. The voltage-current characteristic

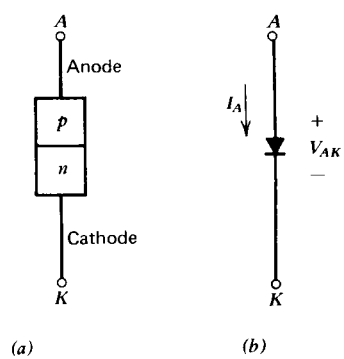


*Fig. A.9* Diode. (*a*) Structure. (*b*) Symbol. (*c*) *V-I* characteristics.

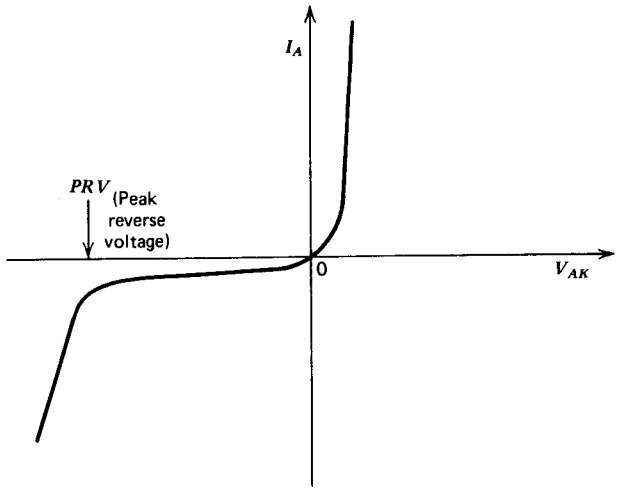


(c)

*Fig. A.9* (*Continued*)

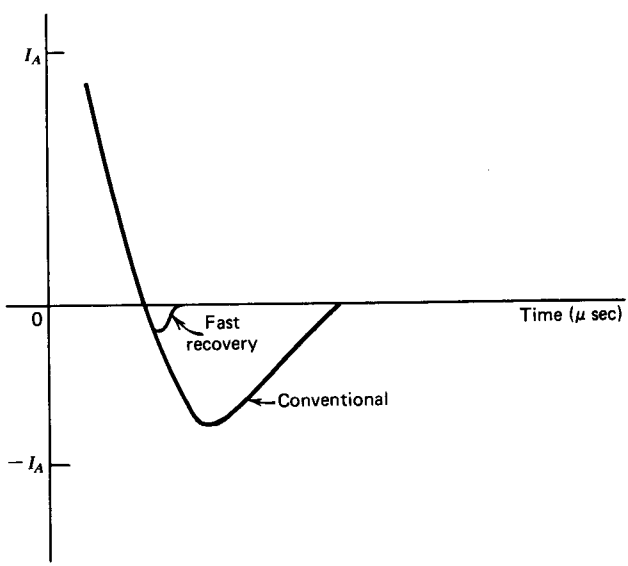


*Fig. A.10* Reverse recovery characteristics of conventional and fast-recovery silicon diodes.

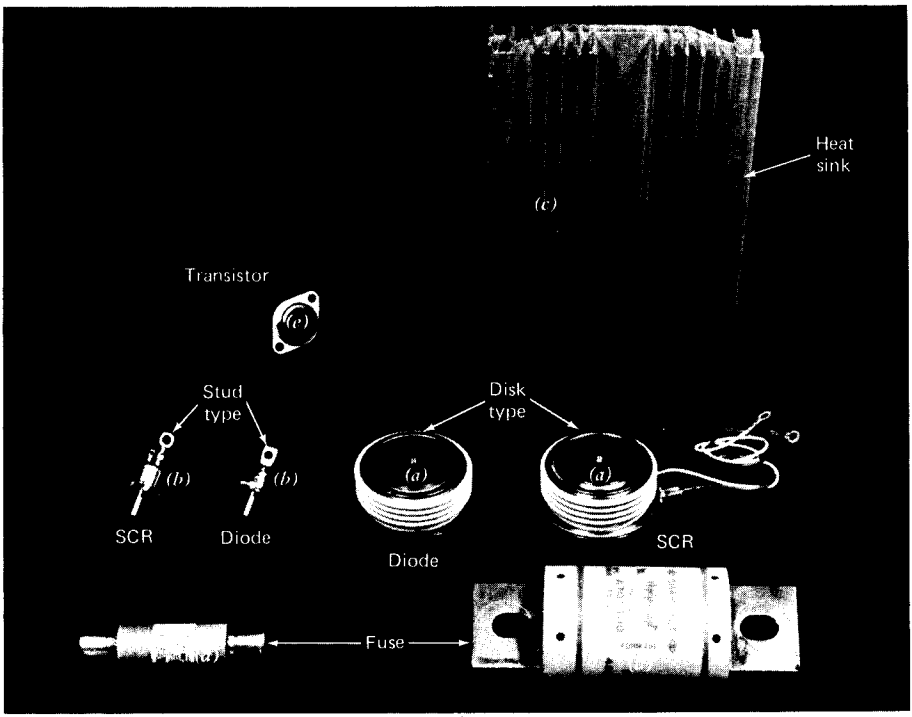


*Fig. A.11* Thyristors, transistors, and diodes, illustrating: (*a*) disk type (hockey puck) devices; (*b*) stud-mounted devices; (*c*) heat-sink; (*d*) semiconductor fuses; and (*e*) transistor.

of a diode is also shown in Fig. A.9. If a reverse voltage is applied across the device, it behaves essentially as an open circuit. If a forward voltage is applied, it starts conducting and behaves essentially as a closed switch. The forward voltage drop when it conducts current is in the range of 0.8 to 1 V. Diodes with ratings as high as 4000 V and 2000 A are available.

Following the end of forward conduction in a diode, a reverse current flows for a short time. The device does not attain its full blocking capability until the reverse current ceases. The time interval during which reverse current flows is called the *rectifier recovery time*. During this time charge carriers stored in the diode at the end of forward conduction are removed. The recovery time is in the range of a few microseconds (1–5 $\mu$sec) in a conventional diode to several hundred nanoseconds in fast-recovery diodes. This recovery time is of great significance in high-frequency applications. The recovery characteristics[5] of conventional and fast-recovery diodes are shown in Fig. A.10.

Figure A.11 shows pictures of thyristors, transistors, and diodes. Two configurations of thyristors and diodes are in common use today: stud-mounted and "hockey-puck" (or "press-pak" or "disk").

## REFERENCES


1 B. R. Pelly, *Thyristor Phase-Controller Converters and Cycloconverters*, Wiley-Interscience, New York, 1971.

2 General Electric Co., *General Electric SCR Manual*, Fifth Edition, Electronics Park, Syracuse, NY, 1977.

3 V. R. Stefanovic and P. Bhagwat, "A Novel Dc Side Commutated Inverter," *IEEE Conference Record*, PESC-80, New York, 1980.

4 S. Krishna and A. J. Yerman, "The Development of a Power Darlington Transistor and Hybrid Integrated Circuit for a DC-to-DC Converter," *IEEE Conference Record*, PESC-79, New York, 1979.

5 S. A. Nasar and L. E. Unnewehr, *Electromechanics and Electric Machines*, John Wiley & Sons Inc., New York, 1979.

# Appendix B

# Firing and Logic Circuits

In this book various phase-controlled converters and chopper converters have been described. It has been assumed that thyristors (SCRs) in these converters are fired at the desired instant for proper operation. The firing instant is controlled by a control signal so that the converter can provide a desired output performance.

There are numerous variations of the firing circuits and the control logic circuits that can be used to control the firing of the thyristors. No two designers will come up with the same circuit, although both circuits will perform the same function. An exhaustive treatment of this subject will not be given here. A few simple and basic schemes are discussed with the hope that a reader who is not an expert in this area may acquire some knowledge and the ability to build these control circuits. The firing and control logic circuits described here are definitely not the best possible ones. Component values are shown in these circuits as an illustration and to indicate the order of magnitude of the components.

## B.1 Phase Control

In phase-controlled converters, discussed in Chapters 2 and 3, thyristors are fired at a firing angle $\alpha$ with respect to a reference point. In single-phase converters, the reference point is the zero crossing of the supply voltage. The firing angle is changed to vary the output dc voltage, which can control the speed of a dc motor. There are two basic approaches to achieve this: linear control of angle,[1] and cosine control of phase angle.[1,2]

### B.1.1 Linear Control of Phase Angle $\alpha$

In this scheme, illustrated in Fig. B.1, a control voltage $E_c$ changes linearly the phase angle $\alpha$. A synchronizing center-tapped transformer steps down the supply voltage to low voltages $v_1$ and $v_2$. The voltage $v_1$ is converted to a square voltage $e_1$ and then to a ramp voltage $e_2$, which is then compared with a control voltage $E_c$. If $e_2$ is higher than $E_c$, a signal $e_\alpha$ is obtained at the

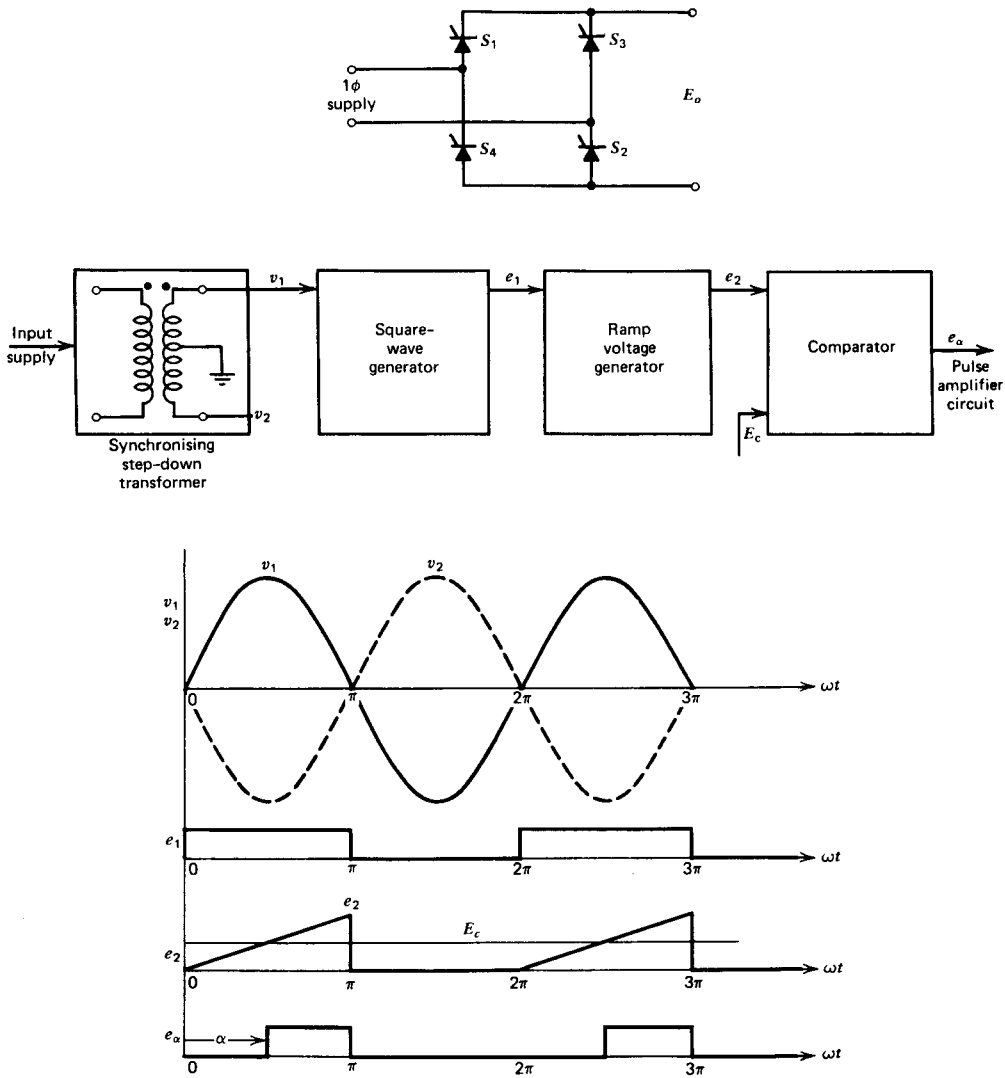


*Fig. B.1* Linear control of phase angle.

output of the comparator. The time at which the rising edge of $e_\alpha$ occurs is proportional to $E_c$ and defines the firing angle $\alpha$. This signal $e_\alpha$ is next fed to a pulse amplifier circuit and is used to fire SCRs $S_1$ and $S_2$ in the positive half-cycle of the input supply. A similar circuit with input $v_2$ provides firing pulses for SCRs $S_3$ and $S_4$ to be fired in the negative half-cycle of the input supply. The firing angle is given by

$$\alpha = k_1 E_c \tag{B.1}$$

From equation 2.23

$$E_o = E_{max}\cos\alpha$$

$$= E_{max}\cos(k_1 E_c) \qquad \text{(B.2)}$$

The transfer characteristic between the converter output voltage $E_o$ and control voltage $E_c$ is therefore nonlinear. However, accuracies of the order of $\pm 1°$ in the firing angle are normally possible.

### B.1.2 Cosine Control of Phase Angle $\alpha$

In this scheme a control voltage $E_c$ generates firing pulses at the crossing point of the control voltage and a cosine voltage derived from the supply voltage. The basic scheme is illustrated in Fig. B.2. The phase angle $\alpha$ is given

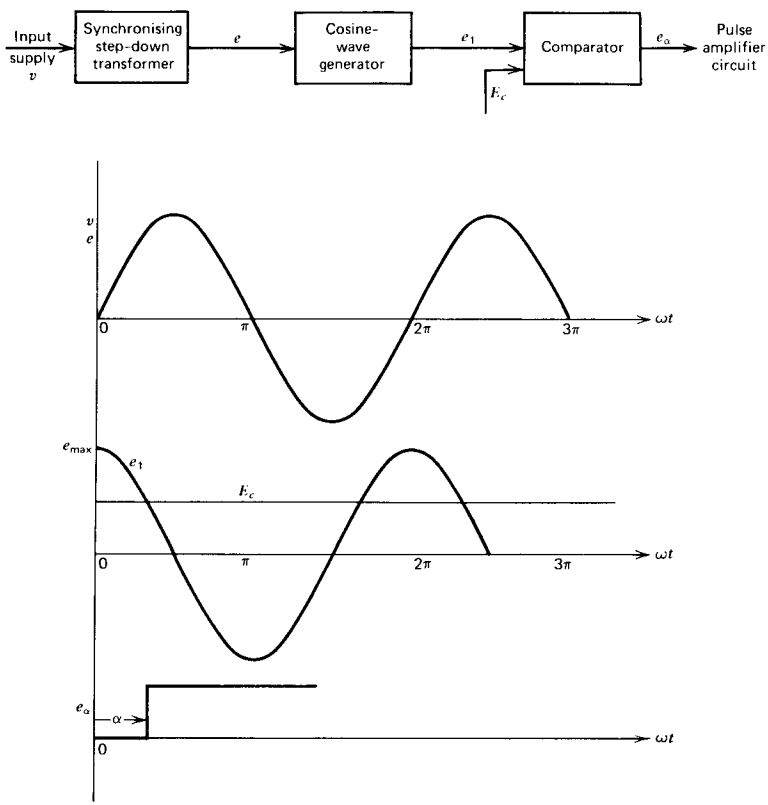


*Fig. B.2* Cosine control of phase angle.

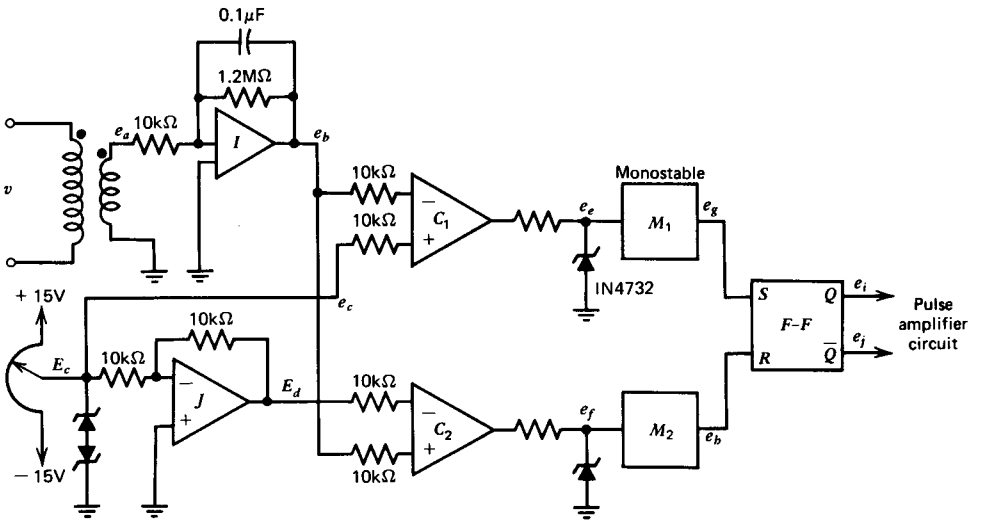


(a)

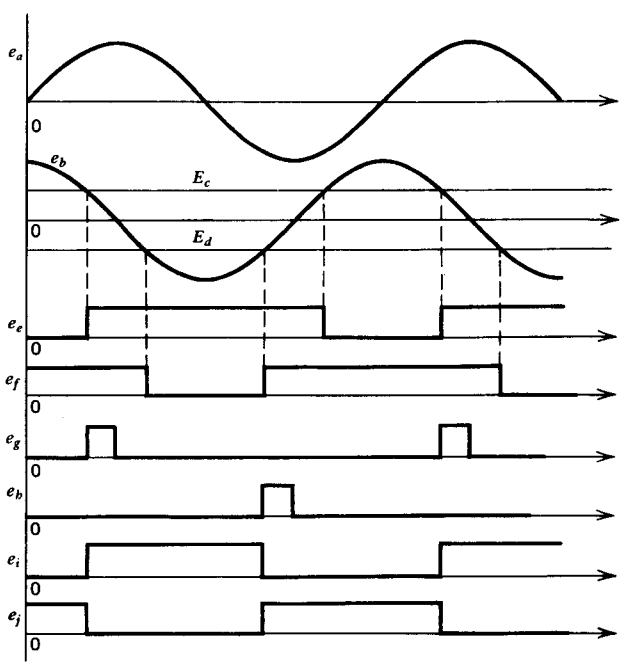


(b)

***Fig. B.3*** Circuit implementation of a cosine firing scheme in phase-controlled converters. (*a*) Circuit. (*b*) Timing diagram.

by

$$\alpha = \cos^{-1}\left[\frac{E_c}{e_{\max}}\right] \tag{B.3}$$

The output voltage of the converter is given by

$$\begin{aligned} E_o &= E_{\max}\cos\alpha \\ &= E_{\max}\cos\left[\cos^{-1}\frac{E_c}{e_{\max}}\right] \\ &= \frac{E_{\max}}{e_{\max}}E_c \\ &= k_2 E_c \end{aligned} \tag{B.4}$$

Therefore the cosine firing scheme provides a linear transfer characteristic between the output voltage $E_o$ and the control voltage $E_c$. This scheme is suitable for application in a closed-loop control drive. In fact, the cosine firing scheme is popular and widely used in industry. A circuit implementation of this scheme is shown in Fig. B.3*a*. A timing diagram is shown in Fig. B.3*b* to facilitate an understanding of the signal processing at various stages.

Signal $e_a$ represents a stepped-down voltage of the input supply voltage $v$ of the converter. The integrator $I$ converts it to a cosine signal $e_b$. The two zener diodes connected back-to-back clamp the control voltage $E_c$ below the peak value of the cosine signal $e_b$. The control voltage $E_c$ is inverted by unity gain operational amplifier $J$ to signal $E_d$. The control voltage $E_c$ and its inverse $E_d$ are compared with the cosine signal $e_b$ in comparators $C_1$ and $C_2$ to produce signals $e_e$ and $e_f$. These are fed to monostables $M_1$ and $M_2$ to produce signals $e_g$ and $e_h$, respectively. These signals $e_g$ and $e_h$ trigger a set-reset flip-flop $F$-$F$ to generate signals $e_j$ and $e_i$. The signal $e_i$ is used to fire SCRs in the positive half-cycle, and $e_j$ is used to fire SCRs in the negative half-cycle.

### B.1.3 Pulse Amplifier

The pulses $e_i$ or $e_j$ in Fig. B.3 may not be strong enough to turn on an SCR. Besides, the gate and cathode terminals of the SCR are at higher potentials of the power circuit, and the control circuit should not be directly connected to the power circuit. An optical isolation or pulse-transformer isolation is commonly used in practice to provide physical isolation between the control circuit and the power circuit. Figure B.4 shows a pulse amplifier circuit using a pulse transformer isolation. A Darlington transistor is used to amplify the

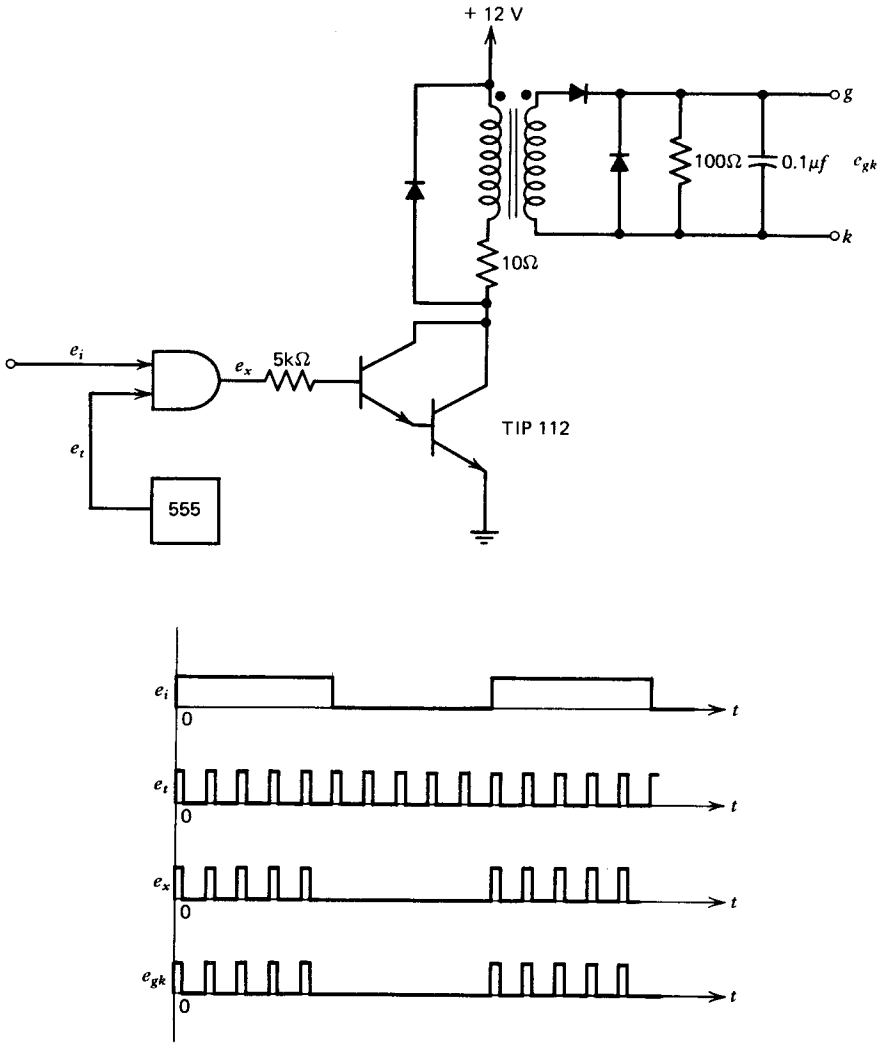


*Fig. B.4* A typical pulse amplifier circuit.

pulse-current. If the pulses are long ($e_i$ or $e_j$ has a width of 180°), they may saturate the pulse-transformer and the whole width of the pulse may not be transmitted. The whole pulse-width may not be necessary. In such a case, the pulse is modulated at a high frequency (10–30 kHz) as shown in Fig. B.4, using a 555 timer. The duty cycle of the timer should be less than 50% so that the flux in the transformer can reset. A modulated pulse also reduces gate dissipation in the SCR. Processing of the pulse signal $e_i$ (obtained from the firing circuit) at various stages is illustrated by the timing diagram in Fig. B.4.

## B.2 CHOPPER CONTROL

Chopper converters in general require firing pulses to turn on a main SCR and a commutating SCR. The time interval between the firing of the two SCRs determines the duty cycle and hence the output voltage. A control voltage is used to control the duty cycle of the chopper.

Figure B.5 shows a chopper firing circuit that consists mainly of four parts: a triangular wave generator, a voltage comparator, edge detection, and pulse amplifiers. The waveforms at various parts of the circuit are also shown in Fig. B.5.

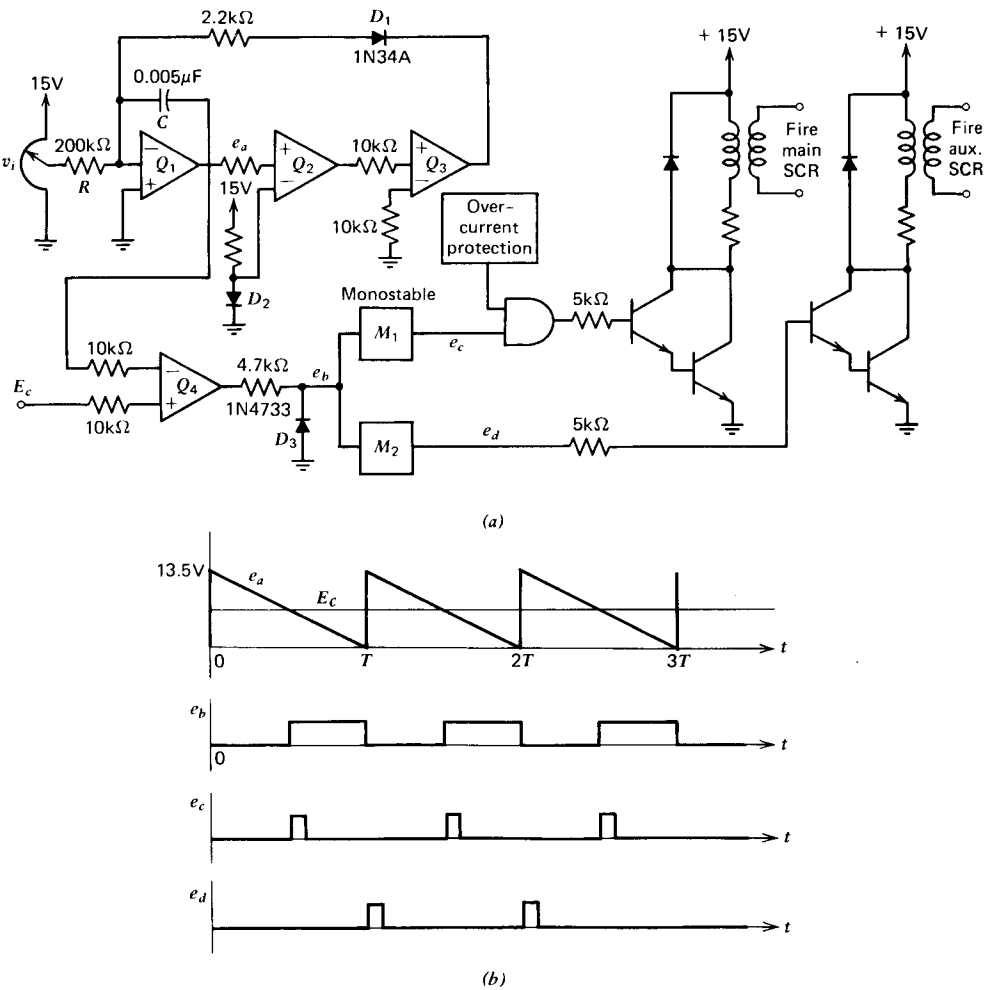


*Fig. B.5* A typical chopper firing circuit. (*a*) Circuit. (*b*) Timing diagram. Op-amp supply ± 15 V.

The three operational amplifiers $Q_1$, $Q_2$, and $Q_3$ together form a triangular wave generator that generates the triangular wave $e_a$ shown in Fig. B.5*b*. As the voltage $e_a$ decreases below 0.6 V (which is the forward bias voltage of the diode $D_2$), the output of $Q_2$ changes from 13.5 V to $-13.5$ V, and it in turn triggers $Q_3$ to change state. The output of $Q_3$, which is now negative ($-13.5$ V), makes $D_1$ forward biased, and the 2.2 k path takes control of the integrator input summing junction. The output of $Q_1$ quickly rises to 13.5 V, which in turn triggers $Q_2$ and $Q_3$ and changes their outputs to positive voltages. Now the diode $D_1$ is reverse biased, the feedback loop through $D_1$ is reverse biased, and the feedback loop through $D_1$ is open. With the diode $D_1$ reverse biased, control of the integrator $Q_1$ reverts to the 200 k path, and the output voltage $e_a$ has a constant slope that depends on the values of the capacitor $C$, the input resistor $R$, and the input voltage $v_i$. In fact, this oscillator can be used as a voltage-controlled oscillator (VCO). The purpose of using $Q_2$ is to introduce a time delay so that there is enough time to charge up the capacitor so that $e_a$ rises to 13.5 V. The diode $D_2$ is used for the offset adjustment so that $e_a$ is always above zero voltage.

The operational amplifier $Q_4$ is used as a voltage comparator. If the control voltage $E_c$ exceeds the voltage $e_a$ the output of $Q_4$ changes as shown by waveform $e_b$ in Fig. B.5*b*.

The two monostable multivibrators are connected in such a way that one of them is triggered by the rising edge and the other by the falling edge of the signal $e_b$. On receiving the rising or falling edge, the monostable multivibrators produce output signals $e_c$ and $e_d$ whose width can be adjusted. A pulse-width in the range of 20 to 200 $\mu$sec is sufficient for firing SCRs. The pulse $e_c$ is used to fire the main SCR, and the pulse $e_d$ is used to fire the commutating SCR of the chopper. For proper operation of the current commutated chopper shown in Fig. 4.6*a* the pulse width of $e_d$ for the auxilliary SCR should be less than $t_4 - t_1$ (Fig. 4.6*b*). A pulse width of $\pi\sqrt{LC} = t_2 - t_1$ is satisfactory.

The firing pulses $e_c$ and $e_d$ are fed to the pulse amplifier circuits consisting of a Darlington transistor and a pulse transformer. The pulse $e_c$ for the main SCR can be "ANDED" with a signal from an over-current protection logic circuit so that when an over-current condition occurs, the pulse $e_c$ is blocked.

## B.3 OPEN-LOOP AND CLOSED-LOOP CONTROL

The control voltage $E_c$ in Figs. B.1, B.2, B.3, and B.5 changes the output voltage of the converter. In an open-loop control as shown in Fig. B.6*a*, the control voltage $E_c$ is varied by using a potentiometer. In a closed-loop control, the control voltage is obtained from the difference between a reference and the quantity to be controlled. For example, if the dc motor armature current is to be controlled in a closed-loop feedback control system, as shown

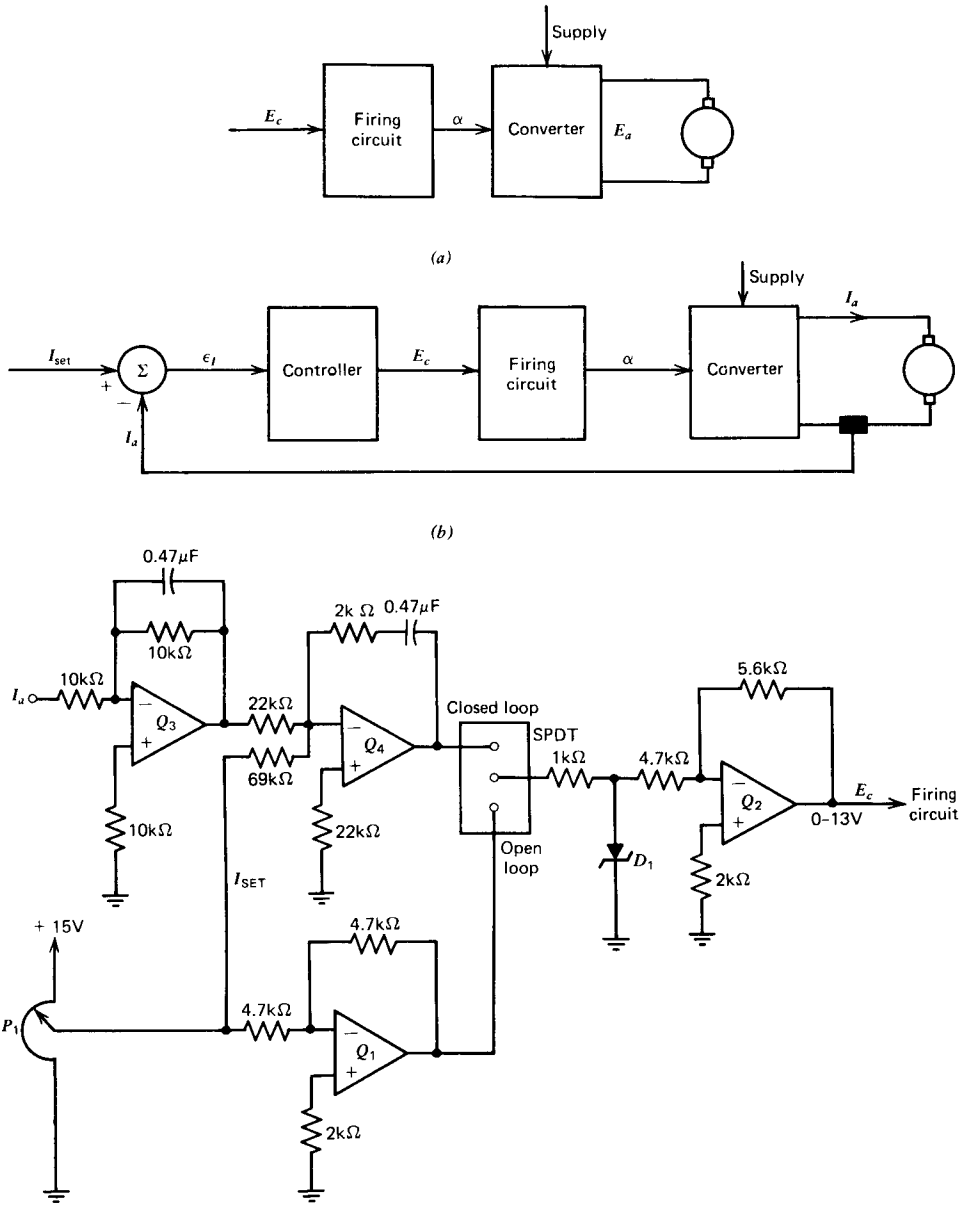


***Fig. B.6*** Open- and closed-loop control. (*a*) Block diagram for open-loop control. (*b*) Block diagram for closed-loop control. (*c*) Logic control circuit.

in Fig. B.6*b*, the control voltage $E_c$ is derived from the difference between the set current and the actual motor current.

Figure B.6*c* shows a logic control circuit in which both open-loop and closed-loop control can be obtained. The single pole double throw (SPDT) switch selects the open-loop voltage control or closed-loop current feedback control. In the open-loop control system, the voltage $E_c$ is obtained from the potentiometer $P_1$ through operational amplifiers $Q_1$ and $Q_2$. In the closed-loop control system, the voltage from the potentiometer $P_1$ represents the current set ($I_{set}$ of Fig. B.6*b*). The signal $I_a$ in Fig. B.6*c* represents a voltage proportional to the motor armature current.

A low-pass filter $Q_3$ smoothes out ripples in the motor current signal $I_a$. A proportional integral controller $Q_4$ provides the gain and desired response. The zener diode $D_1$ is used to limit the output of $Q_2$ to a predetermined maximum voltage. For example, if closed-loop control is required in conjunction with the chopper firing circuit shown in Fig. B.5, the maximum value of $E_c$ should be limited to 13 V if the peak of the triangular wave in Fig. B.5*b* is 13.5 V. Component values as shown in Fig. B.6 are good for a particular drive system and not necessarily for all closed-loop drives. Selection of gains and time constants has significant effects on the behavior of a drive and is a challenge to the circuit designer.

## B.4 OVER-CURRENT PROTECTION

A converter can be protected against high current by tripping the input circuit breaker. If the breaker trips frequently, the contacts in the breaker will deteriorate due to sparking. In addition, the breaker is not fast enough to protect semiconductor devices. Fast-acting semiconductor fuses are used to protect the devices. However, frequent blowing of the fuses is not economical. A simple over-current protection for the converter is achieved by blocking appropriate pulses whenever the current exceeds a preset limit. Figure B.7*a* shows a circuit implementation of a control logic for over-current protection. It consists mainly of three parts: a voltage comparator $Q_1$, a flip-flop *F-F* with preset and clear, and an AND gate *A*. The timing diagram to illustrate the operation of the circuit is shown in Fig. B.7*b*.

In Fig. B.7, if the *Q* output of the flip-flop is high, the firing pulses *X* are transmitted through the AND gate as the *Y* output. When an over-current condition occurs, the *Q* output swings low and the AND gate is disabled so that the firing pulses *X* are blocked. $I_{ref}$ represents the current limit, and $I_o$ represents the converter or motor current. If $I_o$ exceeds $I_{ref}$, output of the comparator $Q_1$ changes (from 13.5 V to $-13.5$ V), and the "clear" input and *Q* output of the flip-flop are driven low. This disables the AND gate and blocks the firing pulses *X*. The AND gate remains disabled until the flip-flop is preset by pressing the preset button. The zener diode is used to limit the input voltage to the flip-flop to 0 to 5V.

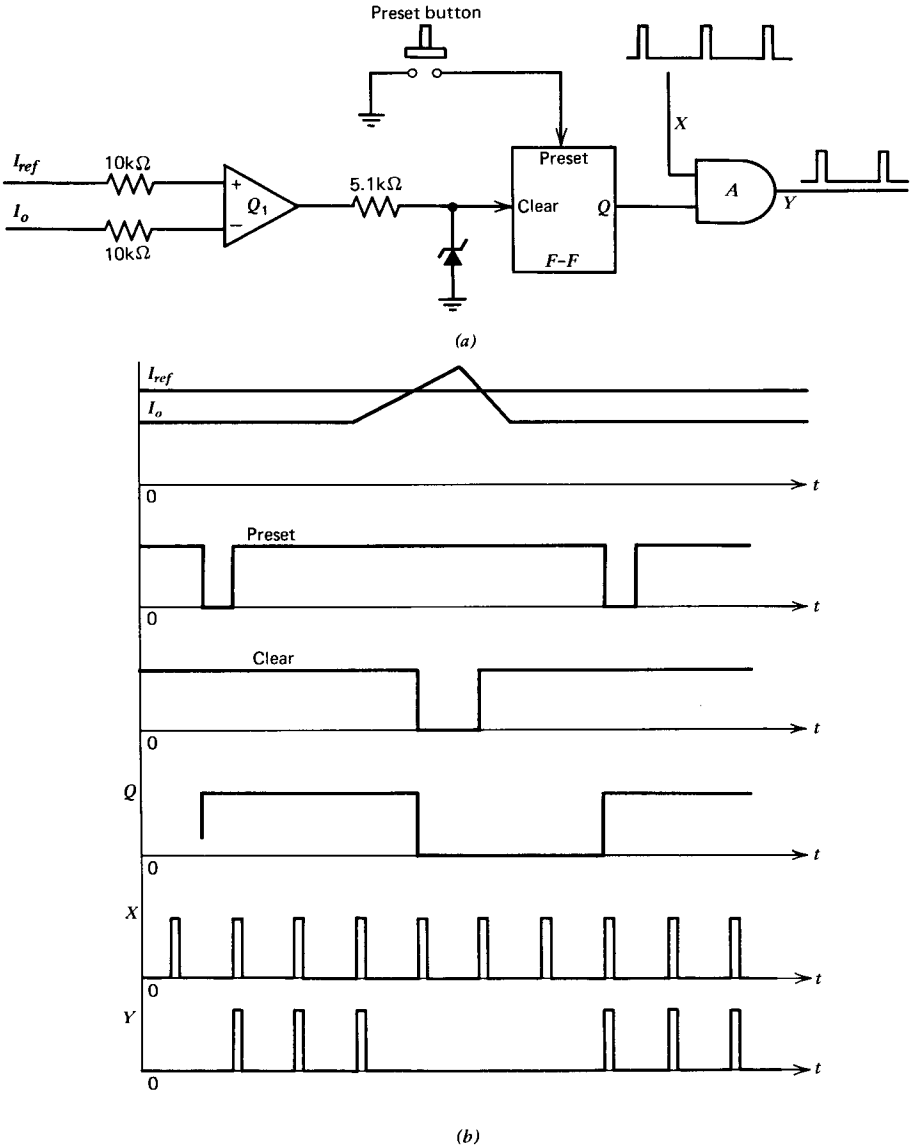


*Fig. B.7* Over-current protection circuit. (*a*) Circuit implementation. (*b*) Timing diagram.

## REFERENCES


1 P. C. Sen, M. MacDonald, and D. J. Clarke, "A Novel Equidistant Pulse Control Scheme for Thyristor Converters," *Canadian Electrical Engineering Journal*, Vol. 3, No. 3, July 1978.

2 B. R. Pelly, *Thyristor Phase-Controlled Converters and Cycloconverters*, Wiley-Interscience, New York, 1971.

# Index


Ac motor, 1, 2, 5
Address bus, 266
Address register, 265
Amplifier:
  power, 133
  pulse, 269, 294
Analog, control, 263
Analysis, 183, 256
  analytical method, 34, 64
  Fourier, 18, 43
  general, 32, 59
  linear system, 238
  numerical method, 33, 64, 248
  state space, 244
Angle:
  displacement, 17, 73, 101, 108
  extinction, 32
  firing, 25, 32, 73
  triggering, 25, 37, 98
Arithmetic logic unit (ALU), 265
Armature current:
  average, 16
  commutation component, 17
  continuous, 21, 37, 60, 99, 137, 183
  discontinuous, 29, 37, 43, 64, 101, 137, 139, 183
  heat producing component, 17
  peak, 17, 48, 70, 191, 193
  reversal, 151
  rms, 16, 54, 70, 186, 191, 194
  torque producing component, 16
Armature heating, 51
Armature inductance, 20, 30, 43, 55, 190, 193
Armature resistance, 20, 55, 209
Armature voltage control, 3, 10, 222, 225
Assembly language, 266
Asymmetrical firing, 78

Back emf, 20, 55
Battery-operated vehicles, 164, 176, 204, 264
Binary codes, 266
Binary instructions, 266
Braking, 204
  dynamic, 12, 205
  electric, 12, 204
  friction, 12, 204, 218
  regenerative, 12, 21, 76, 90, 155, 165, 169, 170, 204, 209
  registors, 12, 204, 205, 207
  power, 205, 209
  torque, 205
  torque-profile, 218
Brushes, 1

Capability, commutating, 51, 187
Capacitance, junction, 278
Capacitor:
  commutating, 174, 178, 182
  electrolytic, 198
  filter, 196
  paper-type, 182
Capital cost of drives, 161, 162
Central processing unit (CPU), 264
Changeover contractors, 150, 151, 160
Chopper, dc, 164
  configuration, 170
  control, 10
  current commutation, 176

drives, 164
firing circuit, 296
first quadrant, 170
four-quadrant, 170
frequency, 187, 193, 197
load commutation, 180
multiphase, 201
period, 166
principles of, 166
regenerative, 170
second quadrant, 170
step-up, 168
two-quadrant:
type A, 170, 213, 283
type B, 170
voltage commutation, 172
Chopper-fed dc motors, 182
Circuit:
commutation, 80
field, 19
firing, 290
hardwired logic, 264
logic, 290
protection, overcurrent, 299
ringing, 174
snubber, 278
Circulating current, 133, 142, 147, 156
reactor, 134, 142, 147
Classical control, dc motor, 205
Clock, 265
frequency, 265, 269
Closed-loop control, 140, 146, 206, 210, 221, 225, 228
logic control circuit, 298
Commutating capability, 51, 187
Commutating capacitor, 174, 178, 182
Commutating inductor, 174, 178
Commutation:
circuit, 80
current, 172, 178
failure , 78, 174, 277, 283
forced, 80, 88, 172, 276
natural or line, 14, 21, 88, 103, 276
voltage, 172
Comparative evaluation, schemes, 94
Computer:
digital, 43
flowchart, 43, 188, 248, 268
study, 43
Constant frequency system, 167
Contractors, changeover, 150, 151, 160
Control:
electronic, 6
extinction angle, 80
derivative, 258
field, 3
hybrid, 261
identical, 122
integral, 258
integral cycle, 10
open-loop, 19, 221, 224, 297
phase, 10
sequential, 78, 85, 90, 122
solid state, 6
symmetrical angle, 83, 88
Control bus, 266
Controller:
field, 216
proportional (P), 226, 228, 234, 242
proportional-integral (PI), 232, 236, 242, 258
Converter:
analog-to-digital (A/D), 269
dc-to-dc, 165
four quadrant, 15, 99, 129
full-, 14, 19, 21, 31, 36, 43, 51, 56, 67, 71, 76, 90, 101, 225
high voltage, 108
one quadrant, 14, 99
phase-controlled, 14, 20, 71, 98
semi-, 14, 19, 21, 31, 35, 43, 51, 56, 67, 74, 76, 85, 98
series, 85
series connected, 107
fully controlled, 110
half controlled, 115
series converter, unshifted voltage, 122
single-phase, 14
three-phase, 14, 98
two-quadrant, 14, 99
CPU, *see* Central processing unit (CPU)
Cross-over philosophy, 141, 147
Current:
commutation, 172, 178
fault, 147
fundamental, 73, 83, 101, 108, 111, 115, 125
harmonic, 18, 198, 200
holding, 275
latching, 274
response, 164
reverse recovery, 276

ripple, 48, 196, 198
supply, 36, 66, 110, 114, 117, 125
surge, 281, 283, 284, 285
transient, 35, 139, 239
Current controller, 228
gain, 240
Current control loop, 229, 256
inner, 140, 228, 262
outer, 141
Current limit, 140, 238
Current transducer, 228

Dampling, 242
Darlington amplifier, 286
Darlington transistor, 285, 294
Data bus, 266
Data register, 265
Dc generator, 5, 204, 209
Dc motor, 1
classical control, 205
separately excited, 19, 43, 104, 168, 186, 206, 210, 215, 222, 239
series, 55, 68, 183, 192, 206, 210, 211, 215, 217
Dc motor model:
separately excited, 223
series, 243
Dead band, 136
Delay time, 275
Derivative control, 258
Design procedure, 239
Digital computer, 43
Digital control system, 264
Digital counter, 264, 269
Digital tachometer, 264, 269
Diode, 286
bridge, 12, 19, 115
conventional, 287
fast recovery, 182, 287
free-wheeling, 15, 21, 32, 88, 99, 166, 174, 178, 181
high power, 286
selenium thynector, 281
Displacement angle, 17, 73, 101, 108
Displacement factor, 17, 74, 80, 83, 94, 107
Distortion factor, current, 107, 114, 121
Drive:
capital cost, 161, 162
chopper, 164, 206, 210
constant horsepower, 2, 69
constant speed, 1, 2
evolution of, 1
high voltage, 85, 107
history of, 1
large horsepower, 98
phase-control, 206, 210
dc drives, 14, 36, 56, 67, 71, 98, 206, 210
regenerative, 149
reversible, 14, 98, 149
single-phase, 14
three-phase, 98
traction, 1, 55, 165
variable speed, 1, 2, 71
Drive selection, 160
Dual-converter, 14, 98, 128, 150, 155, 159, 263, 267
with circulating current, 142, 157
without circulating current, 135, 159
closed-loop control, 140, 146
dual-mode, 147
ideal, 129
nonideal, 133
Duty cycle, 166
Dynamic braking, 12, 205
Dynamic response, 30, 34, 249

Efficiency, 6, 14, 161
Electric car, battery-operated, 12, 164, 176, 204, 264
Electronic crowbar, 283
Energy:
kinetic, 12, 21, 204, 210
recovery, 209
Equation:
basic, 20, 55
characteristic, 242
differential, 32, 59, 244
electrical, 34
electrodynamic, 32, 59
first-order differential, 248
governing, 32, 59, 183, 248
nonlinear differential, 248
torque balance, 222, 239
voltage, 32, 59, 222
Extinction angle control, 80

Fault current, 147
Feedback:
analog servo, 251
closed loop, 251
derivative, 258

integral, 232
motor voltage, 139
tachometer, 19
Field:
circuit, 19
control, 3
controller, 216
current reversal, 158
forcing, 158
generator, 10
series, 55, 213
weakening, 10, 205
windings, cross-connected, 217
Filter, 194, 254
capacitor, 196
L-C, 197, 199
low pass, 258
loop, 254
transfer function, 257
Firing:
asymmetrical, 78
cosine, 132, 225, 292
phase-back, 139
spurious, 147, 281
symmetrical, 80
Firing angle, 25, 32, 73
angle $\alpha$, 21
Firing circuit, 290
Firing control scheme, 131
First order effect, 54
Flowchart, computer, 43, 188, 248, 268
Forward breakover voltage, 273
Fourier analysis, 18, 43
Fourier co-efficients, 18, 73, 74
Fourier series, 18, 73, 199
Free-wheeling action, 19, 30, 33, 35, 59, 65
Frequency:
harmonic, 18
natural, 242
ringing, 175, 197
ripple, 15, 99, 107, 128, 201
Fundamental current, 73, 83, 101, 108, 111, 115, 125
Fuse:
fast acting, 281, 299
$I^2t$ rating, 281, 283

Gate:
blocking, 283
recovery time, 276
Generator:
dc, 5, 204, 209
separately excited, 208
series, 206, 210

Hardware, 267
Hardwired logic circuit, 264
Harmonic:
even, 73, 74, 78, 80, 84
higher order, 76, 84, 94
lower order, 76, 89
lowest order, 95
odd, 73
$n^{th}$ order, 73
Harmonic content, 18, 48
Harmonic current, 18, 198, 200
Harmonic factor, 18, 48, 74, 95
Harmonic frequency, 18
Holding current, 275
Horsepower, constant, 69
Hot spot, 276, 278
Hybrid control, 261

Identical control, 122
Inductor, commutating, 174, 178
Inertia, mechanical, 66
Integral control, 258
Integral cycle control, 10
Interface, input-output, 266
Interpole, 1
Inverter operation, 21, 25, 43, 76, 93, 103, 124, 129, 156
Inverter-rectifier, 164

Junction capacitance, 278

Kinetic energy, 12, 21, 204, 210

Laplace transform, 223, 245
Large scale integration (LSI), 264
Latching current, 274
Linearized model, 244
Load torque, step change, 247, 250
Logic circuits, 290
Look-up tables, 266, 270
Loop filter, 254

Magnetism, residual, 55, 64, 66
Mechanical inertia, 66
Memory, 265
random access (RAM), 266
read only (ROM), 266
Metal oxide varistors (MOV), 281

Microcomputer:
basic architecture, 265
control, 12, 262
of reversing drives, 267
Microprocessing unit (MPU), 264
Microprocessor, 264
Mnemonic codes, 266
Model, linearized, 244
Modes of operation, 32
mode 1, 34, 36, 59, 64
mode 2, 35, 36, 59, 65
mode 3, 36, 60, 65
Modulation:
frequency, 167, 181
index, 84
pulse-width, 83, 167, 254
sinusoidal, 84
Motor:
heating, 10, 187
synchronous, 10, 261
transfer function, 222
voltage, step change, 250
Motor-Generator (M-G) set, 2, 6, 10, 20, 164
Multimotor system, 262

Natural frequency, 242
Newton's method, 84
Nonlinear function, 270
Nonreceptive line, 213
Normalized output voltage, 127

Off-time, 166
On-time, 166
Open-loop control, 19, 221, 244, 297
Optical isolation, 294
Overcurrent protection circuit, 299
Overhauling load, 146

Performance:
characteristic, 36, 66, 187
parameter, 16
motor, 16
supply, 17
Perturbation technique, 244
Phase angle:
control, 71, 87
cosine, 292
linear, 290
Phase-back firing, 139
Phase control, 10
Phase-controlled dc drives, 14, 36, 56, 67, 71, 98, 206, 210
Phase detector, 254
Phase lead compensation, 258
Phase-locked loop (PLL), 254
control, 12, 251
drives, 261
Poles, 235, 237, 256
closed-loop, 257
dominant, 258
open-loop, 256, 257
Pole-zero, 258
Power amplifier, 133
Power factor, 10, 12, 17, 28, 49, 63, 69, 71, 75, 83, 93, 101, 106, 107, 114, 121, 126
characteristics, 126
evaluation, 127
fundamental, 17
improvement, 71
Program, 266
assembler, 266
binary, 266
diagnostic, 270
firmware, 267
object, 266
software, 265, 267
source, 266
symbolic, 266
Proportional (P) controller, 226, 228, 234, 242
Proportional integral (PI) controller, 232, 236, 242, 258
Pulse:
amplifier, 269, 294
speed encoder, 254
transformer, 294

Quasi steady state, 244

RAM, 266
Reactive power, 71
Reactor, smoothing, 194
Rectification mode, 27, 76, 92, 122, 129, 156
Rectifier:
gas-filled, 6
silicon, 286
tube-type, 6
Regeneration, 10, 15, 19, 103
Regulator:
generator field, 6
solid state, 5, 6
tube-type, 4
Relays, 155

Resetting time, 175
Residual magnetism, 55, 64, 66
Residual magnetism voltage, 64, 66
Resistance control, 164
Resonance phenomena, 197
Response:
  current, 227, 232, 233, 236, 238
  second order, 235, 236
  speed, 232, 233, 236, 238
Response study, 250
Reverse breakdown voltage, 273
Reverse recovery current, 276
Reverse recovery time, 276
Reversing switch, 10, 14, 150
Ringing circuit, 174
Ringing frequency, 175, 197
Ripple current, 48, 196, 198
Ripple frequency, 15, 99, 107, 128, 201
Ripple voltage, 133, 143
Rise time, 276
ROM, 265
Root locus:
  plots, 259
  technique, 256
Range kutta (RK) method, 33, 248

Saturable reactor, 7
Saturation, 244, 285
Schemes, comparative evaluation, 94
Selenium thyrector diodes, 281
Sequential control, 78, 85, 122
  of full converters, 90, 122
  of semi-converters, 85
Silicon controlled rectifiers (SCR), 6, 272
Simulation, 256
Single-phase:
  drives, 14, 19
  half-wave circuit, 15, 19
  separately excited dc motor drives, 19
  series dc motor drives, 55
Snubber circuit, 278
Solid state control, 6
Speed:
  base, 3, 10, 153, 216
  closed-loop control, 225
  control, analog, 254, 263
  controller gain, 241
  control loop, 141, 226, 229, 233, 262
  regulation, 12, 25, 29, 43, 104, 106, 253, 269
  reversal, 146, 149, 155, 159
  steady state, 34, 36
Stability, 257, 260
Steady state, 34, 64, 67, 146, 154
  behavior, 248
  error, 232, 240
  quasi, 244
Subway car, 149, 164, 178, 204, 215
Supply current, 36, 66, 110, 114, 117, 125
Surge current, 281, 285
  one-cycle, 283, 284
Switching loss, 96, 276
Symbolic codes, 266
Symmetrical angle control, 83, 88
Symmetrical firing, 80
Synchronous motor, 10, 261

Tachogenerator, 225
  digital, 264
Three-phase drives, 98
Thyristor, 6, 272, 288
  circuit protection, 283
  data sheet, 283
  di/dt protection, 277
  dv/dt protection, 278
  gate protection, 281
  heat sink, 280
  overcurrent protection, 281
  overvoltage protection, 281
  power module, 9
  protection by ringing, 283
  static terminal characteristics, 272
  turn-off characteristics, 276
  turn-on characteristics, 275
Time constant, 257
  armature circuit, 30, 151, 223
  of dc motors, 161
  electrical, 1, 223
  field circuit, 151, 158
  filter, 231
  mechanical, 1, 36, 153, 224
  thermal, 277
Time delay, 158, 229
Time response, 10, 161
Torque:
  accelerating, 216
  average, 20
  constant, 2
  decelerating, 216
  disturbance, 234
    profile, 206, 209, 216
    sharing, 217

speed characteristics, 16, 24, 43, 61, 67, 187, 192, 216
reversing, 153, 158
starting, 1, 243
Traction system, 96, 178
Transfer characteristic, 133, 139
Transfer function, 221, 245, 256
Transient behavior, 248
Transient component of current, 35
Transient current, 139, 239
Transient isolation, 196
Transient overcurrent, 228
Transistor, 284
power, 285
power darlington, 285
switching operation, 284
Transit system, 194, 215
Transportation system, 165
Trapped charges, 276
Turn-off time:
circuit, 174, 178, 277
thyristor, 174, 178, 276
Turn-on time, 276

Up/down counter, 264

Variable frequency system, 167
Vehicles, battery operated, 164, 176, 204, 264
Voltage:
forward breakover, 273
magnetism, residual, 64, 66
oscillation, 197
output, normalized, 127
reverse breakdown, 273
ripple, 133, 143
Voltage-controlled oscillator (VCO), 254

Ward-Leonard system, 2, 14, 129, 149
Windage and friction losses, 153

Zero current detector, 151, 155
Zeros, 237, 256
open-loop, 257
Zero speed regulation, 254, 261